



**FRDC**

FISHERIES RESEARCH &  
DEVELOPMENT CORPORATION

# Investigate oceanographic and environmental factors impacting on the ETBF

Jason R. Hartog, J. Paige Eveson, Thomas Moore, Kylie Scales,  
Toby Patterson, Shane Baylis, Bernadette Sloyan,  
Ash Williams, Claire Spillman, Alistair J. Hobday  
January 2023

FRDC Project No **2017/004**

## ***Please Note – Final Report Requirements – accessibility***

*Under the Disability Discrimination Act 1992, Australian Government agencies are required to ensure information and services are provided in a non-discriminatory accessible manner – the FRDC and as a result all content produced as part of our projects also need to meet these requirements.*

*The Web Content Accessibility Guidelines outlines ways to make digital content more accessible to the broadest audience – <https://guides.service.gov.au/content-guide/accessibility-inclusivity/>*

*While there are many aspects to this, a key focus for principal investigators is to ensure that PDF documents are accessible. To make a PDF accessible you must make sure structural elements such as headings are marked-up so that a screen reader can follow the logical order of the content. The FRDC will update the final report design standard to highlight these requirements. We are regularly working to improve what we deliver to end users and this is part of that.*

© 2023 Fisheries Research and Development Corporation.  
All rights reserved.

## Investigate oceanographic and environmental factors impacting on the ETBF

2017-004

2023

### Ownership of Intellectual property rights

Unless otherwise noted, copyright (and any other intellectual property rights, if any) in this publication is owned by the Fisheries Research and Development Corporation [and CSIRO Environment]

This publication (and any information sourced from it) should be attributed to [Hartog, J.R. et al, CSIRO Environment, 2023, *Investigate oceanographic and environmental factors impacting on the ETBF*, Place of publishing, January. CC BY 3.0]

### Creative Commons licence

All material in this publication is licensed under a Creative Commons Attribution 3.0 Australia Licence, save for content supplied by third parties, logos and the Commonwealth Coat of Arms.



Creative Commons Attribution 3.0 Australia Licence is a standard form licence agreement that allows you to copy, distribute, transmit and adapt this publication provided you attribute the work. A summary of the licence terms is available from <https://creativecommons.org/licenses/by/3.0/au/>. The full licence terms are available from <https://creativecommons.org/licenses/by-sa/3.0/au/legalcode>.

Inquiries regarding the licence and any use of this document should be sent to: [frdc@frdc.com.au](mailto:frdc@frdc.com.au)

### Disclaimer

The authors do not warrant that the information in this document is free from errors or omissions. The authors do not accept any form of liability, be it contractual, tortious, or otherwise, for the contents of this document or for any consequences arising from its use or any reliance placed upon it. The information, opinions and advice contained in this document may not relate, or be relevant, to a readers particular circumstances. Opinions expressed by the authors are the individual opinions expressed by those persons and are not necessarily those of the publisher, research provider or the FRDC.

The Fisheries Research and Development Corporation plans, invests in and manages fisheries research and development throughout Australia. It is a statutory authority within the portfolio of the federal Minister for Agriculture, Fisheries and Forestry, jointly funded by the Australian Government and the fishing industry.

### Researcher Contact Details

Name: Jason Hartog  
Address:  
Phone: 03 6232 5153  
Fax:  
Email: Jason.Hartog@csiro.au

### FRDC Contact Details

Address: 25 Geils Court  
Deakin ACT 2600  
Phone: 02 6122 2100  
Email: [frdc@frdc.com.au](mailto:frdc@frdc.com.au)  
Web: [www.frdc.com.au](http://www.frdc.com.au)

In submitting this report, the researcher has agreed to FRDC publishing this material in its edited form.

# Table of Contents

<b>Acknowledgments</b> .....	<b>x</b>
<b>Abbreviations</b> .....	<b>x</b>
<b>Executive Summary</b> .....	<b>xi</b>
<b>Introduction</b> .....	<b>1</b>
<b>Objectives</b> .....	<b>2</b>
<b>1 Local and Regional Fishery Data</b> .....	<b>3</b>
<b>2 State-of-the-art estimates of ocean state</b> .....	<b>6</b>
2.1 CAFE60 .....	6
2.2 ACCESS-S.....	6
2.3 From coupled climate model output to analysis ready data (ARD) for fisheries applications.....	8
<b>3 Initial Habitat Modelling</b> .....	<b>10</b>
<b>4 Oceanographic background</b> .....	<b>11</b>
4.1 Overview.....	11
4.2 Choice of study regions .....	12
4.3 Catch heatmaps and events .....	14
4.4 Event case studies .....	24
4.4.1 Current index locations with summer / winter conditions .....	24
4.4.2 Ocean climatologies.....	29
4.4.3 Strong ENSO events .....	36
4.5 Discussion.....	49
<b>5 Boosted Regression Trees</b> .....	<b>51</b>
5.1 General BRT methods .....	51
5.2 BRT using CAFE60.....	52
5.2.1 Methods.....	52
5.2.2 Results .....	54
5.3 BRT using ACCESS-S2 .....	69
5.3.1 Methods.....	69
5.3.2 Results.....	69
<b>6 BRT forecasting with ACCESS-S2</b> .....	<b>85</b>
6.1 Methods .....	85
6.2 Results.....	85
6.2.1 Model performance .....	85
6.2.2 Relative contributions of ocean predictors.....	86
6.2.3 Effects of ocean predictors on CPUE .....	86
<b>7 Projecting future patterns – seasonal and decadal forecasts</b> .....	<b>91</b>
7.1 Forecast runs .....	91
7.2 Progress on CAFE decadal (multi-year) forecasts.....	94
<b>8 Categorical approach to prediction of CPUE based on ACCESS-S2 output</b> .....	<b>95</b>
8.1 Background.....	95
8.2 Methods .....	96
8.2.1 Data categorization .....	96

8.2.2	Spatial configuration .....	97
8.2.3	Statistical models .....	98
8.2.4	Ocean model data output.....	99
8.2.5	Model selection .....	99
8.3	Results.....	99
8.3.1	Ocean conditions.....	99
8.3.2	Yellowfin tuna.....	101
8.3.3	Bigeye Tuna .....	102
8.3.4	Broadbill swordfish.....	103
8.3.5	Striped Marlin .....	104
8.3.6	Albacore .....	105
8.3.7	Summary of oceanographic predictors in selected models .....	106
8.3.8	Examples of model prediction for the EAC dominated region.....	107
8.4	Discussion.....	109
8.4.1	Selection of thresholds for categorisation of states.....	110
8.4.2	Spatial configuration .....	111
<b>Discussion and Conclusion .....</b>		<b>112</b>
<b>Implications .....</b>		<b>113</b>
<b>Recommendations .....</b>		<b>114</b>
<b>Further development .....</b>		<b>114</b>
<b>Extension and Adoption .....</b>		<b>115</b>
<b>Project materials developed .....</b>		<b>116</b>
<b>Appendices .....</b>		<b>117</b>
	Appendix 1 – Initial Habitat Modelling exploration (attached) .....	117
	Appendix 2 – Boosted Regression Tree results for all species and regions (attached).....	117
	Appendix 3 – Categorical Timeseries (attached).....	117
	Appendix 4 – Project Staff .....	117
	Appendix 5 – Project Updates (attached) .....	117
	Appendix 6 – SPC Newsletter article (attached) .....	117
	References.....	118

## Tables

Table 1-	available ocean environmental variable from retrospective analyses.....	7
Table 2 -	Physical predictors from CAFE60 ensemble reanalysis, direct and derived products. Bold indicates those used in BRT models .....	52
Table 3 -	Pairwise correlation of physical fields from CAFE60 listed in Table 1. The subset in bold were selected for inclusion in the BRTs since all pairwise correlations are < 0.80. ....	53
Table 4 -	Number of trees fitted for each species/region combination. ....	54
Table 5 -	Proportion of deviance explained by CAFE60-based boosted regression tree (BRT) models, for each species and sub-region (ALL = Western Central and South-West Pacific domain; EAC = East Australian Current domain; CS = Coral Sea/Equatorial; WCP = Western Central Pacific; NZ = New Zealand).....	54
Table 6 -	Pearson correlation ( $R^2$ ) of observed and predicted catch-per-unit-effort (CPUE) values for 2008-2015 model training dataset for the CAFE60-based boosted regression tree (BRT) models. ....	55
Table 7 -	Pearson correlation ( $R^2$ ) of observed and predicted catch-per-unit-effort (CPUE) per 1° grid cell for 2016-2019 independent testing (validation) dataset for the CAFE60-based boosted regression tree (BRT) models.....	55
Table 8 -	Pearson correlation ( $R^2$ ) of observed and predicted catch per 1° grid cell for 2008-15 model training dataset for the CAFE60-based boosted regression tree (BRT) models. ....	55

Table 9 - Pearson correlation ( $R^2$ ) of observed and predicted catch per 1° grid cell for 2016-19 independent testing (validation) dataset for the CAFE60-based boosted regression tree (BRT) models....	55
Table 10 - Root mean squared error (RMSE) values for observed vs predicted CPUE (defined as catch per 10,000 hooks) calculated from the BRT model for each species and region using: the training dataset (2008-2015) for the CAFE60-based boosted regression tree (BRT) models. Mean observed CPUE in parentheses below. ....	56
Table 11 - Root mean squared error (RMSE) values for observed vs predicted CPUE (defined as catch per 10,000 hooks) calculated from the for the CAFE60-based boosted regression tree (BRT) models for each species and region using the validation dataset (2016-2019). Mean observed CPUE in parentheses below. ....	56
Table 12. List of oceanographic variables available from the ACCESS-S2 reanalysis data (direct and derived products), except for bathymetry taken from TerrainBase ( <a href="https://www.ngdc.noaa.gov/mgg/gravity/1999/document/html/tbase.html">https://www.ngdc.noaa.gov/mgg/gravity/1999/document/html/tbase.html</a> ). Bold indicates those included in the BRTs. ....	71
Table 13. Pairwise correlations between all ocean variables listed in Table 12. The subset in bold were selected for inclusion in the BRTs since all pairwise correlations are $< 0.80$ . ....	72
Table 14. Number of trees used in the BRT model for each species and region (ALL = whole domain)...	73
Table 15. Proportion of deviance in catch explained by the BRT model for each species and region using the training dataset. ....	73
Table 16. $R^2$ values for observed vs predicted CPUE (defined as catch per 10,000 hooks) calculated from the BRT model for each species and region using: (left) the training dataset (2008-2015), and (right) the validation dataset (2016-2020). ....	73
Table 17. Root mean squared error (RMSE) values for observed vs predicted CPUE (defined as catch per 10,000 hooks) calculated from the BRT model for each species and region using: (left) the training dataset (2008-2015), and (right) the validation dataset (2016-2020). The mean observed CPUE value is given in parentheses below for reference. ....	74
Table 18. Number of trees used in the BRT forecasting model for each species and region (ALL = whole domain). ....	86
Table 19. Proportion of deviance in catch explained by the BRT forecasting model for each species and region using the training dataset. ....	86
Table 20. $R^2$ values for observed vs predicted CPUE (defined as catch per 10,000 hooks) calculated from the BRT model for each species and region using: (left) the training dataset (2008-2015), and (right) the validation dataset (2016-2020). ....	86
Table 21. $R^2$ values for observed vs predicted CPUE (defined as catch per 10,000 hooks) calculated from the BRT whole-region forecast model for each species run using: (left) the ACCESS-S2 hindcast oceanographic data output for March, April and May 2018 from a February 1 <sup>st</sup> initialisation date; (right) the observed oceanographic data for March, April and May 2018 for comparison. ....	92
Table 22 - observed state transitions for each species for the EAC dominated region. The tables are to be read as the “from state” as rows and “to state” as columns. ....	101
Table 23 - Number of times a given ocean covariate was retained in set of 40 chosen models. ....	107
Table 24 - Deviance explained according to self (S) and adjacent (A) models. ....	107

## Figures

Figure 1: Yellowfin CPUE for the 4 regions in the study area. The dotted lines show the 25 <sup>th</sup> and 85 <sup>th</sup> percentiles of CPUE. ....	3
Figure 2: Albacore CPUE for the 4 regions in the study area. The dotted lines show the 25 <sup>th</sup> and 85 <sup>th</sup> percentiles of CPUE. ....	4
Figure 3: Bigeye CPUE for the 4 regions in the study area. The dotted lines show the 25 <sup>th</sup> and 85 <sup>th</sup> percentiles of CPUE. ....	4
Figure 4: Striped Marlin CPUE for the 4 regions in the study area. The dotted lines show the 25 <sup>th</sup> and 85 <sup>th</sup> percentiles of CPUE. ....	5
Figure 5: Swordfish CPUE for the 4 regions in the study area. The dotted lines show the 25 <sup>th</sup> and 85 <sup>th</sup> percentiles of CPUE. ....	5
Figure 6 - Ratio of EKE to MKE. ....	12

Figure 7 - Four key regions for analysis. EAC = EAC-dominated, CS = Coral Sea and Equatorial, WCP = Western-Central Pacific, NZ = New Zealand. ....	13
Figure 8: ENSO phase across period of study based on the Oceanic Niño Index (ONI).....	14
Figure 9: Heatmap of CPUE categorization for yellowfin tuna in the WCP region.....	15
Figure 10: Heatmap of CPUE categorization for bigeye tuna in the WCP region.....	16
Figure 11: Heatmap of CPUE categorization for albacore in the WCP region.....	17
Figure 12: ENSO phase based on the Oceanic Niño Index (ONI) vs catch state ( “Bad”(0), “Normal”(1), “Good”(2) ) for yellowfin tuna in the WCP region.....	18
Figure 13: ENSO phase based on the Oceanic Niño Index (ONI) vs catch state ( “Bad”(0), “Normal”(1), “Good”(2) ) for bigeye tuna in the WCP region .....	19
Figure 14: ENSO phase based on the Oceanic Niño Index (ONI) vs catch state ( “Bad”(0), “Normal”(1), “Good”(2) ) for albacore tuna in the WCP region .....	20
Figure 15: ENSO phase based on the Oceanic Niño Index (ONI) vs catch state ( “Bad”(0), “Normal”(1), “Good”(2) ) for striped marlin in the WCP region.....	21
Figure 16: ENSO phase based on the Oceanic Niño Index (ONI) vs catch state ( “Bad”(0), “Normal”(1), “Good”(2) ) for swordfish in the WCP region .....	22
Figure 17: ENSO phase based on the Oceanic Niño Index (ONI) vs catch state ( “Bad”(0), “Normal”(1), “Good”(2) ) for yellowfin tuna in the EAC region .....	23
Figure 18: Regional summer conditions with SST, ocean currents, and location of 4 current indices. ....	25
Figure 19: Regional winter conditions with SST, ocean currents, and location of 4 current indices. ....	26
Figure 20: Ocean current index for the South Equatorial Current (SEC) – relative to ENSO (as described by the oceanic Niño index – ONI) .....	27
Figure 21: Ocean current index for the East Australian Current (EAC) – relative to ENSO (as described by the oceanic Niño index – ONI) .....	28
Figure 22: Seasonal climatology for sea surface temperature from ACCESS-S2. ....	29
Figure 23: Seasonal climatology for temperature at 500m from ACCESS-S2.....	30
Figure 24: Seasonal climatology for depth of the 20° isotherm from ACCESS-S2. ....	31
Figure 25: Seasonal climatology for ocean heat content for the upper 300m from ACCESS-S2. ....	32
Figure 26: Seasonal climatology for sea surface salinity from ACCESS-S2. ....	33
Figure 27: Seasonal climatology for mixed layer depth from ACCESS-S2.....	34
Figure 28: Seasonal climatology for sea surface height from ACCESS-S2. ....	35
Figure 29: Monthly anomalies for sea surface temperature from ACCESS-S2 for the 2015-2016 El Niño events.....	36
Figure 30: Monthly anomalies for sea surface salinity from ACCESS-S2 for the 2015-2016 El Niño events .....	37
Figure 31: Monthly anomalies for sea surface height from ACCESS-S2 for the 2015-2016 El Niño events .....	38
Figure 32: Monthly anomalies for temperature at 500m from ACCESS-S2 for the 2015-2016 El Niño events.....	39
Figure 33: Monthly anomalies for depth of the 20 degree isotherm from ACCESS-S2 for the 2015-2016 El Niño events.....	40
Figure 34: Monthly anomalies for mixed layer depth from ACCESS-S2 for the 2015-2016 El Niño events .....	41
Figure 35: Monthly anomalies for heat content in the upper 300m from ACCESS-S2 for the 2015-2016 El Niño events.....	42
Figure 36: Monthly anomalies for sea surface temperature from ACCESS-S2 for the 2010-2012 La Niña events.....	43
Figure 37: Monthly anomalies for sea surface salinity from ACCESS-S2 for the 2010-2012 La Niña events.....	44
Figure 38: Monthly anomalies for sea surface height from ACCESS-S2 for the 2010-2012 La Niña events .....	45
Figure 39: Monthly anomalies for temperature at 500m from ACCESS-S2 for the 2010-2012 La Niña events.....	46
Figure 40: Monthly anomalies for depth of the 20 degree isotherm from ACCESS-S2 for the 2010-2012 La Niña events.....	47
Figure 41: Monthly values for mixed layer depth from ACCESS-S2 for the 2010-2012 La Niña events ..	48

Figure 42: Monthly anomalies for heat content in the upper 300m from ACCESS-S2 for the 2010-2012 La Nina events.....	49
Figure 43 - Relative contributions of physical fields from CAFÉ-60 ensemble to overall deviance explained by models of YFT CPUE in the five model domains (“all” = Western Central and South-West Pacific; “eac” = EAC-dominated region; “cs” = Coral Sea; “wcp” = Western Central Pacific; “nz” = New Zealand). Variable names described in Table 2. ....	57
Figure 44 - Relative contributions of physical fields from CAFÉ-60 ensemble to overall deviance explained by models of BET CPUE in the five model domains (“all” = Western Central and South-West Pacific; “eac” = EAC-dominated region; “cs” = Coral Sea; “wcp” = Western Central Pacific; “nz” = New Zealand).....	58
Figure 45 - Relative contributions of physical fields from CAFÉ-60 ensemble to overall deviance explained by models of ALB CPUE in the five model domains (“all” = Western Central and South-West Pacific; “eac” = EAC-dominated region; “cs” = Coral Sea; “wcp” = Western Central Pacific; “nz” = New Zealand).....	58
Figure 46 - Relative contributions of physical fields from CAFÉ-60 ensemble to overall deviance explained by models of MLS CPUE in the five model domains (“all” = Western Central and South-West Pacific; “eac” = EAC-dominated region; “cs” = Coral Sea; “wcp” = Western Central Pacific; “nz” = New Zealand).....	59
Figure 47 - Relative contributions of physical fields from CAFÉ-60 ensemble to overall deviance explained by models of SWO CPUE in the five model domains (“all” = Western Central and South-West Pacific; “eac” = EAC-dominated region; “cs” = Coral Sea; “wcp” = Western Central Pacific; “nz” = New Zealand).....	59
Figure 48 - Seasonal mean of predicted vs. observed catch-per-unit-effort (CPUE, per 10000 hooks) of YFT for winter (Dec-Feb), predicted from the broad Western Central and South-West Pacific domain and averaged across the testing (validation) dataset, 2016-19. The mean observed CPUE over the EAC sub-region is given in the lower corner of the observed map, whereas Pearson’s $R^2$ value and the root mean squared error (RMSE) are given in the lower corner of the prediction map as an indicator of predictive performance.....	60
Figure 49 - Seasonal mean of predicted vs. observed catch-per-unit-effort (CPUE, per 10000 hooks) of BET for autumn (Mar-May), predicted from the broad Western Central and South-West Pacific domain and averaged across the testing (validation) dataset, 2016-19. The mean observed CPUE over the EAC sub-region is given in the lower corner of the observed map, whereas Pearson’s $R^2$ value and the root mean squared error (RMSE) are given in the lower corner of the prediction map as an indicator of predictive performance.....	61
Figure 50 - Seasonal mean of predicted vs. observed catch-per-unit-effort (CPUE, per 10000 hooks) of ALB for winter (Dec-Feb), predicted from the Coral Sea domain and averaged across the testing (validation) dataset, 2016-19. The mean observed CPUE over the EAC sub-region is given in the lower corner of the observed map, whereas Pearson’s $R^2$ value and the root mean squared error (RMSE) are given in the lower corner of the prediction map as an indicator of predictive performance. ....	61
Figure 51 - Seasonal mean of predicted vs. observed catch-per-unit-effort (CPUE, per 10000 hooks) of SWO for spring (Sept-Nov), predicted from the EAC-dominated model domain and averaged across the testing (validation) dataset, 2016-19. The mean observed CPUE over the EAC sub-region is given in the lower corner of the observed map, whereas Pearson’s $R^2$ value and the root mean squared error (RMSE) are given in the lower corner of the prediction map as an indicator of predictive performance.....	62
Figure 52 - Seasonal mean of predicted vs. observed catch-per-unit-effort (CPUE, per 10000 hooks) of SWO for spring (Sept-Nov), predicted from the broad Western Central and South-West Pacific domain and averaged across the testing (validation) dataset, 2016-19. The mean observed CPUE over the EAC sub-region is given in the lower corner of the observed map, whereas Pearson’s $R^2$ value and the root mean squared error (RMSE) are given in the lower corner of the prediction map as an indicator of predictive performance.....	62
Figure 53 - Marginal effects plots for YFT Western Central and South-West Pacific model, showing most influential predictors.. The rug plot along the top axis marks deciles in the data, so the marginal effect functions are of most relevance within the 10 <sup>th</sup> and 90 <sup>th</sup> deciles (i.e., between the second and tenth marks). ....	63
Figure 54 - Marginal effects plots for BET Western Central and South-West Pacific model, showing most influential predictors. The rug plot along the top axis marks deciles in the data, so the marginal effect	

functions are of most relevance within the 10<sup>th</sup> and 90<sup>th</sup> deciles (i.e., between the second and tenth marks). ..... 64

Figure 55 - Marginal effects plots for ALB Coral Sea model, showing most influential predictors. The rug plot along the top axis marks deciles in the data, so the marginal effect functions are of most relevance within the 10<sup>th</sup> and 90<sup>th</sup> deciles (i.e., between the second and tenth marks). ..... 64

Figure 56 - Marginal effects plots for SWO EAC-dominated model, showing most influential predictors. The rug plot along the top axis marks deciles in the data, so the marginal effect functions are of most relevance within the 10<sup>th</sup> and 90<sup>th</sup> deciles (i.e., between the second and tenth marks). ..... 65

Figure 57 - Marginal effects plots for SWO Western Central and South-West Pacific model, showing most influential predictors. The rug plot along the top axis marks deciles in the data, so the marginal effect functions are of most relevance within the 10<sup>th</sup> and 90<sup>th</sup> deciles (i.e., between the second and tenth marks). ..... 65

Figure 58 - Observed (black line) and predicted (red line) total catch of YFT over the broad Western Central and South-West Pacific (“all”) domain, as sum of total catch across all 1° grid cells per month over the time series 2008-19. Dashed line shows separation of model training (2008-15) and validation (2016-19) datasets. .... 66

Figure 59 - Observed (black line) and predicted (red line) total catch of BET over the broad Western Central and South-West Pacific (“all”) domain, as sum of total catch across all 1° grid cells per month over the time series 2008-19. Dashed line shows separation of model training (2008-15) and validation (2016-19) datasets. .... 67

Figure 60 - Observed (black line) and predicted (red line) total catch of ALB in the Coral Sea domain, as sum of total catch across all 1° grid cells per month over the time series 2008-19. Dashed line shows separation of model training (2008-15) and validation (2008-15) and validation (2016-19) datasets. .... 67

Figure 61 - Observed (black line) and predicted (red line) total catch of SWO in the EAC-dominated region, as sum of total catch across all 1° grid cells per month over the time series 2008-19. Dashed line shows separation of model training (2008-15) and validation (2016-19) datasets. .... 68

Figure 62 - Observed (black line) and predicted (red line) total catch of SWO over the broad Western Central and South-West Pacific (“all”) domain, as sum of total catch across all 1° grid cells per month over the time series 2008-19. Dashed line shows separation of model training (2008-15) and validation (2016-19) datasets. .... 68

Figure 63. Relative contributions of each of the oceanographic variables included in the BRTs for each species and region (all = whole region; eac = EAC-dominated region; cs = Coral Sea; wcp = Western Central Pacific; nz=New Zealand) (see Figure 7). See Table 12 for definitions of oceanographic variables. .... 76

Figure 64. Marginal effect plots for the ocean variables that explain at least 10% of the total deviance in the whole-domain models for (a) YFT, (b) BET and (c) SWO. The rug plot along the top axis marks deciles in the data, so the marginal effect functions are of most relevance within the 10<sup>th</sup> and 90<sup>th</sup> deciles (i.e., between the second and tenth marks). .... 77

Figure 65. Marginal effect plots for the ocean variables that explain at least 10% of the total deviance in the EAC-dominated sub-region models for (a) YFT, (b) BET and (c) SWO. The rug plot along the top axis marks deciles in the data, so the marginal effect functions are of most relevance within the 10<sup>th</sup> and 90<sup>th</sup> deciles (i.e., between the second and tenth marks). .... 78

Figure 66. Spatial maps showing the average observed (left) and average predicted (right) CPUE over all years in the validation/test dataset (2016-2020) for (a) YFT in winter, (b) BET in autumn, and (c) SWO in summer, where CPUE is defined as catch per 10,000 hooks and predictions were made using the whole-domain BRTs. The mean observed CPUE over the whole region is given in the lower corner of the observed map, whereas Pearson’s R<sup>2</sup> value and the root mean squared error (RMSE) are given in the lower corner of the prediction map as an indicator of predictive performance. .... 81

Figure 67. Spatial maps showing the average observed (left) and average predicted (right) CPUE over all years in the validation/test dataset (2016-2020) for (a) YFT in winter, (b) BET in autumn, and (c) SWO in summer, where CPUE is defined as catch per 10,000 hooks and predictions were made using the EAC sub-region BRTs. The mean observed CPUE over the EAC sub-region is given in the lower corner of the observed map, whereas Pearson’s R<sup>2</sup> value and the root mean squared error (RMSE) are given in the lower corner of the prediction map as an indicator of predictive performance. .... 84

Figure 68. Relative contributions of each of the oceanographic variables included in the BRT forecasting models for each species and region (all = whole region; eac = EAC-dominated region; cs = Coral Sea; wcp = Western Central Pacific; nz=New Zealand) (see Figure 7 in Section 4). .....	89
Figure 69. Marginal effect plots for the ocean variables with a relative contribution to explaining the total deviance of at least 20% in the whole-domain BRT forecasting models for (a) YFT, (b) BET and (c) SWO. The rug plot along the top axis marks deciles in the data, so the marginal effect functions are of most relevance within the 10 <sup>th</sup> and 90 <sup>th</sup> deciles (i.e., between the second and tenth marks). .....	89
Figure 70. Marginal effect plots for the ocean variables with a relative contribution to explaining the total deviance of at least 20% in the EAC-dominated sub-region BRT forecasting models for (a) YFT, (b) BET and (c) SWO. The rug plot along the top axis marks deciles in the data, so the marginal effect functions are of most relevance within the 10 <sup>th</sup> and 90 <sup>th</sup> deciles (i.e., between the second and tenth marks). .....	90
Figure 71. Spatial maps showing the predicted CPUE (defined as catch per 10,000 hooks) for February 2022 for (a) YFT, (b) BET, and (c) SWO, obtained using the whole-domain BRT forecast model with ACCESS-S2 forecast data initialised on January 1 <sup>st</sup> 2022 as input. Only grid cells with at least some fishing effort historically are included. (Note that the catch and effort data around New Zealand was only provided at a 1 x 1 degree resolution, hence the sparse appearance of the predictions which are made at a 0.25 x 0.25 degree resolution). .....	93
Figure 72 - Spatial configuration used in the ‘self’ models – as per the figure, there is no spatial dependence. ....	97
Figure 73 - Spatial configuration used in the ‘adjacent’ models for the case of the EAC and NZ blocks at illustrations. The model is configured so that only adjacent blocks influence the focal cell. ....	98
Figure 74 - Monthly time series for the EAC-dominated region (see Figure 7 above). .....	100
Figure 75 - Yellowfin tuna (top) catch rates and (bottom) categorized series of catch states .....	102
Figure 76 - Bigeye tuna (top) catch rates and (bottom) categorized series of catch states. ....	103
Figure 77 - Broadbill swordfish (top) catch rates and (bottom) categorized series of catch states. ....	104
Figure 78 - striped marlin (top) catch rates and (bottom) categorized series of catch states. ....	105
Figure 79 - Albacore (top) catch rates and (bottom) categorized series of catch states. ....	106
Figure 80 - State predictions for each species through time. See text for explanation of the plots. ....	109

# Acknowledgments

The authors wish to acknowledge those who provided reviews of the final report and early contributors to the project.

We gratefully acknowledge the provision of fishing effort data from following countries:

Cook Islands; French Polynesia; New Caledonia; New Zealand; Norfolk Island; Samoa; Solomon Islands; Tokelau; Tonga; Tuvalu; Vanuatu; Fiji and Australia and Peter Williams from SPC for collation into aggregated data that we could use.

We thank the steering committee (consisting of TTRAG members and the FRDC) and early input from Wez Norris.

## Abbreviations

ACCESS-S – Australian Coupled Climate Earth Simulator – Seasonal

ALB – Albacore tuna

BET – Bigeye tuna

BRT – Boosted Regression Tree

CAFE60 - Climate retrospective Analysis and Forecast Ensemble system

CPUE – Catch per Unit Effort

CS – Coral Sea

EAC – East Australia Current

ETBF – Eastern Tuna and Billfish Fishery

MLS – Striped Marlin

NZ – New Zealand

POAMA - Predictive Ocean Atmosphere Model for Australia

SPC – Pacific Community

STM – Striped Marlin

SWO – Broadbill swordfish

TTRAG – Tropical Tuna Resource Assessment Group

WCP – Western Central Pacific

YFT – Yellowfin tuna

# Executive Summary

## What the report is about

This research project was a collaborative project between CSIRO, Bureau of Meteorology and industry and management partners in Australia and the western Pacific region, with primary benefit for the ETBF. The project investigated the influence of local ocean conditions on the main target species availability in eastern Australian waters as well as the wider Pacific region, and how lagged ocean conditions elsewhere can also provide insight. We sought to utilise existing environmental datasets to aid in this investigation and also to develop analysis ready datasets for this project and beyond.

## Background

The five target species of the ETBF (Bigeye Tuna, *Thunnus obesus*; Yellowfin Tuna, *Thunnus albacares*; Albacore, *Thunnus alalunga*; Striped Marlin, *Kajikia audax*; Broadbill Swordfish, *Xiphias gladius*) have a wide distribution outside the Australian EEZ, but the influence of oceanographic factors on their distribution, abundance and phenology within the ETBF fishery region and the adjacent south-west Pacific region is poorly understood, creating uncertainty in current management arrangements. This project investigated the influence of oceanographic conditions on species distribution in the ETBF and the wider region.

## Aims/objectives

The specific project objectives were:

- Enhance AFMA and industry understanding of influence of climate-ocean system drivers upon the spatial and temporal variability of key ETBF species;
- Develop and deliver predictive models at seasonal and decadal time scales to assist management and industry planning;
- Provide operational forecasts of habitat distribution for Australia and the regional partners within the life of the project;
- Inform harvest and allocation discussions at national and international scales.

In meeting these objectives, we used available data on species' locations (rather than collecting new tagging data) and investigate how ocean conditions might affect their distributions in the south-west Pacific.

## Methods

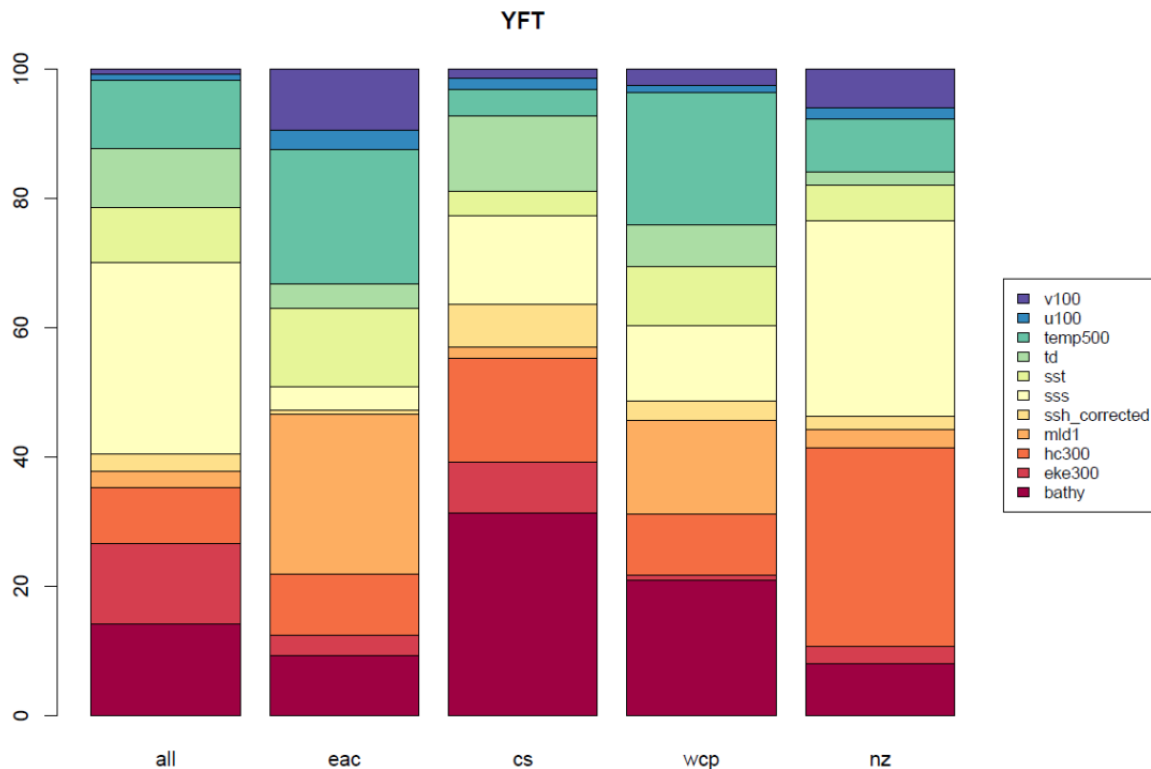
The project team undertook an examination of existing literature and research and held project workshops throughout the project lifetime to reveal current understanding of the focal species distribution. A significant portion of the project resources were used in the collation of fisheries and ocean data to enable this investigation to be done. We initially applied habitat models that had been developed in other marine domains to test how well these models performed in our system. After this assessment we focused our efforts on applying the best model from this initial process to the wider domain and for all five species. We also investigated a new time-series modelling framework that allowed us to include environmental information from both the region being investigated and also including time lagged environmental data from neighbouring regions to assess influence of conditions in one region on an adjacent region in the

future. All of these models were subsequently run using oceanographic input variables that can be forecast, and the results presented as example forecast case studies.

### Key Findings

A key finding of the project was that sub-surface ocean state variables are important in explaining the variance in catch. Previous work has focused on surface variables, as these are ones that have historically been available in seasonal models and models such as IPCC climate models. Modern forecast systems, however, allow us to assess sub-surface variables, and revealed their importance for these target species and as a focus for future work.

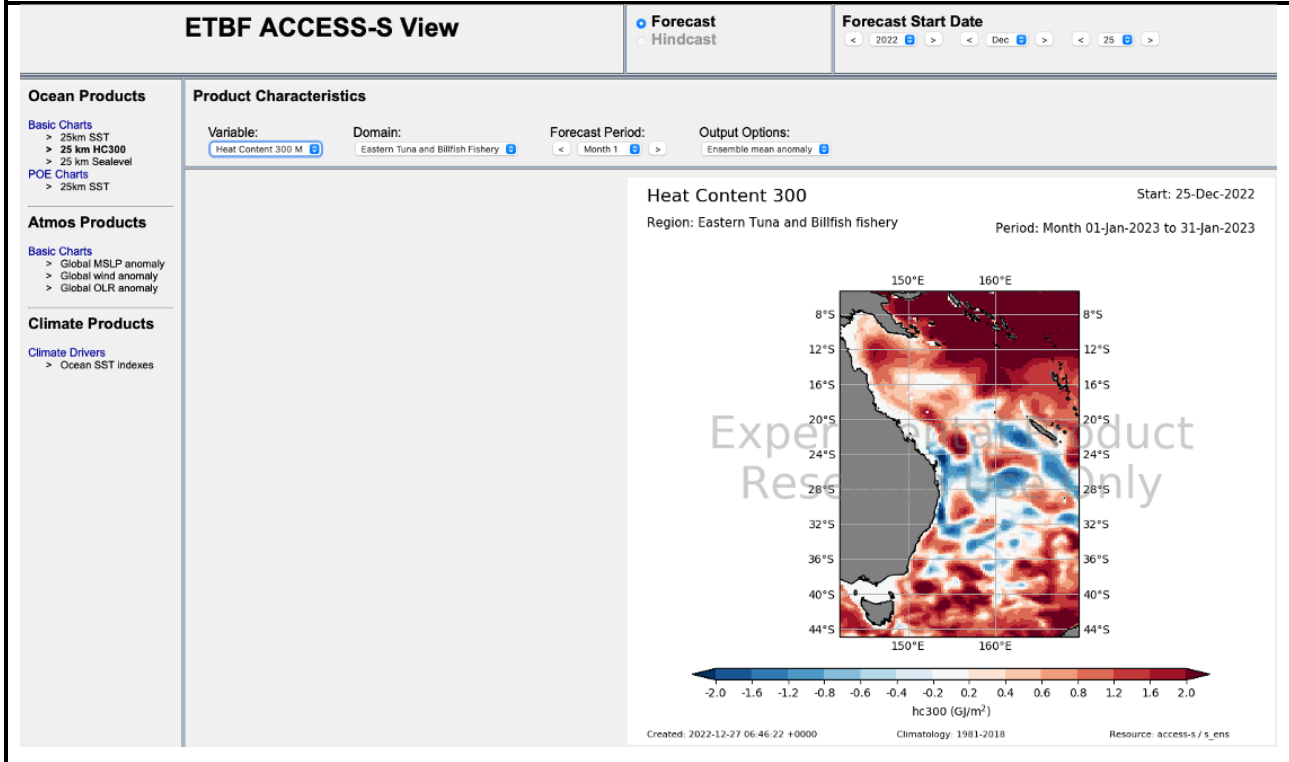
The figure below is taken from Figure 63 (a) in the main report and shows the relative contributions and the variation of each of the oceanographic variables included in the yellowfin tuna (YFT) model for the different study regions. Variables to note are heat content in the upper 300m (hc300), mixed layer depth (mld1) and temperature at 500m (temp500) which are all sub-surface oceanographic variables. The regions on the x-axis are the divisions of the study area: all regions (all); East Australian Current dominated (eac); Coral Sea (cs), Western Central Pacific (wcp) and New Zealand (nz).



A key output from this project is an analysis-ready dataset for use in ongoing scientific investigation, and will be made accessible for management. Additionally, two dedicated websites for real time forecasts of ocean state have been provisioned. The first is a project webpage, hosted by the Bureau of Meteorology, providing seasonal forecasts of ocean state (<http://poama.bom.gov.au/project/etbf/index.html>, Box 1), and the second is a dedicated project page where case studies of habitat model forecasts and project outputs will be located (<http://www.cmar.csiro.au/etbf-oceanographic-influences/index.html>).

Box 1: Example of Forecast Visualisation Tool and how to use it.

1. Choose the Forecast Start Date
2. Select the Basic Chart to view
3. Choose the Domain from the list defined
4. Select the appropriate forecast period (e.g. week 1 and 2, month 1, ...)



### Implications for relevant stakeholders

The outcomes of this work will have utility for fisheries stock assessments and management in the face of climate change. It is expected that as the ocean continues to warm, and fish distributions change, there will be a need to use environmental nowcasts and forecasts to aid support sustainable harvest and management and inform the debate about spatial management tools such as static and dynamic protected areas.

Ongoing provision of environmental status reports and forecasts (situational reports) will be useful for managers involved in natural resource management in a changing environment.

### Recommendations

Based on continual project engagement with end users over four years, there is clear interest and need for continued and improved delivery of oceanographic information and insight to Australian fisheries management and industry. During the evolution of this project, the team has worked closely with Bureau of Meteorology staff and CSIRO oceanographers to incorporate the various reanalysis and forecast products into our work. The outputs of the modelling work show that primary (e.g. temperature at 500m) and derived (depth of the 20°C isotherm, heat content in the upper 300m, and mixed layer depth) sub-surface oceanographic variables are important, and yet these are limited in their availability to be forecast. Many of these variables are yet to be fully assessed for forecast skill (a measure of accuracy), and when this has been done, efforts to make these available should be pursued.

The analysis-ready datasets produced by this project should be considered in the regular workflow of the TTRAG for use in standardising CPUE and providing updates of current ocean state.

Engagement with the Bureau of Meteorology should be continued to promote the ongoing development of operational systems, and the continued provision and assessment of additional ocean variables (that include the sub-surface variables of interest).

A substantial limitation in assessing the environmental influence on tuna and billfish availability in the ETBF and surrounding regions is the limited or absent fishery independent data such as that obtained from electronic tags. Targeted studies of species of interest in the Australian region are needed to explore the influences in more detail. Catch data are clearly influenced by decisions made by fishers and managers, primarily to do with economics (e.g., distance from port, market price or demand), or harvest controls, which confound the ocean influences on fish distribution.

**Keywords**

Habitat modelling, tropical tuna, data assimilation, forecasting, ACCESS-S, CAFE60.

# Introduction

There is an ongoing need for the AFMA, its advisory committees and the ETBF industry to gain a much stronger understanding of past, current and potential future oceanographic and environmental impacts upon (i) the spatial and temporal distribution and level of ETBF catches, catch rates, fishing effort and fish sizes (particularly those indicators used in the ETBF harvest strategy), and (ii) the interactions between focal species in the ETBF with domestic (e.g. recreational) and international fisheries. Using established relationships with regional partners, which allowed comprehensive collation of catch and effort (and investigation of tracking) data for the focal species, habitat models for the whole region were developed.

The abundance and distribution and hence availability of highly migratory tuna and billfish species to fisheries are known to be strongly influenced by oceanographic conditions. The five target species of the ETBF have a wide distribution outside the Australian EEZ, but the influence of oceanographic factors within the ETBF fishery region and the surrounding south-west Pacific region is poorly understood, creating uncertainty in current management arrangements. The waters off the east coast of Australia are also experiencing rapid climate change (Hobday and Pecl 2014), with range expansion already observed for many coastal and pelagic fish species (Last et al 2011; Sunday et al 2016). Changes in distribution over the century are also projected for the key ETBF species in eastern Australia (Hobday 2010; Hartog et al 2011; Dell et al, 2015; Robinson et al, 2015) and the wider Pacific (e.g. albacore, Lehodey et al. 2015).

Habitat models and seasonal forecasting approaches have been developed and used for a range of species, including southern bluefin tuna in eastern Australia (Hobday et al 2011), the Great Australia Bight (Eveson et al 2015) and various applications globally (Muhling et al 2017, Scales et al 2017, Tommasi et al 2017). These approaches have been built upon in this project and modified to use the Bureau of Meteorology's ACCESS-S2 model (Australian examples having previously used the Bureau of Meteorology's POAMA model (Hobday et al. 2016; Hobday et al. 2018).

The project team undertook an examination of existing literature and research and held project workshops throughout the project lifetime to aid current understanding of the focal species' distribution. A significant portion of the project resources were used in the collation of fisheries and ocean data to enable this investigation to be done. We initially applied habitat models that had been developed in other marine domains to test how well these models performed in our system. After this assessment we focused our efforts on applying the best model from this initial process to the wider domain and for all five species. We also investigated a new time-series modelling framework that allowed us to include environmental data from the region being investigated as well as time-lagged environmental data from neighbouring regions to assess influence of conditions in one region on an adjacent region in the future. These models were run using input variables that can be forecast, and used to generate example forecast case studies.

# Objectives

The objectives of the project and how they have been addressed in this project are outlined below:

	<b>Objective</b>	<b>Section where addressed</b>
1	Enhance AFMA and industry understanding of influence of climate-ocean system drivers upon the spatial and temporal variability of key ETBF species.	<ul style="list-style-type: none"> <li>• Section 1: Local and Regional Fishery Data</li> <li>• Section 2: State-of-the-art estimates of ocean state</li> <li>• Section 3 and Section 5: Habitat modelling sections</li> </ul>
2	Develop and deliver predictive models at seasonal and decadal time scales to assist management and industry planning	<ul style="list-style-type: none"> <li>• Section 3: Initial Habitat Modelling</li> <li>• Section 5.2: BRT using CAFE60</li> <li>• Section 5.3: BRT using ACCESS-S2</li> <li>• Section 8: Categorical approach to prediction of CPUE based on ACCESS-S2 output</li> </ul>
3	Provide operational forecasts of habitat distribution for Australia and the regional partners within the life of the project	<ul style="list-style-type: none"> <li>• Section 7: Projecting future patterns – seasonal and decadal forecasts</li> <li>• Provided at project websites:               <ul style="list-style-type: none"> <li>○ <a href="http://poama.bom.gov.au/project/etbf/index.html">http://poama.bom.gov.au/project/etbf/index.html</a></li> <li>○ <a href="http://www.cmar.csiro.au/etbf-oceanographic-influences/index.html">http://www.cmar.csiro.au/etbf-oceanographic-influences/index.html</a></li> </ul> </li> <li>• Article written for               <ul style="list-style-type: none"> <li>○ <a href="https://coastfish.spc.int/en/publications/bulletins/fisheries-newsletter">https://coastfish.spc.int/en/publications/bulletins/fisheries-newsletter</a></li> </ul> </li> </ul>
4	Inform harvest and allocation discussions at national and international scales	<ul style="list-style-type: none"> <li>• Results sections</li> <li>• Discussion and Conclusion</li> <li>• Executive Summary</li> </ul>

# 1 Local and Regional Fishery Data

Catch and effort data from 13 nations and territories across the South-West Pacific region (Cook Islands; French Polynesia; New Caledonia; New Zealand; Norfolk Island; Samoa; Solomon Islands; Tokelau; Tonga; Tuvalu; Vanuatu; Fiji and Australia) were provided by the Western and Central Pacific Fisheries Commission (WCPFC) and Australian Fisheries Management Authority (AFMA) for the five target species in the Eastern Tuna and Billfish Fishery (ETBF). The data for these species (Bigeye Tuna, *Thunnus obesus*; Yellowfin Tuna, *Thunnus albacares*; Albacore, *Thunnus alalunga*; Striped Marlin, *Kajikia audax*; Broadbill Swordfish, *Xiphias gladius*) were provided in a summarised form by month and spatial grid cell from 1990 to 2020, using both a 1°x1° and 0.25°x0.25° grid (noting that the data for New Zealand were only available at the coarser 1°x1° resolution).

Background information on the nature of the fishery from a domestic and international perspective can be found in the supplementary material to this report and further information on the ETBF can be also found at the AFMA website<sup>1</sup>. These both provide context to much of the work to follow.

Figure 1 to Figure 5 illustrate the general decline in longline CPUE from 2000 – 2008/9 for the focal species and the stabilisation from that point on. In the latter sections of the report, we focus on the more stable period from 2008 onwards. The regions shown (EAC, WCP, Coral Sea and NZ) are defined and the rationale for choosing them are shown in section 4.

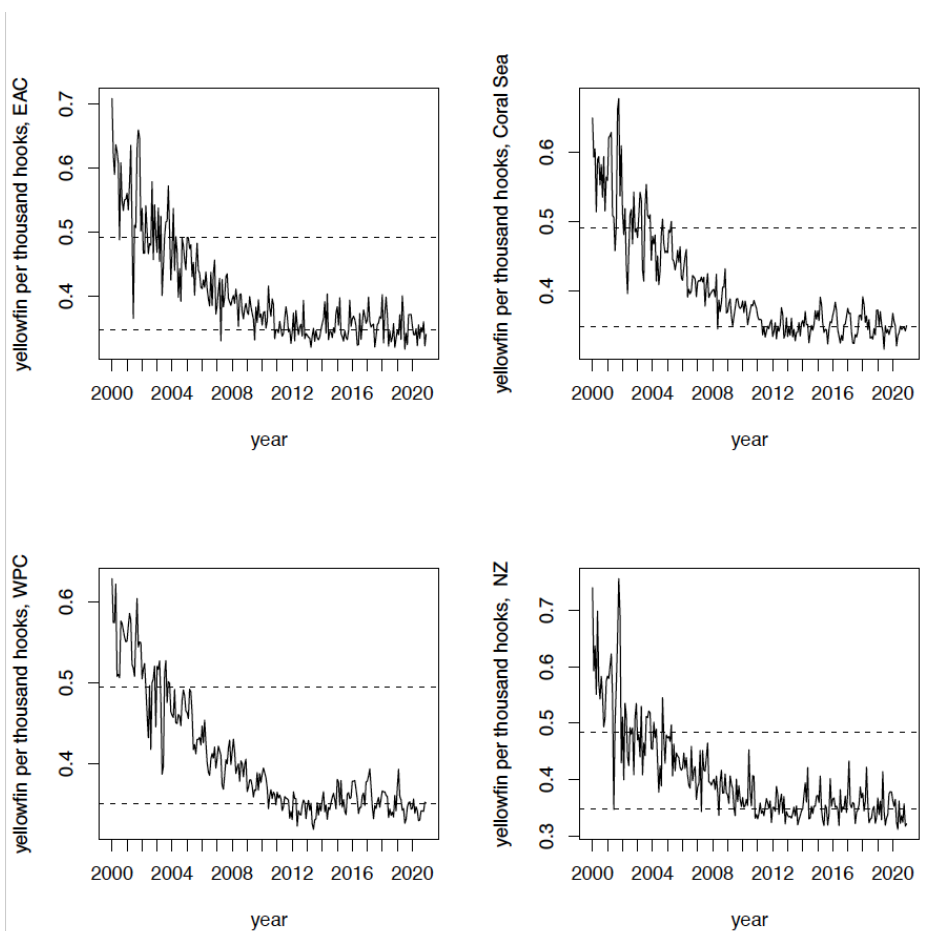


Figure 1: Yellowfin CPUE for the 4 regions in the study area. The dotted lines show the 25<sup>th</sup> and 85<sup>th</sup> percentiles of CPUE.

<sup>1</sup> <https://www.afma.gov.au/fisheries/eastern-tuna-and-billfish-fishery-page>

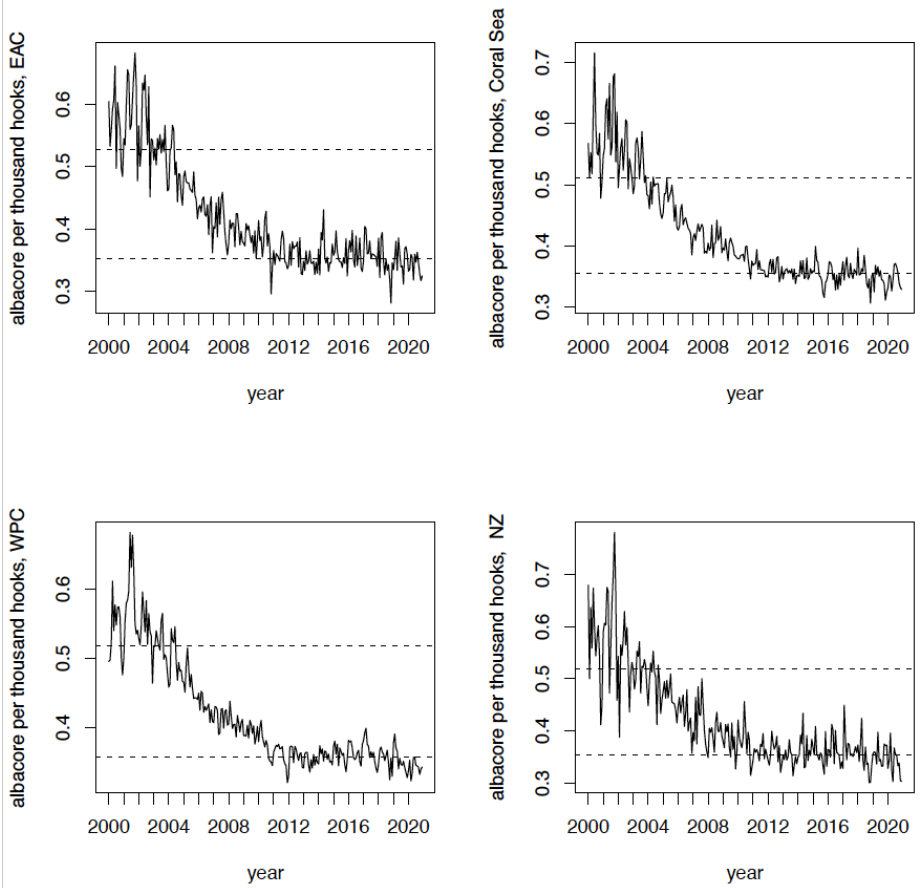


Figure 2: Albacore CPUE for the 4 regions in the study area. The dotted lines show the 25th and 85th percentiles of CPUE.

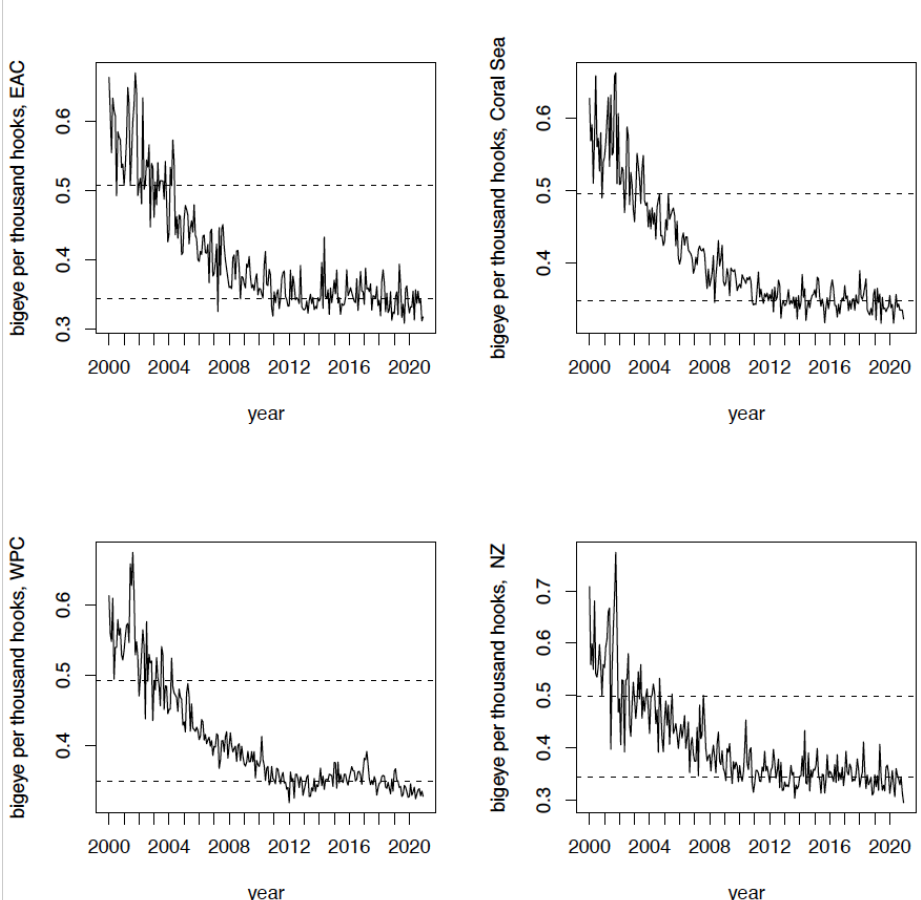


Figure 3: Bigeye CPUE for the 4 regions in the study area. The dotted lines show the 25th and 85th percentiles of CPUE.

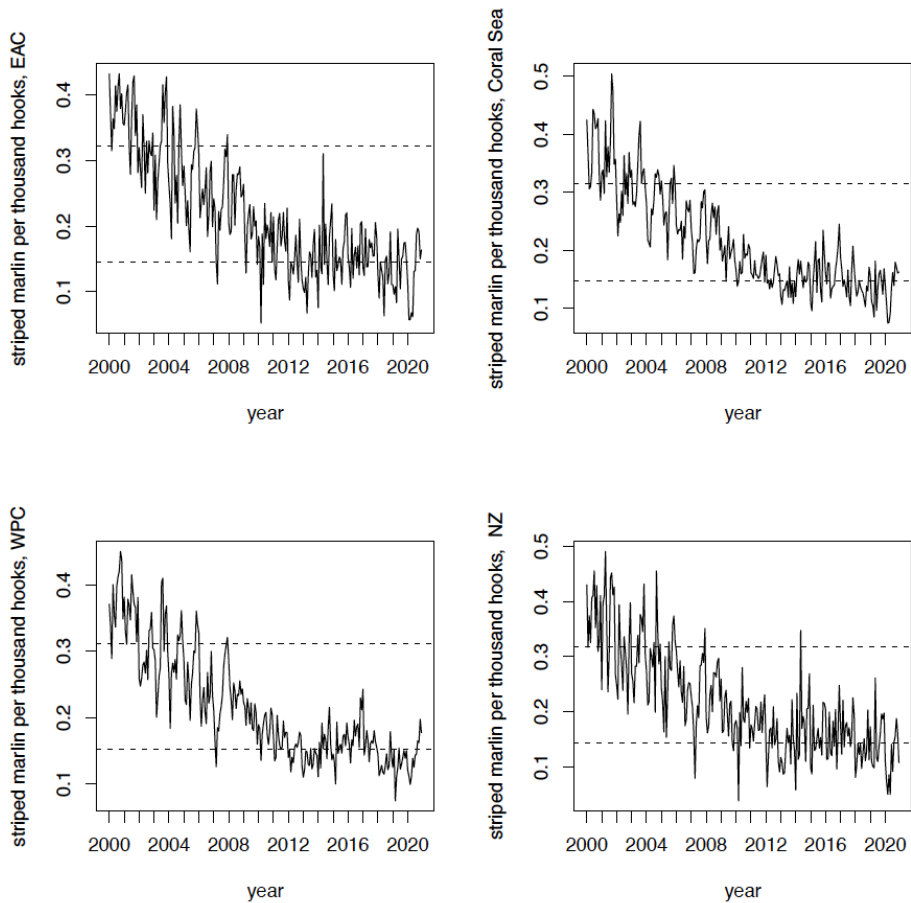


Figure 4: Striped Marlin CPUE for the 4 regions in the study area. The dotted lines show the 25th and 85th percentiles of CPUE.

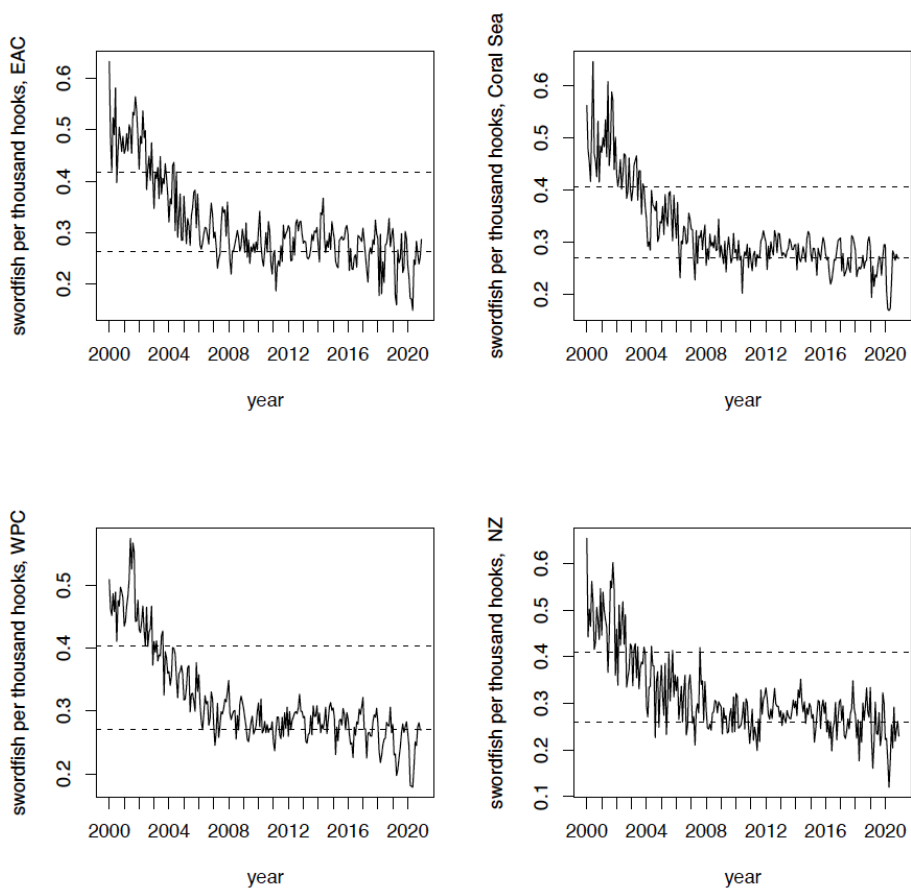


Figure 5: Swordfish CPUE for the 4 regions in the study area. The dotted lines show the 25th and 85th percentiles of CPUE.

## 2 State-of-the-art estimates of ocean state

Our modelling efforts start with estimates of the historical ocean state from two recently released coupled ocean-atmosphere retrospective analysis models. These are both large national scientific efforts requiring significant computational resources and technical teams.

### 2.1 CAFE60

The CSIRO Climate retrospective Analysis and Forecast Ensemble system (CAFE60) provides a large ensemble retrospective analysis of the global climate system from 1960 through 2020. Using an ensemble Kalman filter approach, 96 climate state estimates are generated over the most recent six decades. For the purposes of this project, we have focused on 2008-2020 as the accuracy of any climate reanalysis can be particularly hard to assess (Saha et al. , 2010) prior to the advent of millions of new temperature-salinity subsurface observations from the global array of Argo profiling floats (Wong et al, 2020).

The CAFE60 state estimates are constrained by monthly mean ocean, atmosphere, and sea ice observations, providing a comprehensive climate data resource for studying internal climate variability and predictability in the upper ocean ( O’Kane et al 2021a, O’Kane et al 2021b). In the ocean, satellite (altimetry, sea surface temperature, sea ice concentration) and observed in-situ ocean temperature and salinity profiles are directly assimilated.

The CAFE60 climate model configuration is based on the Geophysical Fluid Dynamics Laboratory’s (GFDL) Climate Model 2.1 (CM2.1) (Delworth et al. 2006). The ocean model configuration uses the 1° ocean grid as described by Bi et al. (2013). The ocean model is coupled to the land, atmospheric and sea ice components from CM2.1, namely, Land Model 2 (LM2), Atmospheric Model 2 (AM2) and Sea Ice Simulator (SIS) respectively. The nominal resolution of the Modular Ocean Model (MOMv4.1) ocean component is 1°, with extra latitudinal resolution in the tropics, 0.33° at the equator, with extra horizontal resolution in the Southern Ocean, corresponding to 0.25° at 75° S. There are 50 vertical levels, with a 10m resolution in the upper ocean, increasing to roughly 300m at depth.

Ocean subgrid processes are adopted from CM2.1, including neutral physics, Brian-Lewis vertical mixing profile, Lagrangian friction scheme and a K-profile parameterisation for the mixed layer calculation. Biases in the mode water structure and deep open ocean convection are reduced by restoring the ocean temperature and salinity below 2000 m to climatology based on World Ocean Atlas observations with a 1-year timescale. Deep restoring further accounts for the poor coverage of in-situ ocean observations that exists throughout the record.

The CAFE60 reanalysis provides historical estimates of the ocean environmental state that defines the structure of the upper water column where ETBF target species spawn, live, and feed.

### 2.2 ACCESS-S

ACCESS-S (Australian Community Climate and Earth-System Simulator-Seasonal) is the Bureau of Meteorology’s coupled ocean-atmosphere seasonal prediction system. It is based on based on the UK Met Office’s global coupled model seasonal forecast system (GloSea5; MacLachlan et al. 2015) and uses the Global Coupled model configuration version 2 (GC2; Williams et al. 2015). ACCESS-S1 (version 1) was operationalised in August 2018 and then was upgraded to ACCESS-S2 (version 2) in October 2021. The model configuration, generation of initial conditions, ensemble generation, and

hindcast performance of ACCESS-S1 is described in Hudson et al (2017), with details of improvements in ACCESS-S2 in Wedd et al (2022).

The ocean model is the Nucleus for European Modelling of the Ocean (NEMO) community model (Madec and NEMO team, 2012), which has an approximate horizontal resolution of 25 x 25 km in the Australian region. There are 75 depth layers, with the top 1-metre layer representing sea surface temperature (SST). Ocean model initial conditions are created using a new weakly coupled data assimilation scheme, which assimilates in situ ocean observations and satellite sea surface temperature data (see Wedd et al. 2022). The resulting gridded ocean data reanalysis was used in this study to provide input subsurface data for training models.

A set of retrospective forecasts (hindcasts) were run using ACCESS-S2 for the period 1982-2018. Three forecasts were run out to 5 months into the future (i.e., lead time 0 – 4 months) on the 1<sup>st</sup> of each month in the period. Three additional forecasts were also run on each of the eight days prior to the 1<sup>st</sup> (giving a total of 9 days) to arrive at a 27-member ensemble forecast for each month. These ensemble forecasts were then averaged to give an ensemble mean for each month being forecast. Anomalies were calculated by removing the monthly model climatologies at each lead time, calculated using the hindcast dataset (see Smith and Spillman 2019).

A skill assessment of ACCESS-S2 is being prepared (Spillman et al, in prep), and will be also made available on the project website.

Table 1- available ocean environmental variable from retrospective analyses

Reanalysis model	Product	Description
<b>CAFE60 variable</b>	sss	Sea Surface Salinity (PSU)
	sst	Sea Surface Temperature (°C)
	temp50	Seawater Potential Temperature at 50m (°C)
	temp100	Seawater Potential Temperature at 100m (°C)
	temp200	Seawater Potential Temperature at 200m (°C)
	temp500	Seawater Potential Temperature at 500m (°C)
	u100	x velocity at 100m (m/s)
	v100	y velocity at 100m (m/s)
	mld	Mixed layer depth (m)
	<b>CAFE60 derived variable</b>	u100_300
v100_300		y velocity depth weighted mean over 100 - 300m (m/s)
D20		Depth of the 20C isotherm (m)
eke300		Eddy kinetic energy depth weighted sum over upper 300 m (cm <sup>2</sup> /s <sup>2</sup> )
eke2000		Eddy kinetic energy depth weighted sum over upper 2000 m (cm <sup>2</sup> /s <sup>2</sup> )
hc200		Heat content upper 200 m (J/m <sup>2</sup> )
hc300		Heat content upper 300 m (J/m <sup>2</sup> )

<b>ACCESS-S2 variable</b>	sss	Sea Surface Salinity (PSU)
	sst	Sea Surface Temperature (°C)
	temp50	Seawater Potential Temperature at 50m (°C)
	temp100	Seawater Potential Temperature at 100m (°C)
	temp200	Seawater Potential Temperature at 200m (°C)
	temp500	Seawater Potential Temperature at 500m (°C)
	u100	x velocity at 100m (m/s)
	v100	y velocity at 100m (m/s)
	D20	Depth of the 20C isotherm (m)
	hc300	Heat content upper 300 m (J/m <sup>2</sup> )
	td	Thermocline Depth (m)
	ssh	Sea Surface Height (m)
	mld1	Kara Mixed Layer Depth (m)
	mld2	Mixed Layer Depth 0.01 (m)
<b>ACCESS-S2 derived variable</b>	eke300	Eddy kinetic energy depth weighted sum over upper 300 m (cm <sup>2</sup> /s <sup>2</sup> )
	eke2000	Eddy kinetic energy depth weighted sum over upper 2000 m (cm <sup>2</sup> /s <sup>2</sup> )
	u100_300	x velocity depth weighted mean over 100 - 300m (m/s)
	v100_300	y velocity depth weighted mean over 100 - 300m (m/s)

## 2.3 From coupled climate model output to analysis ready data (ARD) for fisheries applications.

Both CAFE60 and ACCESS-S2 modelling is done on national supercomputing resources and are typically delivered as a reduced set of model variables across many thousands of individual files in multi-dimensional self-describing NetCDF format. These datasets are large (up to many 10's of terabytes), require specialist tools, and come with significant challenges in terms of computer processing, quality control, and delivery that's ready for ecological applications.

Both CAFE60 and ACCESS-S2 retrospective analysis model output is available to researchers from Australia's National Computational Infrastructure (NCI) supercomputing centre in Canberra, ACT. To make the raw coupled climate model output into analysis ready data (ARD) requires several steps, including:

- **Generating Zarr collections:** Convert substantial number of raw NetCDF files into a single Zarr collection encompassing all variables required for fisheries modelling. This includes building boutique compatibility fixes that are typically required for datasets of this type. A well formatted Zarr collection allows for efficient and practical reduction of larger-than-memory datasets using state-of-the-art open-source coding tools, namely Pangeo (<https://github.com/pangeo-data>) style workflows.
- **Masking and region cropping:** Apply land masking where required and crop dataset regionally to reduce unnecessary processing cost.
- **Regridding:** Convert datasets onto a single common grid for analysis. Computationally expensive regridding is required for compatibility within and between datasets, especially with the staggered Arakawa grid systems commonly used in modelling the climate system.

Alignment with grid systems for fisheries observations is also done to better enable further analyses.

- **Derived variables:** Calculate derived ocean environmental variables from model outputs, combining all required products into a final single Zarr collection. Derived variables like eddy kinetic energy, not directly available from model outputs, enhance the interpretation and value of retrospective analysis products.
- **ARD file:** Run basic tests, formatting, and output final dataset in multi-dimensional or tabular formats required for ecological model analyses.

While model output at NCI is nominally available to partner research organisations and through research flagship allocation schemes, commercial and industry access options exist. We have provided links to open code repositories for both the CAFE60 (<https://github.com/Thomas-Moore-Creative/NCI-CAFE-ARD>) and ACCESS-S2 (<https://github.com/Thomas-Moore-Creative/NCI-ACCESS-S2-ARD>) ARD workflows to assist others making easier use of these retrospective analysis datasets.

### 3 Initial Habitat Modelling

The project plan was designed to deliver oceanographic insights and updates to management and industry in a phased approach. The initial focus was on applying existing habitat model approaches to the ETBF region using catch and effort data and to investigate the availability of electronic tagging datasets and their utility. Environmental datasets were obtained from a variety of sources (Appendix 1 - Table 1). Surface variables were obtained from global satellite data providers (SST - <https://www.ghrsst.org>, <https://www.psl.noaa.gov/data/gridded/data.noaa.oisst.v2.highres.html>; ocean productivity - SeaWIFs and <https://oceandata.sci.gsfc.nasa.gov>). Physical variables below the surface were provided by synTS, an output from the CSIRO Bluelink project (Ridgway et al. 2006).

During this initial period, requests for access to international catch and effort data were sent and support was obtained from regional partners allowing us to further investigate habitat models in domains other than the ETBF. An evaluation of the available electronic tagging data was also undertaken in this initial period and revealed that there were insufficient data in the region relevant to this project for any of the species of interest to pursue these data further.

After investigating different modelling approaches in this early stage, boosted regression trees (BRTs) were deemed to be most suitable, and the decision was made to apply these models to the wider domain and for all species helping us to meet Objectives 2 and 3, and providing information for Objectives 1 and 4.

# 4 Oceanographic background

## 4.1 Overview

El Niño-Southern Oscillation (ENSO) is the most prominent climate variability on interannual time scales. Every few years, the eastern and central tropical Pacific experiences ocean surface warming and weakening of trade winds during El Niño events, while the reverse situations happen during La Niña events. Although it originates in the tropical Pacific via strong air-sea coupling including Bjerknes feedback (Bjerknes, 1969), ENSO extends its influence beyond tropical Pacific via oceanic pathways as well as atmospheric teleconnections (Alexander et al. 2002; Timmerman et al. 2018). There is also an ENSO-like low-frequency climate variability mode in the Pacific on decadal to interdecadal time scales, i.e., the Pacific Decadal Oscillation (PDO; Mantua et al., 1997) or equivalently the Interdecadal Pacific Oscillation (IPO; Folland et al., 2002). The PDO can be regarded as a reddened response to ENSO, or a response to ENSO and atmospheric noise (e.g., Newman et al. 2016). The PDO/IPO and ENSO are highly correlated in the low (decadal period) frequency band (Newman et al., 2016).

The impacts of ENSO and PDO on ocean variables like sea level along the East Coast of Australia is not as strong as those along northern and western coasts of Australia (e.g., Zhang and Church 2012; Frankcombe et al. 2015), because there is no similar direct oceanic pathway via Indonesian Throughflow and coastally trapped waves (e.g., Feng et al. 2004). Holbrook et al. (2011) identified that the sea level in Sydney (Fort Denison) is not well correlated with the Southern Oscillation Index (SOI) at zero lag over the period 1914-2010, but is significantly correlated when lagged (both low-pass filtered with 5-yr running-mean filter), with maximum correlation of 0.54 at 3-year lag (Denison sea level lags the SOI). They also found the sea level anomalies at Fort Denison are highly correlated to baroclinic East Australia Current (EAC) transport anomalies across 33.5S (max correlation 0.58, at 9-mon lag), both of which are related to incoming westward-propagating Rossby waves, from both locally in the Tasman Sea and remotely from the interior of South Pacific (east of New Zealand). This can be favourably explained by the anticyclonic wind stress curl forcing tend to happen in the South Pacific Ocean interior during El Niño events. Similarly, Hill et al. (2008) also found the close connection between temperature and salinity in the Southeast coast of Australia (e.g., at Maria Island) and EAC extension strength for both long-term trends and decadal variability, which can be further linked to subtropical gyre circulation in response to wind stress forcing over a broader region of South Pacific.

The analysis of the time series data from Port Hacking and Maria Island shows that shifts in seasonal phytoplankton cycles along the southeast coast of Australia are likely driven by the increased southward extension of the EAC (Kelly et al., 2015). However, the changes in plankton biomass and primary production at Maria Island reflect a complex relationship between the EAC, its eddy field and subantarctic water masses, and the dynamics that drive the frontal interface between these water masses (Kelly et al., 2015). For the East Australian region, there is a poor correlation between seasonal phytoplankton anomalies and SOI. ENSO variability is not a significant driver of East Australian phytoplankton and marine primary productivity variability.

The Southern Annular Mode (SAM) describes the north–south movement of the westerly wind belt that circles Antarctica, with main impacts in the middle to higher latitudes of the southern hemisphere (e.g., Thompson and Wallace 2000). Because the SAM is mainly confined to middle-high latitudes, it should only affect southeast coast (rather than the whole east coast) of Australia, through adjustments in the ocean gyre circulation and western boundary currents in response to

SAM-related wind stress variability. However, some studies indicate that SAM doesn't play a significant role in climate variability in southeast coast of Australia (e.g., Francombe et al. 2015). For the seasonal anomaly in phytoplankton concentrations, there is a weak positive correlation between SAM index in the East Australian region. This correlation is strongest along the south coast but does extend into the Tasman Sea, and would produce a positive correlation between primary productivity and the SAM index.

## 4.2 Choice of study regions

The South-West Pacific domain was partitioned into four regional sub-domains based on the time-mean ratio of eddy kinetic energy to mean kinetic energy (EKE/MKE – Figure 6). This was generated from BRAN2020, an eddy-resolving, near-global reanalysis (Chamberlain et al., 2021), and used to identify boundaries between regions dominated more by mesoscale eddies than mean currents, and vice versa. By combining the EKE/MKE analysis with a geographical breakdown of Western & Central Pacific Fisheries Commission (WCPFC) nations, four key regions were identified, referred to here as EAC-dominated (EAC), Coral Sea and Equatorial (CS), Western-Central Pacific (WCP) and New Zealand (NZ) (Figure 7).

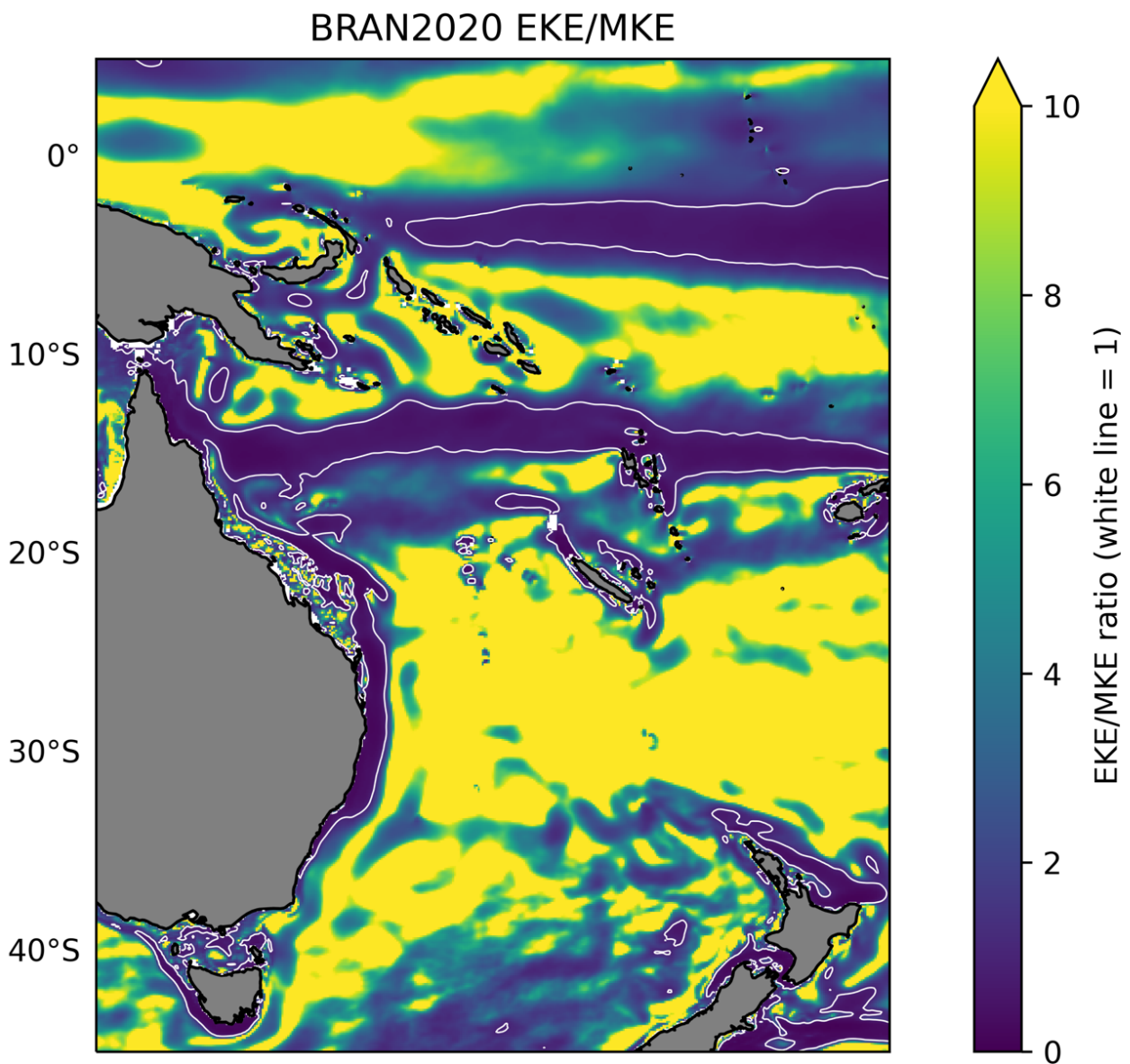


Figure 6 - Ratio of EKE to MKE.

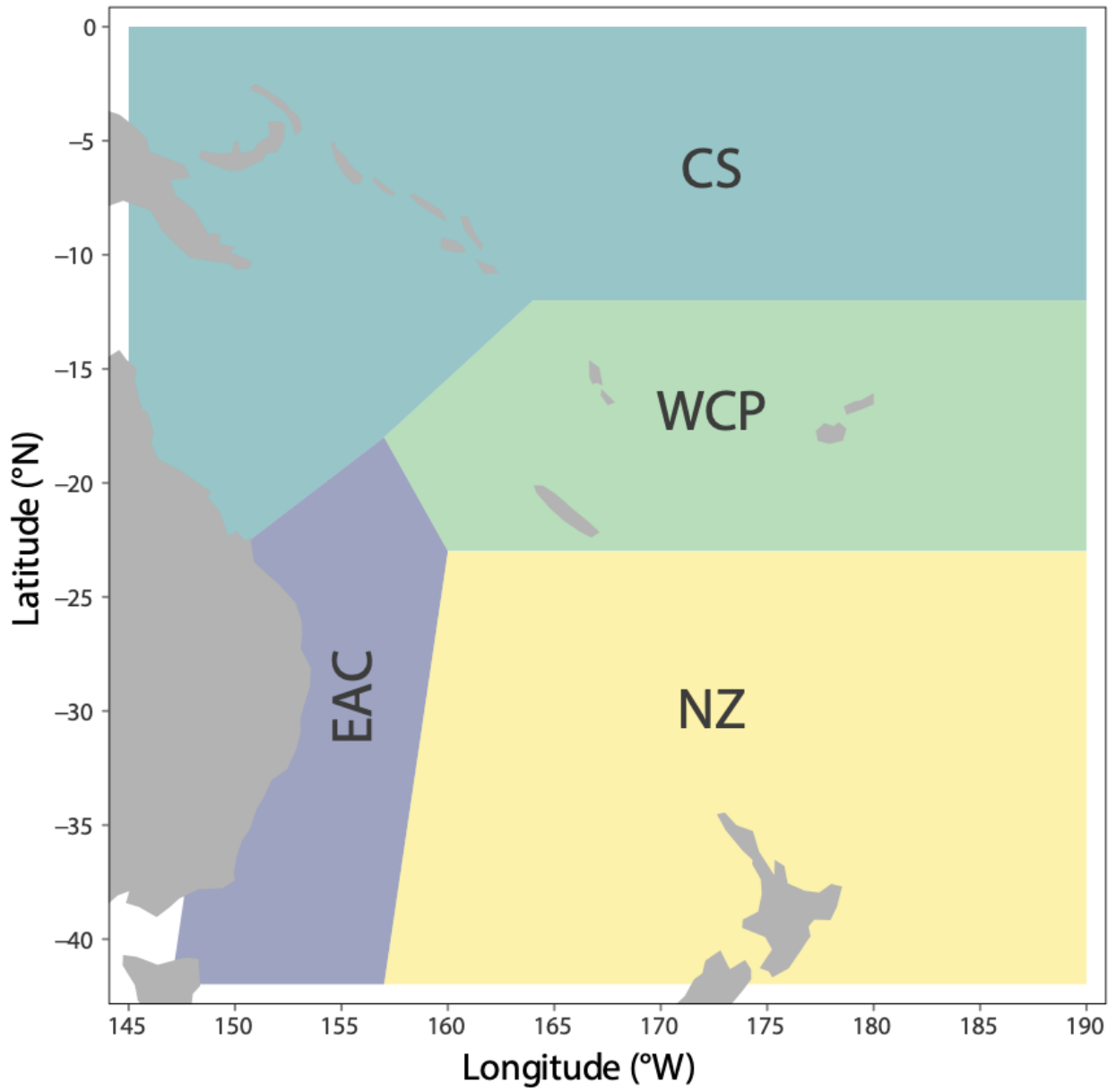


Figure 7 - Four key regions for analysis. EAC = EAC-dominated, CS = Coral Sea and Equatorial, WCP = Western-Central Pacific, NZ = New Zealand.

### 4.3 Catch heatmaps and events

In section 8, we define a categorical approach to investigating CPUE trends. This approach defines CPUE as being in one of three states (bad, medium or good), based on percentiles of the CPUE distribution (less than the 25<sup>th</sup>, between the 25<sup>th</sup> and 85<sup>th</sup>, and above the 85<sup>th</sup>) respectively. For a formal definition, see section 8.2.1. CPUE heat maps demonstrated a link to two of the larger events of the 2009 – 2020 period, namely the strong El Nino conditions in 2015 through early 2016 contrasted with long and strong La Nina conditions from late 2010 through early 2012 (Figure 8). Categorical CPUE heatmaps for YFT, BET, and ALB for the WCP region are shown (Figure 9, Figure 10, Figure 11).

In this region links between ENSO and mixed layer depth and the extent of the 20° isotherm and other measures of ocean heat may be a driver given the preferred temperature range of tuna species (Lehodey 2005).

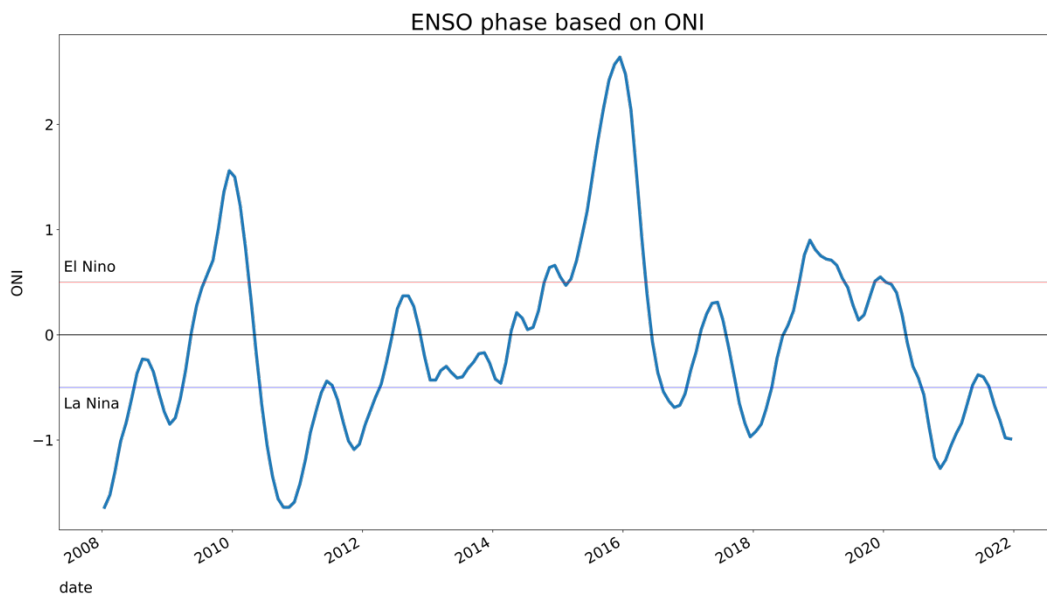


Figure 8: ENSO phase across period of study based on the Oceanic Niño Index (ONI)

(0)Bad-(1)Normal-(2)Good YFT CPUE for WCP islands region  
 (0-25% / 25-85% / 85-100%)

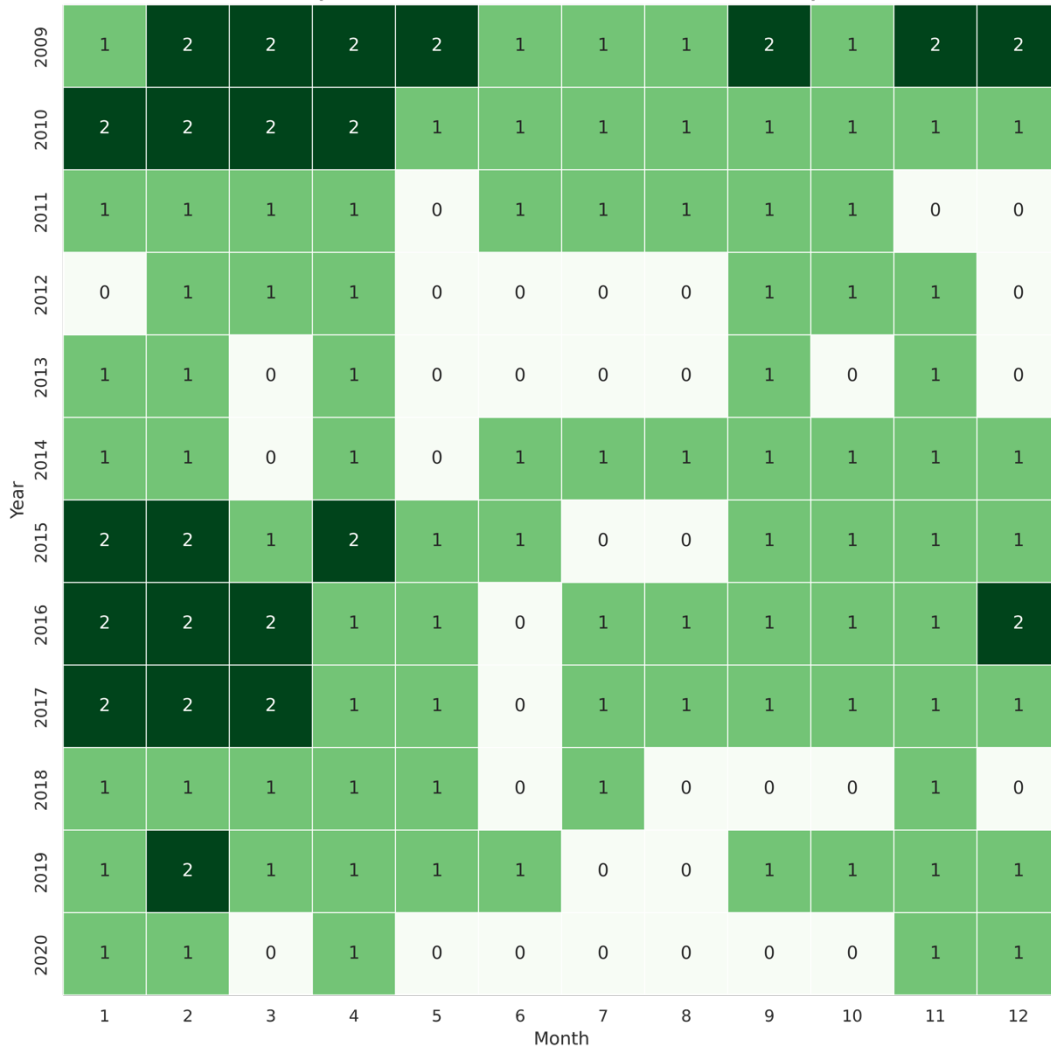


Figure 9: Heatmap of CPUE categorization for yellowfin tuna in the WCP region

(0)Bad-(1)Normal-(2)Good BET CPUE for WCP islands region  
(0-25% / 25-85% / 85-100%)

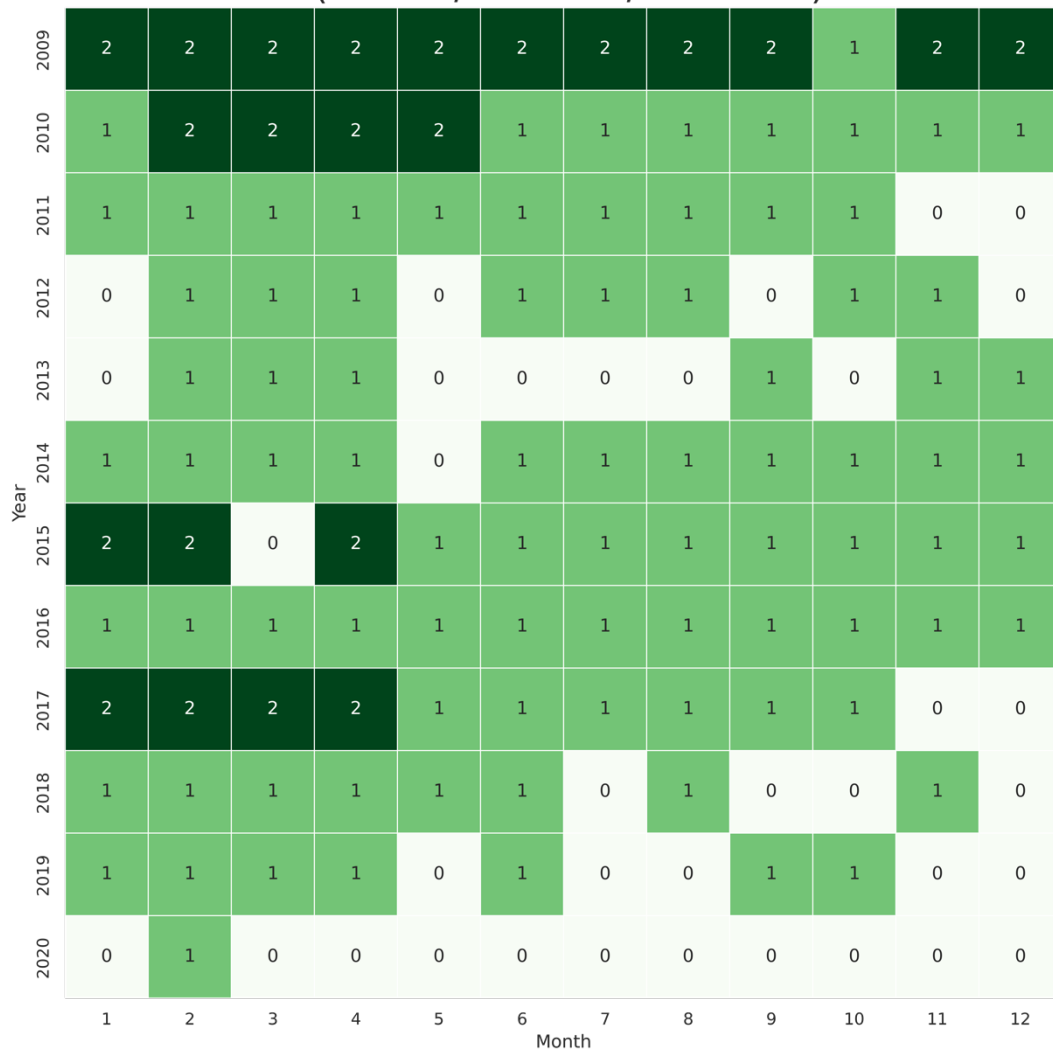


Figure 10: Heatmap of CPUE categorization for bigeye tuna in the WCP region

(0)Bad-(1)Normal-(2)Good ALB CPUE for WCP islands region  
(0-25% / 25-85% / 85-100%)

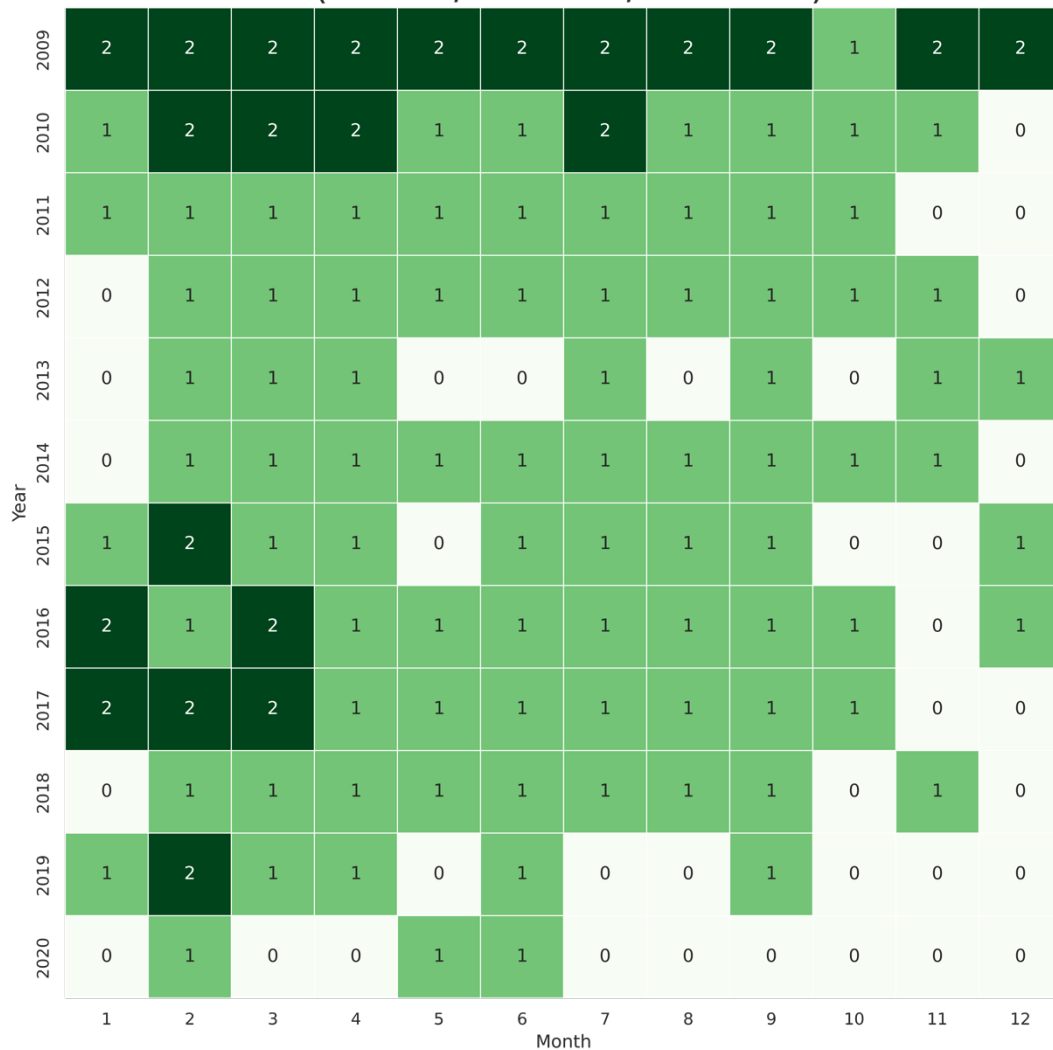


Figure 11: Heatmap of CPUE categorization for albacore in the WCP region

Examining timeseries of ENSO phase based on the Oceanic Nino Index (ONI) against CPUE categories for tuna species (Figure 12 - Figure 14) and STM (Figure 15) in the WCP, we see some relationship between the category of catch state and ENSO phase. For species like SWO, with less restriction to upper ocean and mixed layer, this relationship is less clear (Figure 16). Outside of the WCP, for example in the EAC region (Figure 17), even YFT show little relationship to ENSO phase, possibly due to the weaker links between east coast ocean dynamics and ENSO variability.

ENSO phase based on ONI  
vs  
YFT catch state in WCP  
bad(0) - normal(1) - good(2)

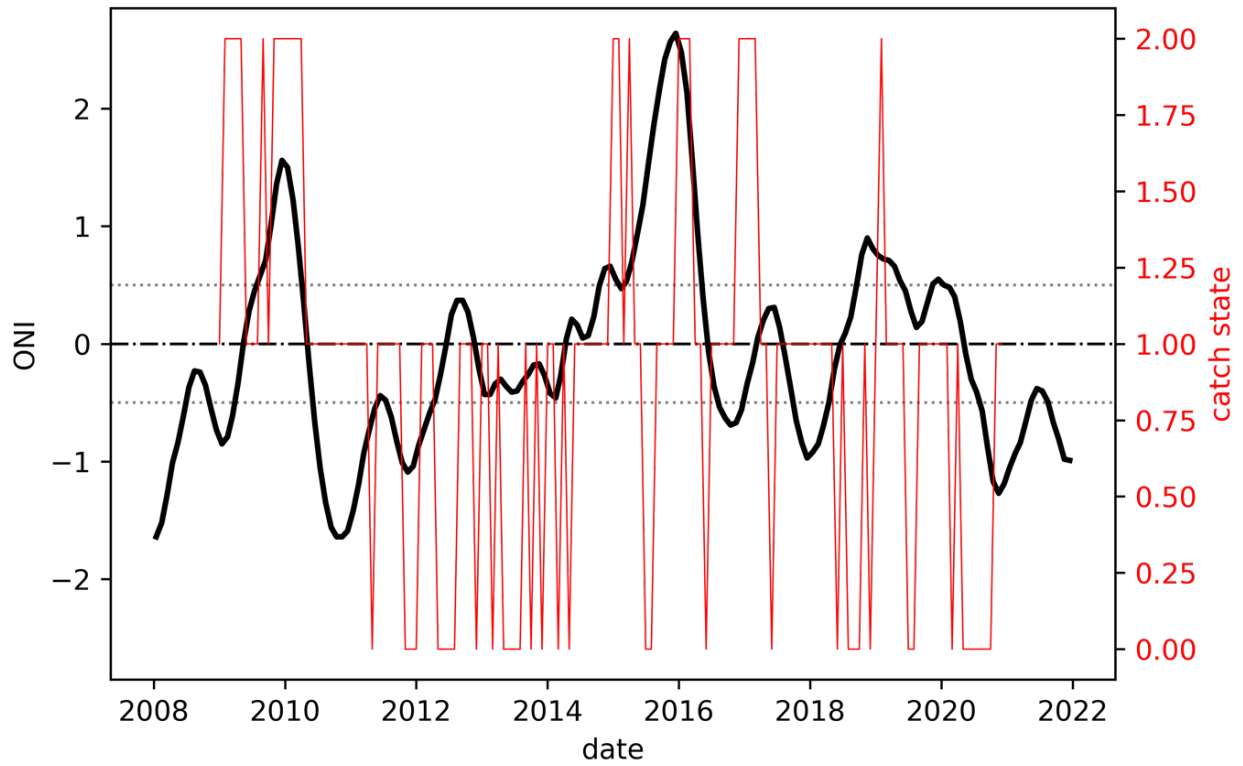


Figure 12: ENSO phase based on the Oceanic Niño Index (ONI) vs catch state ( "Bad"(0), "Normal"(1), "Good"(2) ) for yellowfin tuna in the WCP region.

ENSO phase based on ONI  
vs  
BET catch state in WCP  
bad(0) - normal(1) - good(2)

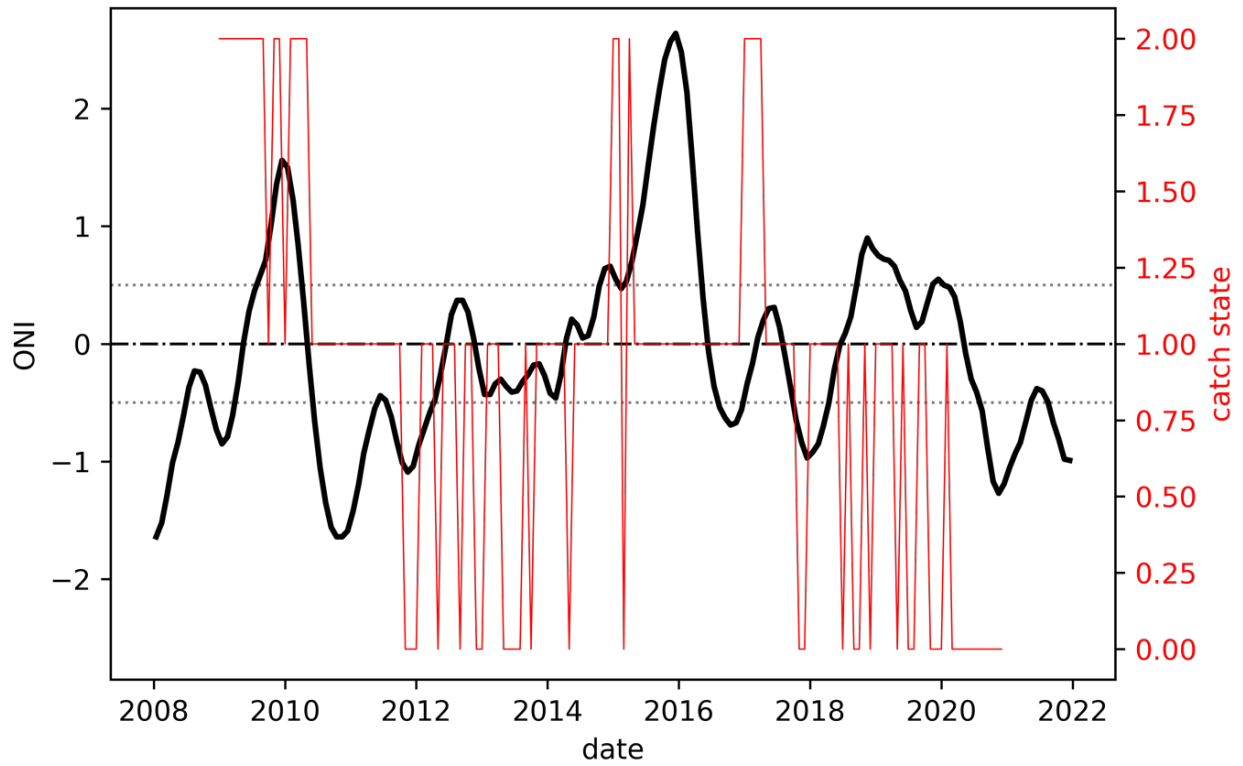


Figure 13: ENSO phase based on the Oceanic Niño Index (ONI) vs catch state ( "Bad"(0), "Normal"(1), "Good"(2) ) for bigeye tuna in the WCP region

ENSO phase based on ONI  
vs  
ALB catch state in WCP  
bad(0) - normal(1) - good(2)

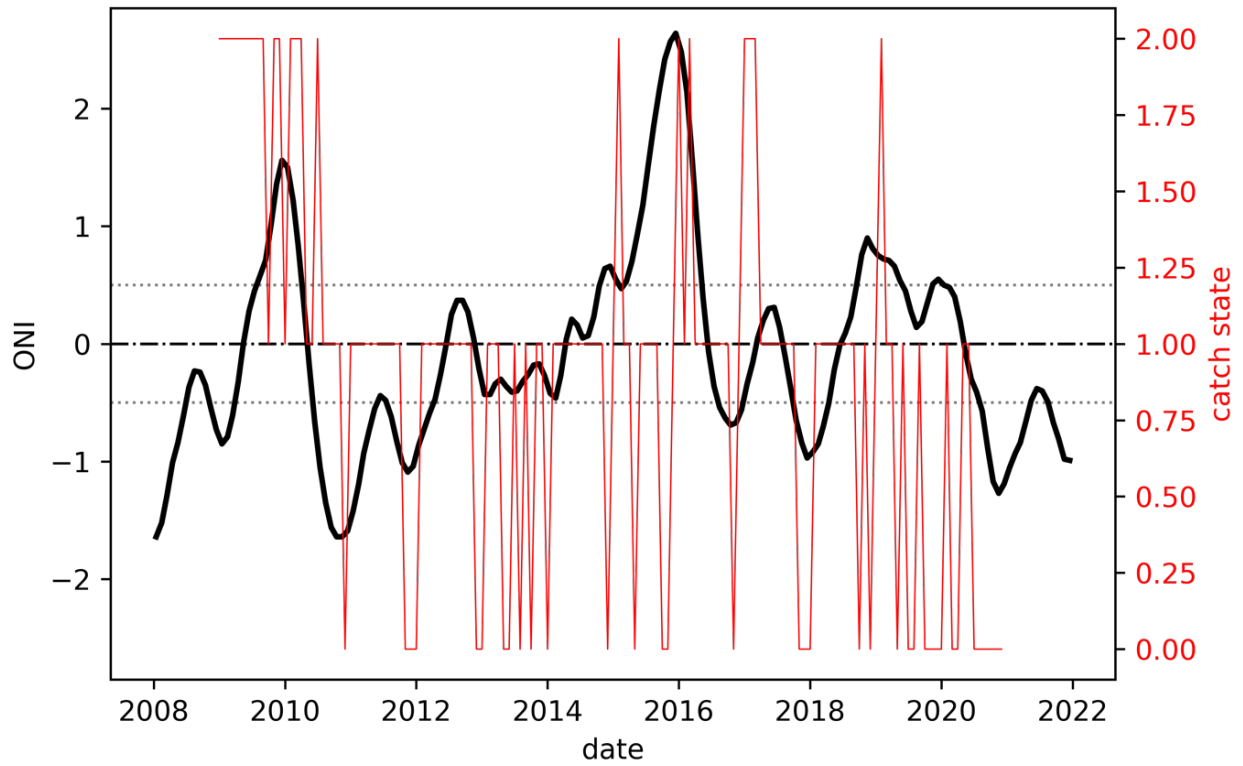


Figure 14: ENSO phase based on the Oceanic Niño Index (ONI) vs catch state ( "Bad"(0), "Normal"(1), "Good"(2) ) for albacore tuna in the WCP region

ENSO phase based on ONI  
vs  
STM catch state in WCP  
bad(0) - normal(1) - good(2)

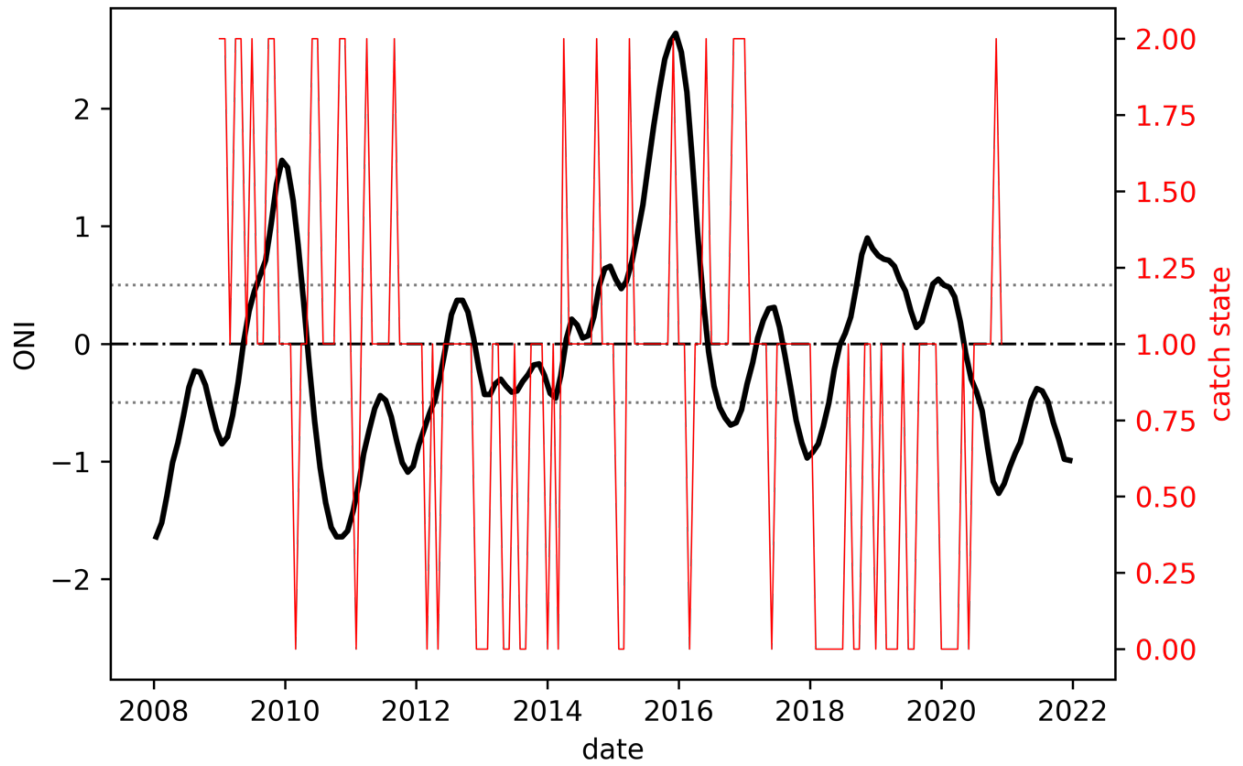


Figure 15: ENSO phase based on the Oceanic Niño Index (ONI) vs catch state ( "Bad"(0), "Normal"(1), "Good"(2) ) for striped marlin in the WCP region

ENSO phase based on ONI  
vs  
SWO catch state in WCP  
bad(0) - normal(1) - good(2)

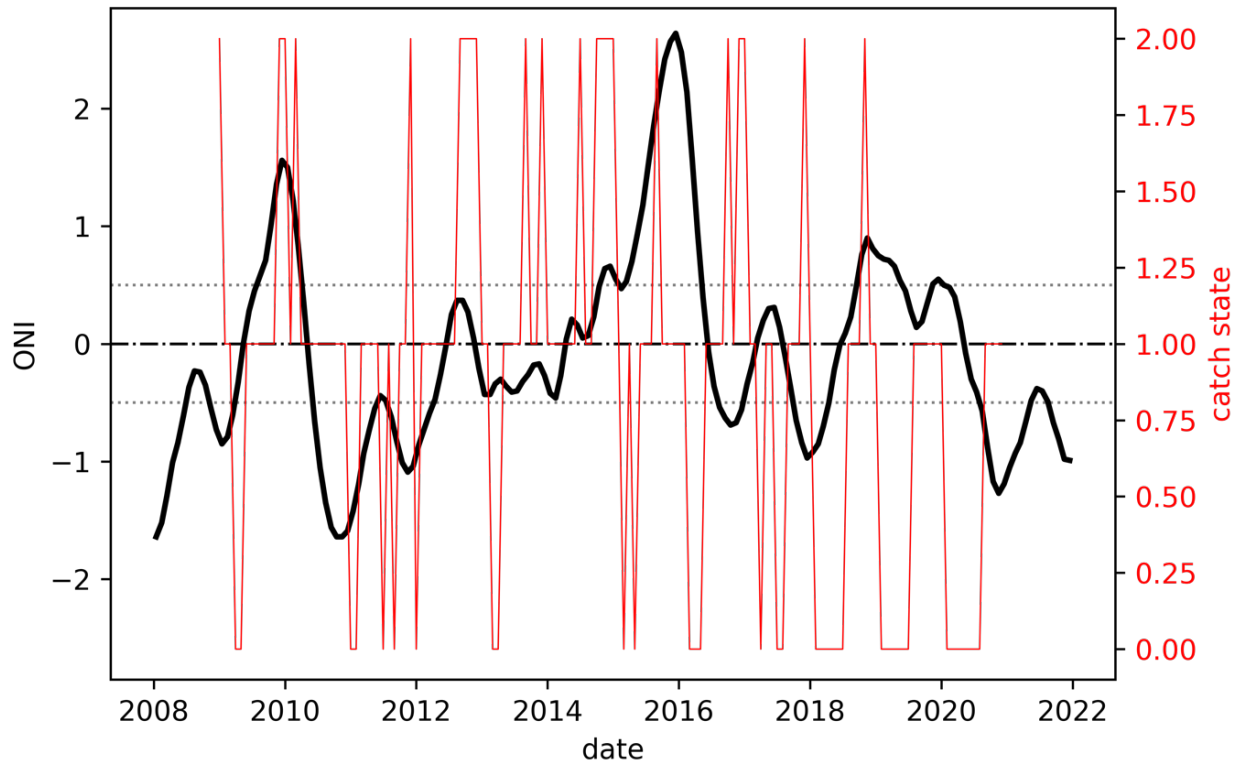


Figure 16: ENSO phase based on the Oceanic Niño Index (ONI) vs catch state ( "Bad"(0), "Normal"(1), "Good"(2) ) for swordfish in the WCP region

ENSO phase based on ONI  
vs  
YFT catch state in EAC  
bad(0) - normal(1) - good(2)

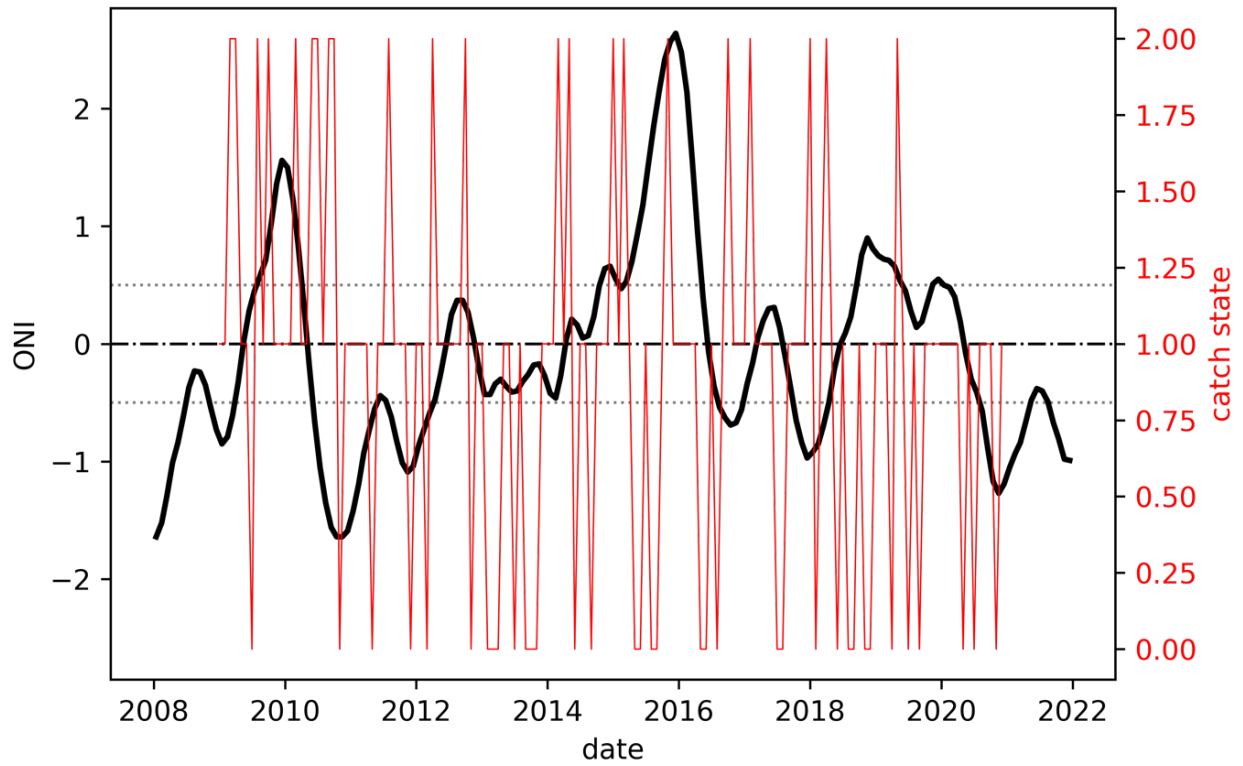


Figure 17: ENSO phase based on the Oceanic Niño Index (ONI) vs catch state ( "Bad"(0), "Normal"(1), "Good"(2) ) for yellowfin tuna in the EAC region

## **4.4 Event case studies**

In this section we first show the overall climatology of regional oceanographic environmental variables available from the BoM's ACCESS-S2 reanalysis product. We then examine the two major ENSO events in the 2009 – 2020 period considered in the previous section (4.3), namely the strong El Nino conditions in 2015 through to early 2016 contrasted with long and strong La Nina conditions from late 2010 through early 2012.

### **4.4.1 Current index locations with summer / winter conditions**

Figure 18 & Figure 19 show summer and winter climatological conditions for SST with mean currents while providing the overall view of our study region, including the location of the four current indices that were produced for this project.

Figure 20 and Figure 21 show the relationship between a current system with a strong relationship to ENSO (the SEC index), with a correlation of 0.4 at zero lag increasing to 0.5 at a 3-month lag, and a weak one (the EAC index) with overall poor correlation.

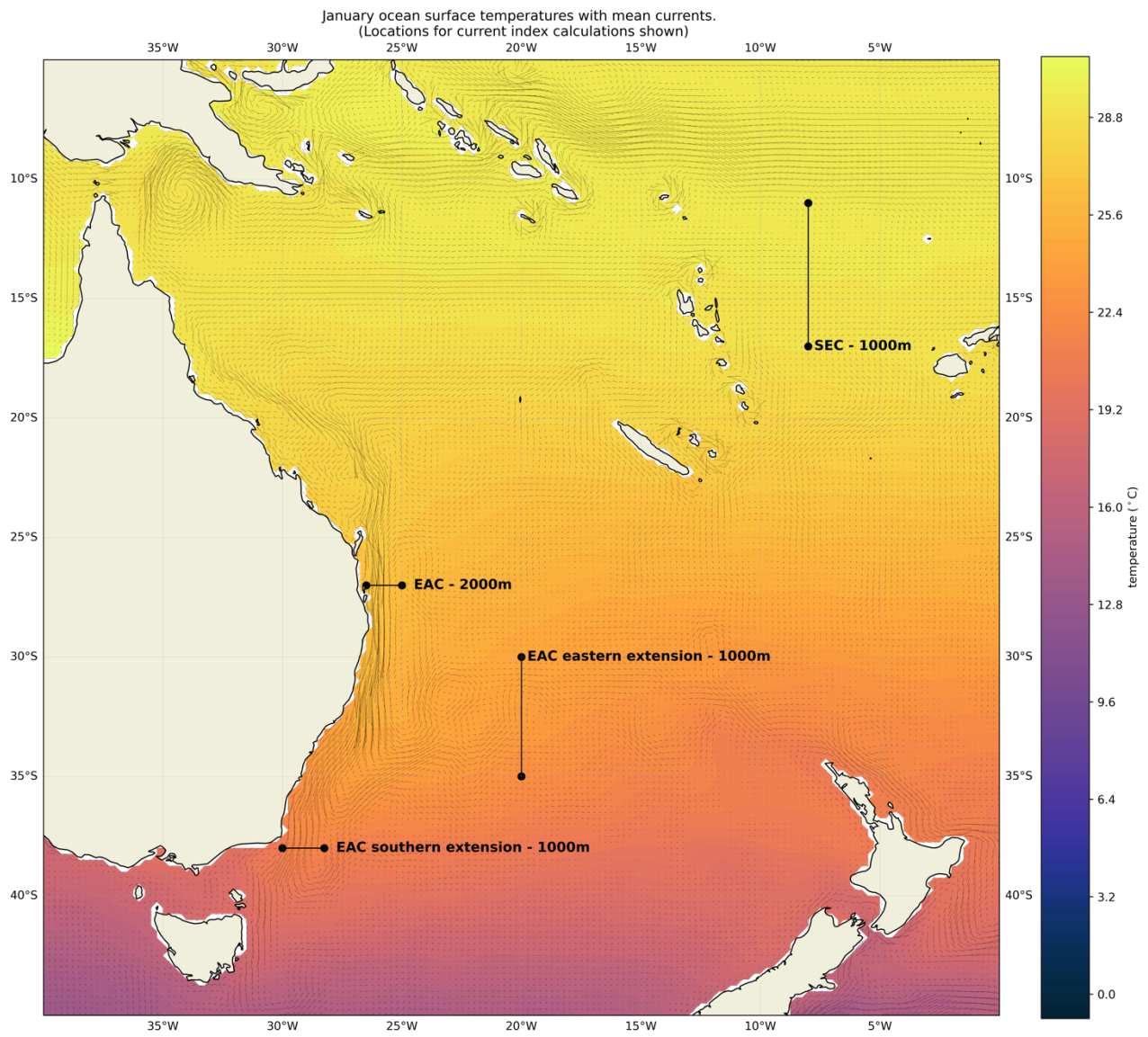


Figure 18: Regional summer conditions with SST, ocean currents, and location of 4 current indices.

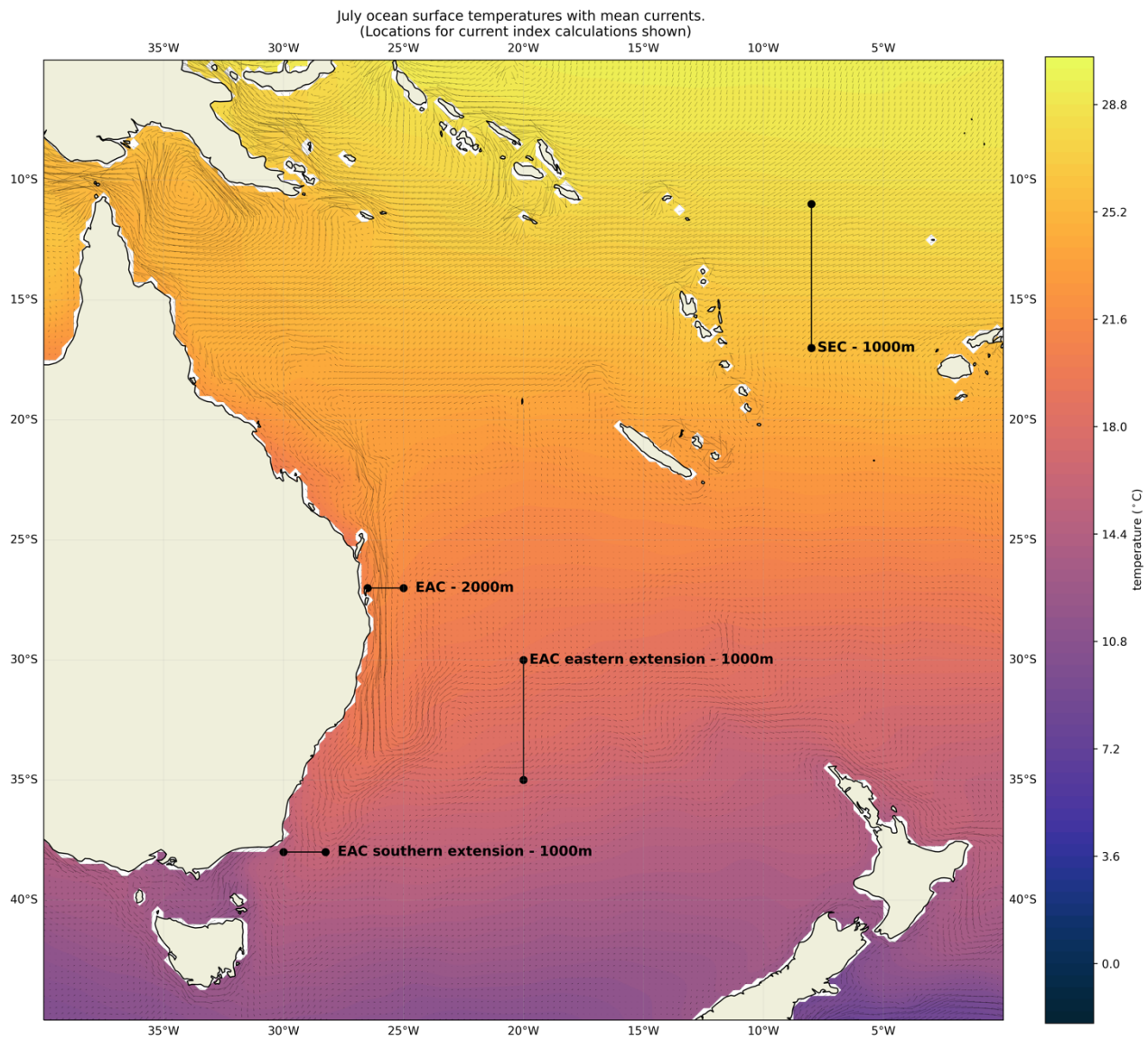


Figure 19: Regional winter conditions with SST, ocean currents, and location of 4 current indices.

ENSO phase based on ONI  
vs  
SEC index

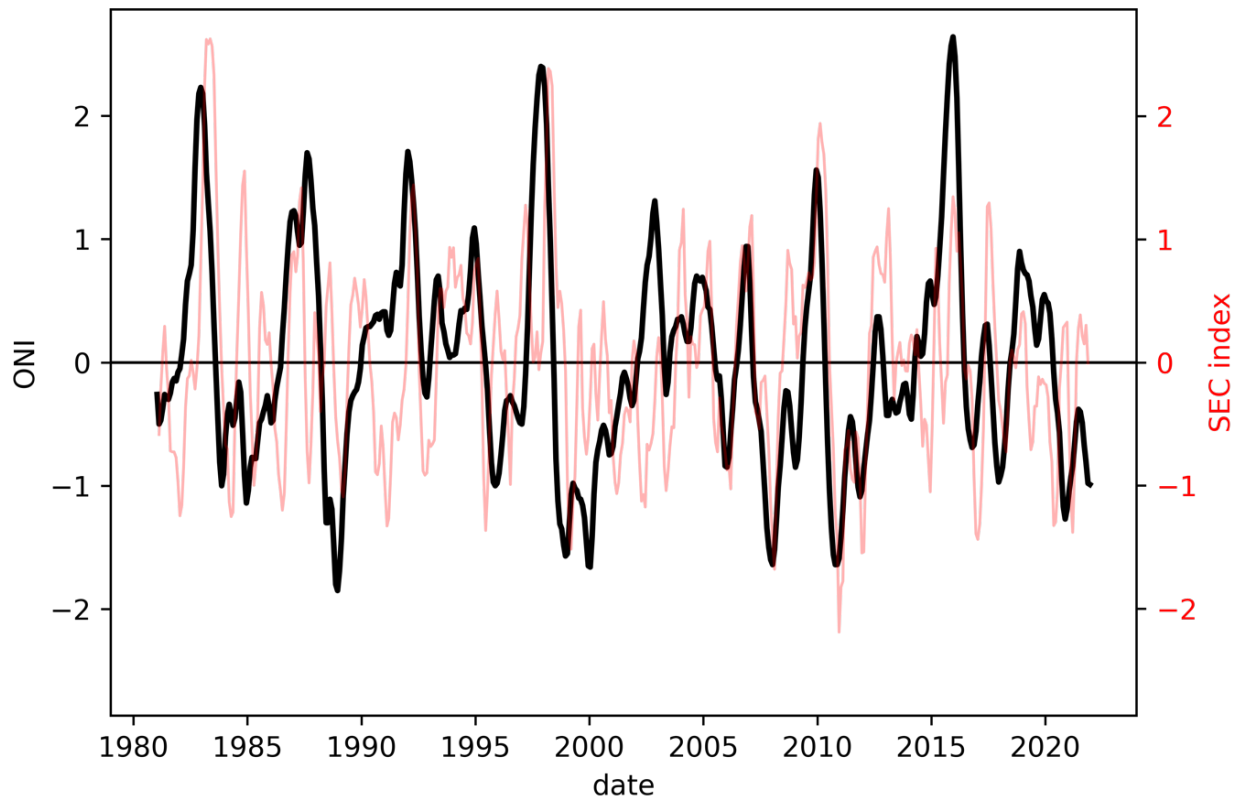


Figure 20: Ocean current index for the South Equatorial Current (SEC) – relative to ENSO (as described by the oceanic Niño index – ONI)

ENSO phase based on ONI  
vs  
EAC index

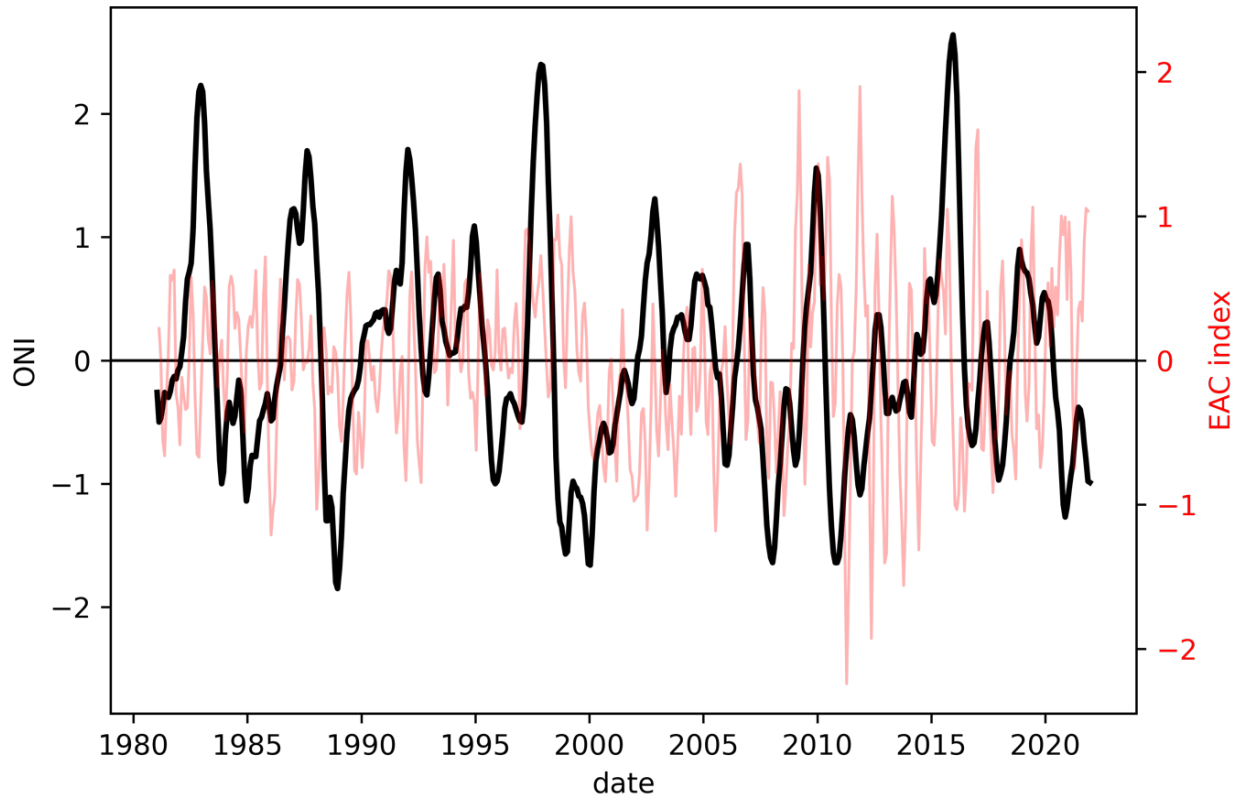


Figure 21: Ocean current index for the East Australian Current (EAC) – relative to ENSO (as described by the oceanic Nino index – ONI)

#### 4.4.2 Ocean climatologies

Figure 22 to Figure 28 show the seasonal climatologies for a selection of ACCESS-S2 reanalysis ocean variables, namely sea surface temperature (SST in °C), temperature at 500 metres (Temp500 in °C), depth of the 20° isotherm (d20 in metres), ocean heat content over the upper 300 metres (hc300 in J), seas surface salinity (SSS in psu), mixed layer depth (MLD in metres), and sea surface height (SSH in metres).

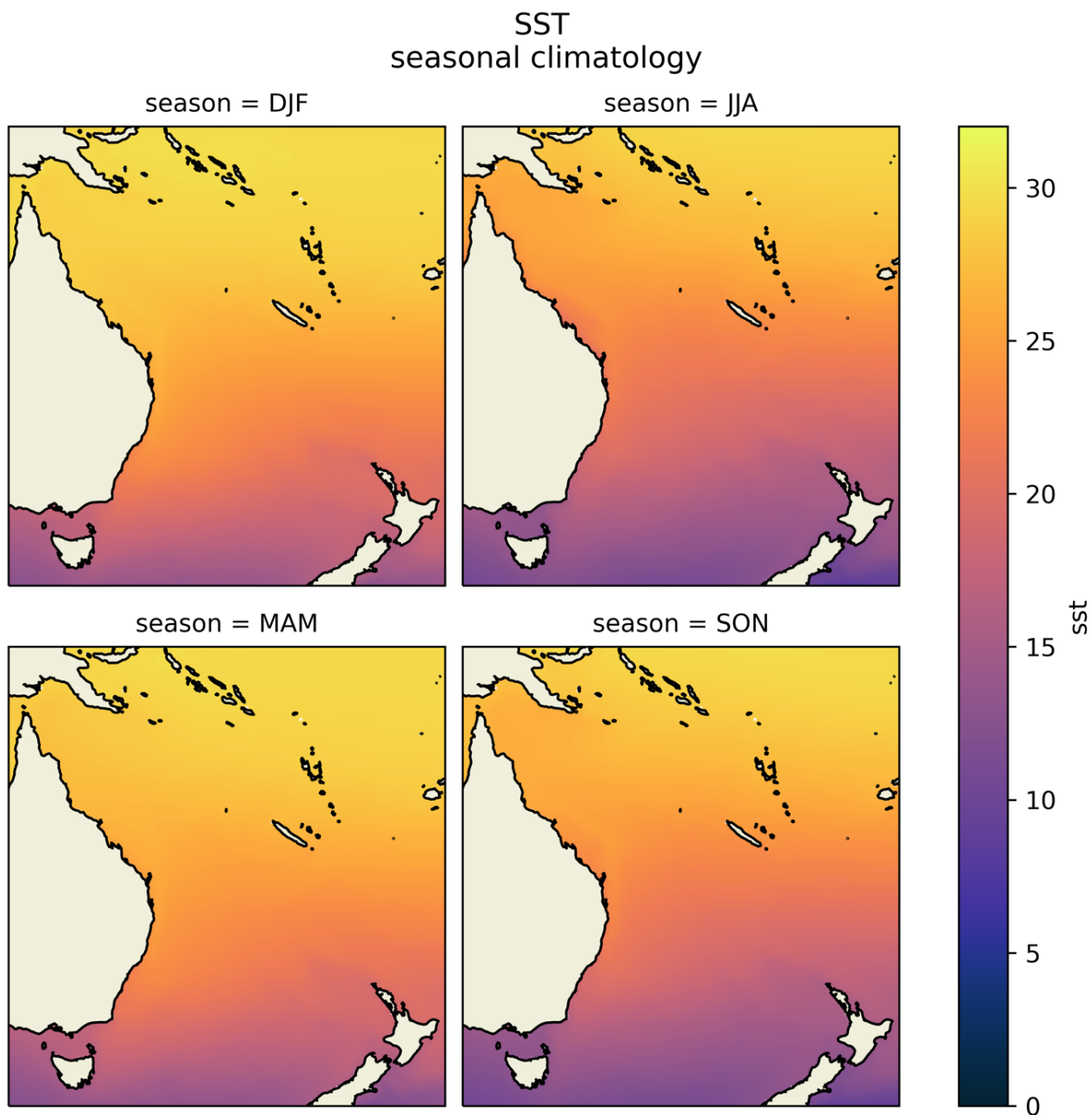


Figure 22: Seasonal climatology for sea surface temperature from ACCESS-S2.

Temp500  
seasonal climatology

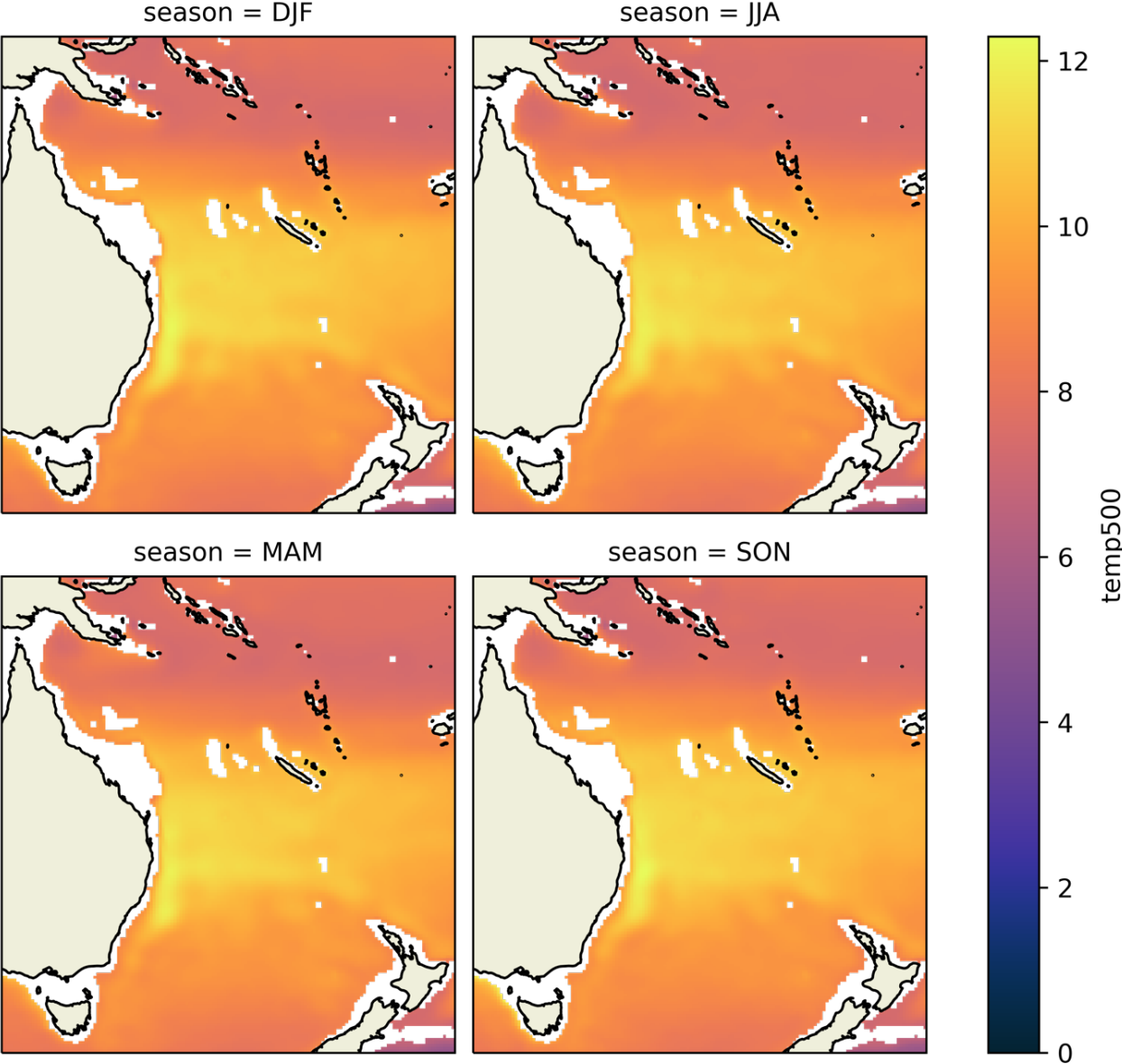


Figure 23: Seasonal climatology for temperature at 500m from ACCESS-S2.

d20  
seasonal climatology

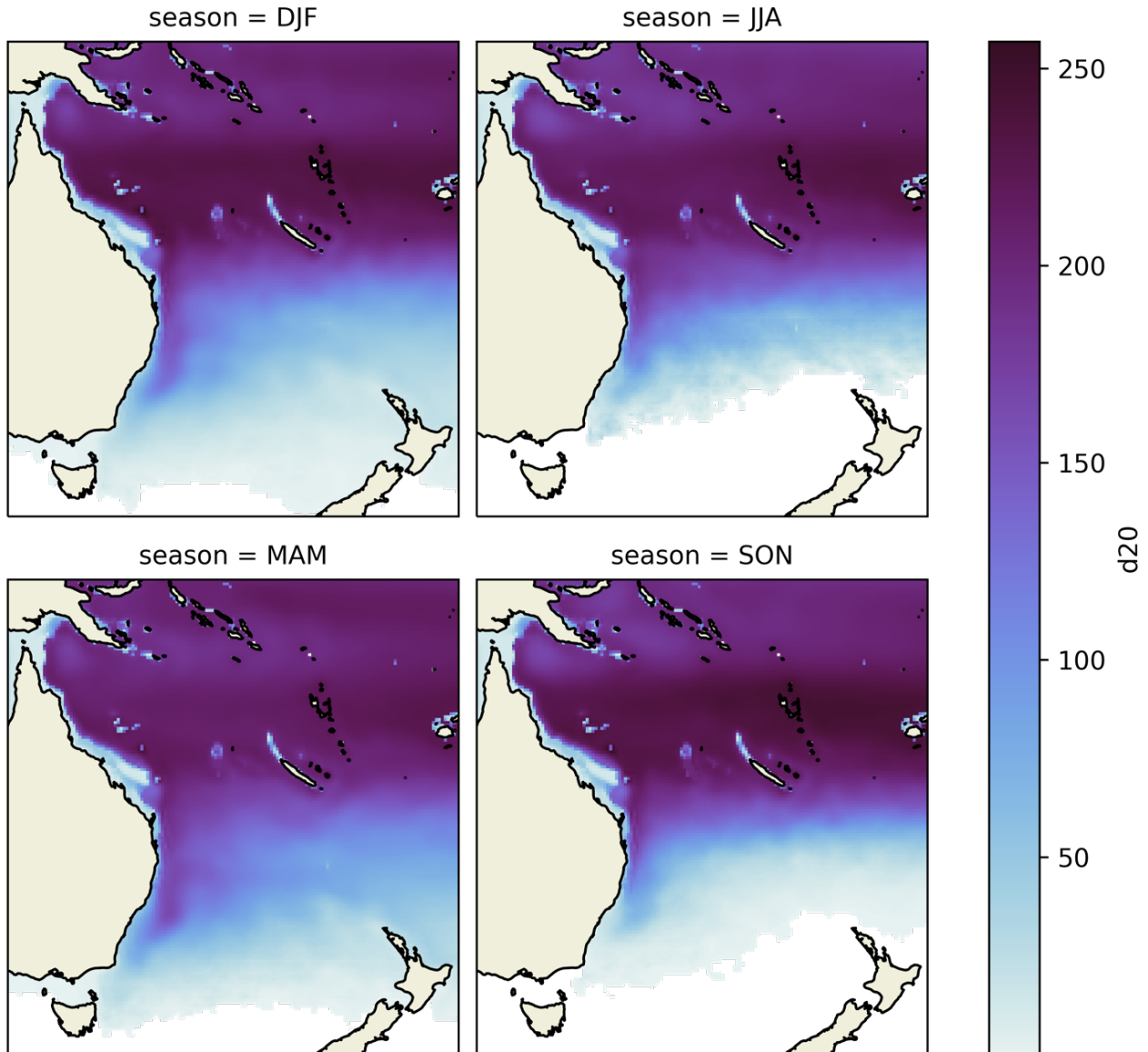


Figure 24: Seasonal climatology for depth of the 20° isotherm from ACCESS-S2.

hc300  
seasonal climatology

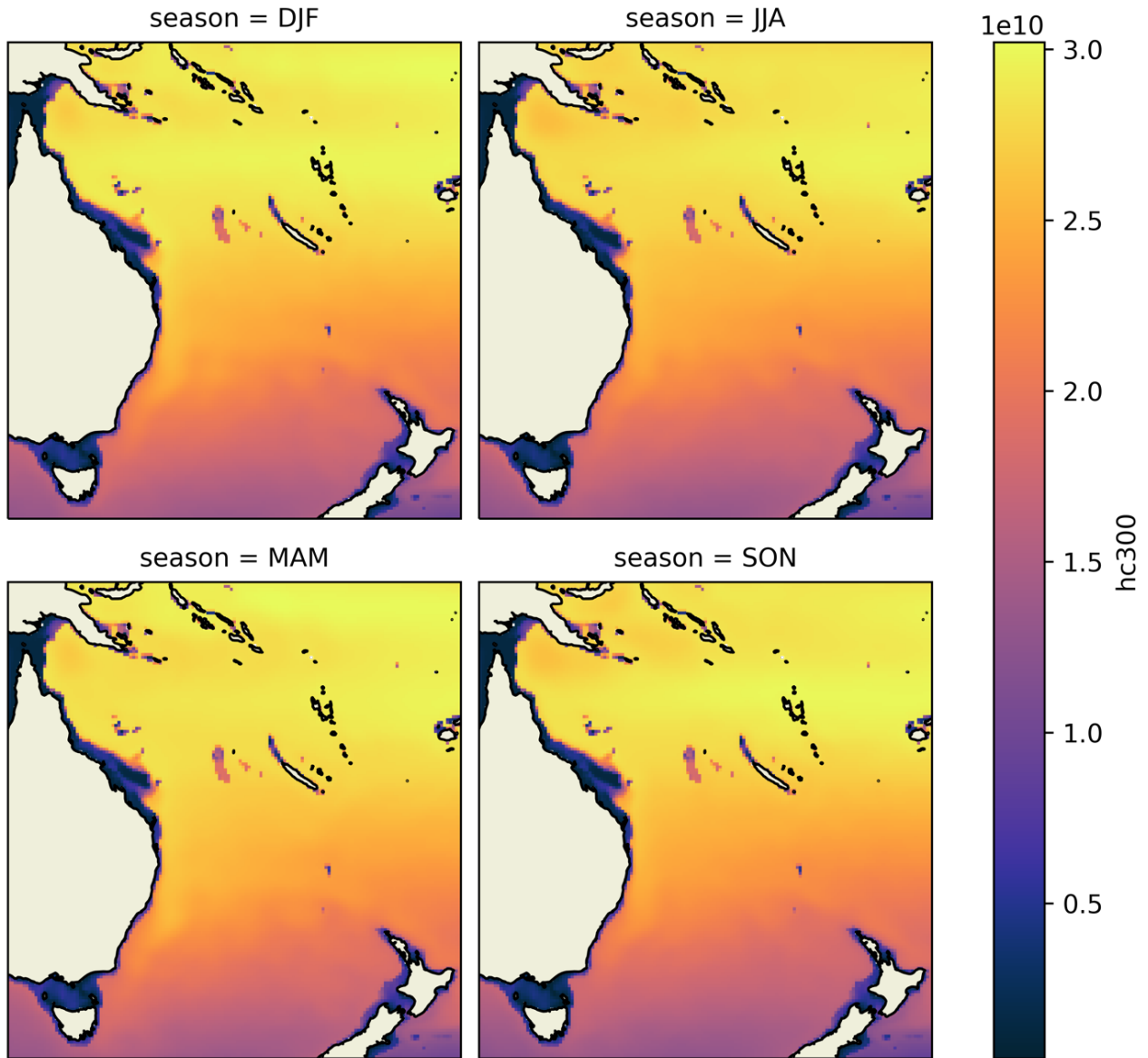


Figure 25: Seasonal climatology for ocean heat content for the upper 300m from ACCESS-S2.

# SSS seasonal climatology

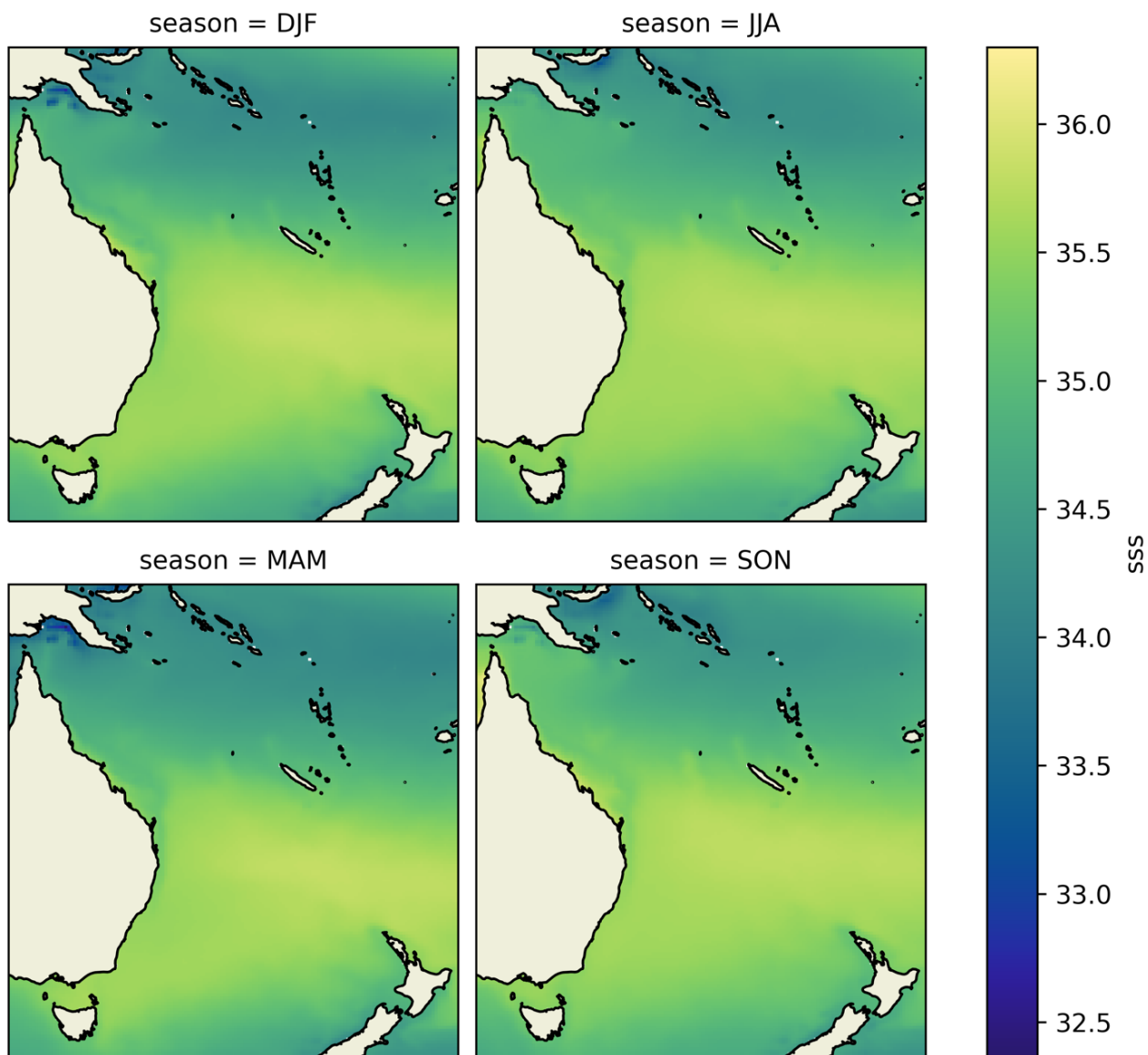


Figure 26: Seasonal climatology for sea surface salinity from ACCESS-S2.

# MLD seasonal climatology

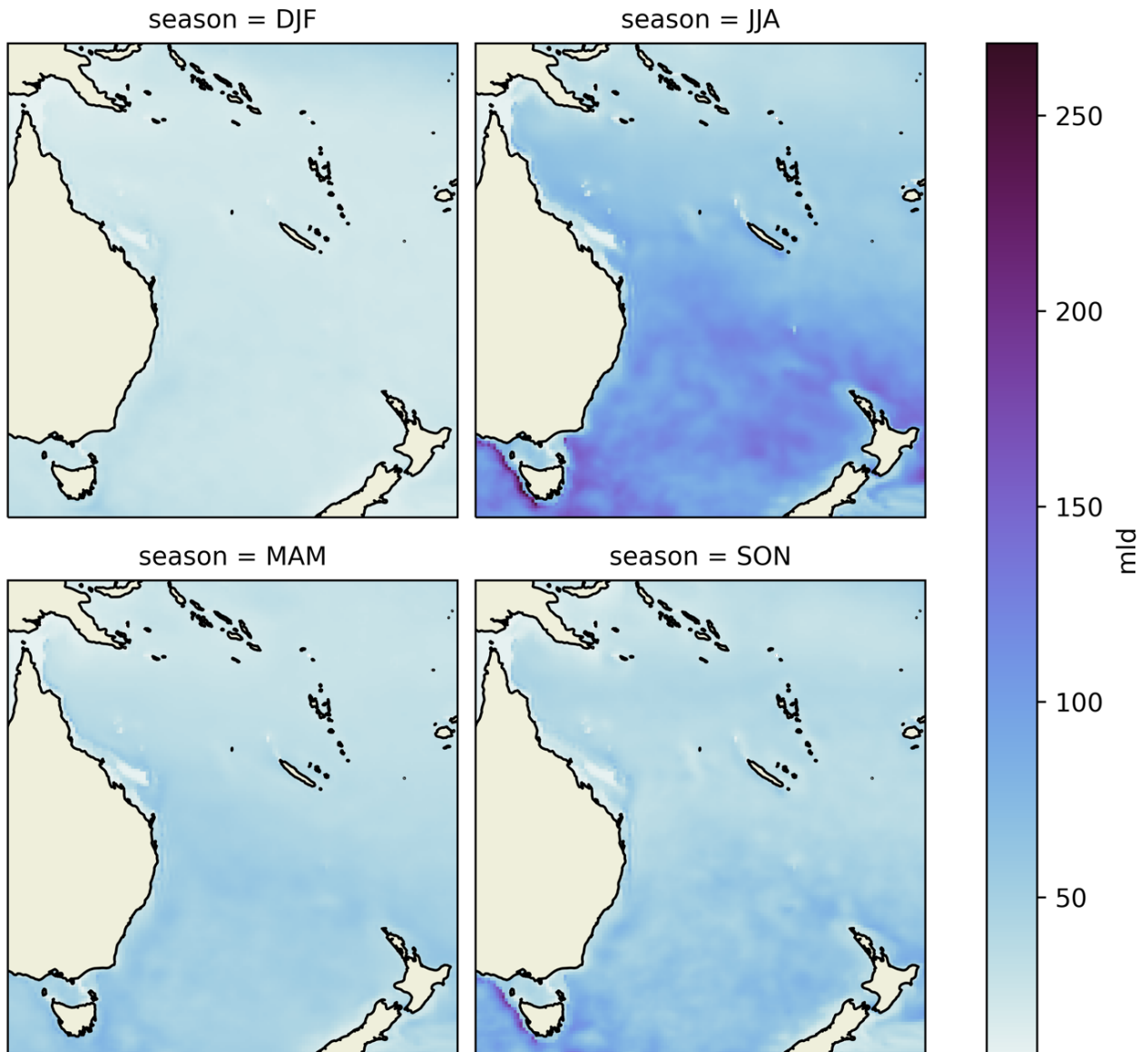


Figure 27: Seasonal climatology for mixed layer depth from ACCESS-S2.

SSH  
seasonal climatology

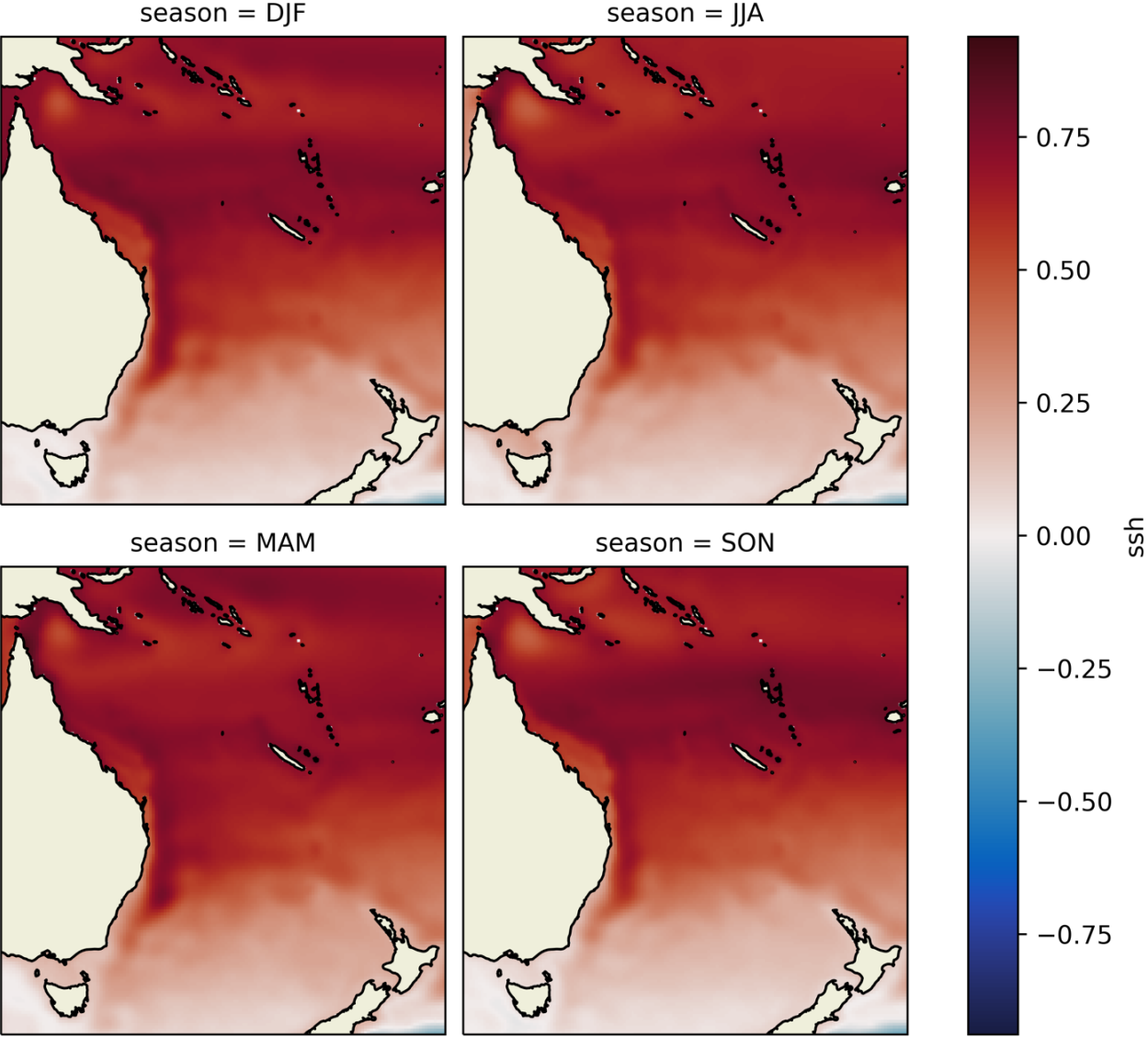


Figure 28: Seasonal climatology for sea surface height from ACCESS-S2.

### 4.4.3 Strong ENSO events

For two strong historical ENSO events (El Nino 2015-2016 and La Nina 2010-2012), we identified the months of strong El Nino / La Nina using the ONI characterisation of +0.5/-0.5 respectively. For each of these events the monthly anomalies across the event as it progressed are shown for each of the above seven ocean environmental variables (El Nino: Figure 29 to Figure 35; La Nina: Figure 36 to Figure 42).

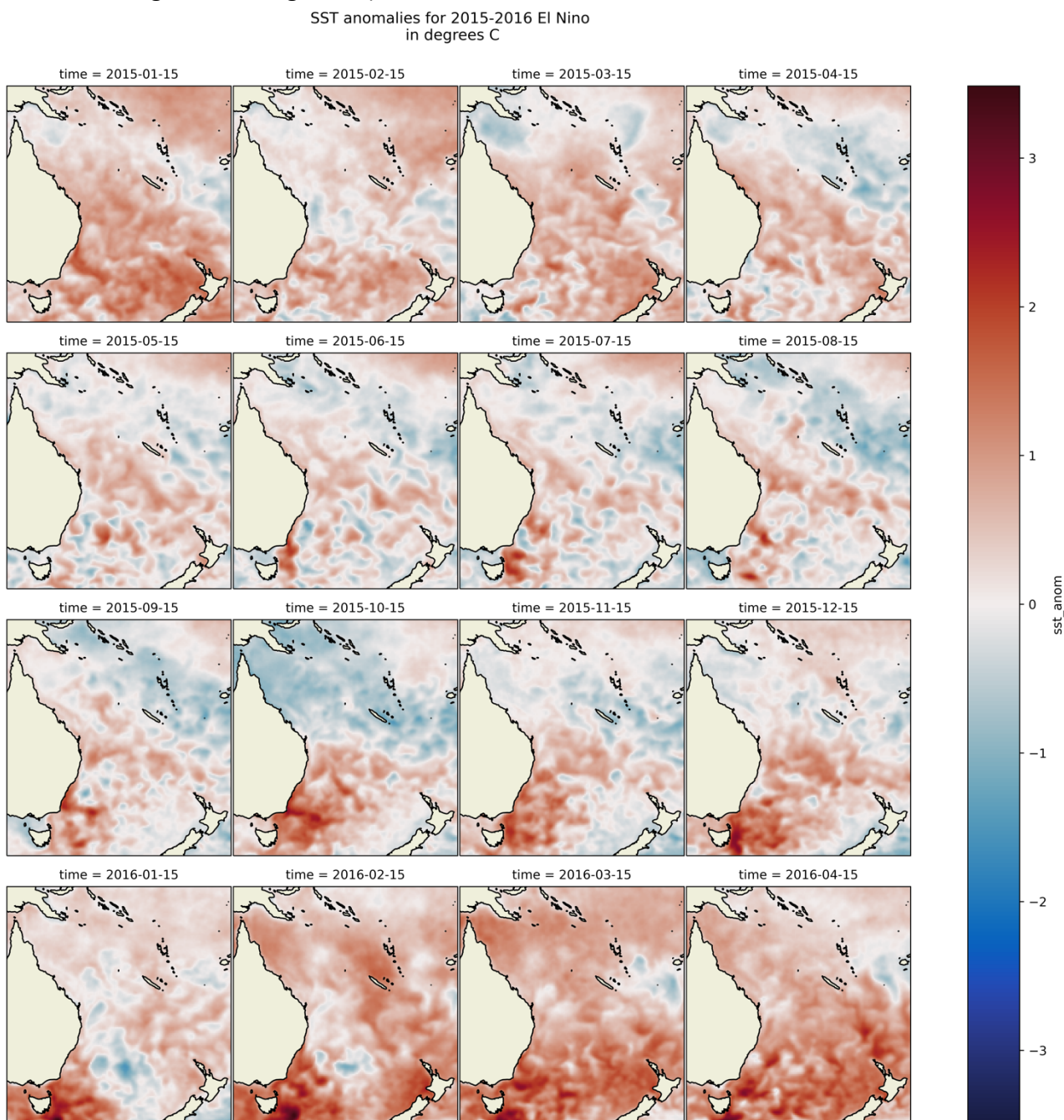


Figure 29: Monthly anomalies for sea surface temperature from ACCESS-S2 for the 2015-2016 El Niño events

SSS anomalies for 2015-2016 El Nino  
in psu

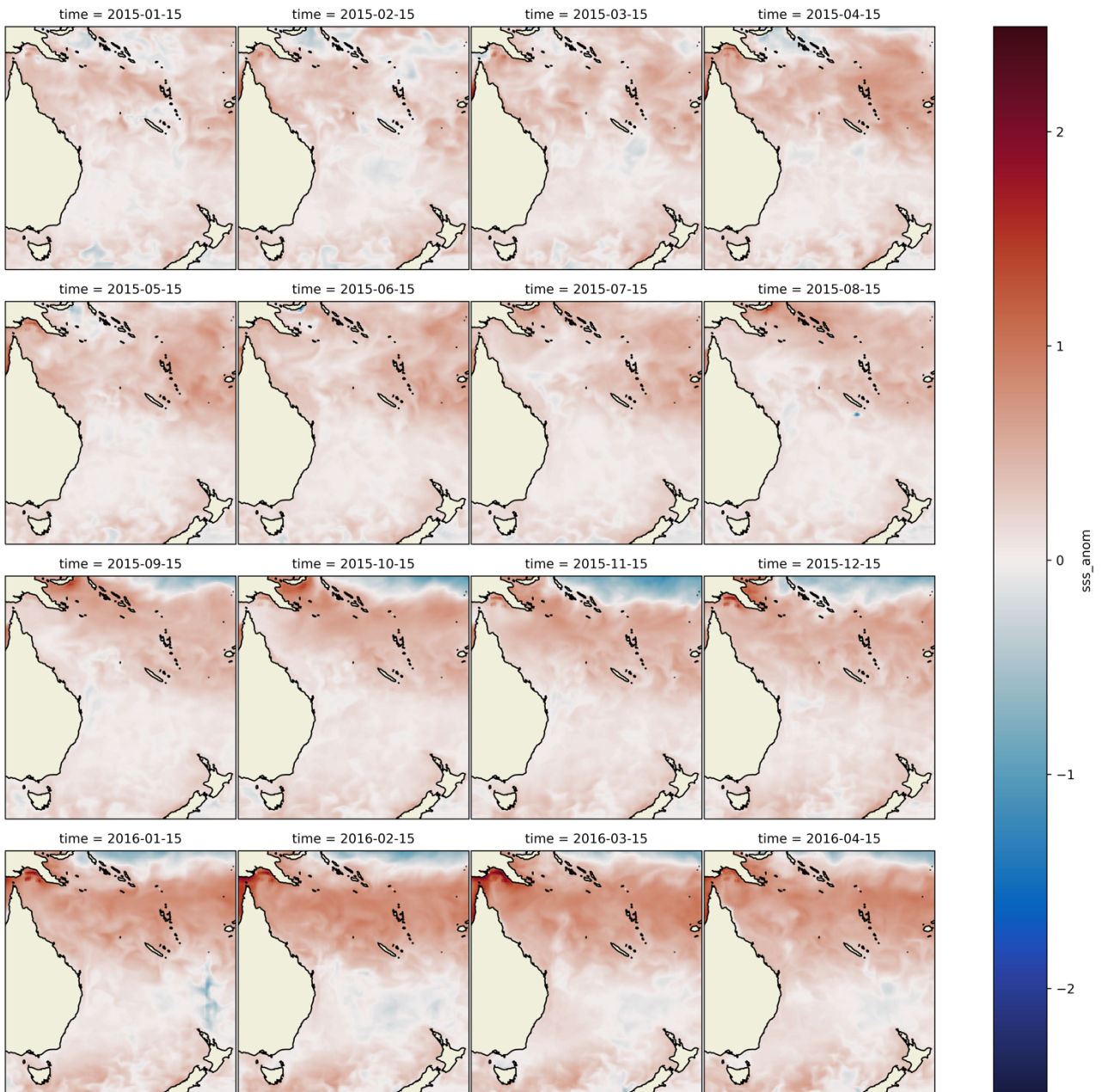


Figure 30: Monthly anomalies for sea surface salinity from ACCESS-S2 for the 2015-2016 El Nino events

SSH anomalies for 2015-2016 El Nino  
in m

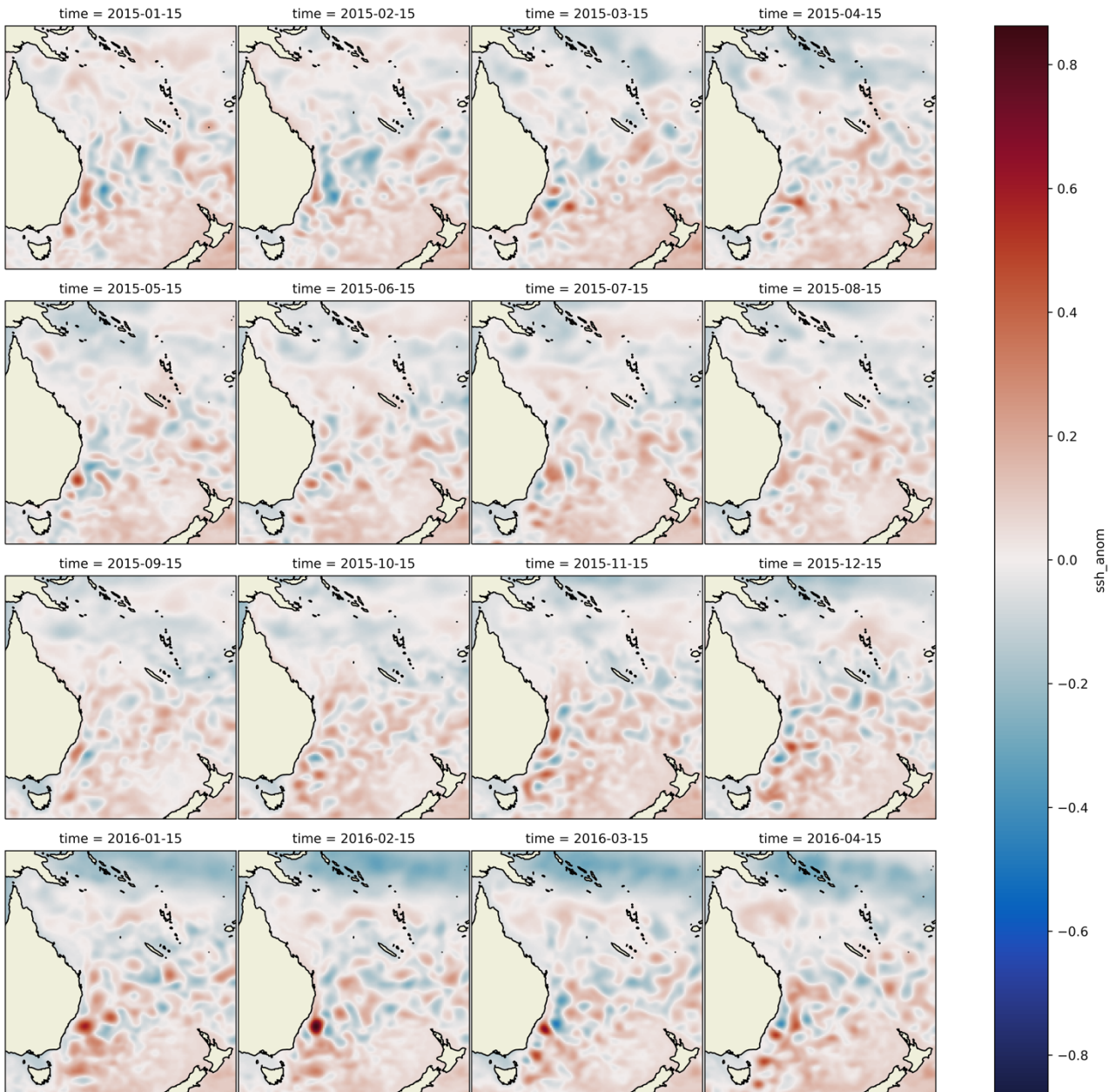


Figure 31: Monthly anomalies for sea surface height from ACCESS-S2 for the 2015-2016 El Niño events

Temp500 anomalies for 2015-2016 El Nino  
in degrees C

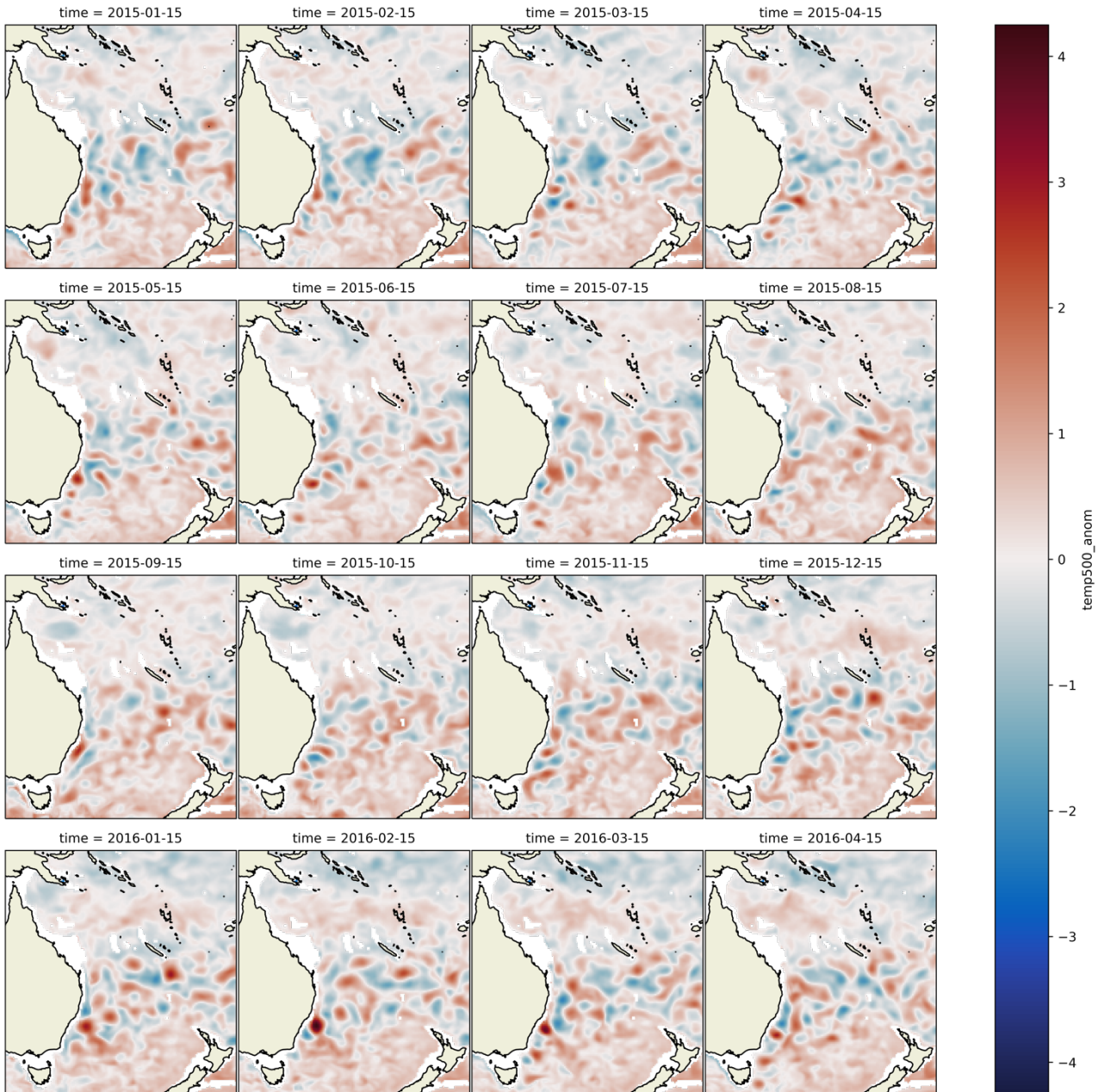


Figure 32: Monthly anomalies for temperature at 500m from ACCESS-S2 for the 2015-2016 El Nino events

d20 anomalies for 2015-2016 El Nino  
in m

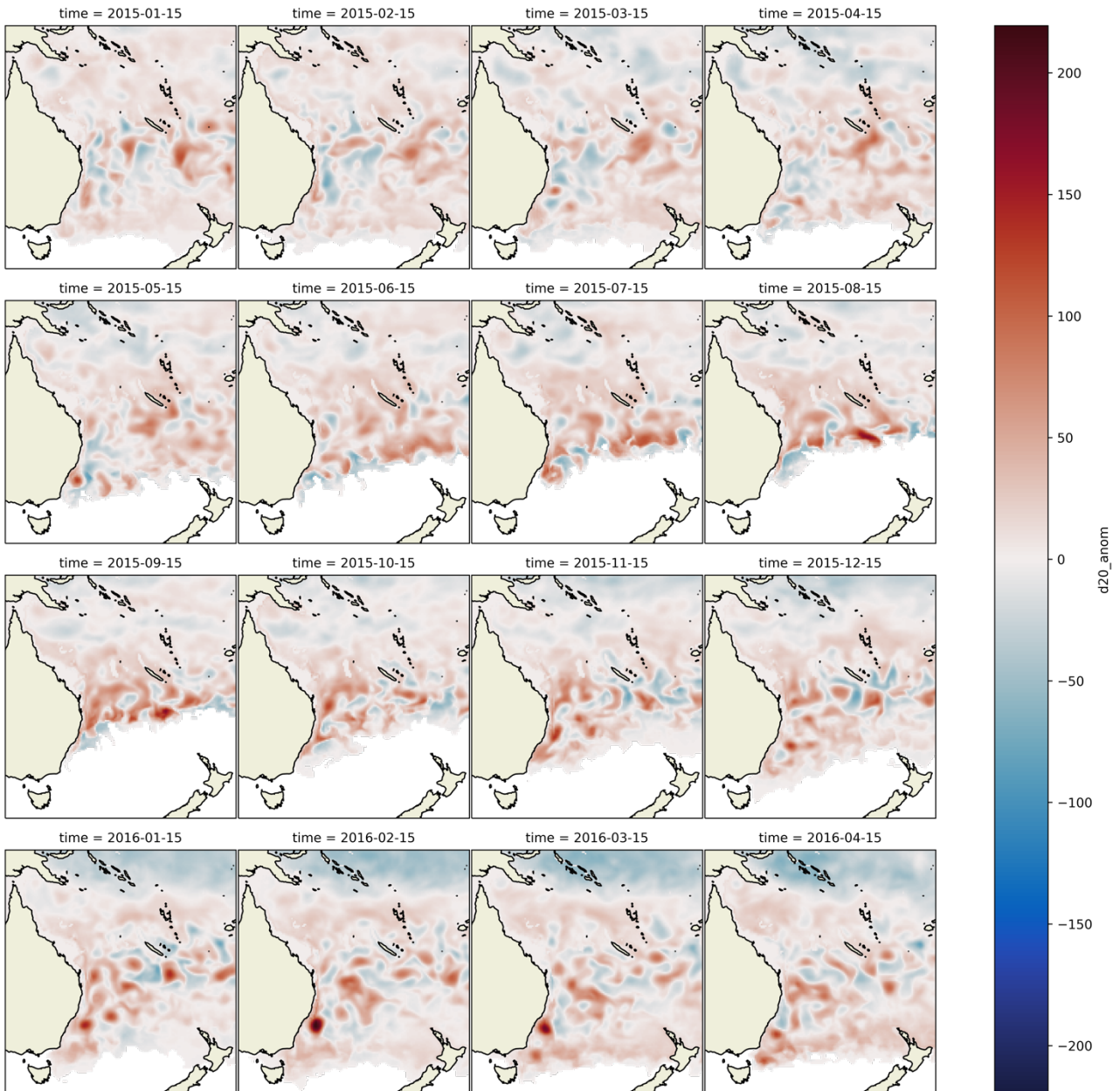


Figure 33: Monthly anomalies for depth of the 20 degree isotherm from ACCESS-S2 for the 2015-2016 El Nino events

MLD anomalies for 2015-2016 El Nino  
in m

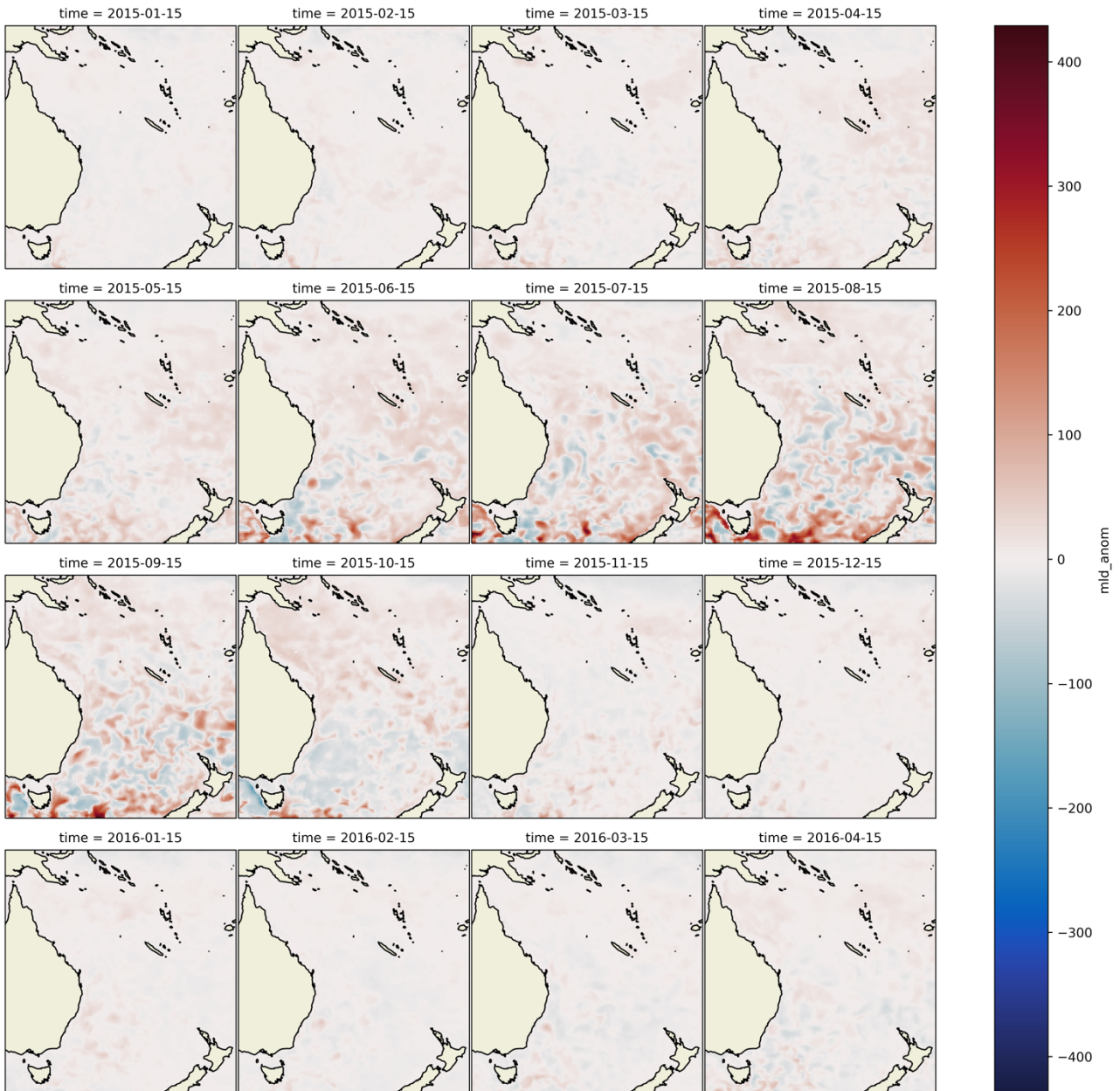


Figure 34: Monthly anomalies for mixed layer depth from ACCESS-S2 for the 2015-2016 El Niño events

hc300 anomalies for 2015-2016 El Nino  
in J

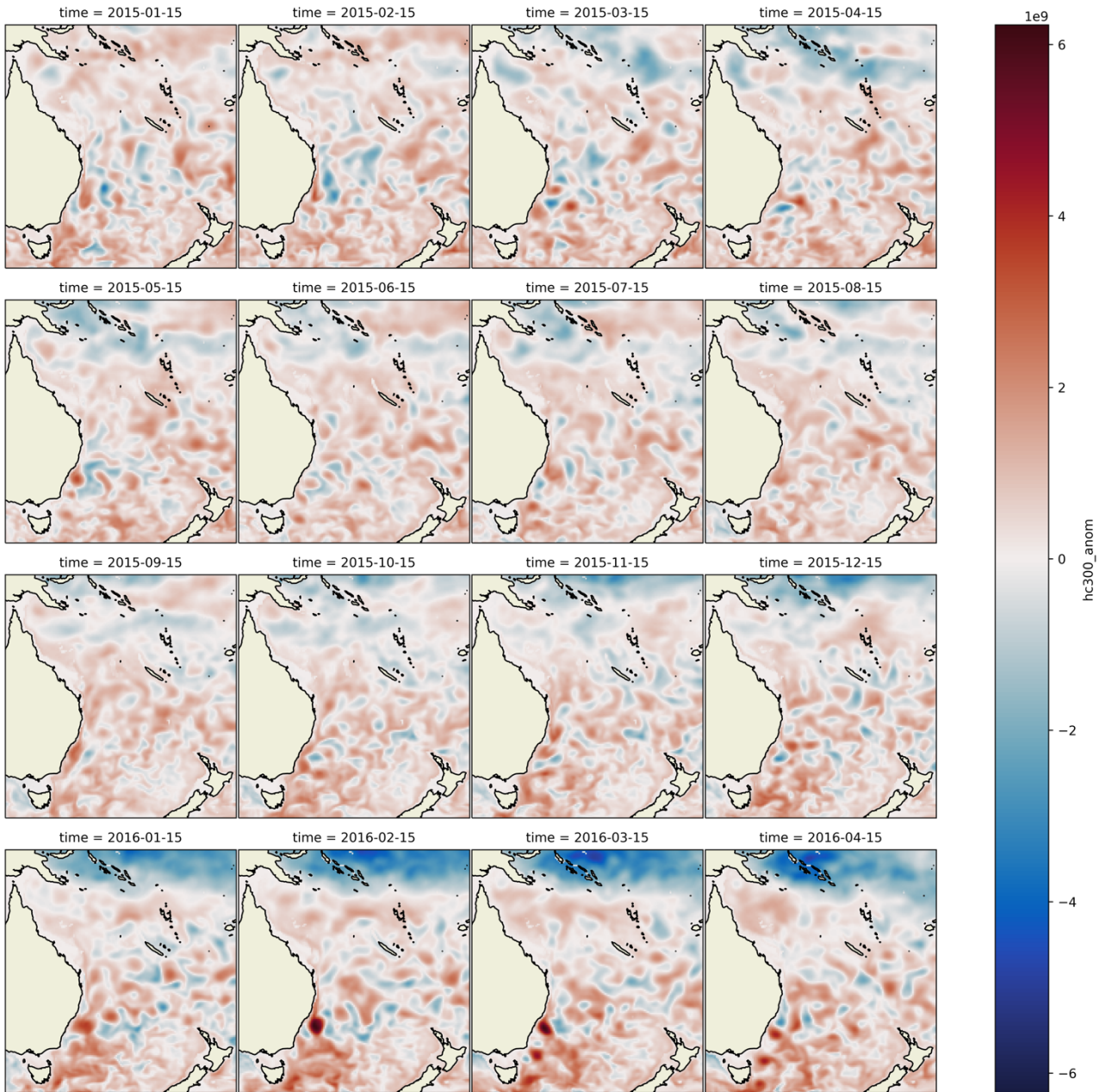


Figure 35: Monthly anomalies for heat content in the upper 300m from ACCESS-S2 for the 2015-2016 El Niño events

SST anomalies for 2010-2012 La Nina  
in degrees C

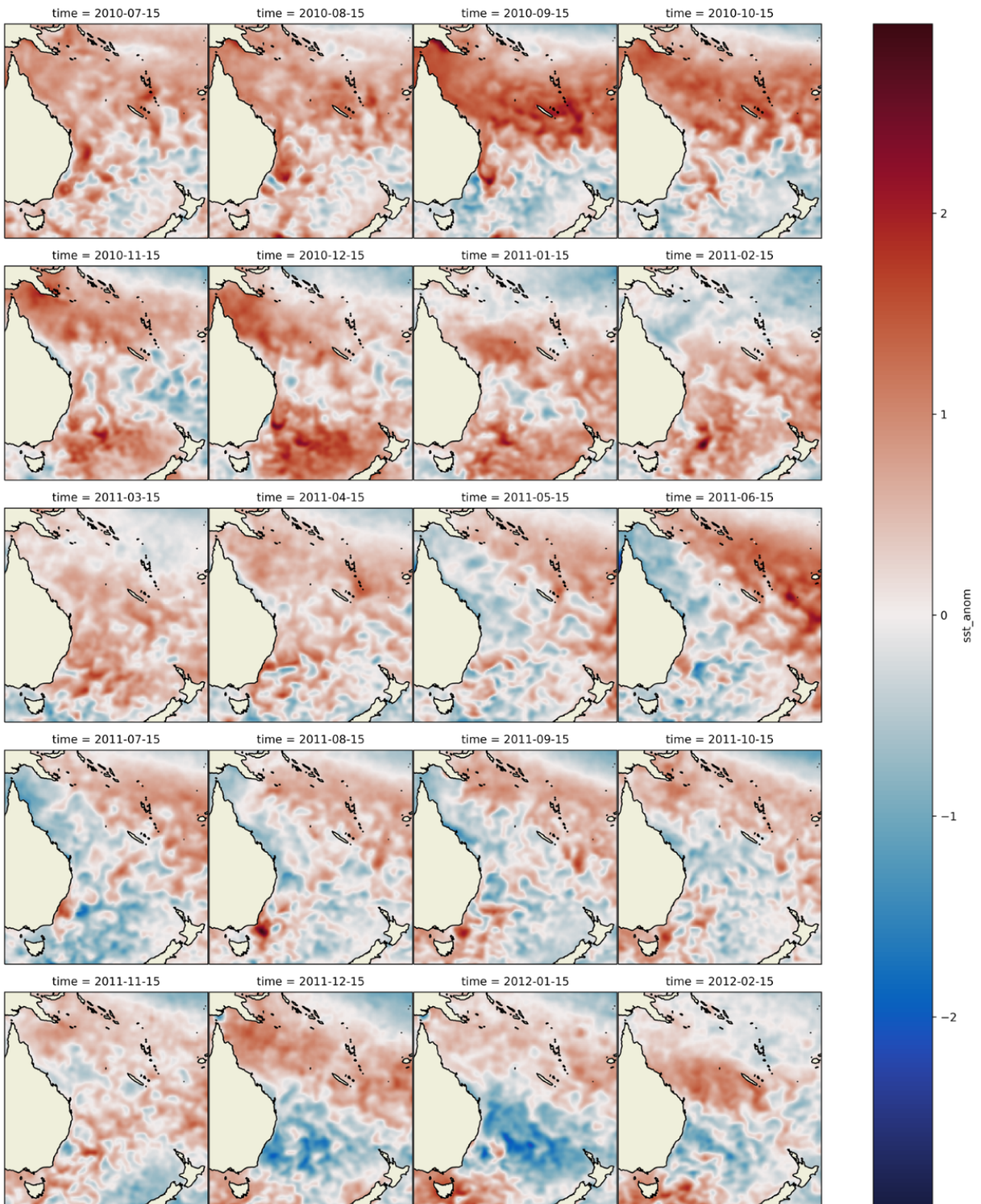


Figure 36: Monthly anomalies for sea surface temperature from ACCESS-S2 for the 2010-2012 La Nina events

SSS anomalies for 2010-2012 La Nina  
in psu

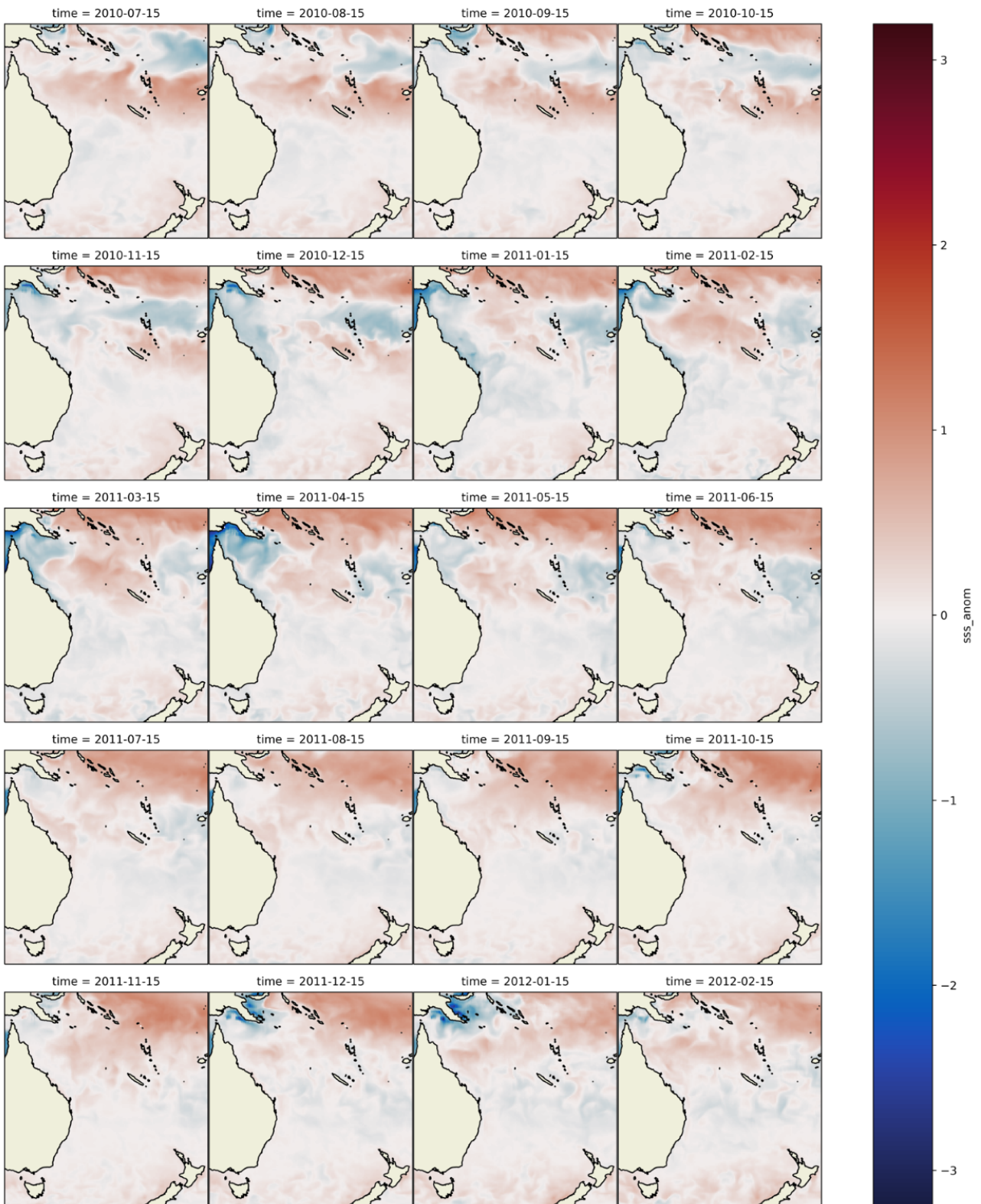


Figure 37: Monthly anomalies for sea surface salinity from ACCESS-S2 for the 2010-2012 La Nina events

SSH anomalies for 2010-2012 La Nina  
in m

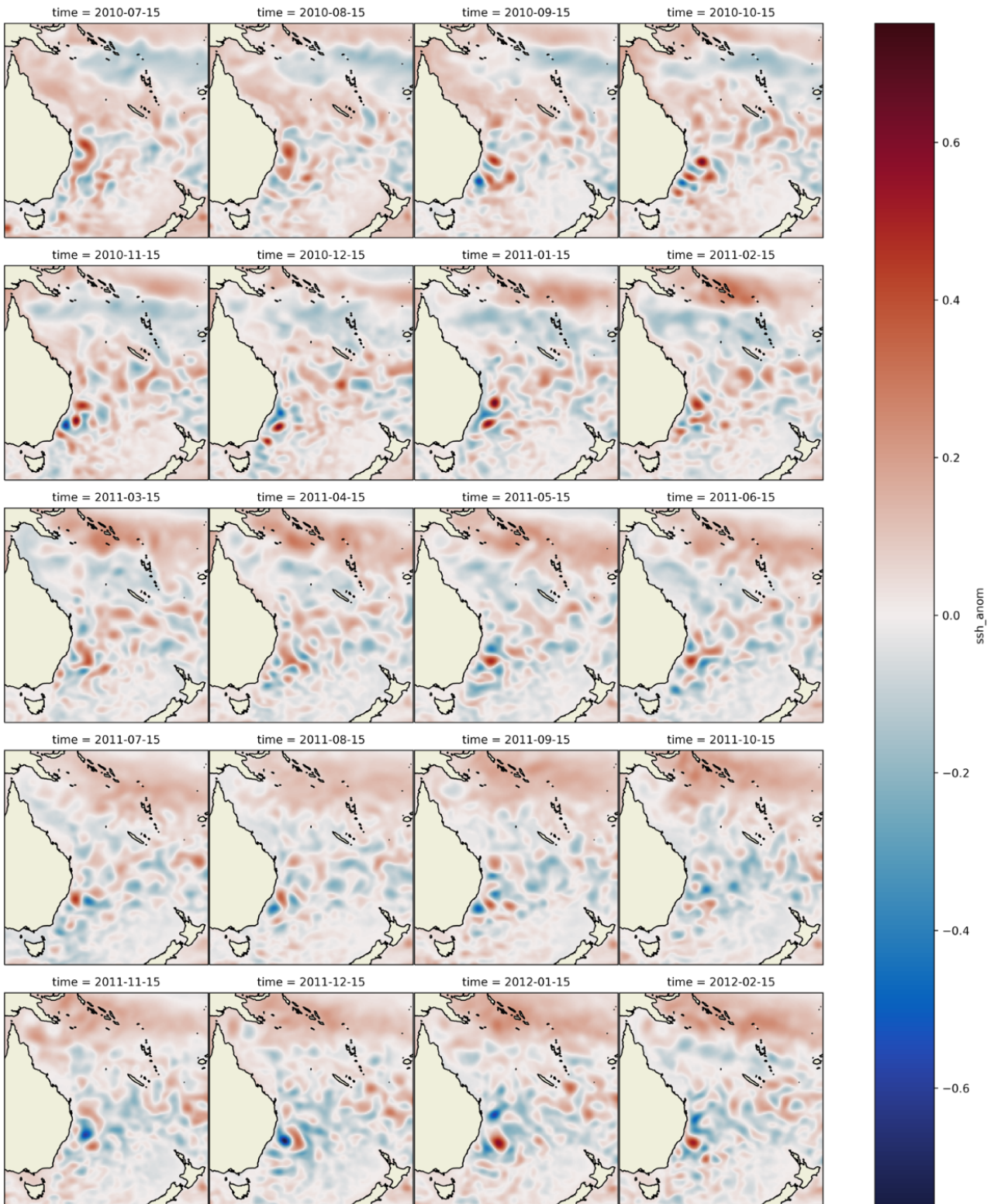


Figure 38: Monthly anomalies for sea surface height from ACCESS-S2 for the 2010-2012 La Nina events

Temp500 anomalies for 2010-2012 La Nina  
in degrees C

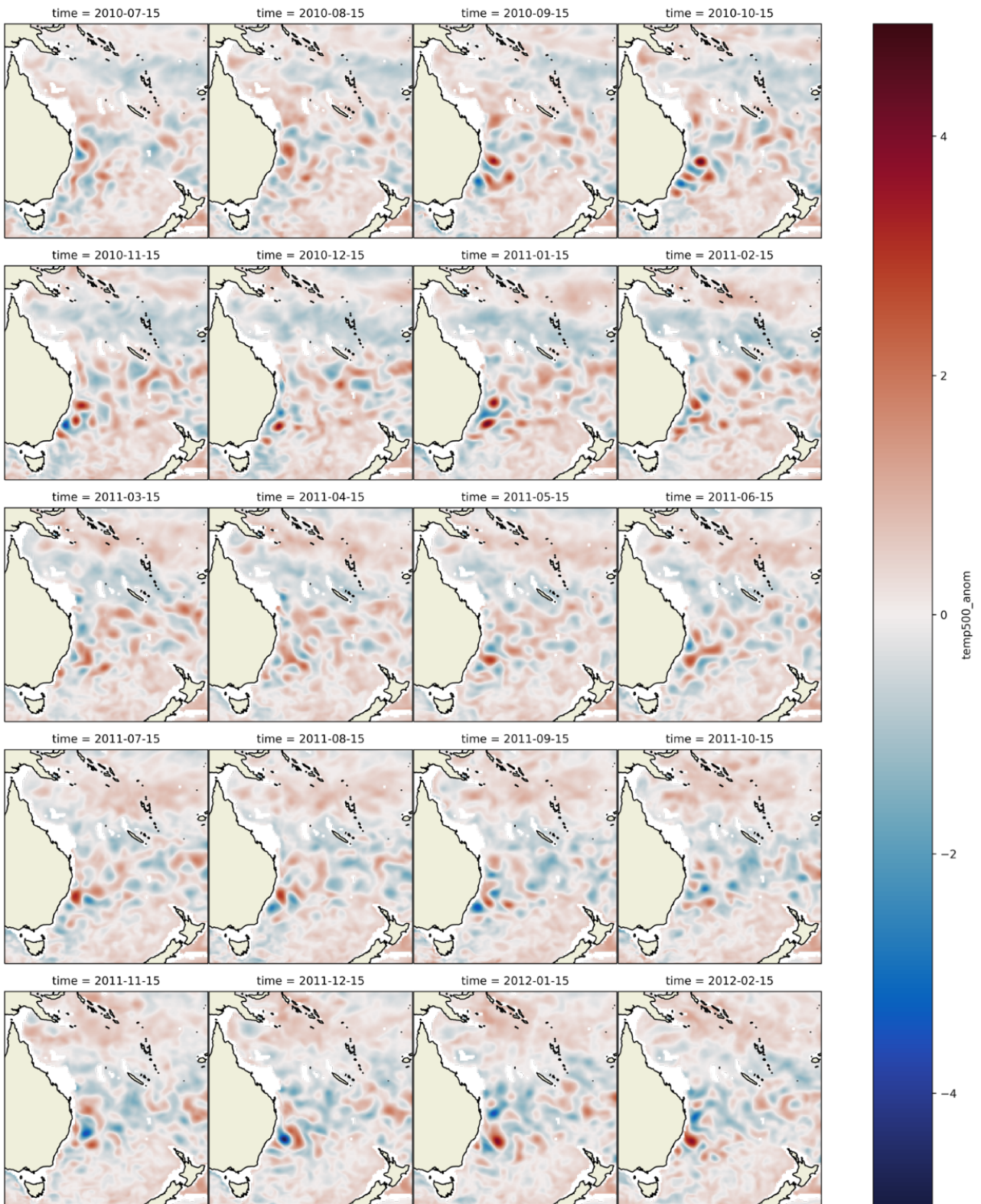


Figure 39: Monthly anomalies for temperature at 500m from ACCESS-S2 for the 2010-2012 La Nina events

d20 anomalies for 2010-2012 La Nina  
in m

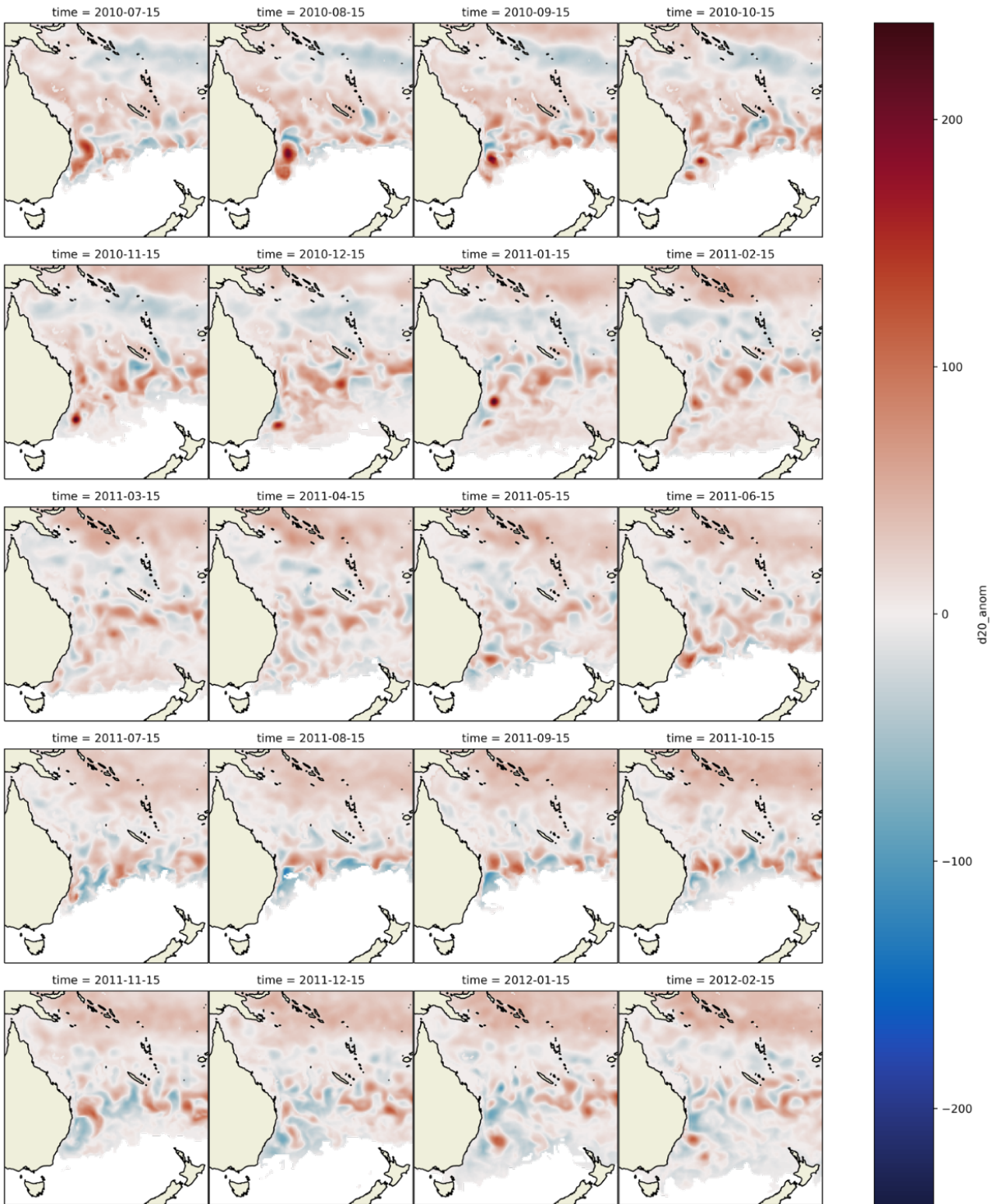


Figure 40: Monthly anomalies for depth of the 20 degree isotherm from ACCESS-S2 for the 2010-2012 La Nina events

MLD anomalies for 2010-2012 La Nina  
in m

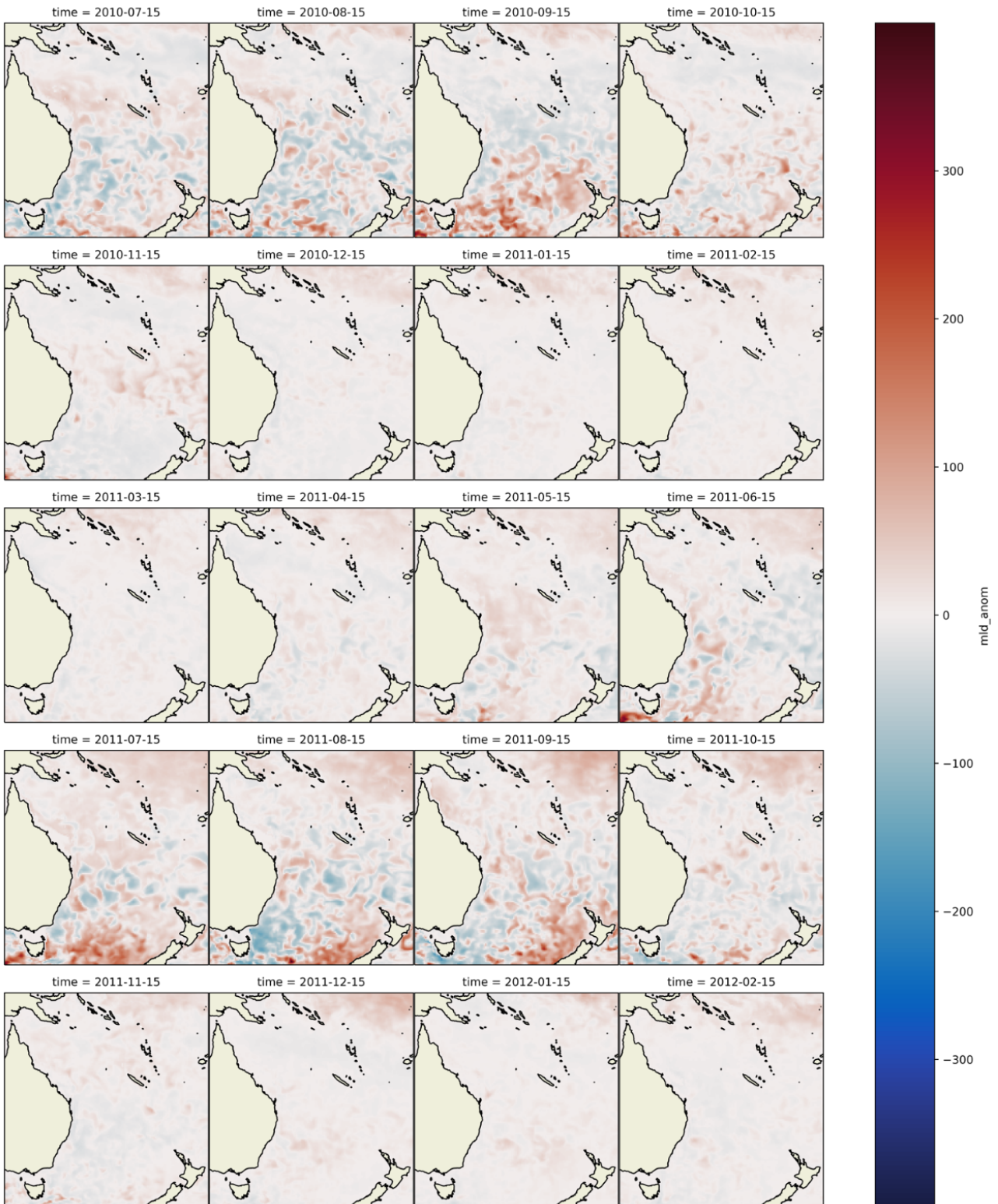


Figure 41: Monthly values for mixed layer depth from ACCESS-S2 for the 2010-2012 La Nina events

hc300 anomalies for 2010-2012 La Nina  
in J

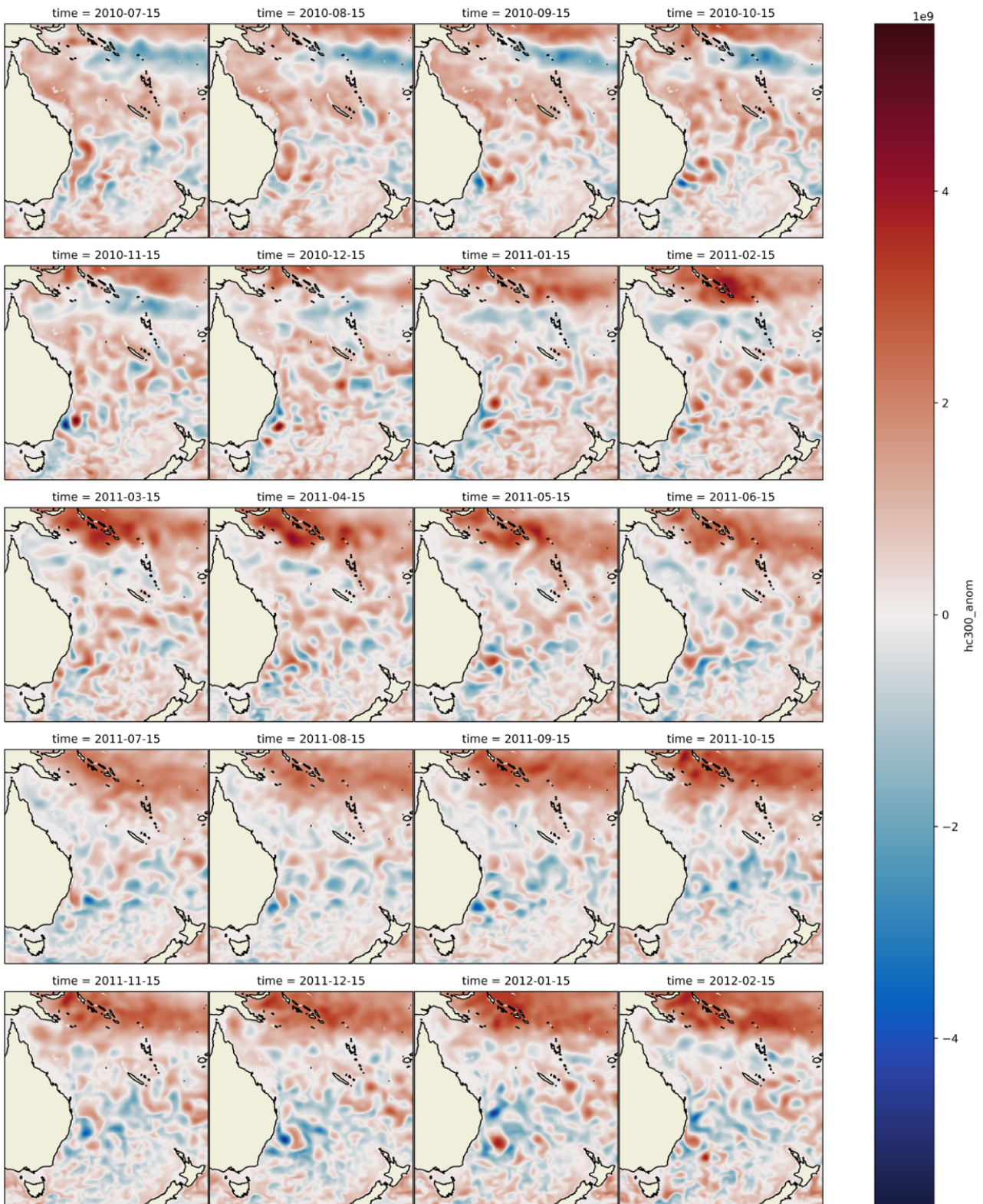


Figure 42: Monthly anomalies for heat content in the upper 300m from ACCESS-S2 for the 2010-2012 La Nina events

## 4.5 Discussion

The habitat modelling sections that follow show that sub-surface variables representing upper ocean structure and stored heat can have the greatest relative contribution in explaining the variability in catch rates of tuna and billfish species. While location specific, this may be

particularly important in general for species with specific thermal envelopes for which the ocean mixed layer is their primary environment. This highlights an opportunity to move beyond the use of ocean observations and estimates focused solely on the sea surface.

To expand their usefulness for catch prediction applications, products like the BoM ACCESS-S2 model would need to provide regularly updated reanalyses for model building, tuning, and training, as well as near-real-time hindcast output of the same full suite of ocean environmental variables to enable verification and testing. In looking towards a truly operational fisheries prediction system, forecast ocean inputs for the statistical catch modelling would need to be available in a regular and ongoing fashion to keep up with the decision trigger points for the industry. Contemporary seasonal climate forecast products like ACCESS-S2 show real progress towards these needs.

# 5 Boosted Regression Trees

## 5.1 General BRT methods

Catch and effort data from 13 nations and territories across the South-West Pacific region (Cook Islands; French Polynesia; New Caledonia; New Zealand; Norfolk Island; Samoa; Solomon Islands; Tokelau; Tonga; Tuvalu; Vanuatu; Fiji and Australia) were provided by the Western and Central Pacific Fisheries Commission (WCPFC) and Australian Fisheries Management Authority (AFMA) for the five target species (see section 1). The data were provided in a summarised form by month and spatial grid cell from 1990 to 2020, using both a  $1^\circ \times 1^\circ$  and  $0.25^\circ \times 0.25^\circ$  grid (noting that the data for New Zealand were only available at the coarser  $1^\circ \times 1^\circ$  resolution).

For each of the five target species, boosted regression trees (BRTs) were used to model the observed catch in each grid cell in each month assuming a Poisson distribution and including the number of hooks as an offset and the chosen oceanographic variables as predictors. The spatial resolution used depended on the resolution of the oceanographic data ( $1^\circ \times 1^\circ$  for CAFE60 and  $0.25^\circ \times 0.25^\circ$  for ACCESS-S2). Although the catch data were provided for years 1990-2020, only data from 2008 onwards were used since fishing pressure increased and catch rates declined steadily during the 2000-2007 period for most of the target species (see section 1). The data were split into a training dataset (2008-2015) and test (or validation) dataset (2016-2020<sup>2</sup>) to allow validation of model performance. We used the `gbm.step()` function from the BRT fitting protocols developed by Elith et al. (2008) as extensions to functions available in the `gbm` package for R (Greenwell et al. 2020). `gbm.step()` implements a cross-validation method for identifying the optimal number of trees for a given learning rate, bag fraction and tree complexity. BRT fitting parameters were tuned using an iterative process to prevent overfitting to the training data, resulting in models with a ten-fold cross-validation, a bag fraction of 0.7, an interaction depth (or tree complexity) of 1, and using a maximum of 4000 trees. We trialled learning rates between 0.03 and 0.05 to identify an optimal learning rate that resulted in at least 1000 trees, as recommended in Elith et al. (2008), selecting a learning rate of 0.04 for model fitting on the 2008-15 training dataset. Model performance was evaluated by calculating Pearson's correlation ( $R^2$ ) and root-mean-square error (RMSE) for both the training and test datasets, and deviance explained for the training dataset. However, deviance explained should be treated with caution since it calculates the deviance of catch values explained by the model and not CPUE, and hence includes number of hooks used. Since number of hooks is itself a predictor of catch, CPUE is more reliable as a metric of model performance as it removes the influence of number of hooks and relates to the predictive performance of the 'ocean-only' component of each model.

Once the best-performing model was identified for each species based on the training dataset, the model was used to make spatial predictions of CPUE for each month and year in the test dataset. Maps were generated showing the average observed versus average predicted CPUE in each season across all years in the test dataset, where the seasons were defined as Dec-Jan-Feb (summer), Mar-Apr-May (autumn), Jun-Jul-Aug (winter), Sep-Oct-Nov (spring).

Next, the South-West Pacific domain was partitioned into four regional sub-domains based on dominant oceanographic modes and timescales of variability in each region (see Section 4.2). Four key regions were identified (Figure 7), referred to here as EAC-dominated (EAC), Coral Sea and Equatorial (CS), Western-Central Pacific (WCP) and New Zealand (NZ). Species-specific models

---

<sup>2</sup> 2019 for the BRTs using oceanographic data from CAFE60 since that was the extent of the CAFE60 reanalysis at the time of running the models.

were then fitted to the data from each of these regional sub-domains following the same protocol as for the whole-domain model, and with model performance evaluated using the same methods.

## 5.2 BRT using CAFE60

### 5.2.1 Methods

BRTs were fit to the catch and effort data for each of the five target species following the methods described in section 5.1, using as inputs:

- catch and effort data compiled on a 1°x1° spatial grid
- physical fields derived from CAFE60 ensemble and compiled on the same 1°x1° spatial grid.

Although a suite of ocean variables is available from CAFE60, only those with suitably low pairwise correlation (<0.80) were chosen for inclusion in the BRTs (see Table 2 and Table 3). The same set of variables was used in the whole-region model and sub-region models for all species. The number of trees used in each model, as selected by the cross-validation method described in section 5.1, is provided in Table 4.

Table 2 - Physical predictors from CAFE60 ensemble reanalysis, direct and derived products. Bold indicates those used in BRT models

Variable	Description	Note
<b>sst</b>	Sea Surface Temperature (°C)	equivalent to potential temperature from the top grid cell
<b>sss</b>	Sea Surface Salinity (psu)	
temp50	Temperature at 50m (°C)	potential temperature nearest to 50m depth
temp100	Temperature at 100m (°C)	potential temperature nearest to 50m depth
temp200	Temperature at 200m (°C)	potential temperature nearest to 50m depth
<b>temp500</b>	Temperature at 500m (°C)	potential temperature nearest to 50m depth
<b>mld</b>	Mixed layer depth (m)	standard MOM5 metric based on density criteria
<b>u100, v100</b>	Zonal (U) and meridional (V) velocities at 100m (m/s)	
u100_300, v100_300	Zonal (U) and meridional (V) velocities, depth-integrated 100m-300m (m/s)	
<b>eke300</b>	Mean eddy kinetic energy (EKE) in upper 300m	
hc200	Ocean heat content in upper 200m	
<b>hc300</b>	Ocean heat content in upper 300m	
<b>D20</b>	Depth of 20°C isotherm (m)	Where 20°C isotherm exists in ocean

Table 3 - Pairwise correlation of physical fields from CAFE60 listed in Table 1. The subset in bold were selected for inclusion in the BRTs since all pairwise correlations are < 0.80.

	<i>D20</i>	<i>eke2000</i>	<i>eke300</i>	<i>hc200</i>	<i>hc300</i>	<i>mld</i>	<i>sss</i>	<i>sst</i>	<i>temp100</i>	<i>temp200</i>	<i>temp50</i>	<i>temp500</i>	<i>u100</i>	<i>u100_300</i>	<i>v100</i>	<i>v100_300</i>
<i>D20</i>	1	-0.01	0	0.73	<b>0.79</b>	<b>0.03</b>	<b>-0.08</b>	<b>0.53</b>	0.6	0.81	0.6	<b>-0.43</b>	<b>-0.06</b>	-0.13	<b>0.2</b>	0.2
<i>eke2000</i>	-	1	0.96	0.33	0.21	-0.01	-0.17	0.32	0.35	0	0.35	-0.33	-0.31	-0.38	0.02	0.04
<i>eke300</i>			1	0.3	<b>0.2</b>	<b>-0.05</b>	<b>-0.22</b>	<b>0.3</b>	0.32	0.02	0.33	<b>-0.3</b>	<b>-0.24</b>	-0.32	<b>0</b>	0.04
<i>hc200</i>				1	0.96	-0.19	-0.2	0.85	0.98	0.78	0.91	-0.73	-0.39	-0.58	0.18	0.24
<i>hc300</i>					1	<b>-0.18</b>	<b>-0.15</b>	<b>0.75</b>	0.91	0.91	0.8	<b>-0.6</b>	<b>-0.28</b>	-0.45	<b>0.19</b>	0.23
<i>mld</i>						1	<b>0.34</b>	<b>-0.48</b>	-0.15	-0.2	-0.27	<b>0.15</b>	<b>-0.11</b>	-0.06	<b>-0.02</b>	-0.04
<i>sss</i>							1	<b>-0.31</b>	-0.16	-0.01	-0.25	<b>0.08</b>	<b>-0.18</b>	-0.02	<b>0.14</b>	0.03
<i>sst</i>								1	0.87	0.67	0.95	<b>-0.68</b>	<b>-0.33</b>	-0.49	<b>0.15</b>	0.22
<i>temp100</i>									1	0.73	0.96	-0.74	-0.41	-0.61	0.17	0.23
<i>temp200</i>										1	0.71	-0.41	-0.09	-0.24	0.21	0.19
<i>temp50</i>											1	-0.75	-0.39	-0.58	0.16	0.22
<i>temp500</i>												1	<b>0.39</b>	0.54	<b>-0.18</b>	-0.26
<i>u100</i>													1	0.89	-0.26	-0.2
<i>u100_300</i>														1	-0.22	-0.22
<i>v100</i>															1	0.9
<i>v100_300</i>																1

Table 4 - Number of trees fitted for each species/region combination.

	<b>ALL</b>	<b>EAC</b>	<b>CS</b>	<b>WCP</b>	<b>NZ</b>
<b>YFT</b>	2350	2050	2000	2750	1850
<b>BET</b>	2300	1700	1900	1850	1700
<b>ALB</b>	2300	1400	2150	1500	2000
<b>MLS</b>	3650	2100	1950	2100	2200
<b>SWO</b>	4000	2350	1650	1900	2750

## 5.2.2 Results

### 5.2.2.1 Model performance

Models trained on a 2008-2015 subset of the time series explained a high proportion of deviance observed in the catch in the same training data set for most species and regions (Table 5). Over the broad Western Central and South-West Pacific domain (“all”), models performed well for YFT, BET, ALB and reasonably well for SWO, but deviance explained was notably lower for MLS, presumably owing to a smaller number of records and lower catch numbers. In some cases, sub-regional models performed better than the broad domain model. For example, models for YFT, BET and SWO in the EAC-dominated region, and YFT, BET and ALB in the Coral Sea performed slightly better than the broad domain model (see Table 5).

$R^2$  values for the observed versus predicted CPUE (defined as catch per 10,000 hooks) calculated from the BRT model for each species and region using the training dataset ranged from 0.06-0.46, with values tending to be lowest in the WCP and highest in the EAC and NZ regions (Table 6). The  $R^2$  values for the whole-region model are slightly lower for the validation dataset than the training dataset, whereas they tend to be quite a bit lower for the sub-region models (Table 7). The RMSE values for the validation dataset are very similar to those for the training dataset (Table 10 and Table 11). Overall, however, the predictive performance of the models is low for the validation dataset, with  $R^2$  values rarely above 0.20 (Table 7)

Table 5 - Proportion of deviance explained by CAFE60-based boosted regression tree (BRT) models, for each species and sub-region (ALL = Western Central and South-West Pacific domain; EAC = East Australian Current domain; CS = Coral Sea/Equatorial; WCP = Western Central Pacific; NZ = New Zealand).

	<b>ALL</b>	<b>EAC</b>	<b>CS</b>	<b>WCP</b>	<b>NZ</b>
<b>YFT</b>	0.78	0.81	0.82	0.69	0.80
<b>BET</b>	0.73	0.82	0.76	0.65	0.71
<b>ALB</b>	0.83	0.80	0.83	0.86	0.89
<b>MLS</b>	0.48	0.74	0.40	0.40	0.65
<b>SWO</b>	0.72	0.82	0.52	0.51	0.81

Table 6 - Pearson correlation ( $R^2$ ) of observed and predicted catch-per-unit-effort (CPUE) values for 2008-2015 model training dataset for the CAFE60-based boosted regression tree (BRT) models.

	<b>ALL</b>	<b>EAC</b>	<b>CS</b>	<b>WCP</b>	<b>NZ</b>
<b>YFT</b>	0.20	0.24	0.15	0.10	0.46
<b>BET</b>	0.23	0.21	0.19	0.06	0.21
<b>ALB</b>	0.15	0.32	0.27	0.11	0.31
<b>MLS</b>	0.24	0.24	0.22	0.21	0.26
<b>SWO</b>	0.33	0.43	0.19	0.11	0.37

Table 7 - Pearson correlation ( $R^2$ ) of observed and predicted catch-per-unit-effort (CPUE) per 1° grid cell for 2016-2019 independent testing (validation) dataset for the CAFE60-based boosted regression tree (BRT) models.

	<b>ALL</b>	<b>EAC</b>	<b>CS</b>	<b>WCP</b>	<b>NZ</b>
<b>YFT</b>	0.13	0.09	0.04	0.05	0.07
<b>BET</b>	0.16	0.10	0.07	0.05	0.12
<b>ALB</b>	0.14	0.26	0.15	0.08	0.22
<b>MLS</b>	0.20	0.16	0.05	0.17	0.07
<b>SWO</b>	0.34	0.24	0.19	0.09	0.24

Table 8 - Pearson correlation ( $R^2$ ) of observed and predicted catch per 1° grid cell for 2008-15 model training dataset for the CAFE60-based boosted regression tree (BRT) models.

	<b>ALL</b>	<b>EAC</b>	<b>CS</b>	<b>WCP</b>	<b>NZ</b>
<b>YFT</b>	0.67	0.75	0.74	0.60	0.81
<b>BET</b>	0.63	0.79	0.67	0.52	0.71
<b>ALB</b>	0.79	0.74	0.79	0.85	0.90
<b>MLS</b>	0.43	0.73	0.40	0.33	0.71
<b>SWO</b>	0.61	0.85	0.51	0.42	0.77

Table 9 - Pearson correlation ( $R^2$ ) of observed and predicted catch per 1° grid cell for 2016-19 independent testing (validation) dataset for the CAFE60-based boosted regression tree (BRT) models.

	<b>ALL</b>	<b>EAC</b>	<b>CS</b>	<b>WCP</b>	<b>NZ</b>
<b>YFT</b>	0.58	0.59	0.55	0.46	0.12
<b>BET</b>	0.54	0.47	0.56	0.56	0.41
<b>ALB</b>	0.79	0.64	0.59	0.84	0.76
<b>MLS</b>	0.43	0.63	0.10	0.24	0.27
<b>SWO</b>	0.56	0.71	0.41	0.37	0.45

Table 10 - Root mean squared error (RMSE) values for observed vs predicted CPUE (defined as catch per 10,000 hooks) calculated from the BRT model for each species and region using: the training dataset (2008-2015) for the CAFE60-based boosted regression tree (BRT) models. Mean observed CPUE in parentheses below.

	ALL	EAC	CS	WCP	NZ
<b>YFT</b>	47.5 (35.9)	57.1 (45.5)	67.2 (64.8)	38.0 (31.0)	10.5 (5.8)
<b>BET</b>	15.2 (12.0)	17.1 (14.1)	19.4 (18.4)	7.0 (5.1)	14.9 (11.1)
<b>ALB</b>	88.8 (95.0)	99.5 (82.6)	70.7 (66.4)	85.7 (113.5)	114.5 (118.7)
<b>MLS</b>	2.5 (0.9)	6.2 (4.6)	1.3 (0.3)	1.6 (0.6)	3.7 (1.8)
<b>SWO</b>	17.5 (5.7)	23.0 (25.8)	7.4 (1.6)	2.5 (0.7)	47.1 (44.3)

Table 11 - Root mean squared error (RMSE) values for observed vs predicted CPUE (defined as catch per 10,000 hooks) calculated from the for the CAFE60-based boosted regression tree (BRT) models for each species and region using the validation dataset (2016-2019). Mean observed CPUE in parentheses below.

	ALL	EAC	CS	WCP	NZ
<b>YFT</b>	42.1 (35.0)	52.5 (40.2)	64.5 (57.9)	35.0 (31.4)	19.1 (9.0)
<b>BET</b>	14.5 (11.2)	17.9 (9.9)	19.3 (17.9)	6.4 (5.3)	15.9 (10.0)
<b>ALB</b>	82.4 (85.0)	114.6 (91.5)	70.6 (58.2)	78.9 (102.6)	123.0 (109.0)
<b>MLS</b>	2.4 (0.8)	4.8 (3.7)	1.1 (0.2)	1.2 (0.4)	5.3 (2.1)
<b>SWO</b>	12.7 (4.1)	26.0 (19.0)	3.6 (1.0)	1.5 (0.5)	40.0 (27.4)

### 5.2.2.2 Relative contributions of physical predictors from CAFE60 ensemble

Sub-surface variables that represent upper ocean structure and heat content had the greatest relative contribution in explaining the variability in catch rates of tuna and billfish species over the time series. For YFT, temperature at 500m (temp500), depth of the 20°C isotherm (D20), ocean heat content in the upper 300m (hc300), and mixed-layer depth (mld) contributed the most to the predictive skill of the broad Western Central and South-West Pacific domain model. Indeed, temp500 contributed ~67% to the overall explanation of deviance in the training dataset, with D20, hc300 and mld each contributing ~5%. For BET, temperature at 500m (temp500) remained the most informative predictor in the broad domain (“all”) model (42%), with mixed-layer depth, depth of the 20°C isotherm (D20), and sea surface salinity (sss) also making contributions of >10% to overall predictive skill. For ALB, temp500 contributed ~23% to the overall explanation of deviance in the training dataset, with sst, sss, u100, D20 each also contributing >10%. For MLS, sst (29%), D20 (26%) and hc300 (21%) made the highest relative contributions, although this model

had much lower deviance explained (48%) than for other species in this broad-scale region (Table 5). For SWO, hc300 (39%), temp500 (24%), D20 (14%), v100 (13%) were the most informative predictors of CPUE.

Temperature at 500m emerged as an informative predictor of CPUE for all species in the broad Western Central and South-West Pacific region, with the exception of MLS. Metrics of upper ocean structure and heat content including D20, hc300 and mld were informative predictors across several species, notably for tuna, indicating that these predictors capture some of the variability in the physical environment that contributes to the spatial structuring of CPUE of tuna and billfish across the Western Central and South-West Pacific.

Relative variable importance in regional sub-domain models was notably different in comparison with the whole Western Central and South-West Pacific model for particular species/regions combinations. For example, sst and hc300 were of greater relative importance in the YFT model for the EAC-dominated region than for the broader domain model. For BET and ALB, mld and hc300 were of increased influence in the EAC region with respect to the broader domain, and for SWO, the influence of v100 was markedly higher in the EAC region. These results are in accordance with our understanding of the physical dynamics of the EAC-dominated region, in which mesoscale and sub-mesoscale variability dominates around the southward flowing, warm-water western boundary current.

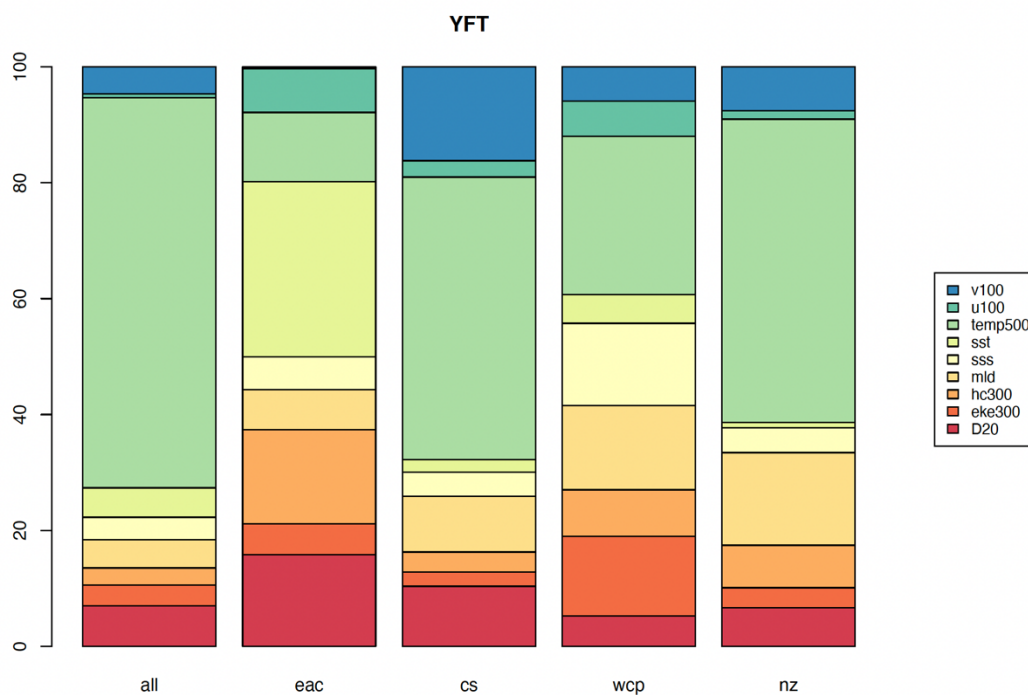


Figure 43 - Relative contributions of physical fields from CAFÉ-60 ensemble to overall deviance explained by models of YFT CPUE in the five model domains (“all” = Western Central and South-West Pacific; “eac” = EAC-dominated region; “cs” = Coral Sea; “wcp” = Western Central Pacific; “nz” = New Zealand). Variable names described in Table 2.

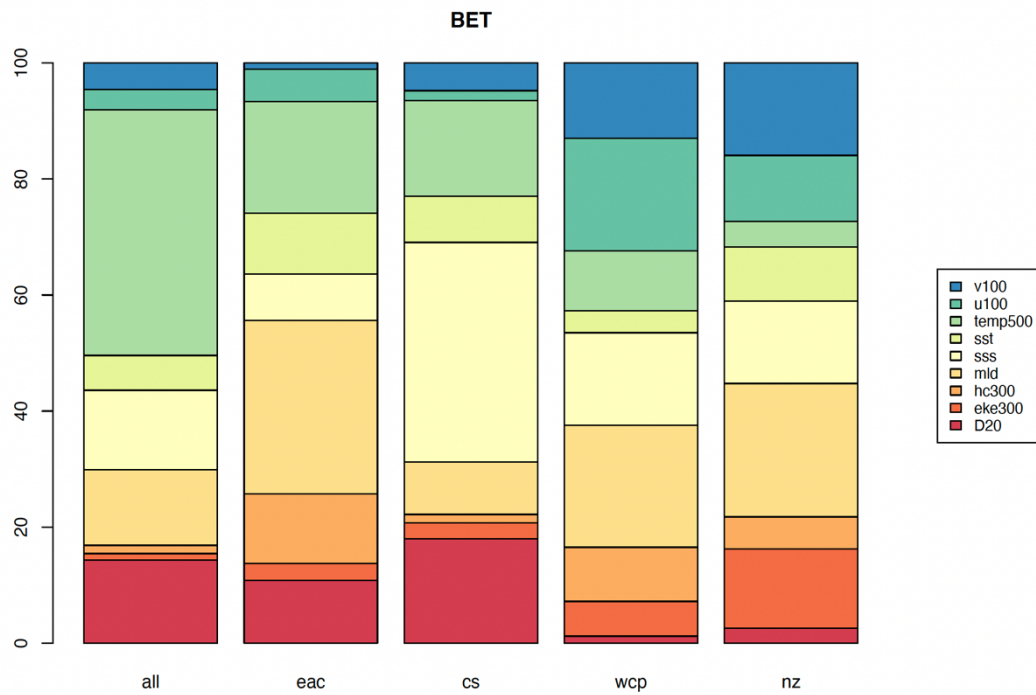


Figure 44 - Relative contributions of physical fields from CAFÉ-60 ensemble to overall deviance explained by models of BET CPUE in the five model domains (“all” = Western Central and South-West Pacific; “eac” = EAC-dominated region; “cs” = Coral Sea; “wcp” = Western Central Pacific; “nz” = New Zealand).

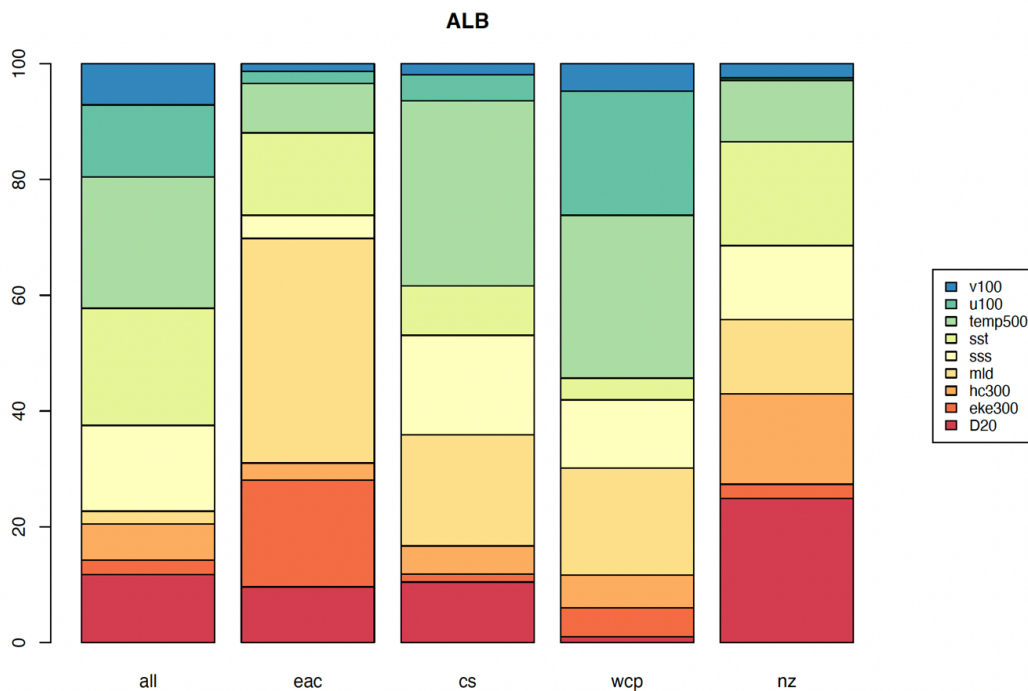


Figure 45 - Relative contributions of physical fields from CAFÉ-60 ensemble to overall deviance explained by models of ALB CPUE in the five model domains (“all” = Western Central and South-West Pacific; “eac” = EAC-dominated region; “cs” = Coral Sea; “wcp” = Western Central Pacific; “nz” = New Zealand).

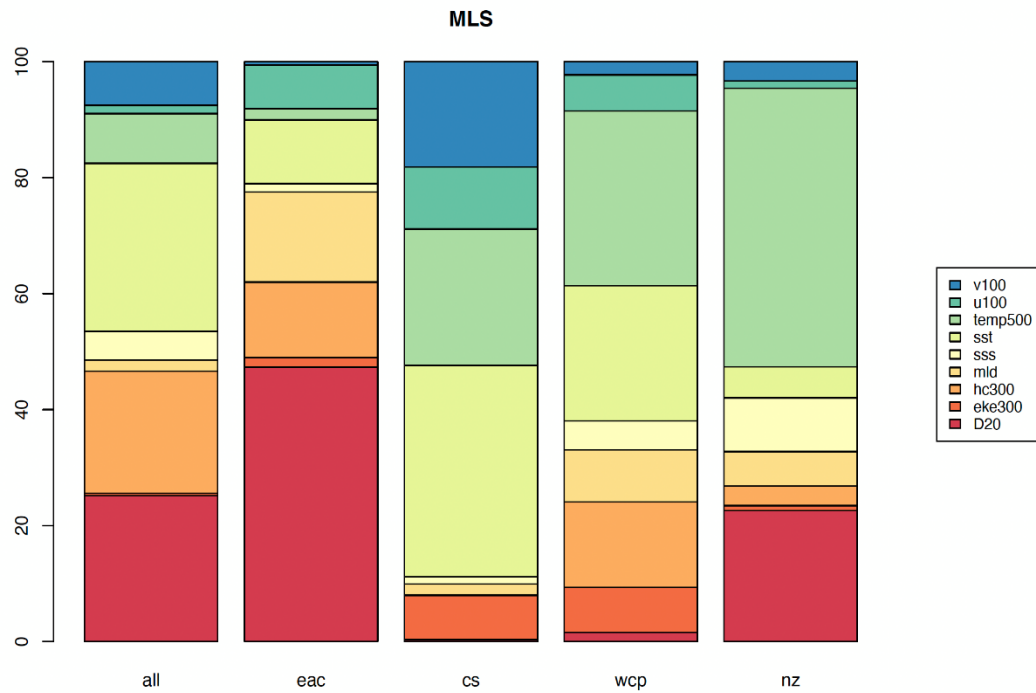


Figure 46 - Relative contributions of physical fields from CAFÉ-60 ensemble to overall deviance explained by models of MLS CPUE in the five model domains (“all” = Western Central and South-West Pacific; “eac” = EAC-dominated region; “cs” = Coral Sea; “wcp” = Western Central Pacific; “nz” = New Zealand).

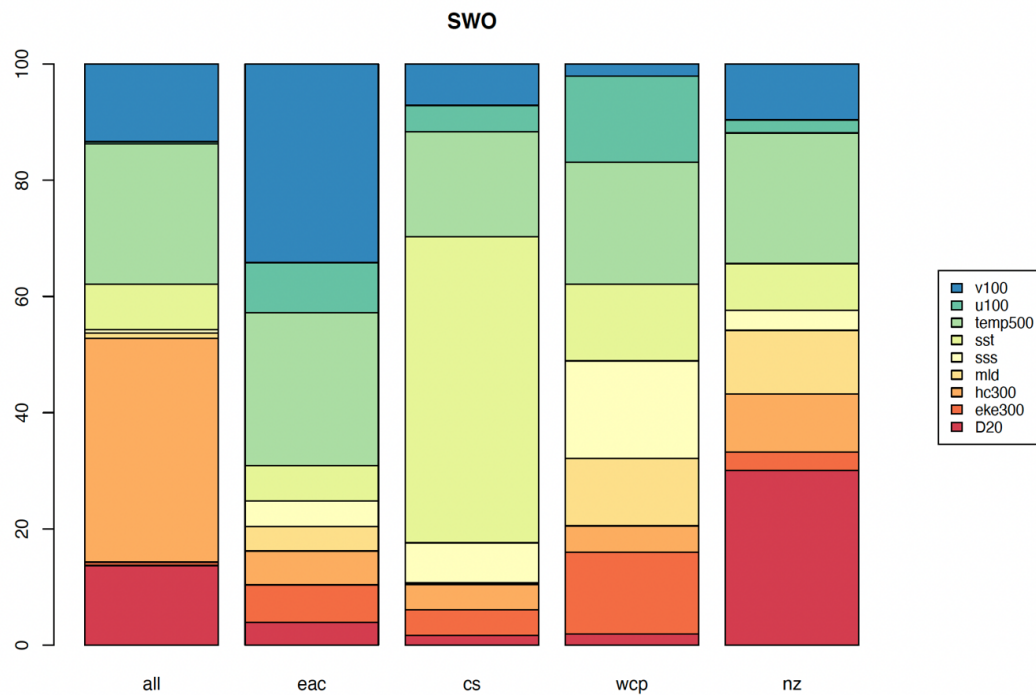


Figure 47 - Relative contributions of physical fields from CAFÉ-60 ensemble to overall deviance explained by models of SWO CPUE in the five model domains (“all” = Western Central and South-West Pacific; “eac” = EAC-dominated region; “cs” = Coral Sea; “wcp” = Western Central Pacific; “nz” = New Zealand).

### 5.2.2.3 Spatial predictions of CPUE

Models were able to capture some of the seasonal spatial structuring of CPUE, with spatial predictions generally mirroring the observed distribution of CPUE at seasonal timescales. Seasonal spatial CPUE predictions resulting from the best performing species-region combination models

are shown in Figure 48 - Figure 52, with additional plots of spatial predictions of each species-region combination included in Appendix 2.

Mean predicted CPUE for YFT in winter (Dec-Feb), the season of peak YFT catches in Australia's Eastern Tuna and Billfish Fishery, approximated the observed mean seasonal CPUE over the same time period (model validation period, 2016-19), highlighting high CPUE around the Solomon Islands, Western Central Pacific, Coral Sea and East Australian Current regions (Figure 48). Similarly, the BET model for the broad Western Central and South-West Pacific recreated the general pattern of spatial structuring of CPUE for Autumn (Mar-May) for the model validation time period, 2016-19 (Figure 49).

Some smoothing of observed CPUE hotspots into gradients of high-low CPUE is evident in the spatial predictions, owing to the gradients in physical ocean data fields used to predict from the models (Figure 48 - Figure 52). This may represent more generalisable patterns in what might be expected in terms of CPUE at seasonal timescales than the more patchy observed CPUE, which is driven by a range of fishery, ecological and physical factors that may not have been adequately represented in this correlative modelling based on physical variability as a sole driver of CPUE variability in space and time.

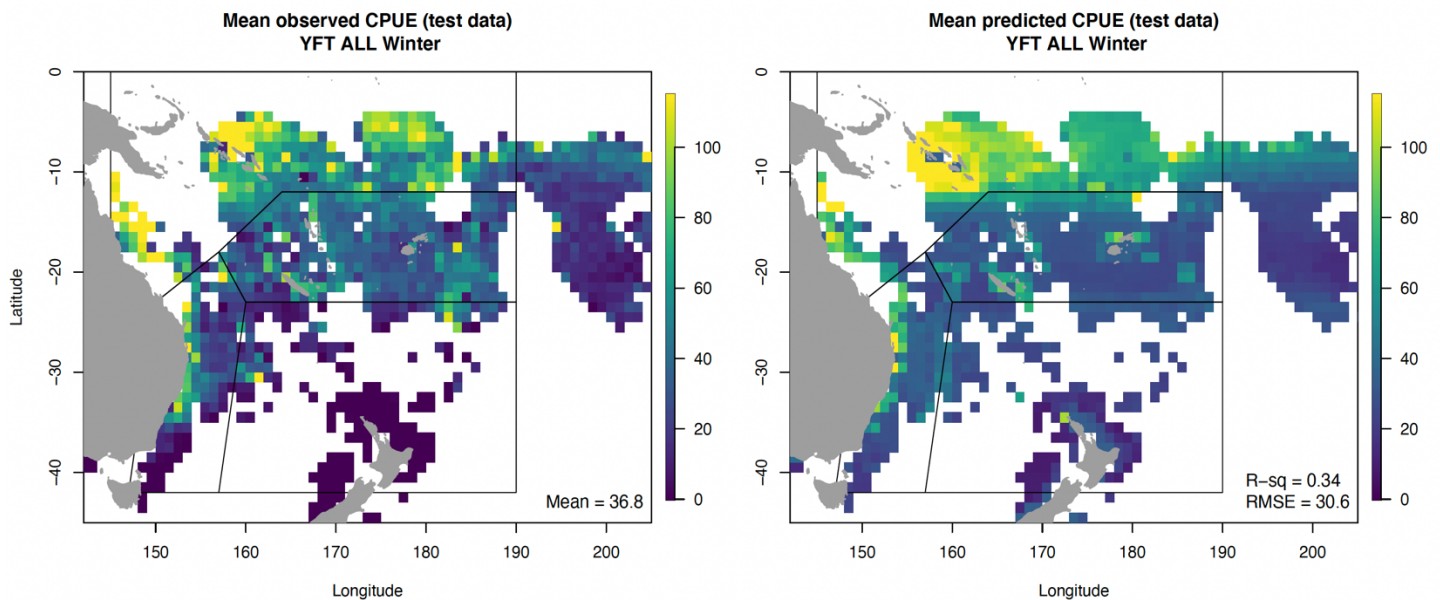


Figure 48 - Seasonal mean of predicted vs. observed catch-per-unit-effort (CPUE, per 10000 hooks) of YFT for winter (Dec-Feb), predicted from the broad Western Central and South-West Pacific domain and averaged across the testing (validation) dataset, 2016-19. The mean observed CPUE over the EAC sub-region is given in the lower corner of the observed map, whereas Pearson's  $R^2$  value and the root mean squared error (RMSE) are given in the lower corner of the prediction map as an indicator of predictive performance.

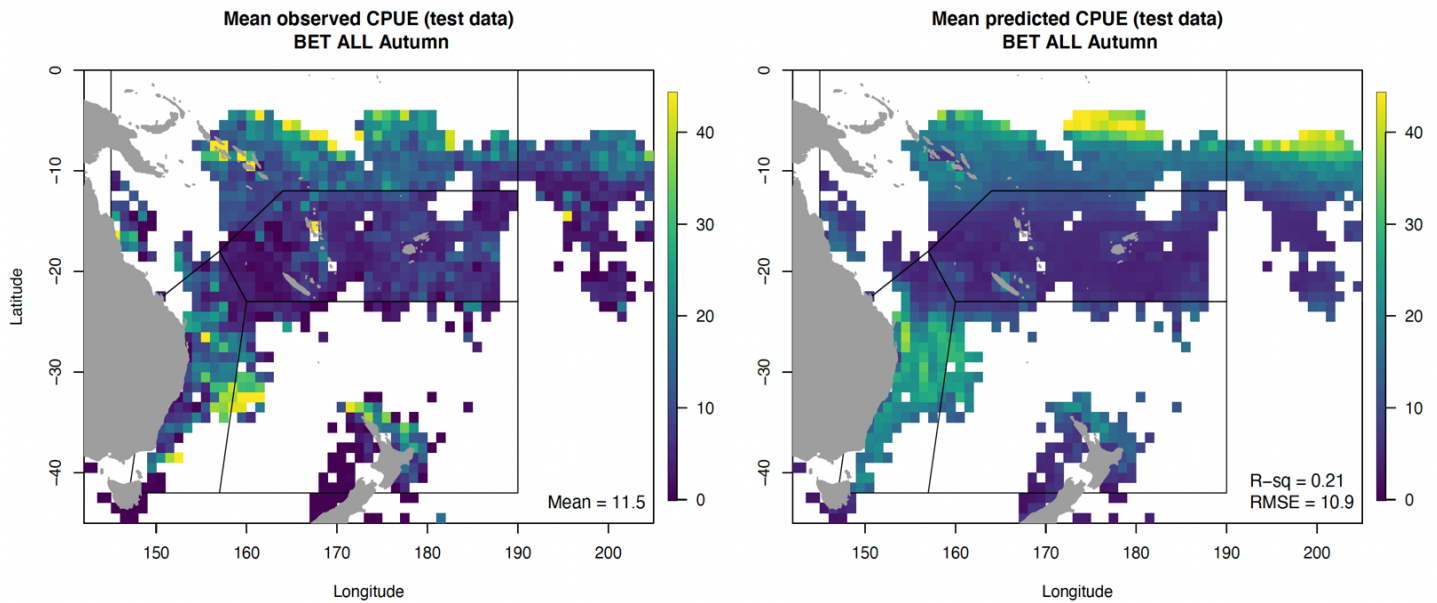


Figure 49 - Seasonal mean of predicted vs. observed catch-per-unit-effort (CPUE, per 10000 hooks) of BET for autumn (Mar-May), predicted from the broad Western Central and South-West Pacific domain and averaged across the testing (validation) dataset, 2016-19. The mean observed CPUE over the EAC sub-region is given in the lower corner of the observed map, whereas Pearson's  $R^2$  value and the root mean squared error (RMSE) are given in the lower corner of the prediction map as an indicator of predictive performance.

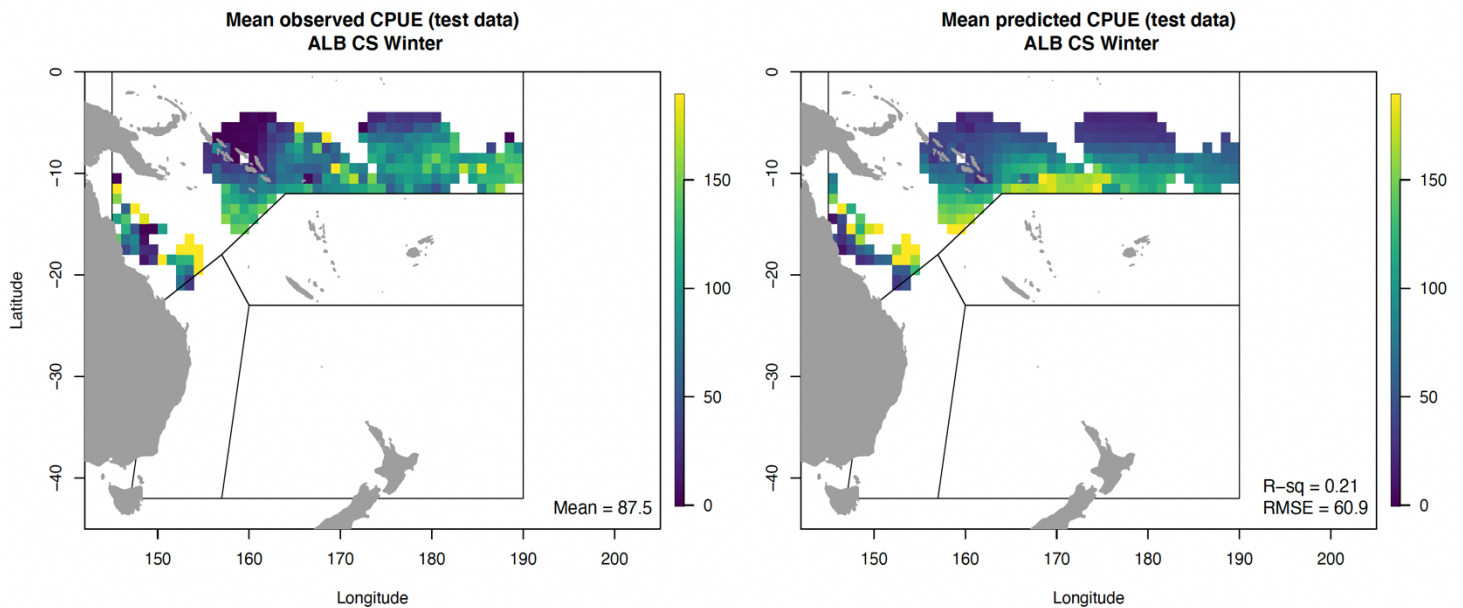


Figure 50 - Seasonal mean of predicted vs. observed catch-per-unit-effort (CPUE, per 10000 hooks) of ALB for winter (Dec-Feb), predicted from the Coral Sea domain and averaged across the testing (validation) dataset, 2016-19. The mean observed CPUE over the EAC sub-region is given in the lower corner of the observed map, whereas Pearson's  $R^2$  value and the root mean squared error (RMSE) are given in the lower corner of the prediction map as an indicator of predictive performance.

The mean predicted CPUE per 10,000 hooks for SWO in Spring (Sept-Nov) in the EAC region, the time of peak catches in the ETBF, also reflects the observed distribution of CPUE for this species during the model validation time period, 2016-19 (Figure 51, Figure 52). Highest CPUE values ( $\leq 50$  per 10,000 hooks) were predicted in the central, offshore quadrant of the EAC-dominated region, as per the corresponding seasonal observations for Spring. The EAC-dominated sub-region model exhibited marginally greater predictive skill ( $R^2 = 0.3$ ; Figure 51; Table 5 - Table 9) than the broad Western Central and South-West Pacific model, but both captured the overall spatial structuring of SWO catch in Spring, with the broader domain model also highlighting higher CPUE

in the mid-latitudes east of the EAC-dominated region and to the north-west of New Zealand (Figure 52).

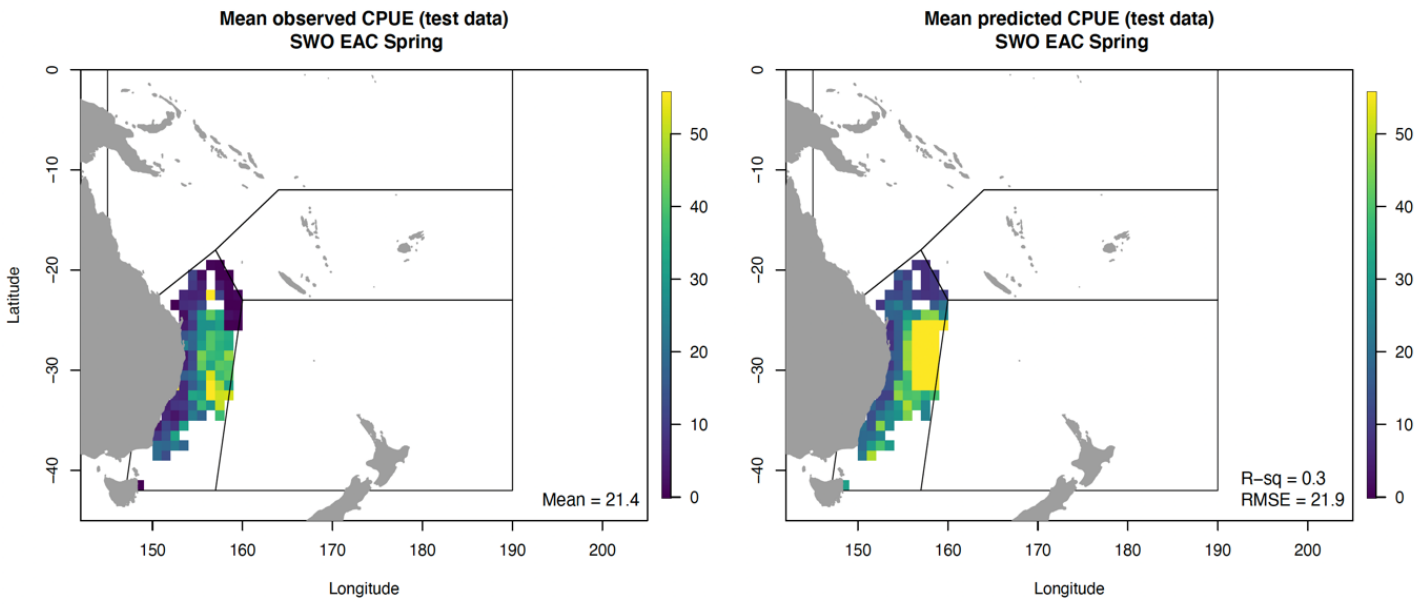


Figure 51 - Seasonal mean of predicted vs. observed catch-per-unit-effort (CPUE, per 10000 hooks) of SWO for spring (Sept-Nov), predicted from the EAC-dominated model domain and averaged across the testing (validation) dataset, 2016-19. The mean observed CPUE over the EAC sub-region is given in the lower corner of the observed map, whereas Pearson's  $R^2$  value and the root mean squared error (RMSE) are given in the lower corner of the prediction map as an indicator of predictive performance.

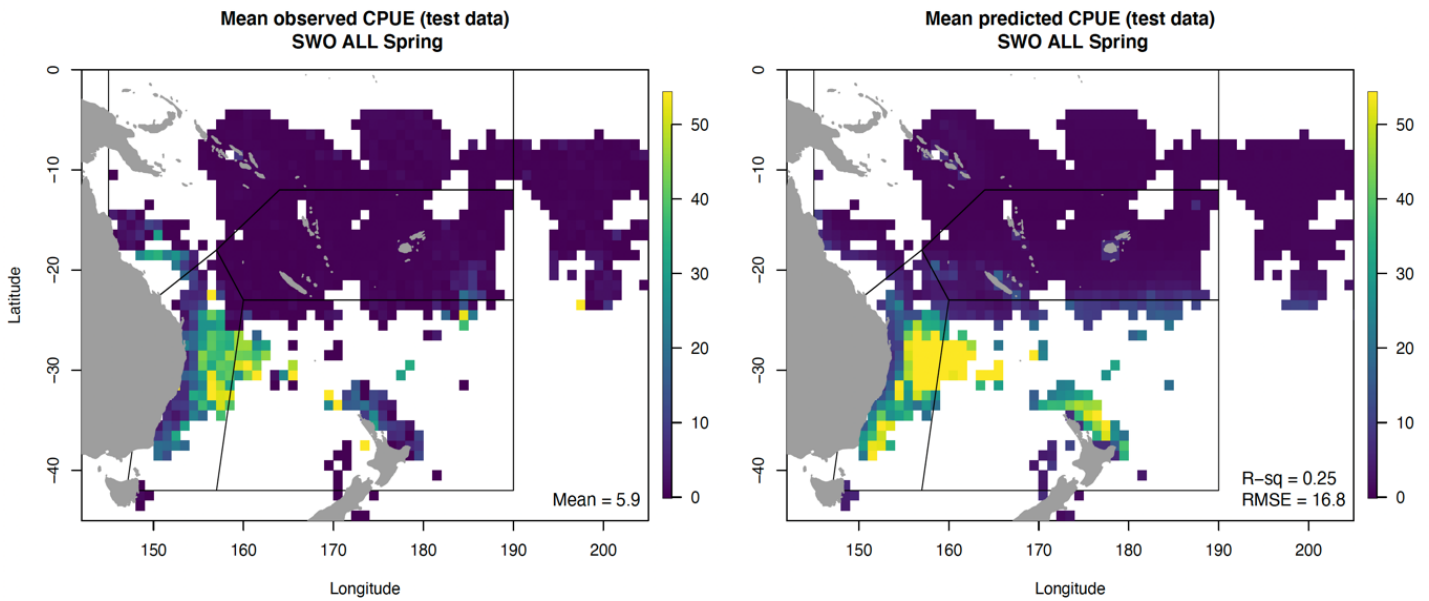


Figure 52 - Seasonal mean of predicted vs. observed catch-per-unit-effort (CPUE, per 10000 hooks) of SWO for spring (Sept-Nov), predicted from the broad Western Central and South-West Pacific domain and averaged across the testing (validation) dataset, 2016-19. The mean observed CPUE over the EAC sub-region is given in the lower corner of the observed map, whereas Pearson's  $R^2$  value and the root mean squared error (RMSE) are given in the lower corner of the prediction map as an indicator of predictive performance.

#### 5.2.2.4 Effects of physical predictors from CAFE60 ensemble on CPUE

Physical predictors from the CAFE60 ensemble had different effects on predicted CPUE of each species in each region. Figures below show the most influential predictors for case studies highlighted in spatial plots above, with complete sets for each species/region combination included in Appendix 2.

For example, for YFT and BET, cooler temperatures at 500m (<8°C) were associated with higher predicted CPUE (Figure 53, Figure 54) in the broad Western Central and South-West Pacific model, and for ALB in the Coral Sea, while warmer temperatures at 500m (>10C) were associated with higher SWO CPUE in both the broad domain and EAC-dominated region. Our hypothesis is that the importance of temperature at depth relates to both the thermal physiological limits of the fish as well as vertical habitat compression pushing fish higher into the water column, into the depth range of the fishery and thus increasing catchability. For YFT, which are thermally constrained predominantly to the mixed layer in the upper ocean, cooler temperatures at depth may increase catchability through vertical habitat compression. For SWO, which are known to perform diurnal dives to greater depths than YFT, warmer temperatures at depth may be more likely to increase the likelihood of presence in that general location, as areas with warmer temperatures at 500m would be more broadly favourable habitat for SWO.

Depth of the 20°C isotherm (D20) was an influential predictor across several of the models for YFT, BET, ALB and SWO, particularly in the broad Western Central and South-West Pacific domain (Figure 53 - Figure 56). In all cases, CPUE decreased as the depth of the 20° isotherm increased, particularly beyond 150-200m. This reinforces our hypothesis of vertical habitat compression influencing CPUE, as a deeper 20°C isotherm would enable thermally constrained, vertically migrating fish to access deeper habitats and reducing catchability in the upper 200m of the water column. However, D20 was found to have an inverse effect for ALB in the Coral Sea (Figure 55), with a shoaling isotherm increasing ALB catchability. Sea surface salinity (sss) was also important for ALB in the Coral Sea, with higher CPUE associated with less saline water masses, presumably owing to the relatively uniform nature of temperature in the Coral Sea with respect to salinity.

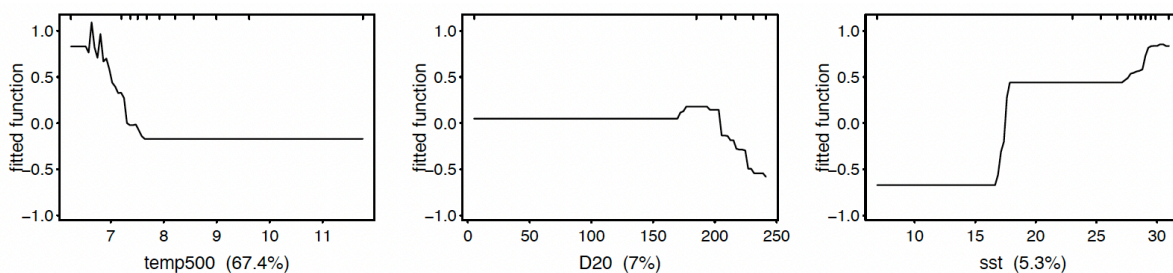


Figure 53 - Marginal effects plots for YFT Western Central and South-West Pacific model, showing most influential predictors.. The rug plot along the top axis marks deciles in the data, so the marginal effect functions are of most relevance within the 10<sup>th</sup> and 90<sup>th</sup> deciles (i.e., between the second and tenth marks).

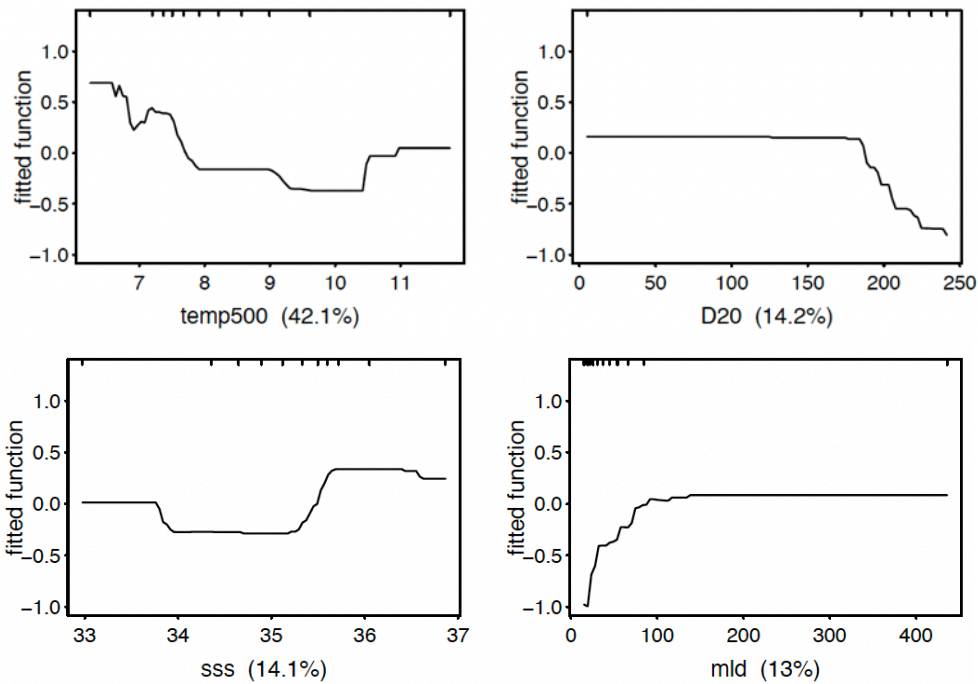


Figure 54 - Marginal effects plots for BET Western Central and South-West Pacific model, showing most influential predictors. The rug plot along the top axis marks deciles in the data, so the marginal effect functions are of most relevance within the 10<sup>th</sup> and 90<sup>th</sup> deciles (i.e., between the second and tenth marks).

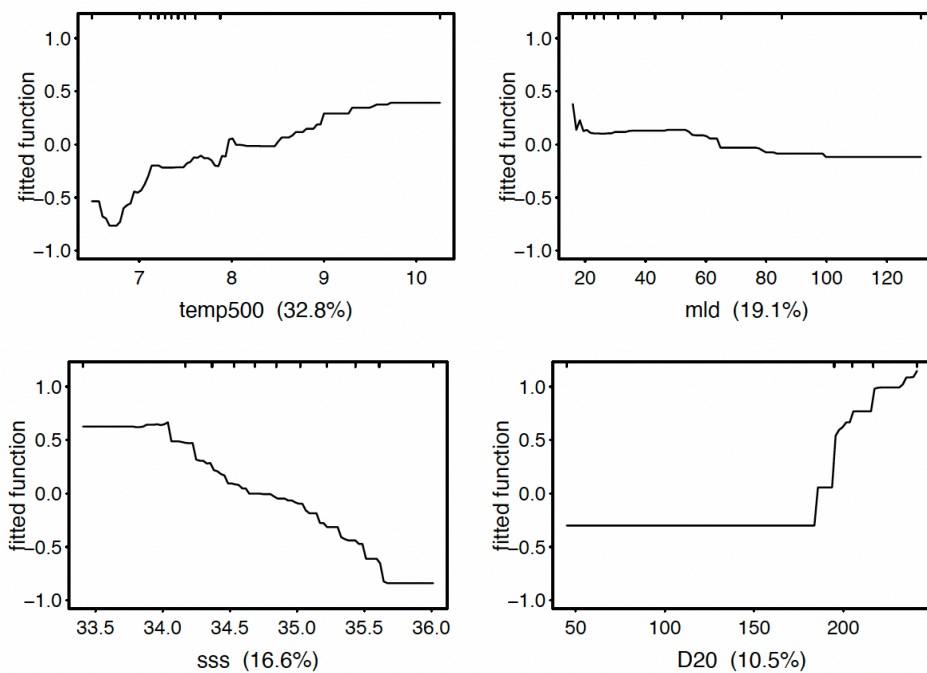


Figure 55 - Marginal effects plots for ALB Coral Sea model, showing most influential predictors. The rug plot along the top axis marks deciles in the data, so the marginal effect functions are of most relevance within the 10<sup>th</sup> and 90<sup>th</sup> deciles (i.e., between the second and tenth marks).

Southward zonal velocity (v100) was an influential predictor of SWO CPUE, both in the EAC-dominated regional model and the broad Western Central and South-West Pacific model, which is to be expected given the dominance of the southward-flowing East Australian Current in this sub-region, and the high CPUE for SWO co-located with the EAC and to its east.

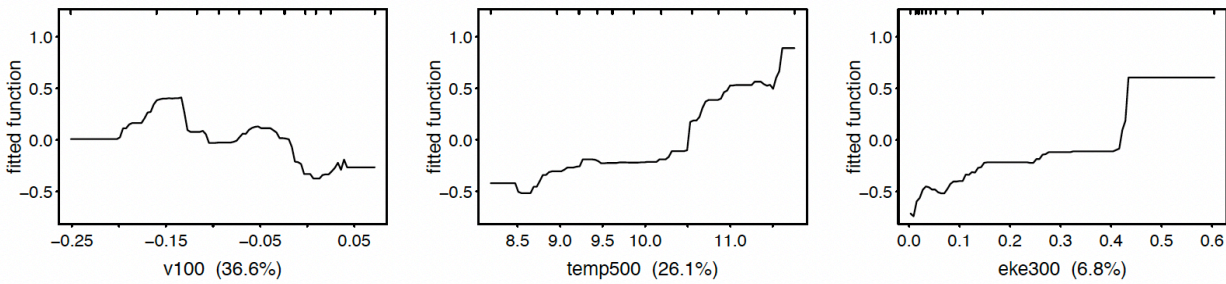


Figure 56 - Marginal effects plots for SWO EAC-dominated model, showing most influential predictors. The rug plot along the top axis marks deciles in the data, so the marginal effect functions are of most relevance within the 10<sup>th</sup> and 90<sup>th</sup> deciles (i.e., between the second and tenth marks).

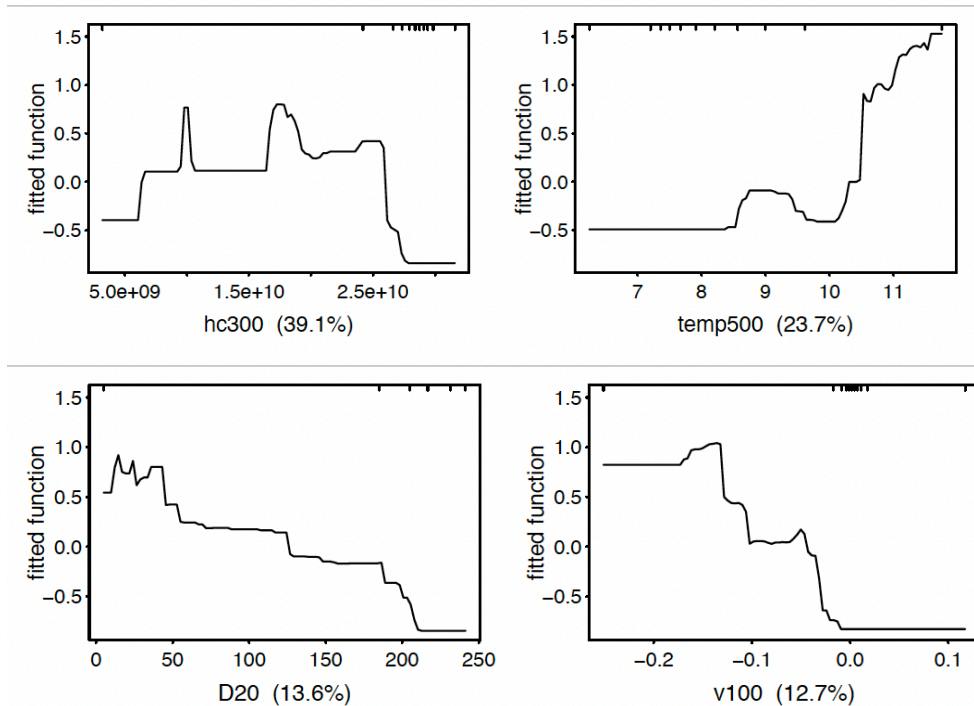


Figure 57 - Marginal effects plots for SWO Western Central and South-West Pacific model, showing most influential predictors. The rug plot along the top axis marks deciles in the data, so the marginal effect functions are of most relevance within the 10<sup>th</sup> and 90<sup>th</sup> deciles (i.e., between the second and tenth marks).

### 5.2.2.5 Total catch, observed and predicted over 2008-19 time series

Inter-annual trends in total catch of each species over the broad Western Central and South-West Pacific model domain were reproduced reasonably well for YFT ( $R^2=0.858$ ; Figure 58) and BET ( $R^2=0.91$ ; Figure 59), demonstrating some level of skill in the model, although the magnitude of extreme peak catches (e.g. YFT in 2012, 2014; BET in 2012, 2015) were not captured in model predictions. Extreme peak catches of ALB in the Coral Sea were similarly not captured by model predictions, although the model recreated inter-annual trends in total catch for the independent validation period with some skill ( $R^2=0.82$ ; Figure 60). The failure of models to capture extreme peaks and troughs is likely a result of an incapacity of correlative statistical modelling techniques such as boosted regression trees to capture the multifaceted drivers of fish catchability, including population-level processes occurring at ocean-basin scales. Models presented here capture only the proximate influence of physical variability on catch rates and so cannot represent population fluctuations or changing recruitment, etc., that influence inter-annual variability in total catch.

Inter-annual trends in total catch of SWO in the EAC-dominated region were captured by the model with reasonable skill ( $R^2=0.60$ ), particularly during the model training period (2008-15), but less so in the independent validation dataset, presumably owing to similar population-level or stock-level processes that our models have not captured, non-stationarity in fish and fisher responses to environmental conditions, and/or inter-periodic variability in environmental conditions. However, the EAC-dominated regional model did outperform the broad Western Central and South-West Pacific model for SWO, which dramatically over-predicted total catch of SWO in the independent model validation period (2016-19). It should be noted that predictions of total catch include the number of hooks used in each grid cell in addition to ocean data fields.

Inter-annual trends in observed and predicted total catch for other species/region combinations are shown in Appendix 2.

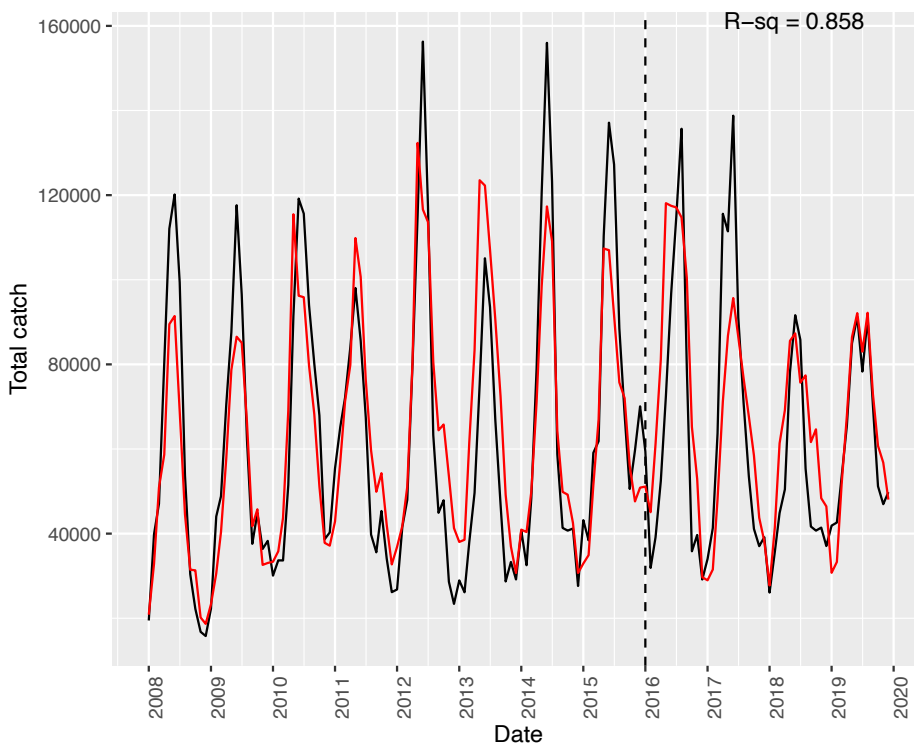


Figure 58 - Observed (black line) and predicted (red line) total catch of YFT over the broad Western Central and South-West Pacific ("all") domain, as sum of total catch across all 1° grid cells per month over the time series 2008-19. Dashed line shows separation of model training (2008-15) and validation (2016-19) datasets.

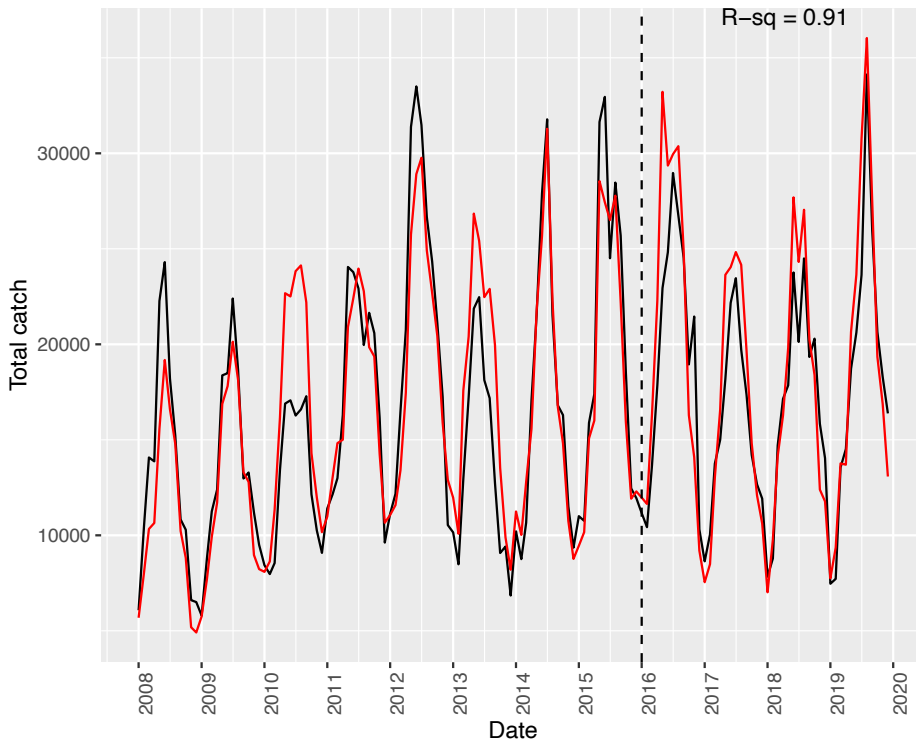


Figure 59 - Observed (black line) and predicted (red line) total catch of BET over the broad Western Central and South-West Pacific (“all”) domain, as sum of total catch across all 1° grid cells per month over the time series 2008-19. Dashed line shows separation of model training (2008-15) and validation (2016-19) datasets.

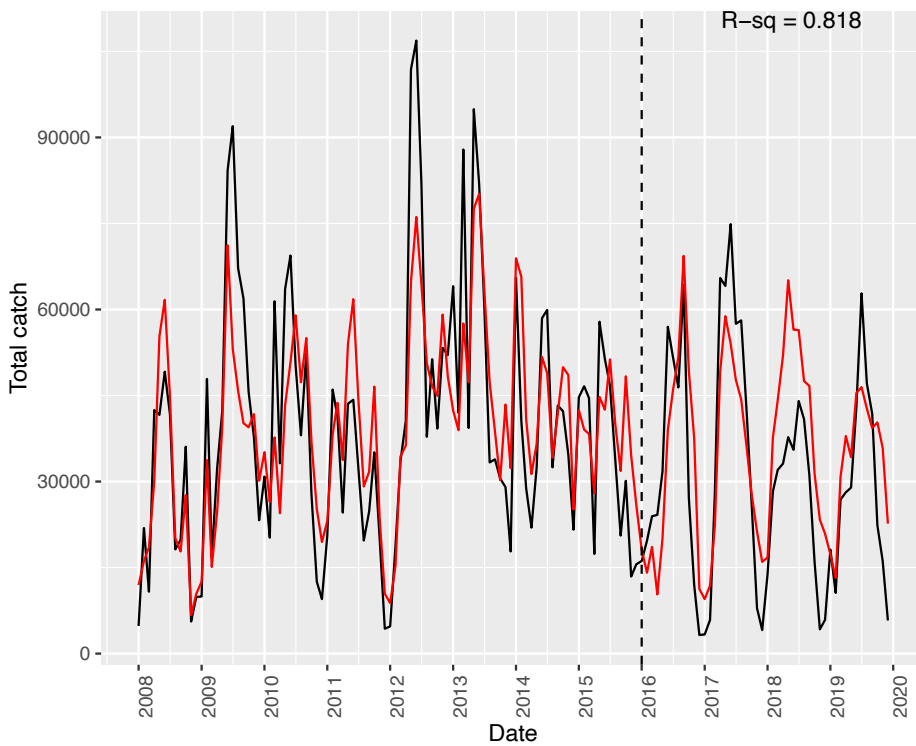


Figure 60 - Observed (black line) and predicted (red line) total catch of ALB in the Coral Sea domain, as sum of total catch across all 1° grid cells per month over the time series 2008-19. Dashed line shows separation of model training (2008-15) and validation (2016-19) datasets.

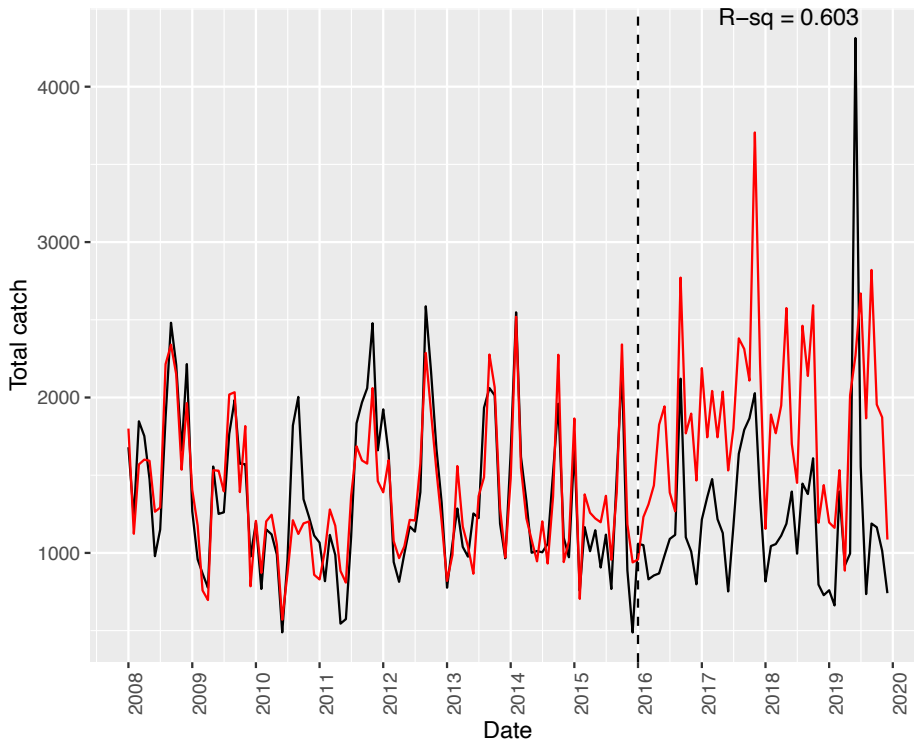


Figure 61 - Observed (black line) and predicted (red line) total catch of SWO in the EAC-dominated region, as sum of total catch across all 1° grid cells per month over the time series 2008-19. Dashed line shows separation of model training (2008-15) and validation (2016-19) datasets.

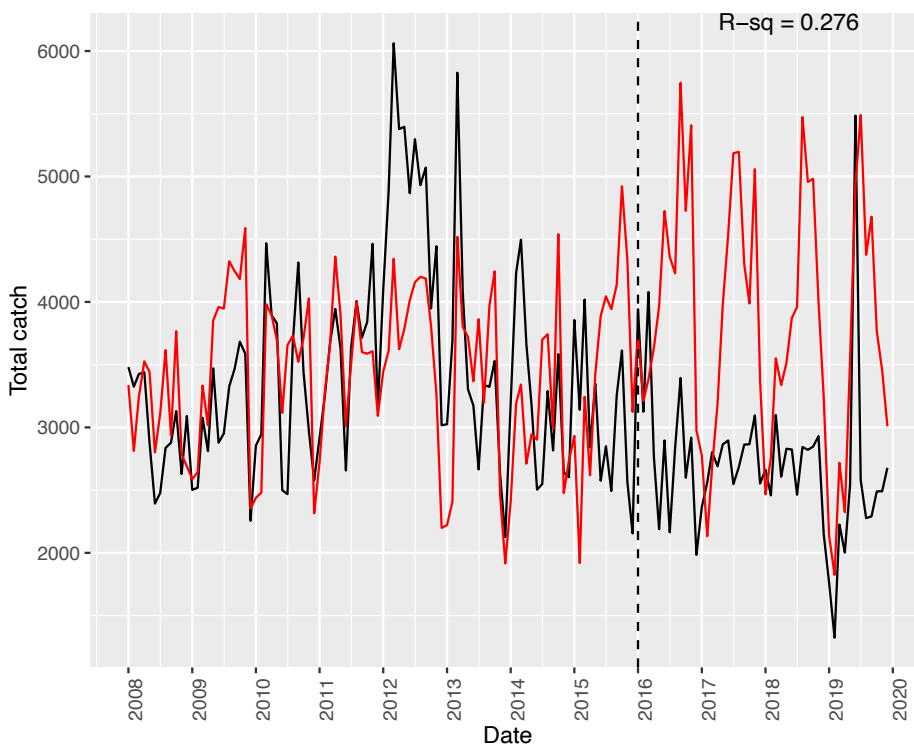


Figure 62 - Observed (black line) and predicted (red line) total catch of SWO over the broad Western Central and South-West Pacific (“all”) domain, as sum of total catch across all 1° grid cells per month over the time series 2008-19. Dashed line shows separation of model training (2008-15) and validation (2016-19) datasets.

## 5.3 BRT using ACCESS-S2

### 5.3.1 Methods

BRTs were fit to the catch and effort data for each of the five target species following the methods described in section 5.1, using as inputs:

- catch and effort data compiled on a 0.25° x 0.25° spatial grid
- ACCESS-S2 oceanographic data compiled on the same 0.25° x 0.25° spatial grid.

Although a suite of ocean variables is available from ACCESS-S2, only those with suitably low pairwise correlation (<0.80) were chosen for inclusion in the BRTs (see Table 12 and Table 13). The same set of variables was used in the whole-region model and sub-region models for all species. The number of trees used in each model, as selected by the cross-validation method described section 5.1, is provided in Table 14.

### 5.3.2 Results

#### 5.3.2.1 Model performance

The BRT models explained a reasonably high proportion of deviance in the catch data (>0.50) for most species and regions, with exceptions for MLS in all regions but the NZ sub-region, all species except ALB in the WCP sub-region, and SWO in the CS sub-region (Table 4). Lower performance for these species and regions may, at least in part be, due to lower catch numbers. However, as was cautioned in section 5.1, these deviance-explained statistics pertain to the catch, and include the number of hooks in determining how much of the deviance was explained by the model. It's not surprising that catch is strongly correlated with number of hooks; what we are interested in here is how much the ocean variables influence the catch rate (CPUE), and which ones have the strongest influence. As such, we will focus on performance statistics ( $R^2$  and RMSE) measuring how well CPUE is predicted by the models.

$R^2$  values for the observed versus predicted CPUE (defined as catch per 10,000 hooks) calculated from the BRT model for each species and region using the training dataset ranged from 0.05-0.39, with values tending to be lowest in the WCP and highest in the EAC and NZ regions (Table 16, left). The  $R^2$  values for the whole-region model are only slightly lower for the validation dataset than the training dataset, whereas they tend to be quite a bit lower for the sub-region models (Table 16, right). The RMSE values for the validation dataset are very similar to those for the training dataset, and even slightly lower in some cases (Table 17). Overall, however, the predictive performance of the models is low for the validation dataset, with  $R^2$  values < 0.20 for all species and regions except SWO for the whole domain and the EAC and NZ sub-regions, and RMSE values greater than the mean CPUE for almost all species and regions.

#### 5.3.2.2 Relative contributions of ocean predictors

Although predictive power of the models is generally low, it is still of interest to consider which ocean variables are contributing the most to explaining the deviance in the CPUE for each species and region. As can be seen in Figure 63(a-e), the variables that are most influential vary significantly, both between region for a given species and between species for a given region. For example, for YFT, sea surface salinity (sss) was the most influential variable in the whole domain model, whereas mixed layer depth (mld1) and temperature at 500 m (temp500) came out as most

influential in the EAC sub-region. For BET, sea surface temperature (sst) and depth of the thermocline (td) were most influential in the whole domain model, whereas mld1 came out as the best predictor in the EAC sub-region. For SWO, temp500 dominated in all of the sub-region models, even though, interestingly, sea surface temperature (sst) and heat content in the upper 300 m (hc300) were most influential in the whole domain model.

### **5.3.2.3 Effects of ocean predictors on CPUE**

Once the most influential variables were identified, it was of interest to see what relationship they have with CPUE. For example, in the whole-domain models, marginal effects plots show that CPUE is expected to decrease as sss increases for YFT, and to increase as sst and td increase for BET (Figure 64a,b). For SWO, CPUE tends to decrease as hc300 increases, but the relationship with sst is more complex, and in fact appears relatively flat over the range of sst values most common in the dataset (Figure 64c). In the EAC sub-region models, CPUE of YFT is expected to decrease as temp500 increases, but the relationship with mld1 is more complex and suggests CPUE first declines then increases slightly as mld1 increases from 0 to 90 m (the range over which most of the data occur) (Figure 65). The relationship between CPUE and mld1 for BET in the EAC sub-region is simpler to interpret, with CPUE showing an almost linear increase as mld1 increases over the range of most relevance (Figure 65b). Similarly, for SWO in the EAC sub-region, CPUE shows an almost linear increase as temp500 increases (Figure 65c).

Although we have chosen to concentrate on results for YFT, BET and SWO from the whole-domain models and the EAC sub-region model, the full set of marginal effects plots for all species and regions can be found in Appendix 2.

### **5.3.2.4 Spatial predictions of CPUE**

Spatial maps showing the average observed and average predicted CPUE values for a given species, region and season are useful for highlighting areas where the models perform better or worse. The whole-domain models tend to do a reasonable job at capturing the overall pattern in CPUE across space, but often do not succeed in predicting specific areas of high and low CPUEs (Figure 66). For example, the whole-domain model for YFT in winter underestimates the high CPUE values observed off the north-eastern coast of Australia in the CS sub-region, in the eastern part of the WCP sub-region, and along the coast in the south of the EAC sub-region (Figure 66a). For BET, the whole domain model tends to predict more average CPUE values across space than was observed in autumn (i.e., it tends to underpredict high CPUEs and overpredict low CPUEs) (Figure 66b). The SWO model performs well at predicting the high catch rates off the central east coast of Australia in summer but overestimates the lower catch rates directly to the south (Figure 66c).

In some cases, the sub-region models were able to improve upon the predictive performance of whole-domain models. For example, for YFT in the winter, the EAC sub-region model better predicts the higher CPUEs along the coast, although tends to slightly overestimate them (Figure 67a). For SWO in summer, the EAC sub-region model does not overestimate the CPUE off the

southeast coast as much as the whole domain model while still predicting the high values off the central east coast (Figure 67c).

Although we have chosen to concentrate on results for YFT, BET and SWO from the whole-domain models and the EAC sub-region model, the full set of observed and predicted spatial maps for all species, regions and seasons can be found in Appendix 2.

*Table 12. List of oceanographic variables available from the ACCESS-S2 reanalysis data (direct and derived products), except for bathymetry taken from TerrainBase (<https://www.ngdc.noaa.gov/mgg/gravity/1999/document/html/tbase.html>). Bold indicates those included in the BRTs.*

Variable name	Description
d20	Depth of 20°C isotherm
eke2000	Eddy kinetic energy - weighted sum of 0-300m
<b>eke300</b>	Eddy kinetic energy - weighted sum of 0-2000m
<b>hc300</b>	Heat content - upper 300m
<b>mld1</b>	Mixed layer depth
<b>ssh</b>	Sea surface height (corrected)
<b>sss</b>	Sea surface salinity
<b>sst</b>	Sea surface temperature
<b>td</b>	Thermocline depth
t100	Temperature at 100m
t200	Temperature at 200m
t50	Temperature at 50m
<b>t500</b>	Temperature at 500m
<b>u100</b>	East/west velocity at 100m
u100-300	East/west velocity - weighted mean of 100-300m
<b>v100</b>	North/south velocity at 100 m
v100-300	North/south velocity - weighted mean of 100-300m
<b>bathy</b>	Bathymetry

Table 13. Pairwise correlations between all ocean variables listed in Table 12. The subset in bold were selected for inclusion in the BRTs since all pairwise correlations are < 0.80.

	d20	eke2000	<b>eke300</b>	<b>hc300</b>	mld1	ssh	sss	sst	td	temp100	temp200	temp50	<b>temp500</b>	u100	u100-300	<b>v100</b>	v100-300	<b>bathy</b>
d20	1.00	-0.29	-0.30	0.84	-0.01	0.66	-0.08	0.61	0.22	0.69	0.87	0.63	-0.37	-0.08	-0.13	0.15	0.14	-0.08
eke2000		1.00	0.93	-0.16	0.05	-0.12	-0.02	-0.15	0.01	-0.14	-0.24	-0.14	0.15	0.11	0.11	-0.19	-0.19	-0.09
<b>eke300</b>			1.00	<b>-0.18</b>	<b>0.04</b>	<b>-0.12</b>	<b>0.00</b>	<b>-0.18</b>	<b>-0.02</b>	-0.18	-0.24	-0.18	<b>0.18</b>	<b>0.13</b>	0.12	<b>-0.20</b>	-0.20	<b>-0.06</b>
<b>hc300</b>				1.00	<b>-0.13</b>	<b>0.70</b>	<b>-0.14</b>	<b>0.77</b>	<b>0.21</b>	0.89	0.94	0.83	<b>-0.44</b>	<b>-0.11</b>	-0.18	<b>0.12</b>	0.12	<b>-0.23</b>
mld1					1.00	<b>-0.09</b>	<b>0.36</b>	<b>-0.43</b>	<b>0.58</b>	-0.11	-0.08	-0.28	<b>0.17</b>	<b>-0.01</b>	0.01	<b>-0.06</b>	-0.06	<b>-0.10</b>
ssh						1.00	<b>-0.28</b>	<b>0.57</b>	<b>0.08</b>	0.62	0.78	0.58	<b>0.13</b>	<b>-0.01</b>	-0.08	<b>0.05</b>	0.03	<b>0.03</b>
sss							1.00	<b>-0.35</b>	<b>0.23</b>	-0.26	0.01	-0.34	<b>0.24</b>	<b>-0.05</b>	0.00	<b>0.00</b>	-0.02	<b>-0.13</b>
sst								1.00	<b>-0.02</b>	0.88	0.66	0.97	<b>-0.61</b>	<b>-0.10</b>	-0.15	<b>0.10</b>	0.11	<b>-0.15</b>
td									1.00	0.32	0.25	0.12	<b>-0.19</b>	<b>-0.03</b>	-0.05	<b>0.01</b>	0.00	<b>-0.22</b>
temp100										1.00	0.76	0.94	-0.63	-0.11	-0.18	0.10	0.11	-0.21
temp200											1.00	0.69	-0.27	-0.11	-0.18	0.11	0.11	-0.05
temp50												1.00	-0.66	-0.10	-0.16	0.09	0.10	-0.19
<b>temp500</b>													1.00	<b>0.12</b>	0.15	-0.10	-0.13	0.21
u100														1.00	0.93	<b>-0.08</b>	-0.06	<b>0.04</b>
u100-300															1.00	-0.08	-0.07	0.04
<b>v100</b>																1.00	0.95	<b>-0.02</b>
v100-300																	1.00	-0.01
<b>bathy</b>																		1.00

Table 14. Number of trees used in the BRT model for each species and region (ALL = whole domain).

	ALL	EAC	CS	WCP	NZ
YFT	3150	2000	2700	3000	2550
BET	3500	2900	2400	2300	2550
ALB	3550	3000	3800	2050	3000
MLS	2200	2500	550	2550	1650
SWO	4000	2850	3000	2500	4000

Table 15. Proportion of deviance in catch explained by the BRT model for each species and region using the training dataset.

	ALL	EAC	CS	WCP	NZ
YFT	0.60	0.66	0.64	0.46	0.62
BET	0.52	0.65	0.57	0.39	0.71
ALB	0.67	0.69	0.66	0.74	0.82
MLS	0.32	0.45	0.18	0.22	0.59
SWO	0.68	0.60	0.30	0.22	0.81

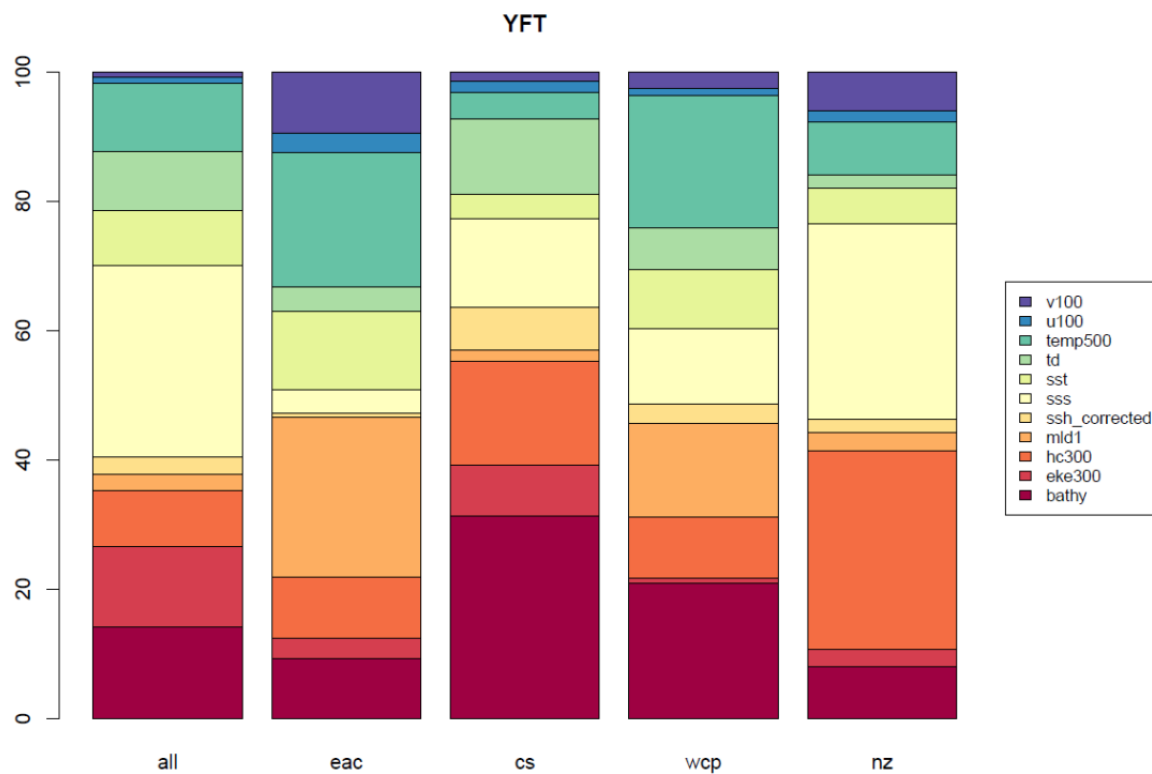
Table 16.  $R^2$  values for observed vs predicted CPUE (defined as catch per 10,000 hooks) calculated from the BRT model for each species and region using: (left) the training dataset (2008-2015), and (right) the validation dataset (2016-2020).

	Training dataset					Validation dataset				
	ALL	EAC	CS	WCP	NZ	ALL	EAC	CS	WCP	NZ
YFT	0.13	0.17	0.08	0.08	0.36	0.10	0.08	0.04	0.04	0.09
BET	0.15	0.17	0.12	0.05	0.15	0.10	0.07	0.04	0.03	0.11
ALB	0.11	0.26	0.19	0.11	0.30	0.11	0.19	0.13	0.09	0.17
MLS	0.18	0.20	0.12	0.12	0.24	0.16	0.08	0.04	0.12	0.10
SWO	0.38	0.35	0.16	0.05	0.39	0.35	0.21	0.14	0.04	0.23

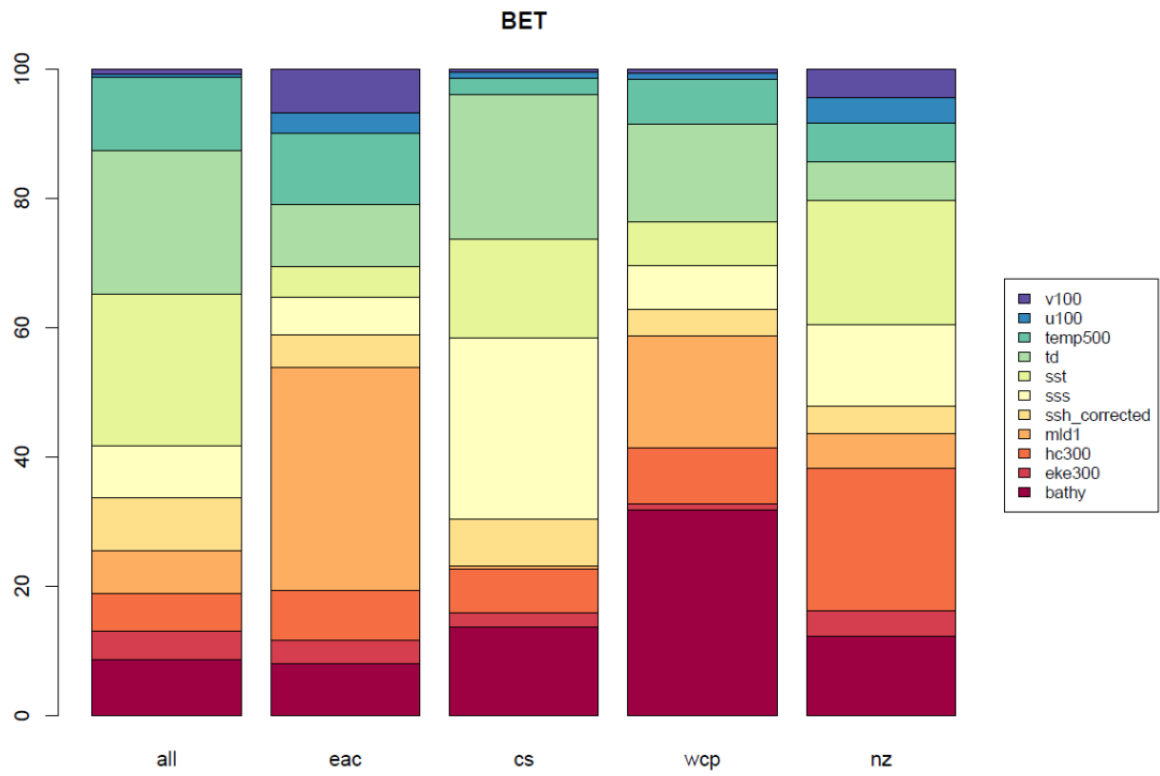
Table 17. Root mean squared error (RMSE) values for observed vs predicted CPUE (defined as catch per 10,000 hooks) calculated from the BRT model for each species and region using: (left) the training dataset (2008-2015), and (right) the validation dataset (2016-2020). The mean observed CPUE value is given in parentheses below for reference.

	Training dataset					Validation dataset				
	ALL	EAC	CS	WCP	NZ	ALL	EAC	CS	WCP	NZ
<b>YFT</b>	60.1 (38.2)	69.7 (46.6)	84.2 (67.5)	45.2 (29.3)	15.5 (8.9)	51.6 (37.7)	71.1 (47.9)	70.9 (60.9)	43.4 (32.9)	23.1 (14.0)
<b>BET</b>	17.4 (11.2)	21.8 (16.2)	21.6 (16.1)	8.7 (5.1)	19.2 (10.1)	15.3 (10.0)	20.6 (10.4)	18.5 (14.5)	7.6 (5.3)	16.2 (8.7)
<b>ALB</b>	104.4 (104.2)	115.4 (85.2)	93.2 (76.5)	102.3 (121.4)	136.9 (149.3)	85.5 (87.9)	140.8 (103.1)	73.7 (58.6)	83.3 (101.2)	138.9 (141.2)
<b>MLS</b>	2.8 (0.8)	9.0 (4.8)	1.5 (0.2)	1.8 (0.5)	4.0 (1.8)	2.3 (0.7)	6.6 (3.8)	1.1 (0.1)	1.4 (0.3)	4.6 (1.8)
<b>SWO</b>	11.6 (3.4)	27.6 (27.4)	5.6 (1.2)	2.4 (0.6)	42.9 (35.6)	10.0 (2.3)	26.6 (18.2)	3.4 (0.7)	1.7 (0.4)	34.9 (20.1)

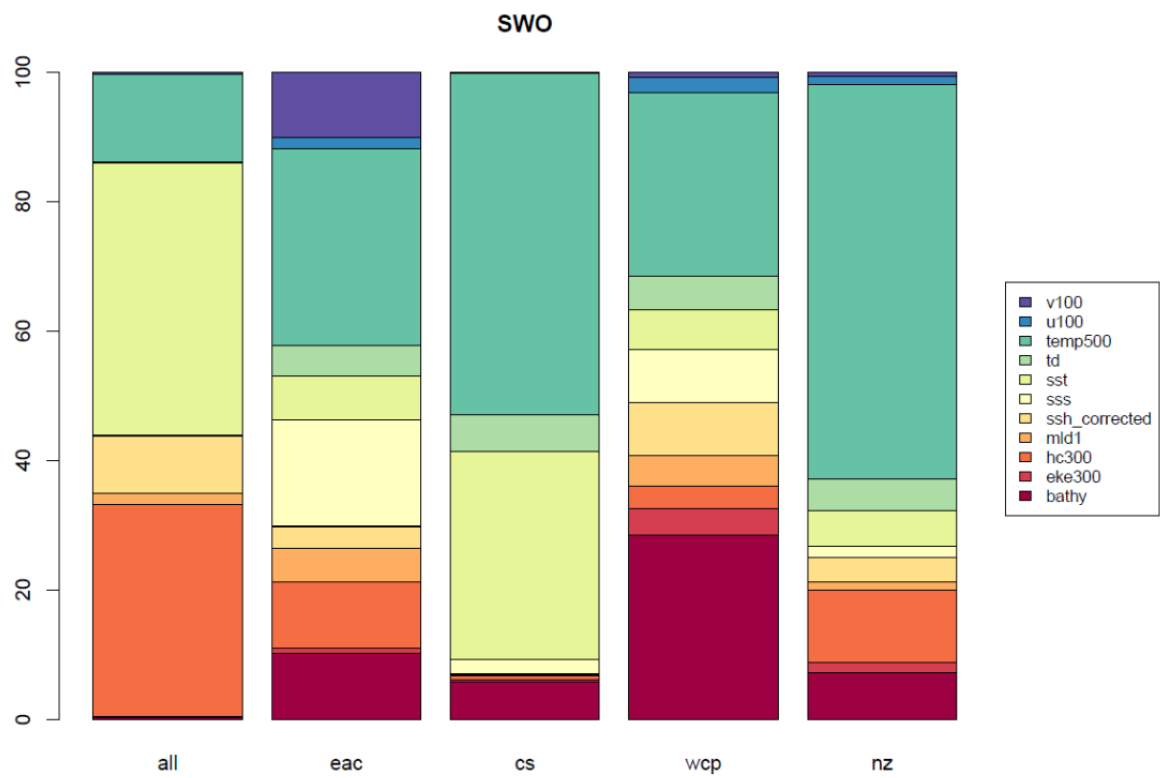
(a)



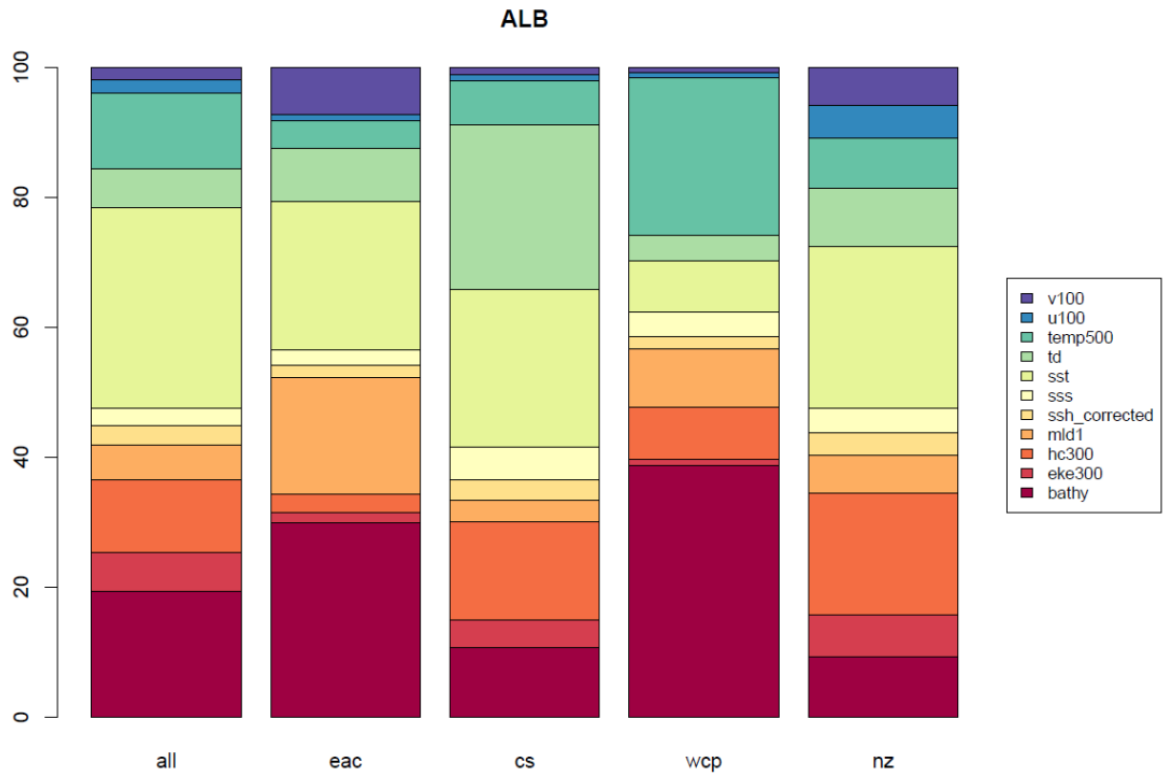
(b)



(c)



(d)



(e)

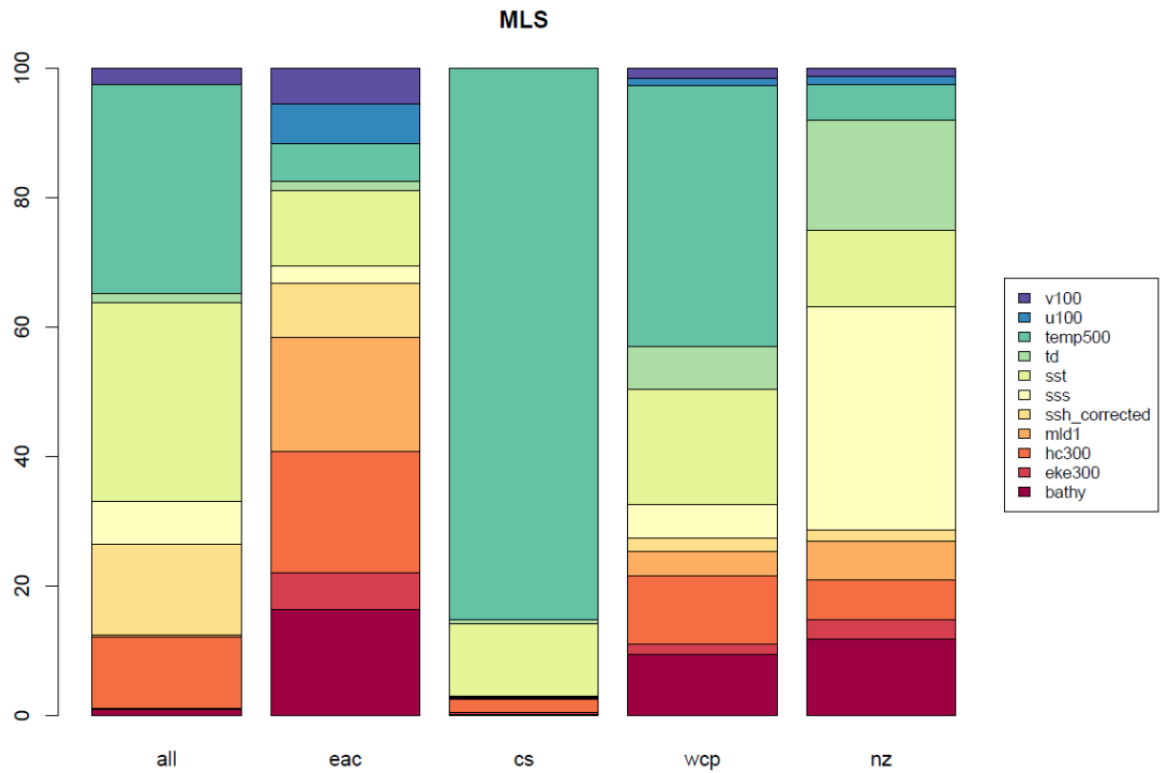
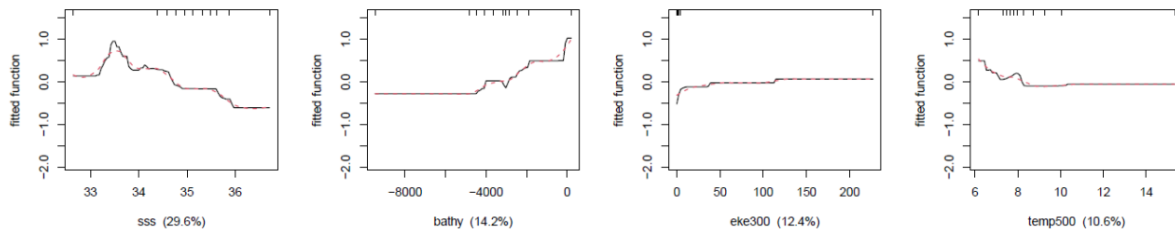
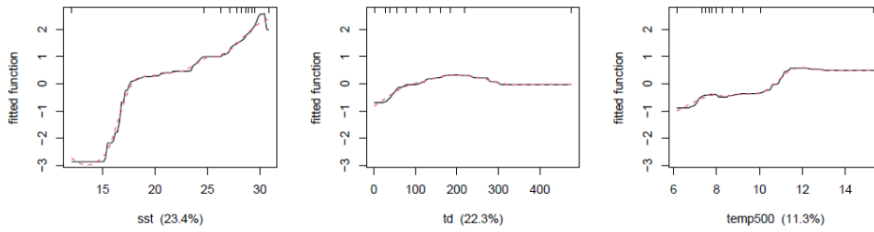


Figure 63. Relative contributions of each of the oceanographic variables included in the BRTs for each species and region (all = whole region; eac = EAC-dominated region; cs = Coral Sea; wcp = Western Central Pacific; nz = New Zealand) (see Figure 7). See Table 12 for definitions of oceanographic variables.

(a) YFT



(b) BET



(c) SWO

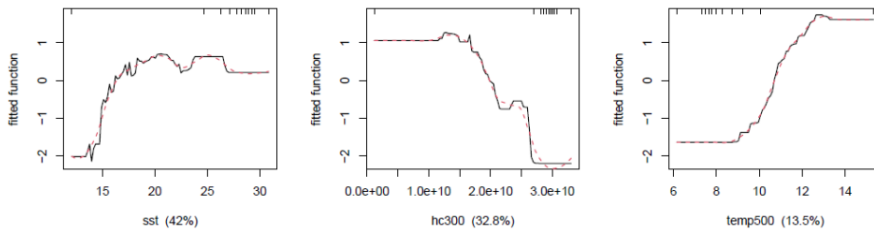
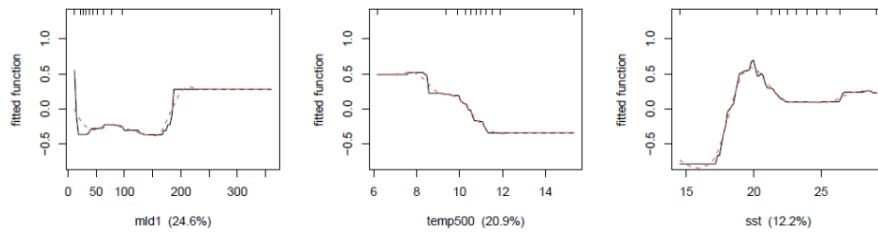
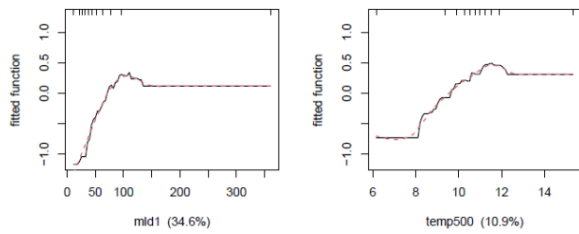


Figure 64. Marginal effect plots for the ocean variables that explain at least 10% of the total deviance in the whole-domain models for (a) YFT, (b) BET and (c) SWO. The rug plot along the top axis marks deciles in the data, so the marginal effect functions are of most relevance within the 10<sup>th</sup> and 90<sup>th</sup> deciles (i.e., between the second and tenth marks).

(a) YFT



(b) BET



(c) SWO

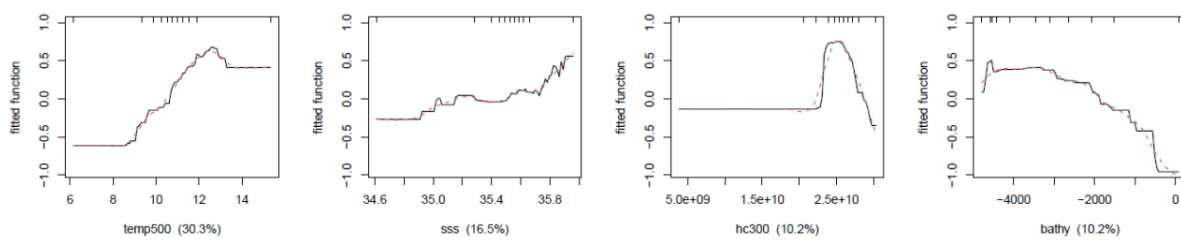
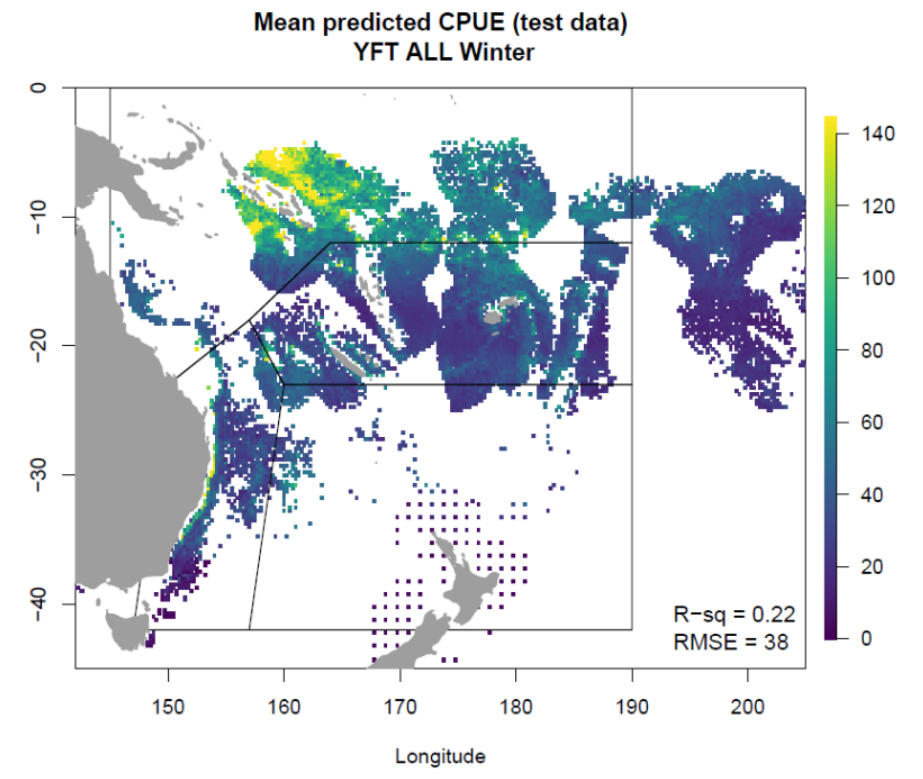
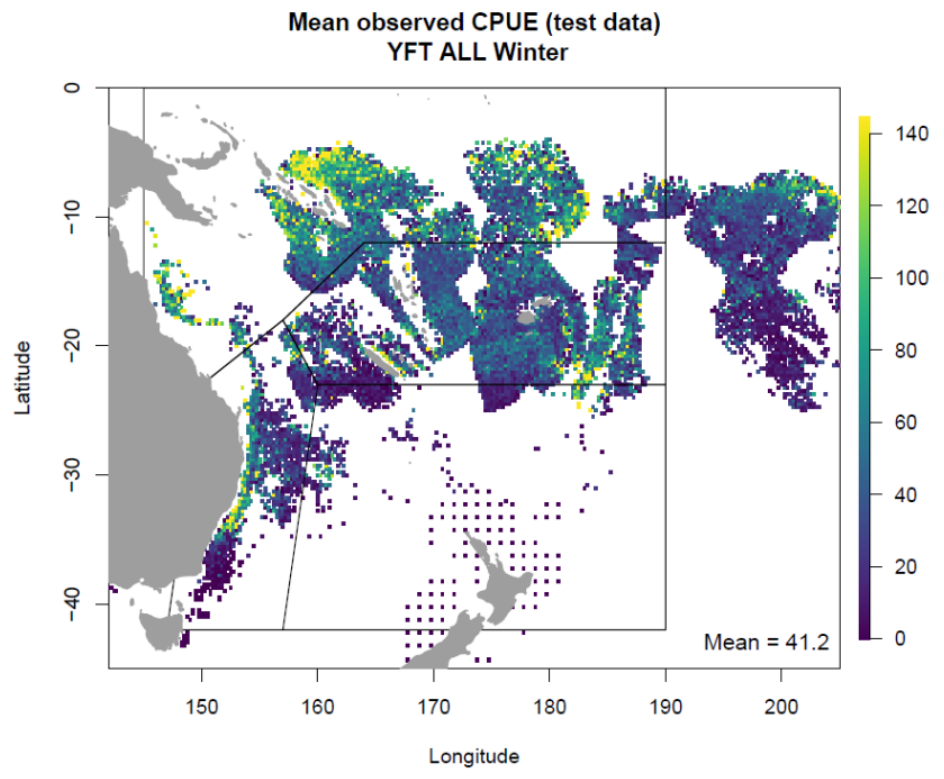
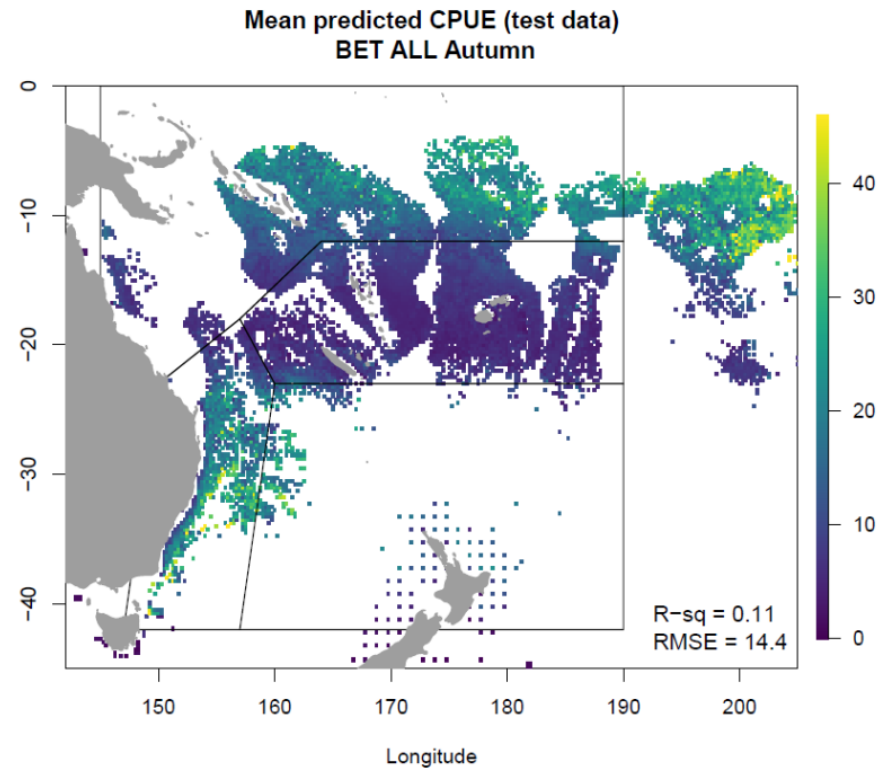
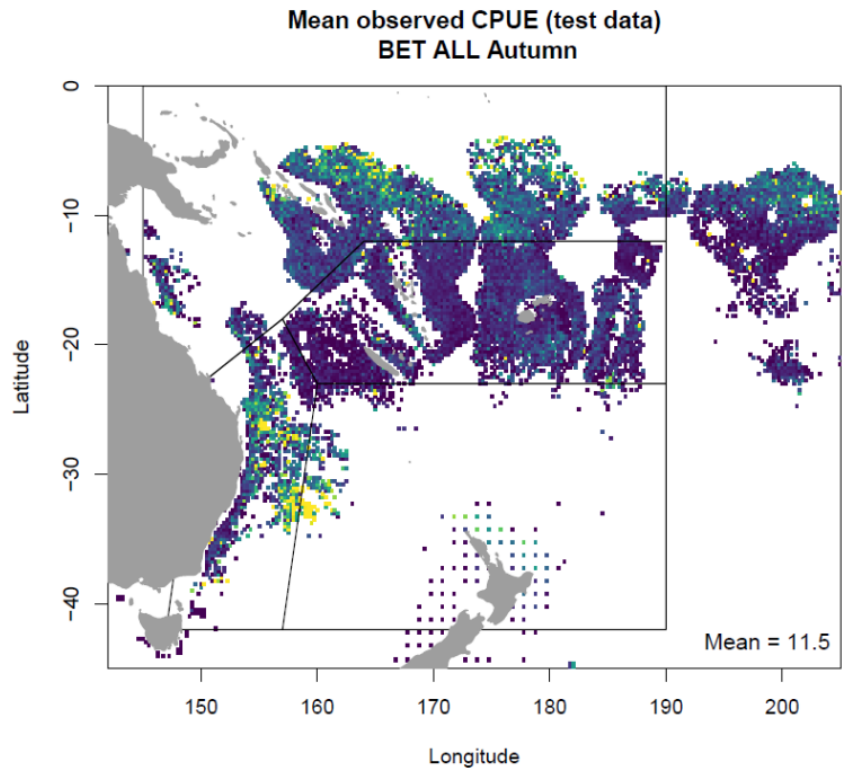


Figure 65. Marginal effect plots for the ocean variables that explain at least 10% of the total deviance in the EAC-dominated sub-region models for (a) YFT, (b) BET and (c) SWO. The rug plot along the top axis marks deciles in the data, so the marginal effect functions are of most relevance within the 10<sup>th</sup> and 90<sup>th</sup> deciles (i.e., between the second and tenth marks).

(a)



(b)



(c)

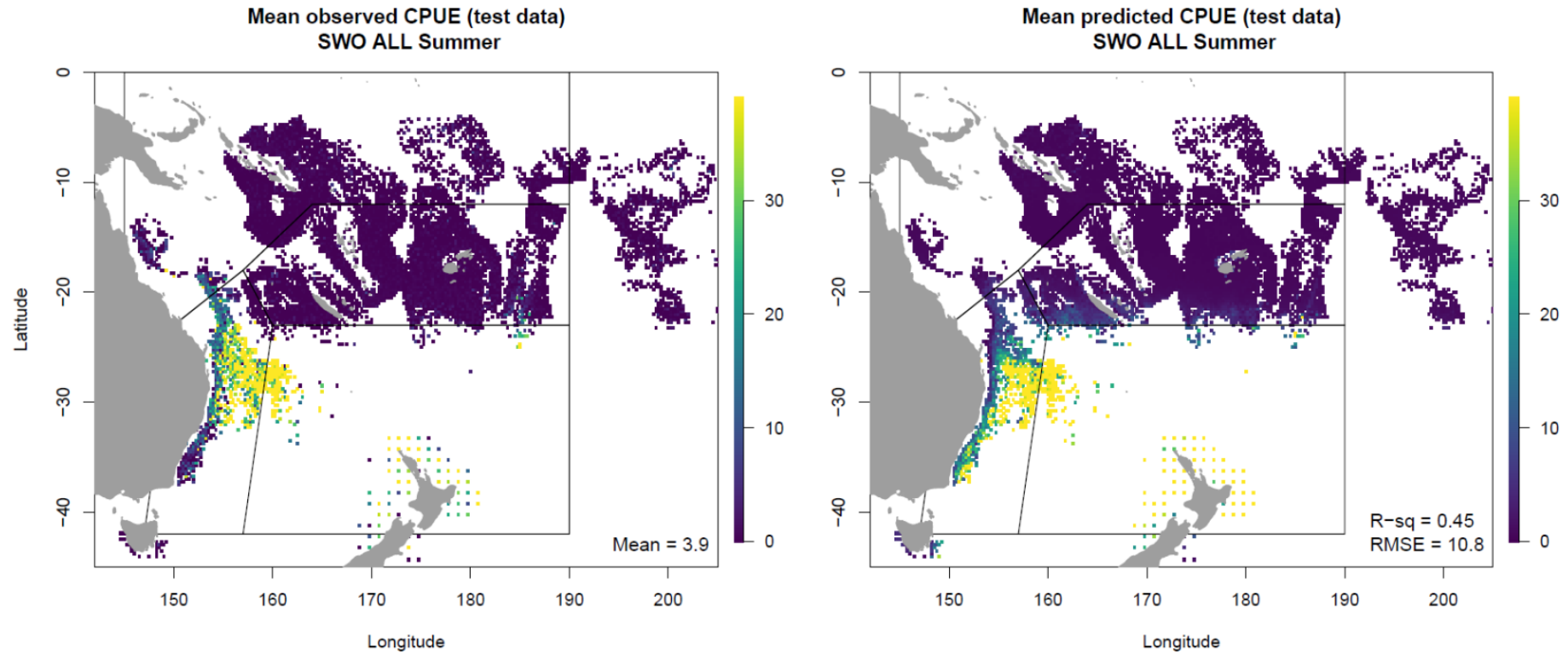
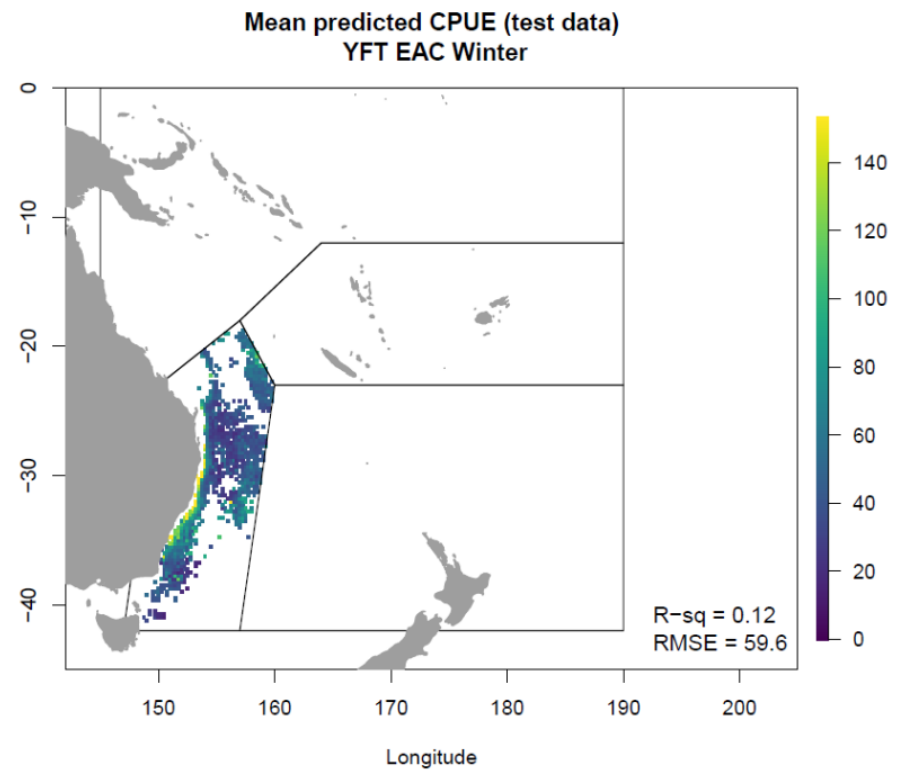
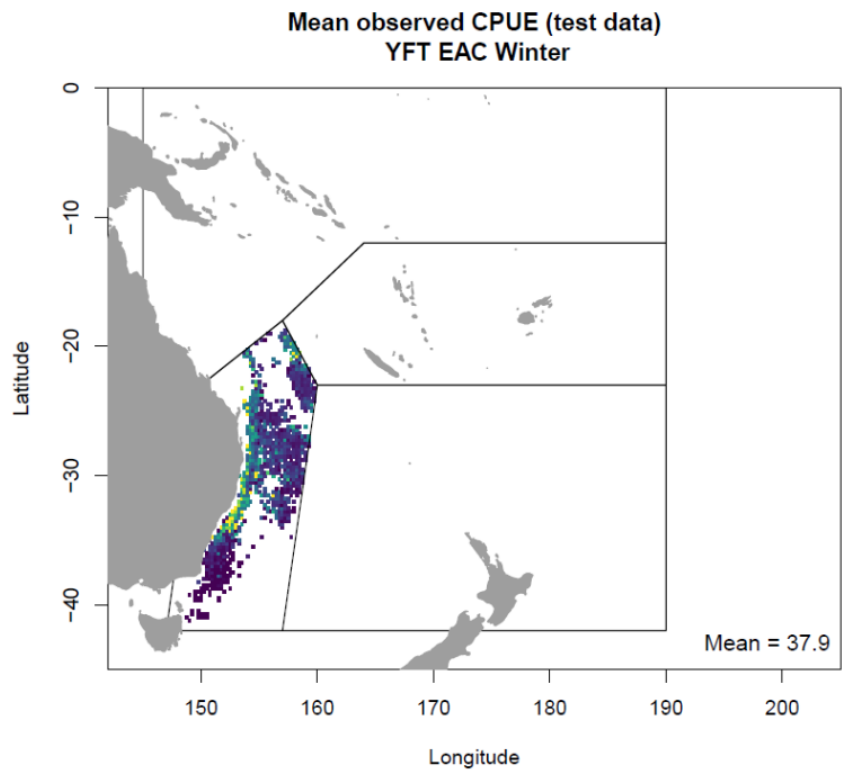
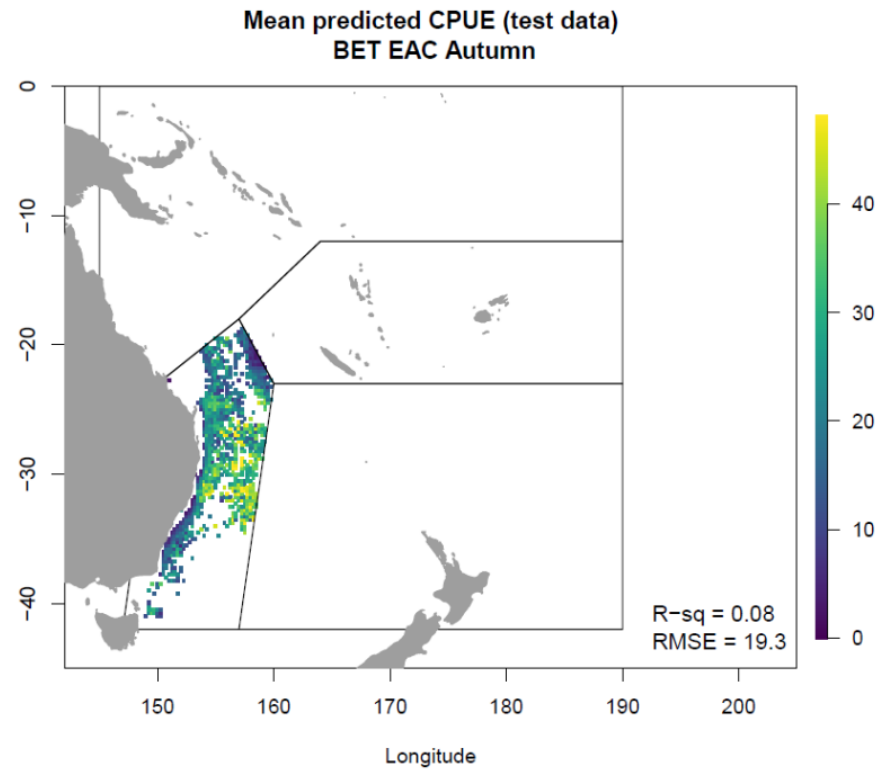
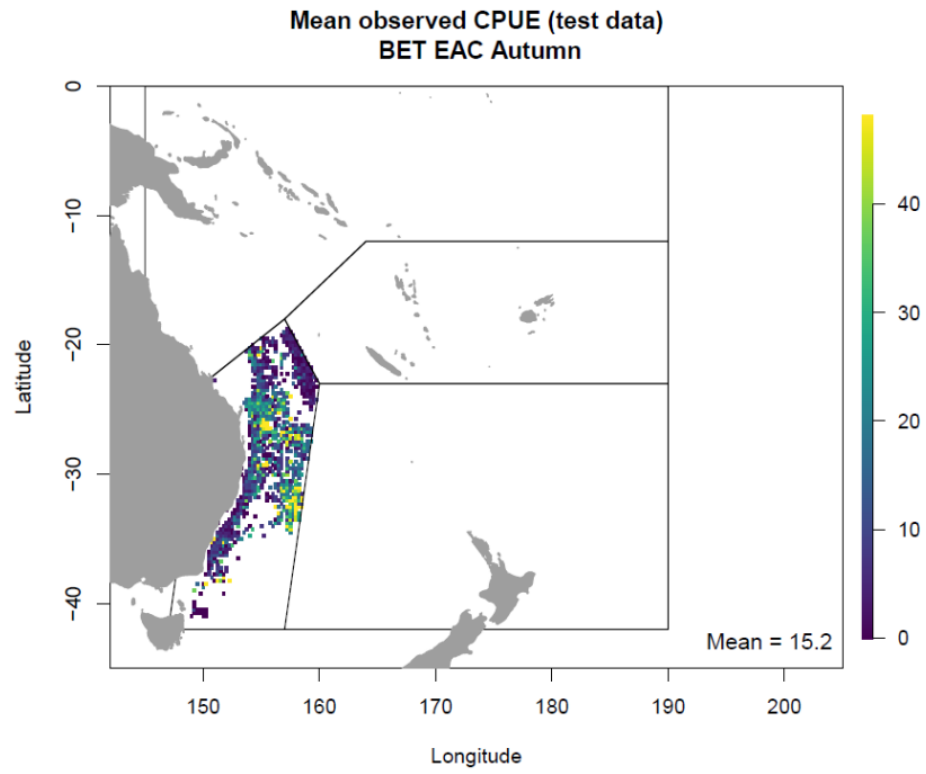


Figure 66. Spatial maps showing the average observed (left) and average predicted (right) CPUE over all years in the validation/test dataset (2016-2020) for (a) YFT in winter, (b) BET in autumn, and (c) SWO in summer, where CPUE is defined as catch per 10,000 hooks and predictions were made using the whole-domain BRTs. The mean observed CPUE over the whole region is given in the lower corner of the observed map, whereas Pearson's  $R^2$  value and the root mean squared error (RMSE) are given in the lower corner of the prediction map as an indicator of predictive performance.

(a)



(b)



(c)

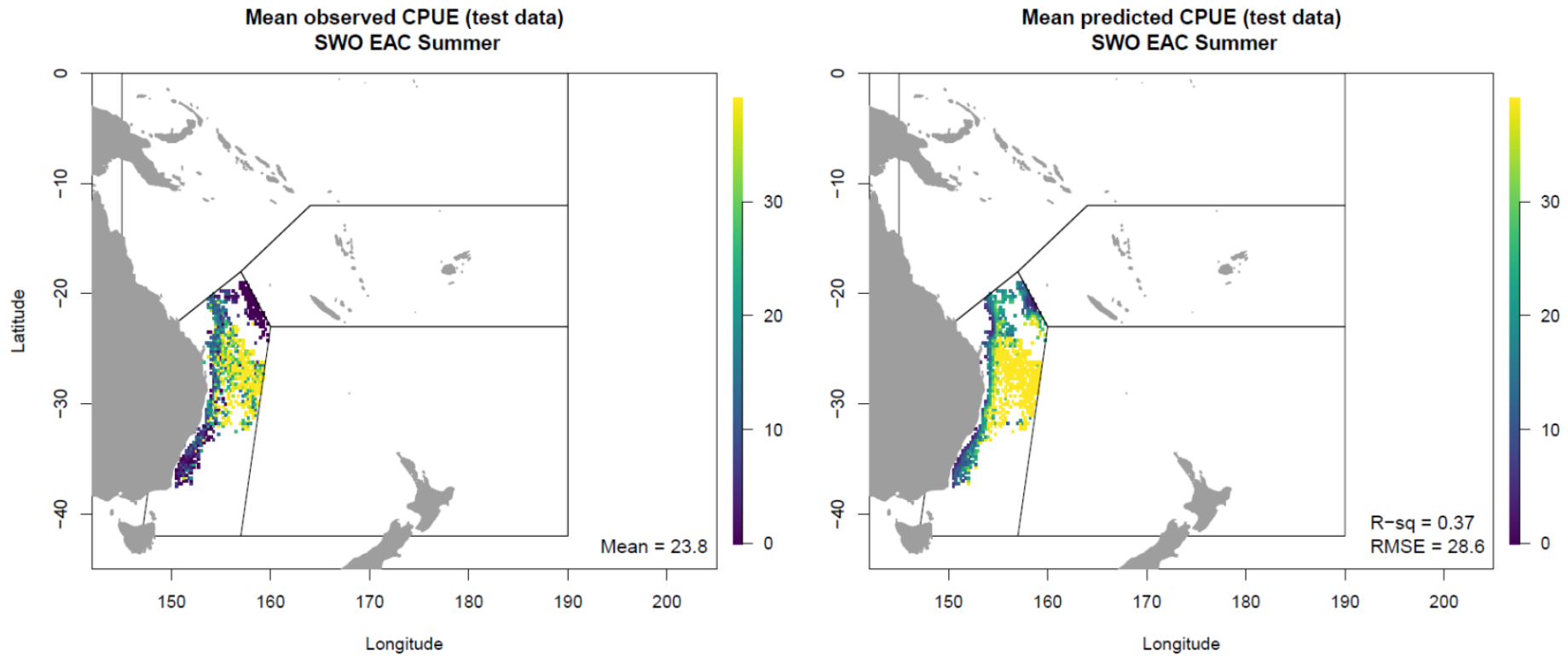


Figure 67. Spatial maps showing the average observed (left) and average predicted (right) CPUE over all years in the validation/test dataset (2016-2020) for (a) YFT in winter, (b) BET in autumn, and (c) SWO in summer, where CPUE is defined as catch per 10,000 hooks and predictions were made using the EAC sub-region BRTs. The mean observed CPUE over the EAC sub-region is given in the lower corner of the observed map, whereas Pearson's  $R^2$  value and the root mean squared error (RMSE) are given in the lower corner of the prediction map as an indicator of predictive performance.

# 6 BRT forecasting with ACCESS-S2

## 6.1 Methods

One of the goals of the project was to investigate forecasts of fish distribution for the five key species for Australia and regional partners based on the habitat models developed. Although the BRTs are modelling catch, not fish abundance, they can still be used to provide forecasts of catch distribution (rather than fish distribution). Unfortunately, not all of the ocean variables that were included in developing the ACCESS-S2 BRT models in the previous section are available in forecast mode. There are, however, four variables available: sea surface temperature (sst), sea surface height (ssh), mixed layer depth (mld; mld2 is used in this section as a better calculation of mld) and heat content in the upper 300 m (hc300). Thus, in order to use the BRTs to provide forecasts, the models needed to be re-run using only these variables. Bathymetry could also be included given it is a static variable, resulting in a total of five variables.

The exact same methods were followed to generate BRTs as in the previous section, but only using the five variables available for forecasting. The optimal number of trees selected for each species and region is given in Table 14. Note that the BRT for MLS in the CS sub-region did not converge due to insufficient data.

## 6.2 Results

### 6.2.1 Model performance

As expected, the performance of the models degraded with a reduced set of predictors; however, it did not degrade markedly. The proportion of deviance in the catch explained by the models tended to only drop by a few percent (Table 19 compared with the equivalent table in the previous section). As explained in section 5.1, the performance statistics for CPUE are of more interest here than the catch statistics, as they measure the influence of the ocean predictors independent of the number of hooks set. The  $R^2$  values for the observed versus predicted CPUE (defined as catch per 10,000 hooks) for each species and region were only slightly lower using the forecasting variables than the full set of variables (Table 20 compared to Table 16 in previous section). Thus, the same comments from the models using the full set of variables apply here, namely:

- For the training dataset,  $R^2$  values tended to be lowest in the WCP and highest in the EAC and NZ regions (Table 16, left).
- For the validation dataset, the  $R^2$  values for the whole-region model are only slightly lower for the validation dataset than the training dataset, but tend to be much lower for the sub-region models (Table 5, right).
- Overall, the predictive performance of the models is low for the validation dataset, with  $R^2$  values  $< 0.20$  for most species and regions.

## 6.2.2 Relative contributions of ocean predictors

Figure 63 shows the relative contribution by each of the forecasting variables in explaining the deviance in the CPUE for each species and region. For the whole domain models, sst is most influential for all species; however, in the sub-regions, the variables that are most influential vary. For instance, in the EAC-dominated sub-region, mld2 is most influential for YFT and BET, compared to bathymetry and sst for ALB, and bathymetry and hc300 for SWO.

## 6.2.3 Effects of ocean predictors on CPUE

Figure 69 shows the relationship between CPUE and the most influential forecasting variables for YFT, BET and SWO in the whole-domain models. For YFT and BET, CPUE is expected to increase as sst increases, whereas the opposite is true for SWO (over the majority of the data, as indicated by the rug plot along the x-axis). For the EAC sub-region models, CPUE for YFT and BET is expected to increase as the mixed layer deepens, and CPUE for SWO is expected to decrease in shallow waters (as bathymetry increases, Figure 70).

The full set of marginal effects plots for the BRT forecasting models for all species and regions can be found in Appendix 2.

Table 18. Number of trees used in the BRT forecasting model for each species and region (ALL = whole domain).

	ALL	EAC	CS	WCP	NZ
<b>YFT</b>	2850	1350	2350	2550	1400
<b>BET</b>	2500	1450	2700	1850	1650
<b>ALB</b>	2600	3450	3200	1300	2450
<b>MLS</b>	3550	2700	NA	2750	3000
<b>SWO</b>	4000	2500	3500	1950	4000

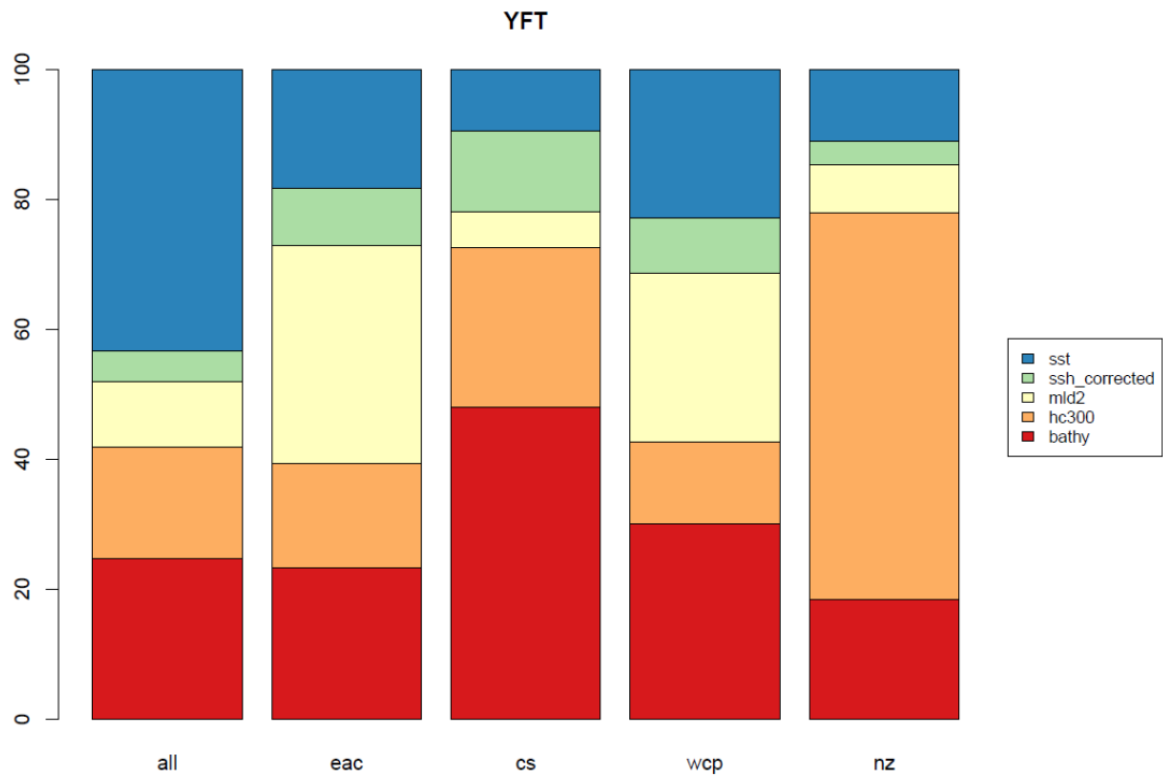
Table 19. Proportion of deviance in catch explained by the BRT forecasting model for each species and region using the training dataset.

	ALL	EAC	CS	WCP	NZ
<b>YFT</b>	0.56	0.61	0.61	0.45	0.56
<b>BET</b>	0.47	0.61	0.53	0.38	0.67
<b>ALB</b>	0.65	0.65	0.61	0.72	0.80
<b>MLS</b>	0.29	0.44	NA	0.21	0.58
<b>SWO</b>	0.62	0.55	0.25	0.20	0.80

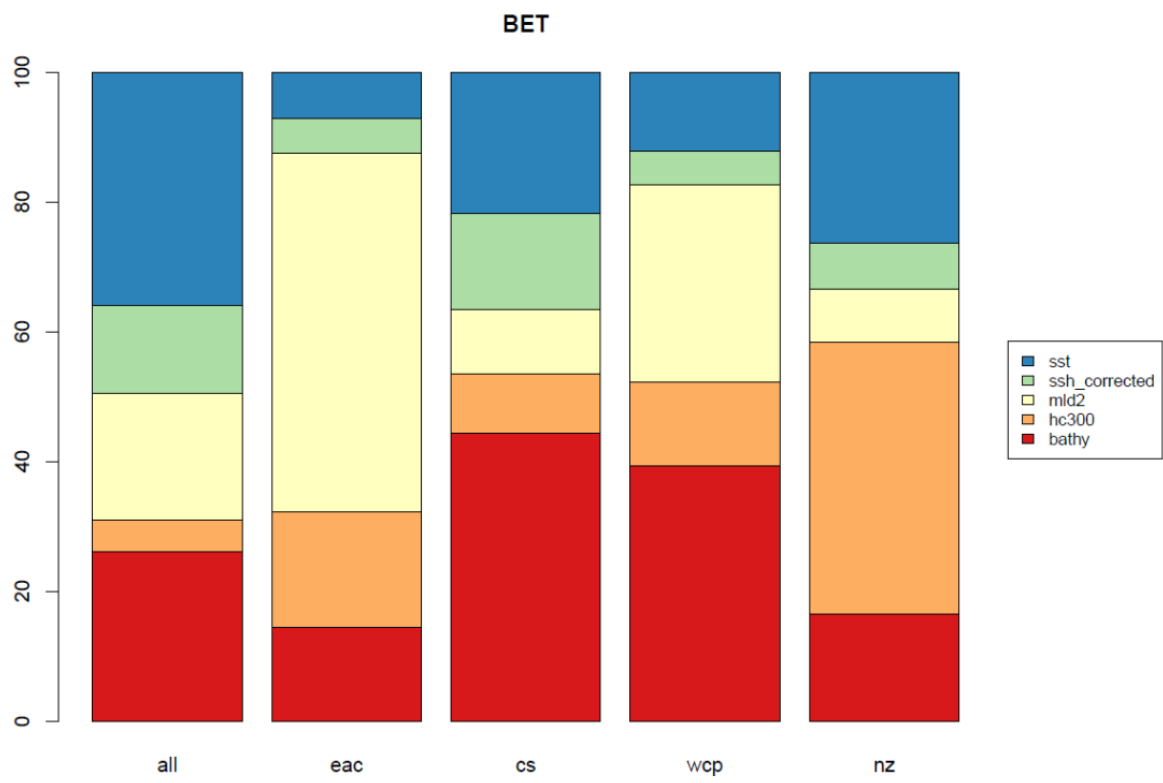
Table 20.  $R^2$  values for observed vs predicted CPUE (defined as catch per 10,000 hooks) calculated from the BRT model for each species and region using: (left) the training dataset (2008-2015), and (right) the validation dataset (2016-2020).

	Training dataset					Validation dataset				
	ALL	EAC	CS	WCP	NZ	ALL	EAC	CS	WCP	NZ
<b>YFT</b>	0.09	0.12	0.06	0.07	0.31	0.07	0.05	0.03	0.03	0.08
<b>BET</b>	0.10	0.13	0.10	0.04	0.11	0.06	0.06	0.03	0.02	0.11
<b>ALB</b>	0.07	0.22	0.13	0.07	0.26	0.08	0.17	0.08	0.06	0.21
<b>MLS</b>	0.16	0.20	NA	0.11	0.23	0.13	0.08	NA	0.10	0.11
<b>SWO</b>	0.31	0.27	0.11	0.04	0.37	0.29	0.16	0.12	0.04	0.23

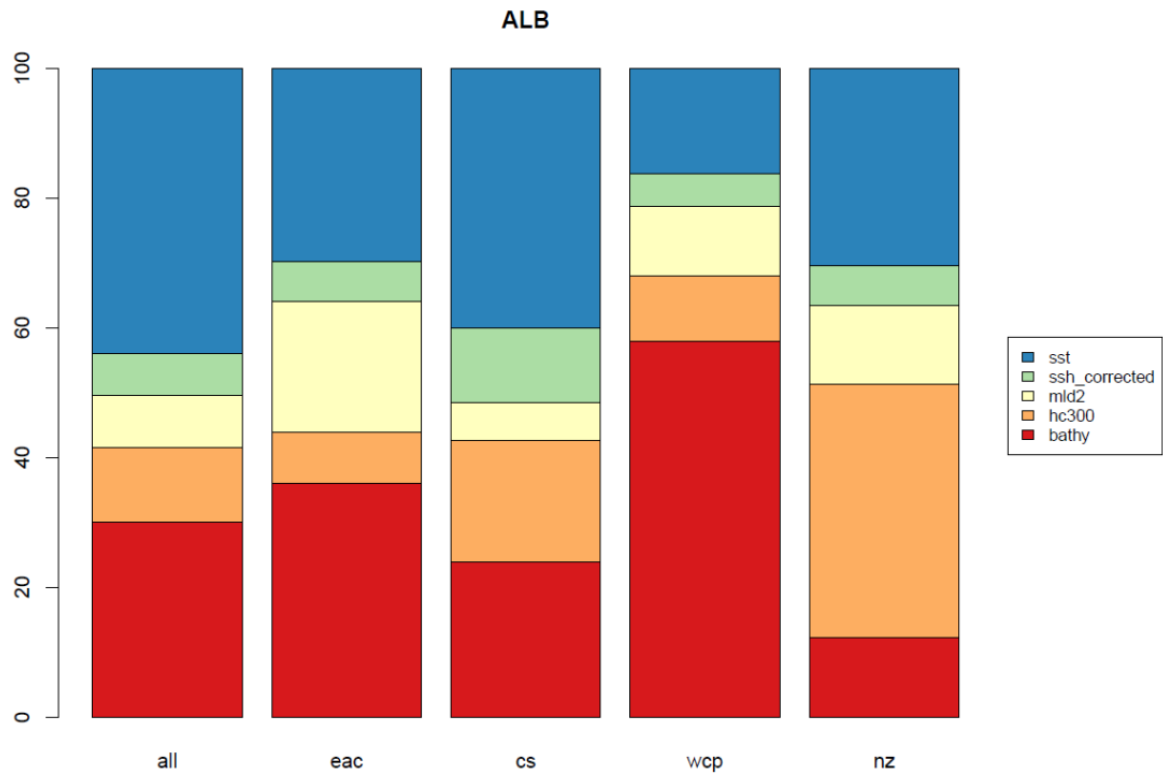
(a)



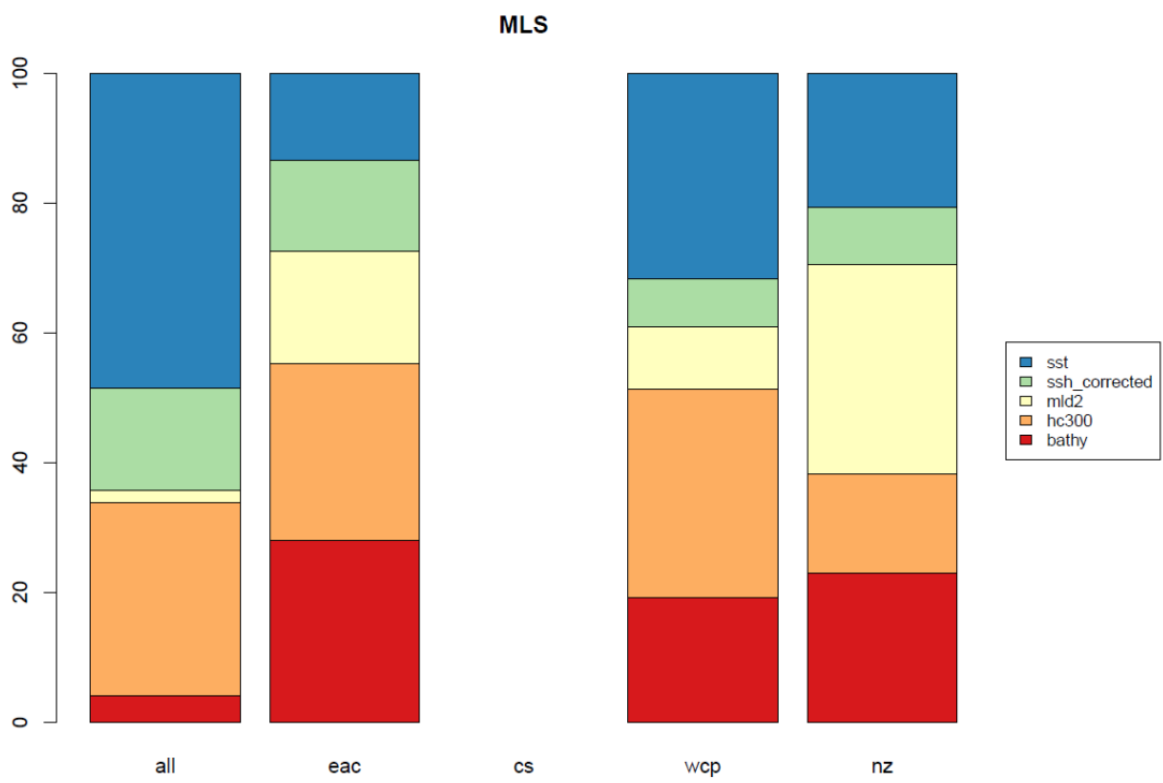
(b)



(c)



(d)



(e)

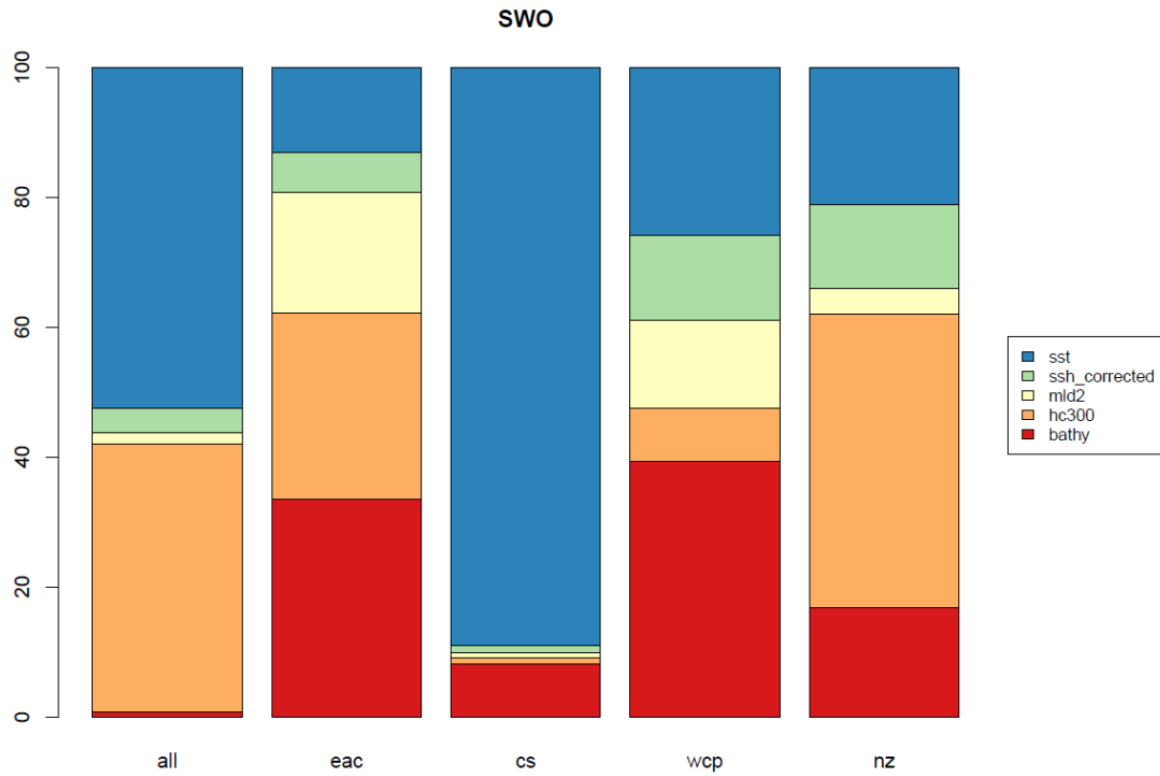
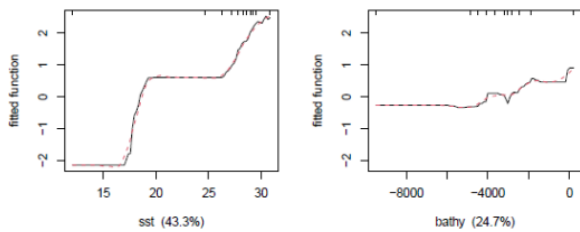
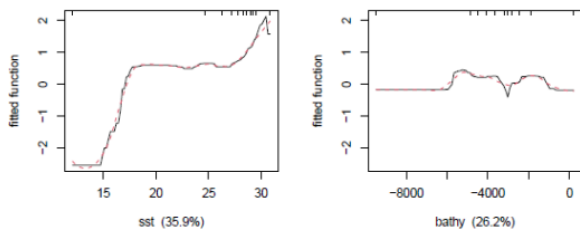


Figure 68. Relative contributions of each of the oceanographic variables included in the BRT forecasting models for each species and region (all = whole region; eac = EAC-dominated region; cs = Coral Sea; wcp = Western Central Pacific; nz = New Zealand) (see Figure 7 in Section 4).

(a) YFT



(b) BET



(c) SWO

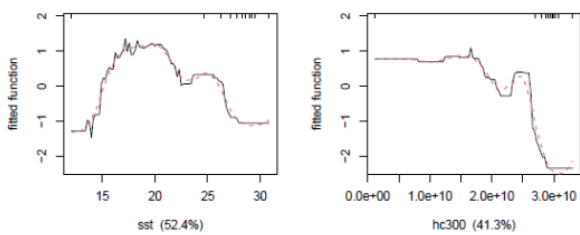
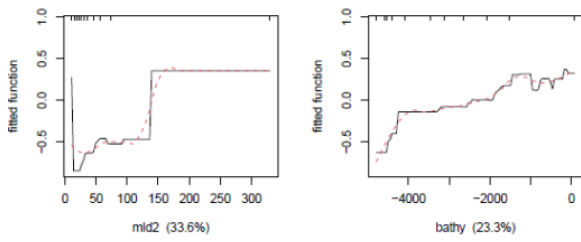
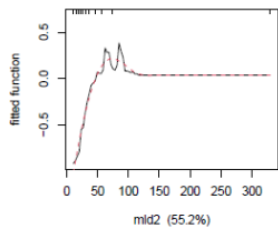


Figure 69. Marginal effect plots for the ocean variables with a relative contribution to explaining the total deviance of at least 20% in the whole-domain BRT forecasting models for (a) YFT, (b) BET and (c) SWO. The rug plot along the top axis marks deciles in the data, so the marginal effect functions are of most relevance within the 10<sup>th</sup> and 90<sup>th</sup> deciles (i.e., between the second and tenth marks).

(a) YFT



(b) BET



(c) SWO

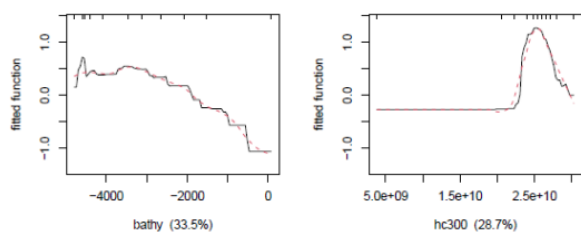


Figure 70. Marginal effect plots for the ocean variables with a relative contribution to explaining the total deviance of at least 20% in the EAC-dominated sub-region BRT forecasting models for (a) YFT, (b) BET and (c) SWO. The rug plot along the top axis marks deciles in the data, so the marginal effect functions are of most relevance within the 10<sup>th</sup> and 90<sup>th</sup> deciles (i.e., between the second and tenth marks).

# 7 Projecting future patterns – seasonal and decadal forecasts

A selection of case study forecasts has been made available at the following project website:

- <http://www.cmar.csiro.au/etbf-oceanographic-influences/index.html>

along with a suite of timeseries plots of identified key ocean state variables for the regions identified and also for a selection of finer scale regions in the EAC domain.

## 7.1 Forecast runs

Using the ACCESS-S2 hindcast data set as input to the BRT forecast models, seasonal hindcasts of catch, i.e., retrospective forecasts run in the past, were run at one, two, and three month lead times from a summer initialisation date of February 2018, providing hindcasts for March-April-May 2018. The predicted spatial catch distribution for each species, region and month could be contrasted with the observed catch and effort data to assess how well the models performed at predicting patterns in catch.  $R^2$  values were calculated between the observed and predicted CPUE (catch per 10000 hooks) in each month for each species and region using the ACCESS-S2 hindcast data, and these were compared to the  $R^2$  values obtained using the reanalysis ocean dataset. Somewhat surprisingly, the hindcast  $R^2$  values were very similar to the reanalysis values, and could by chance be slightly better in some cases (Table 21; note that only results for the whole domain model are shown but that the general findings were similar for all regions). This is because the correlation between the ACCESS-S2 hindcast data and the re-analysis data for these months is very high, even for May (where we would expect the greatest divergence given the 3-month lead time). Assuming similar performance in other months and years, this suggests that the predictive power of the BRTs should not be degraded much by using forecasted ocean data up to 3 months lead time.

To demonstrate an actual catch forecast, catch forecasts were run in January 2022 at one-, two- and three-month lead times from an initialisation date of 1 January 2022, providing “real-time” forecasts for February-March-April 2022. Maps showing the forecasted spatial distribution of catch per 10000 hooks in February 2022 for YFT, BET and SWO for the whole domain are given in Figure 71.

For provision of forecasted input data (sst, hc300 etc) for the eastern Australian region, there is currently a dedicated project page hosted at:

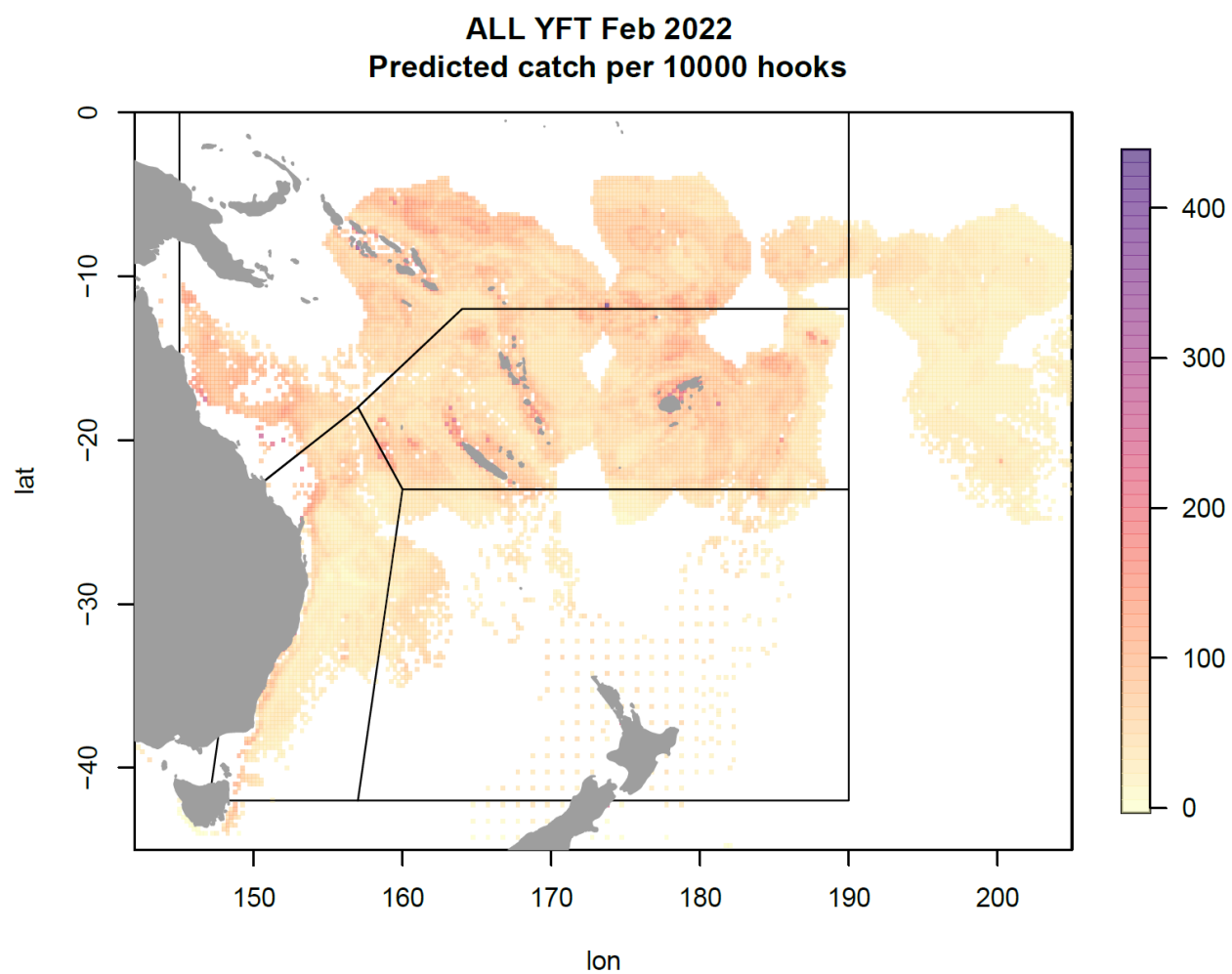
- <http://poama.bom.gov.au/access-s/etbf/>

which is username and password protected, and this can be provided upon request.

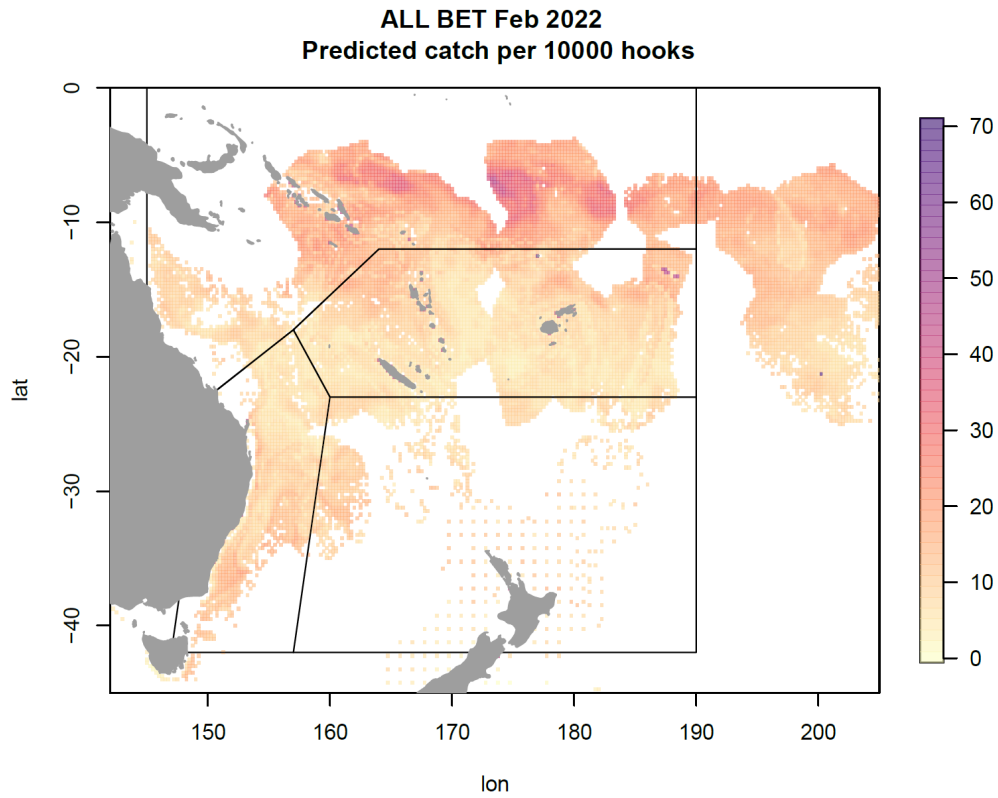
Table 21.  $R^2$  values for observed vs predicted CPUE (defined as catch per 10,000 hooks) calculated from the BRT whole-region forecast model for each species run using: (left) the ACCESS-S2 hindcast oceanographic data output for March, April and May 2018 from a February 1<sup>st</sup> initialisation date; (right) the observed oceanographic data for March, April and May 2018 for comparison.

	ACCESS-S2 hindcast data			Observed data		
	March	April	May	March	April	May
<b>YFT</b>	0.025	0.012	0.099	0.020	0.017	0.099
<b>BET</b>	0.098	0.092	0.073	0.072	0.085	0.073
<b>ALB</b>	0.018	0.031	0.052	0.028	0.059	0.069
<b>MLS</b>	0.240	0.147	0.106	0.243	0.138	0.095
<b>SWO</b>	0.357	0.424	0.363	0.416	0.492	0.433

(a)



(b)



(c)

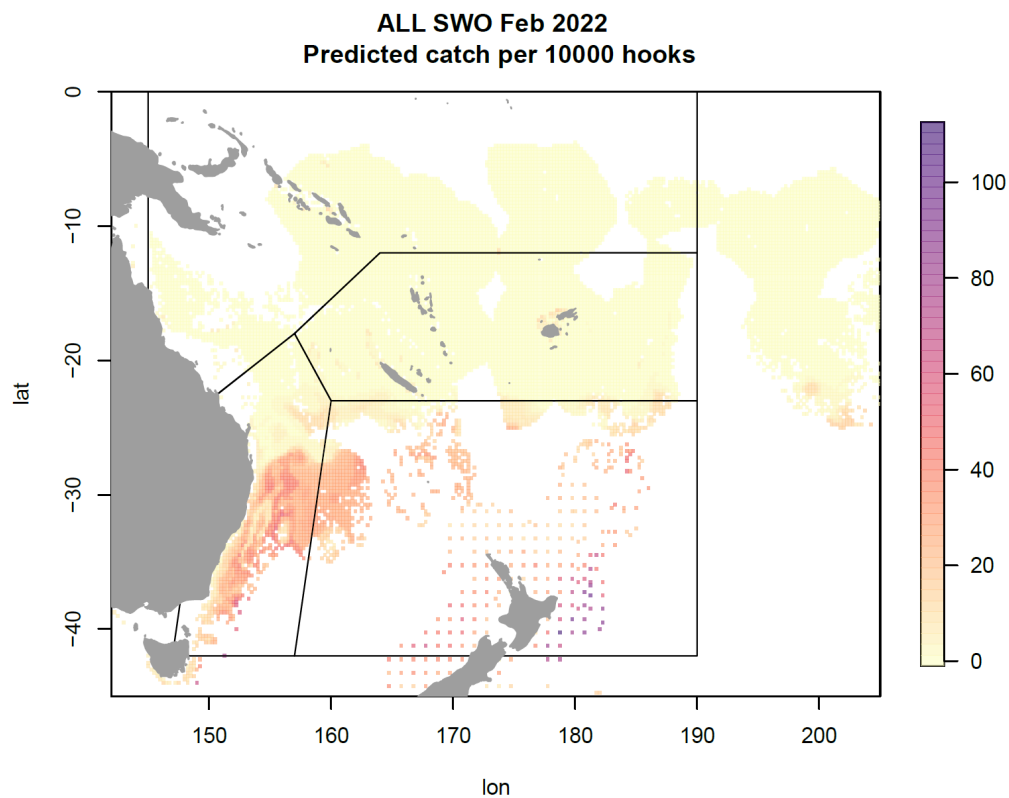


Figure 71. Spatial maps showing the predicted CPUE (defined as catch per 10,000 hooks) for February 2022 for (a) YFT, (b) BET, and (c) SWO, obtained using the whole-domain BRT forecast model with ACCESS-S2 forecast data initialised on January 1<sup>st</sup> 2022 as input. Only grid cells with at least some fishing effort historically are included. (Note that the catch and effort data around New Zealand was only provided at a 1 x 1 degree resolution, hence the sparse appearance of the predictions which are made at a 0.25 x 0.25 degree resolution).

## 7.2 Progress on CAFE decadal (multi-year) forecasts

Multi-year prediction is a less mature field than weather or seasonal prediction. Bridging the gap between shorter-term forecasts and longer-term climate projections to predict conditions in the multi-year period is recognised as a substantial scientific “grand challenge” but one that is of great societal relevance and benefit. One of the risks in embarking on these efforts are unknown challenges effecting workplan timeframes.

CSIRO’s CAFE decadal hindcast/forecast dataset, including historical baselines for the hindcasts allowing exploration of the value of initialisation vs forcing, have only recently been completed. A “generic” global evaluation of the decadal hindcast/forecast product, while not yet complete, is well underway. Documentation will be published and once available will be linked on the project website.

In the decadal forecasting space, which covers predictions over a multi-year period, we ran 9, 12, 18, 24, and 36 month model hindcasts for both summer and winter initialisation dates for a year that best spans the variability in available CPUE data. These results are available on the project website.

Once the generic evaluation is complete there is an opportunity to perform a more specific assessment of the decadal forecast product in relation to ETBF applications, informed in part by the results of the current project.

# 8 Categorical approach to prediction of CPUE based on ACCESS-S2 output

## 8.1 Background

In this section of the report, we consider a simplified approach to prediction of catch in relation to ocean conditions. Instead of trying to predict continuous values of catch-per-unit-effort (CPUE) given certain ocean conditions, we simply try to predict if the catch rates will be “normal”, “higher-than normal” or “lower than normal” over a defined spatial region. We therefore categorized regional CPUE observations into three states: (1) medium (25-85th percentile), (2) bad (less than 25th percentile) and (3) good (above 85th percentile). We used time-dependent multinomial generalized additive models (GAMs) to predict current state as a function of previous state and ocean variables. Broad scale spatial aspects of the SW pacific were incorporated by using the state of catches in adjacent regions to predict the focal region’s state.

The difficulty in developing predictive habitat models for target species based on observed ocean data or reanalysis output has been noted (Section 3 and Section 5). Using catch as a proxy for favoured habitat conditions of the fish necessarily means viewing the process through the lens of fishery dependent data. Therefore, the dynamics of the fishing process, such as market forces, management decisions etc. as well as the influence of fishing on stock abundance, determine the response between fishing effort and catch. Additionally, the process of observing and compiling catch data and the aggregation involved, and, finally, ocean and habitat conditions, add to the fishery dynamics to ultimately create an inherently noisy set of observations of what is a highly complex ecological process.

Even without the complications of fishing as a sampling “tool”, the link between top-order ocean predators’ abundance in space and time and the physical dynamics of the ocean is not necessarily direct. Key variables such as temperature will influence the broad distribution of species (e.g. warm water species such as YFT are less likely to persist in temperate waters). But within these distribution, small scale features such as fronts, local prey density, eddy fields are also likely to be influential in determining spatiotemporal distribution. All these factors mean that making spatiotemporal predictions of target species based purely on ocean data is challenging.

However, industry knowledge has shown that there are particular seasons which have better catch rates of particular species throughout the ETBF. In discussions with fishery operators and managers in the TTRAG, the researchers asked if there was interest in pursuing an approach where the goal of the modelling was simply to predict whether the current fishing year was likely to be roughly the same as current conditions (and similar to recent average years) or substantially better or worse. This idea was positively received and hence investigated in the project.

Additionally, fishers raised the potential for catches in foreign EEZs to be predictors of later catches in the Australian region. The methods used in section 5, are not easily adapted to use observations of lagged covariates (e.g. past catch rates).

To deal with this, the method we detail below categorizes monthly CPUE into a series of discrete states which simply describe if the catch rates were “Good”, “Medium” or “Bad” as a function of the state at a previous time and other covariates. Therefore these statistical models attempt to predict the current state in a particular region as a function of: (a) The state of CPUE (Good/Medium/Bad) in the last month; (b) optionally, the state of CPUE for the previous month in

neighbouring regions in order to simply model spatiotemporal dependence and (c) local ocean conditions.

From a scientific perspective and given the challenges inherent in full spatiotemporal prediction (see section 5), there was interest in determining whether there are advantages in effectively reducing the problem of predicting continuous CPUE values to a much simpler set of outcomes. The aim was for the coarse features of the system to be captured by aggregating the complex and or noisy aspects of the ecological and fishing processes.

It is necessary to be clear from the outset, that it was not apparent whether this would be the case or not. On the one hand there is potential that although the signals are less detailed, that they may be more robust or predictable. On the other, there was every chance that the aforementioned complexity and noise would simply swamp any overall signal.

In this section we describe the statistical approach and present the model selection results for all species in the analysis. We focus on the results of YFT, BBL and BET with a focus on the EAC region (see below for map and see section 4) as a case study to present the degree to which the models detailed below were able to predict the categorized states.

## 8.2 Methods

### 8.2.1 Data categorization

Nominal catch per unit effort data (total catch / hooks)  $U_t$  was used as described in section 1 and 5. There was a clear decreasing trend across all CPUE target species time series (see Figure 1 to

Figure 5) which was likely due to both structural changes in the fisheries and depletion of the harvest species by fishing: factors independent of oceanography having a strong influence on the catch rates. We therefore opted to consider the period from January 2009 onwards as the CPUE series tended to be more stable over this time span.

For each month and region, CPUE was categorized into three states according to the following simple method.

1. The 25<sup>th</sup> and 85<sup>th</sup> percentiles of the data ( $q_{25}$  and  $q_{85}$ ) were calculated.
2. These were used to assign states according to the following:

$$S_{t,i} = \begin{cases} U_{t,i} < q_{25}, & \textit{Bad} \\ q_{25} \leq U_{t,i} < q_{85} & \textit{Medium} \\ U_{t,i} > q_{85}, & \textit{Good} \end{cases}$$

This was used to generate a series of observations  $S_t$  for each region  $i$  (see section 8.2.2) and for the species considered in this study.

The aim of the analysis was to predict  $S_{t,i}$ , the categorical state of CPUE at time  $t$  in region  $i$  given  $S_{t-1,i}$ , oceanographic conditions, and the state in other regions in the previous timestep. In its most general form, the model needs to provide the probability of the state in region  $i$  at time  $t$  given the state in the previous month and other covariates  $Y_t$  which can be expressed as  $\Pr(S_{t,i} | S_{t-1,j}, Y_t)$ . The form of this probability implies a first-order Markov model with covariates. This can be estimated as a multinomial linear model (further details below).

## 8.2.2 Spatial configuration

In order to capture the notion that there is a spatial component to patterns of the states  $S_t$ , we used the same set of regions defined in section 4.2. A series of  $S_t$  was therefore created for each region  $i$  (see Figure 72) and these series were used as predictors in generalized additive models (see section 8.2.3). According to the structure of dependence on adjacent regions, the models in this report are either labelled as 'self' models, or 'adjacent' models. 'Self' models include the catch state in a polygon as a function of the catch state in this polygon at the previous time-step. 'Self' models treat catch rates (and the categorized state  $S_{t,i}$ ) as spatially independent. Therefore according to the self models,  $S_{t,i}$  will change through time or in response to environmental conditions, but state in one polygon does not affect any other polygon. The maps in Figure 72 illustrate 'self' models in the EAC and New Zealand polygons, where a looped arrow illustrates the previous month's catch state being used to help predict the current month's catch state.

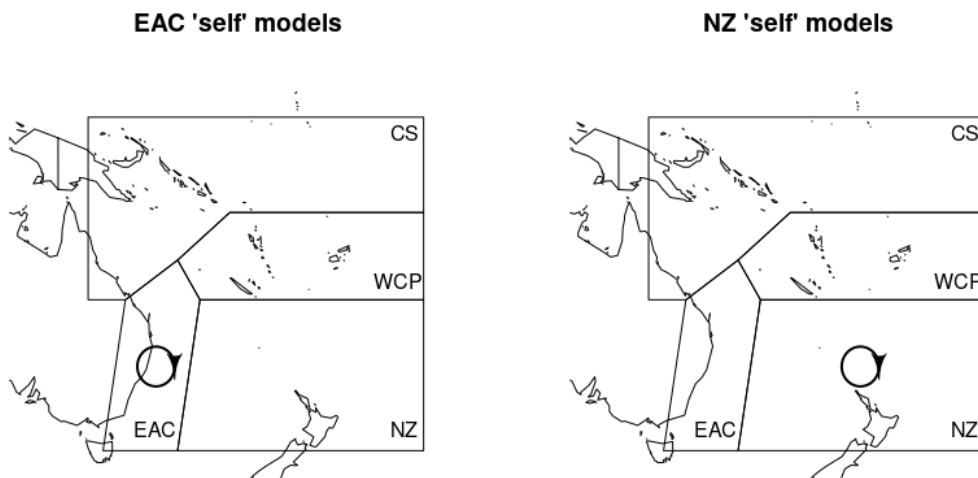


Figure 72 - Spatial configuration used in the 'self' models – as per the figure, there is no spatial dependence.

In contrast, 'adjacent' models model the catch state in a polygon as a function of the catch state in this polygon at the previous time-step, as well as the catch states in all adjacent polygons in the previous time-step.

'Adjacent' models treat  $S_{t,i}$  as spatially dependent. In other words, the state in a neighbouring cell influences the state in the focal cell. We note that the exact nature of this dependence is not really described in these models. For example, spatial dependence could be due to a combination of factors such as literal fish movement, changes in abundance or catchability or spatiotemporally correlated ocean conditions.

The following maps illustrate 'self' models in the EAC and New Zealand polygons, where an arrow illustrates the previous month's catch state at the base of the arrow being used to help predict the current month's catch state at the tip of the arrow.

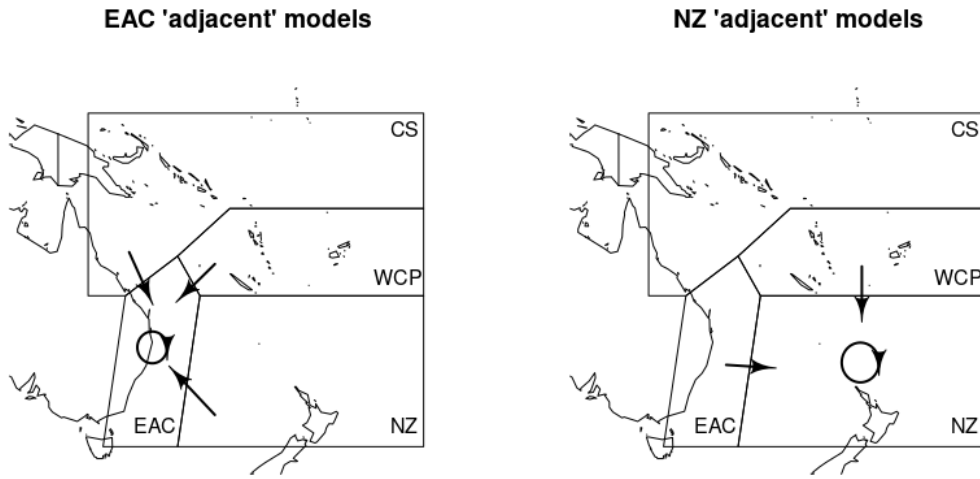


Figure 73 - Spatial configuration used in the 'adjacent' models for the case of the EAC and NZ blocks at illustrations. The model is configured so that only adjacent blocks influence the focal cell.

### 8.2.3 Statistical models

The approach used to predict  $S_{t,i}$  was to employ multinomial Generalized additive models fit using the MGCV library (Wood, 2006) in R (R Core Team, 2019). These allow prediction of categorical data which is assumed to be distributed according to a multinomial distribution, as a function of linear predictors. The model has  $K$  linear predictors, each dependent on smooth functions of predictor variables  $y_{t,j}$  as is usual for GAMS (Wood, 2006). If the response variable is  $S_{t,i} \in \{0, \dots, K\}$ , then the likelihood for  $S_{t,i} = \exp(y_{t,j}) / \{1 + \sum_j \exp(y_{t,j})\}$ . If  $S_{t,i}=0$  the likelihood is  $1 / \{1 + \sum_j \exp(y_{t,j})\}$ . In the two-class case, this becomes a binary logistic regression model (Wood, Pya and Saefken, 2016).

We use the following notation to describe 'self' and 'adjacent' cases, as outlined above. For 'self' models, the GAMS take the form:

$$S_{t,i} \sim \beta_0 + \beta_1 S_{t-1,i} + \beta_2 f(\text{month}) + \sum_{i>2} \beta_i f_i(O_i)$$

Where  $\beta$  are estimated coefficients, month is a factor term for month of the year and  $O_i$  are the set of ocean covariates described in chapter (see section 4). The  $f(\cdot)$  are non-parametric smoothing splines. The term  $f(\text{month})$  was a cyclic smooth (Wood, 2006) where a periodic smooth is used to model an annual cyclic effect.

For 'adjacent' models, the GAMS take the form:

$$S_{t,i} \sim \beta_0 + \beta_1 S_{t-1,i} + \beta_2 \text{month} + \sum_{k \in \mathcal{A}(S)} \beta_k S_{t-1,k} + \sum_{i>2} \beta_i f_i(O_i)$$

which is the same as the previous model structure except that it includes the  $k$  extra parameters for adjacent states (here denoted by  $\mathcal{A}(S)$ .) We included the observed catch states in the previous month in each polygon adjacent to the polygon under investigation as another set of predictors.

## 8.2.4 Ocean model data output

As a simple descriptor of ocean state, we used extracted data from the ACCESS-S2 model output and averaged across each month/region for the time series. For full details of the ACCESS-S2 model see section 2).

## 8.2.5 Model selection

The model selection aimed to narrow down the space of possible models. We therefore aimed to select both a self model and an adjacent model for each species/region combination. To do this we employed the following procedure.

First, we fit reduced models that each included a single oceanographic predictor, separately for each oceanographic predictor. These reduced models were divided into:

- 1. Reduced 'self' models which included the previous state in the polygon, month, and a single oceanographic predictor.
- 2. Reduced 'adjacent' models which also included the previous state in the polygon and all adjacent polygons, as well as month, and a single oceanographic predictor

We recorded the deviance explained by each reduced model in both 1 and 2 above.

To select a 'chosen' model, we started with the reduced model that explained the highest proportion of the deviance, then sequentially added oceanographic predictors from the reduced model that explained the second-most deviance, then third-most, and so on, stopping when:

1. Adding another additional variable did not result in a model that explained a higher proportion of the deviance, or
2. Adding the next predictor resulted in a singular model, or
3. The model contained six oceanographic predictors, at which point adding further predictors was infeasible for reasons of computer power.

The final model in this process was added to the set of 'chosen' models which consists of one 'self' and one 'adjacent' model for each species for each area.

## 8.3 Results

### 8.3.1 Ocean conditions

Figure 74 below shows the times series of monthly averaged ocean data fields from ACCESS-S2 for the EAC region. Clearly there are some variables (such as SST/ HC300/TD) which show very clear seasonal signals. Immediately this indicates that there are likely to be correlations with the month term. Other variables (e.g v100/u100/eke2000) do not have this same signal. However, there is evidence of strong autocorrelation in most variables.

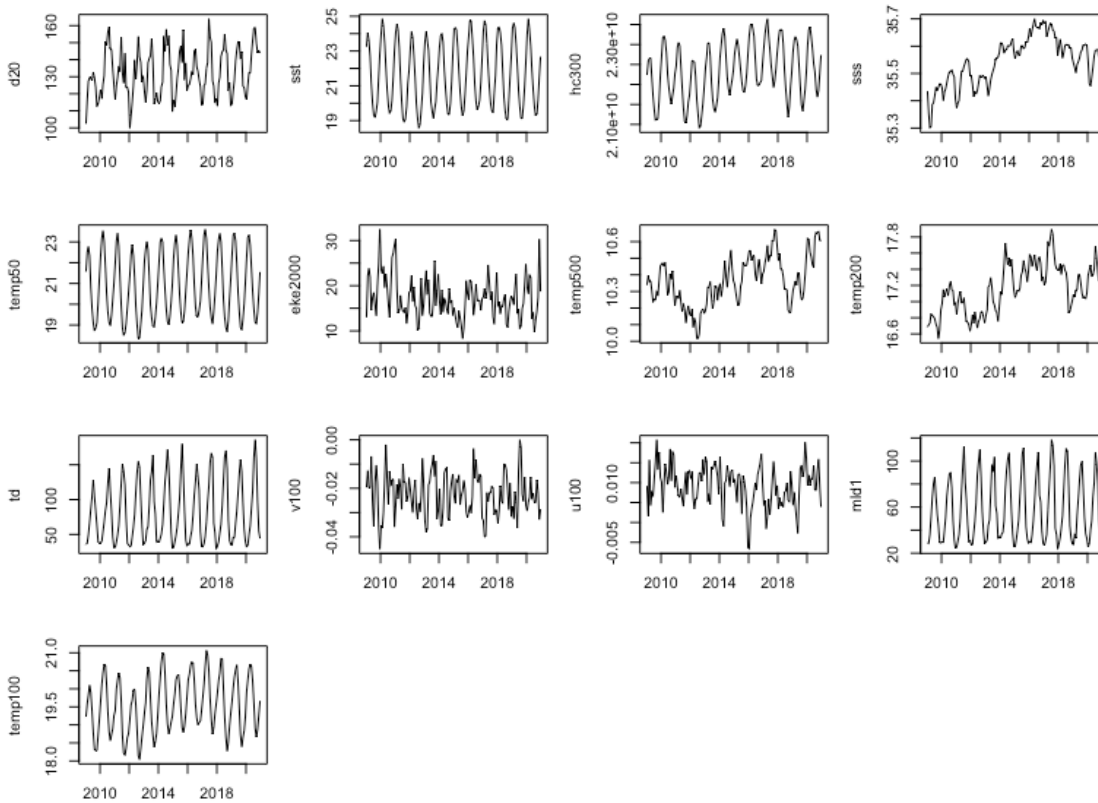


Figure 74 - Monthly time series for the EAC-dominated region (see Figure 7 above).

CPUE and categorized state sequences (Table 22) shows the observed state transitions after categorisation for each species in the EAC region. The time series themselves and resultant time series of categorized data are shown in subsequent figures. Apparent from Table 22 is that the transitions are dominated by Medium->Medium transitions. This is a function of the use of the 25th/85th percentile thresholds and means that the proportion of time in state is equal across all species' time series. We consider how other approaches to choosing thresholds should be considered in any extension of this project in the discussion section below. The consequence of this is that the model has less "information" on transitions to and from the other states. If the percentile thresholds we used do correspond to the typical experience of operators in the industry as to what catch rates are poor/average or good, then this would be unavoidable. However, it would be better if the thresholds were based on direct information from fishers.

Table 22 - observed state transitions for each species for the EAC dominated region. The tables are to be read as the “from state” as rows and “to state” as columns.

<b>YFT</b>	bad	medium	good
bad	10	24	2
medium	21	50	14
good	4	12	6
<b>BET</b>	bad	medium	good
bad	13	20	3
medium	19	53	13
good	3	13	6
<b>SWO</b>	bad	medium	good
bad	16	19	1
medium	18	53	14
good	2	13	7
<b>ALB</b>	bad	medium	good
bad	10	24	2
medium	21	50	14
good	4	12	6
<b>STM</b>	bad	medium	good
bad	15	20	1
medium	19	51	16
good	2	14	5

We now detail the categorized time series and percentiles for each species. By definition, 15% of observations for each species are considered 'good', 60% of observations are 'medium', and 25% of observations are 'bad'.

### 8.3.2 Yellowfin tuna

Figure 75 (a) shows the monthly CPUE for YFT in the EAC. There is still some indication of a downward trend in catch rates from 2009-2013. However, there are still periods of high catch rates – although these were generally less than those from the pre-2009 period (not shown).

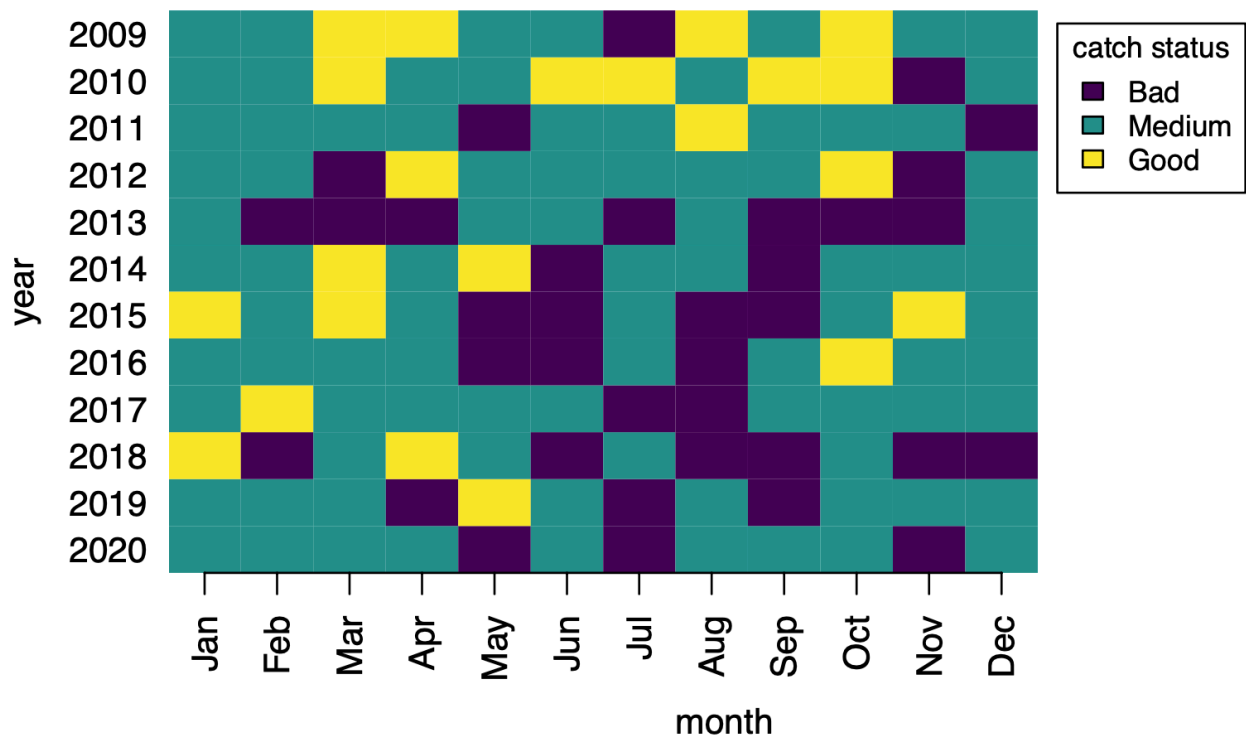
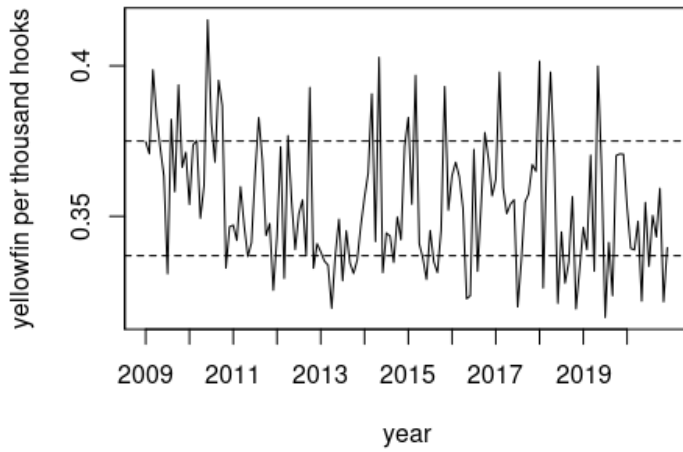


Figure 75 - Yellowfin tuna (top) catch rates and (bottom) categorized series of catch states

### 8.3.3 Bigeye Tuna

Figure 76(a) shows the monthly CPUE for BET in the EAC. As per the data for YFT, there was still some indication of a downward trend in catch rates, though visually it appears that these stabilized earlier -- from 2011. Relative to YFT there are a greater proportion of monthly CPUE observations that fall into the medium state.

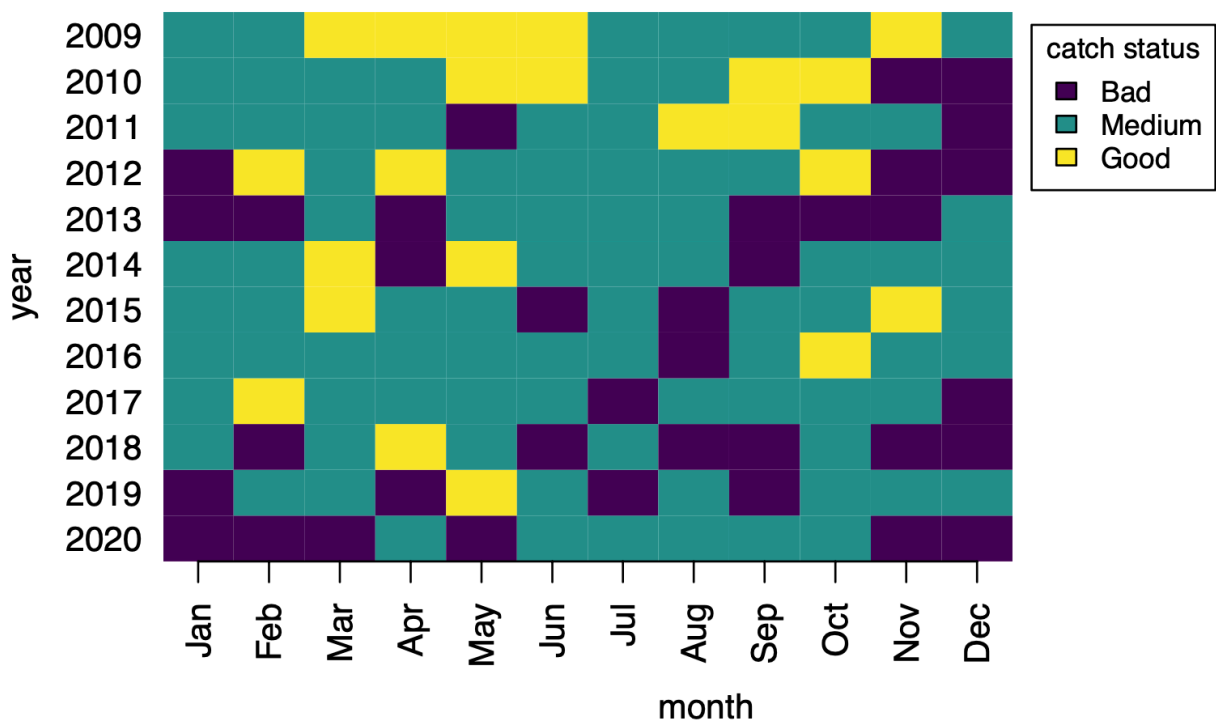
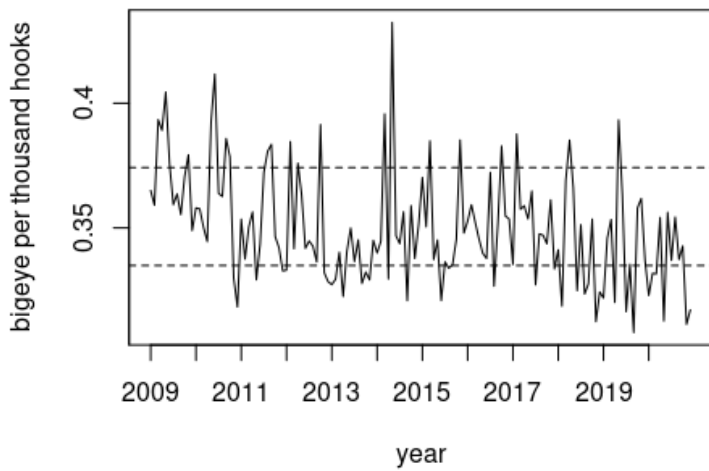


Figure 76 - Bigeye tuna (top) catch rates and (bottom) categorized series of catch states.

### 8.3.4 Broadbill swordfish

The SWO monthly CPUE series shows a period of downward trend for 2009-2011 (interspersed with two Good state observations) and then a period of relatively stable catches from 2013-2017. In the latter part of the time series there appears to be a greater degree of variability with a series of particularly low monthly CPUE values (Figure 77a).

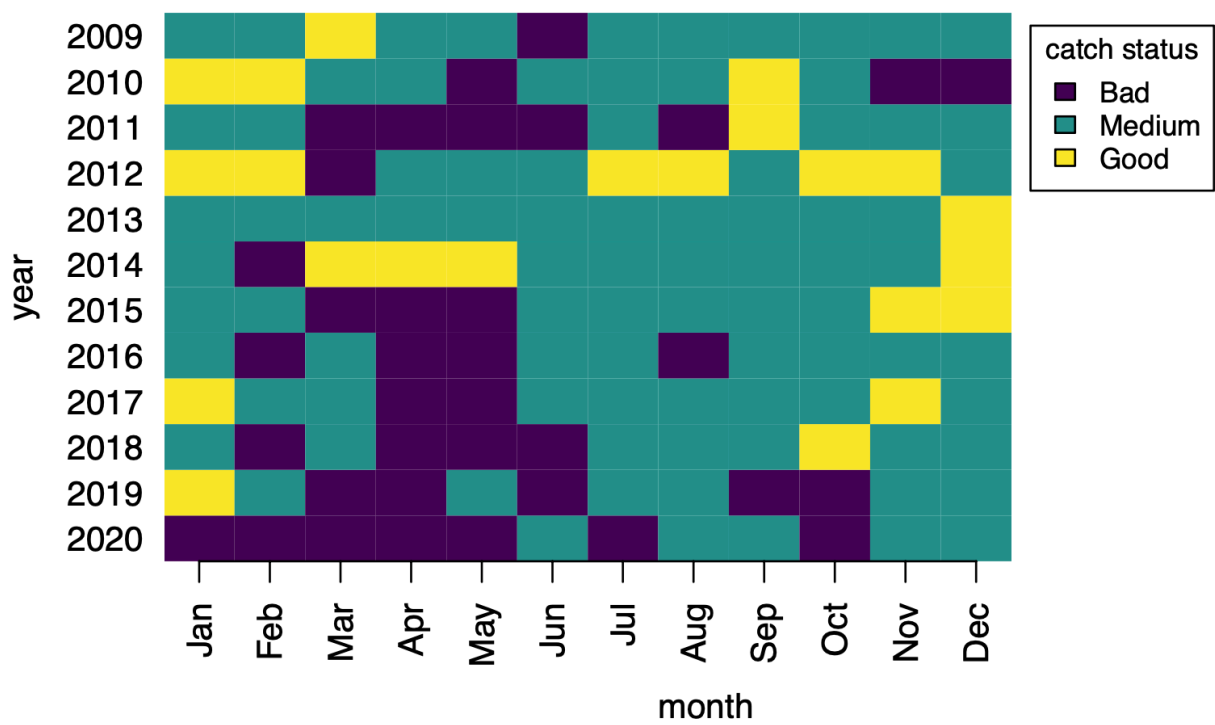
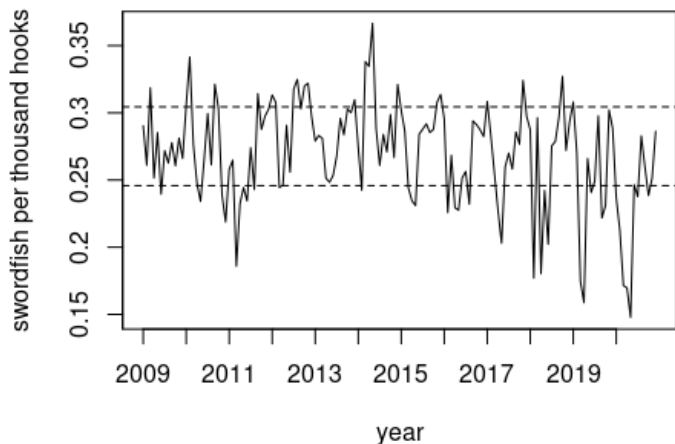


Figure 77 - Broadbill swordfish (top) catch rates and (bottom) categorized series of catch states.

### 8.3.5 Striped Marlin

The STM monthly CPUE series shows a period of downward trend for 2009-2013, and then a period of relatively stable catches from 2013-2017. After 2017, there appears to be another drop in catches, and no 'good' catches occur in the last three years of the data series (Figure 78a). The STM series does not appear to be strongly seasonal.

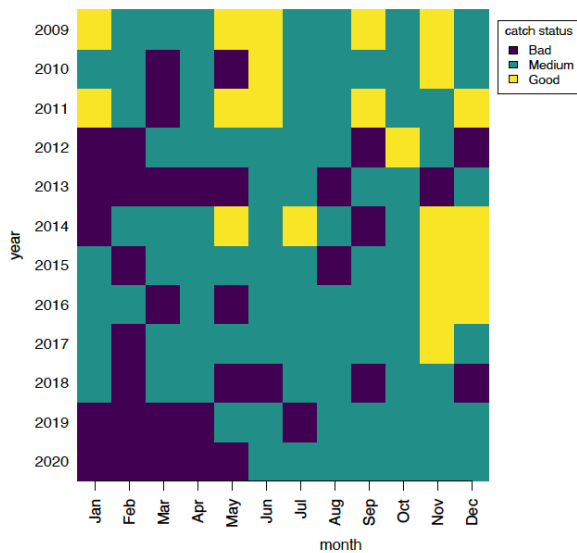
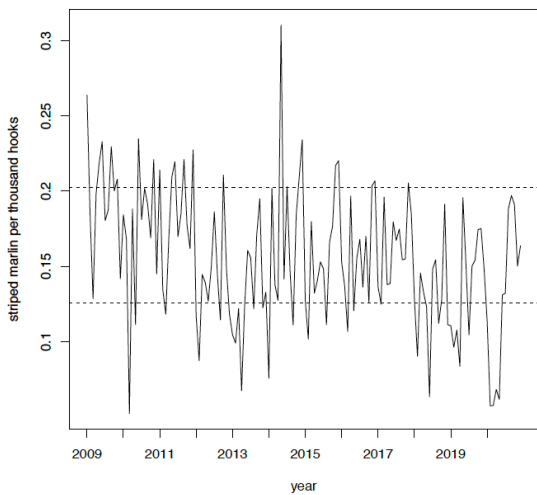


Figure 78 - striped marlin (top) catch rates and (bottom) categorized series of catch states.

### 8.3.6 Albacore

The ALB monthly CPUE series shows an apparent decline from 2009 – 2013, a period of flat CPUE from 2013 – 2018, and another period of apparent decline through to the end of 2020. The series features three outstanding months – very low months in late 2010 and late 2018, and very high in early 2014 (Figure 79). The ALB series show a seasonal pattern, in that good catches are most likely to occur in Feb – May, whereas bad catches are most likely to occur Oct- Jan.

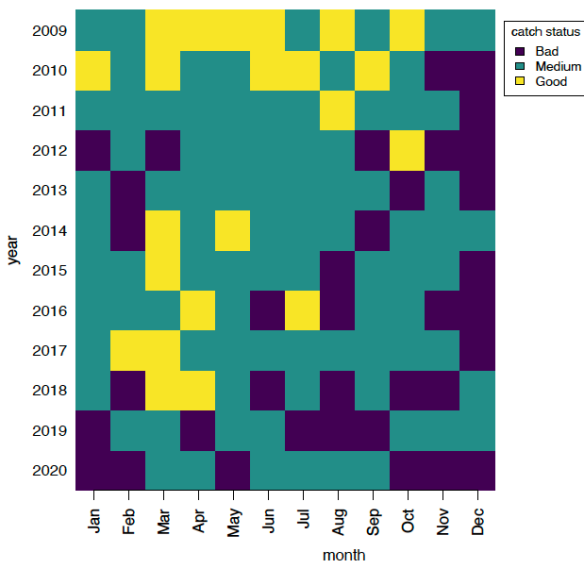
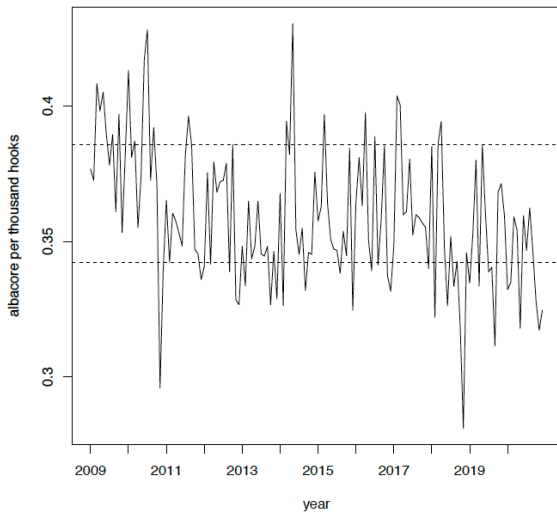


Figure 79 - Albacore (top) catch rates and (bottom) categorized series of catch states.

### 8.3.7 Summary of oceanographic predictors in selected models

The number of times each oceanographic predictor was used in a ‘chosen’ model in each oceanographic region, and across all oceanographic regions is shown in Table 23.

Although causal assignment is impossible for this exercise, the oceanographic predictors that appear in many of our ‘chosen’ models are consistently predictive of catch per unit effort across a suite of species and locations. This may indicate that these variables may drive differences in catchability for the species studied. The top few predictors, in decreasing order of number of ‘chosen’ models are temp100, SSS, temp50, eke2000, temp500, and u\_100, which may indicate that catchability is driven in part by sub-surface temperature (temp100, temp50, and temp500), ocean transport (eke2000 and u\_100), and surface chemistry variables (SSS). On the other end of the spectrum, ocean mixing variables unrelated to temperature, such as mld1 and d20, appear in relatively few models and may be less indicative of differences in catchability.

Table 23 - Number of times a given ocean covariate was retained in set of 40 chosen models.

Variable	CS	WCP	NZ	ETBF	total
d20	1	1	1	1	4
Td	1	5	4	1	11
eke2000	3	5	1	3	12
<b>mld1</b>	0	0	2	5	7
Nino	1	6	2	1	10
<b>hc300</b>	0	3	3	2	7
Sss	6	7	1	1	15
<b>Sst</b>	3	0	2	3	8
temp50	5	6	1	1	13
temp100	0	7	6	4	17
temp200	0	0	1	1	2
temp500	5	2	3	2	12
u_100	6	2	2	2	12
v_100	4	1	5	1	11

### 8.3.8 Examples of model prediction for the EAC dominated region.

For comparisons between ‘self’ and ‘adjacent’ forms of models, our primary metric model performance is the Akaike Information Criterion (AIC). On this criterion, ‘adjacent’ models outperform ‘self’ models for most (14 / 20) pairs of models, with a further 2 pairs being tied between the ‘self’ and ‘adjacent’ forms. Given that AIC should penalize models with many extra parameters, then this could suggest that there is some signal of spatial dependence at the monthly scale in this data and could be due to a combination of movement processes, correlated ocean conditions at large scales and similarities in habitat requirements across the region. This analysis does not have sufficient information to pull out the relative influence of these aspects – largely because of the complexity of disentangling ocean dynamics, target species ecology and fisheries dynamics from catch data alone.

The amount of deviance described by these models was small (See Tables in Appendix 3 for the full set). The best models for STM and SWO explained just only 23.1% and 23.5% of the deviance, respectively. However, this does not automatically mean they are poor predictors of state.

In the rest of this section, we detail the results from EAC region to demonstrate how the models perform. Because ‘adjacent’ models generally outperform ‘self’ models, we will focus our case studies on adjacent models for Yellowfin Tuna, Bigeye Tuna, and Swordfish, in the ETBF polygon.

Table 24 - Deviance explained according to self (S) and adjacent (A) models.

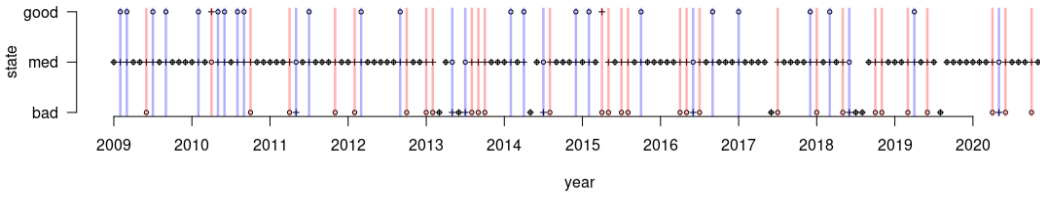
Species	YFT		ALB		BET		STM		SWO	
Model type	S	A	S	A	S	A	S	A	S	A
Deviance	5.60%	10%	5.90%	19.70%	10.40%	16.70%	18.60%	23.10%	19%	23.50%

To examine the model predictions graphically, we employed a 'bullseye chart'. For each month in a bullseye chart, we have an observed catch state, and a maximum-likelihood catch state derived from our oceanographic model. A bullseye chart is simply the observed and modelled catch state, plotted together for each month. The observed catch state is plotted as a round plotting symbol, and the predicted catch state is plotted as a plus-sign. If the observed and predicted states were the same, they line up to produce a cross-hairs, indicating that we 'hit our target' that month. To make it easier to spot patterns, we have also plotted transparent bars over each month where our modelled and observed catch states differed: blue if our modelled state was worse than the real state (a 'pessimistic' model error), and red if the modelled state was better than the real state (an 'optimistic' model error).

The maximum-likelihood predictions for each month are catch states: 'good', 'medium', or 'bad'. These three states are not equally likely a priori, by definition. For instance, a 'good' year is defined as one in the top 15% of all years, so the a priori probability of a 'good' year is 0.15, and the probability of randomly calling a 'good' year when it really happens to be a 'good' year is  $0.15^2 = 0.0225$ . Considering all three states, the probability of randomly calling the 'correct' state 0.445. Alternatively, a non-random strategy of always guessing 'medium' every month will be correct 60% of the time, because 60% of all observations are contained between the 25th and 85th percentiles (which are our 'bad' and 'good' cutoffs, respectively). For each plot, we provide the percentage of 'correct' calls provided by the model, noting that 44.5% of all calls would be correct if our models were simply predicting at random, or 60% of calls would be correct if the models always guessed 'medium'. This again points to the need for an independent and case- or usage- specific set of thresholds between the states.

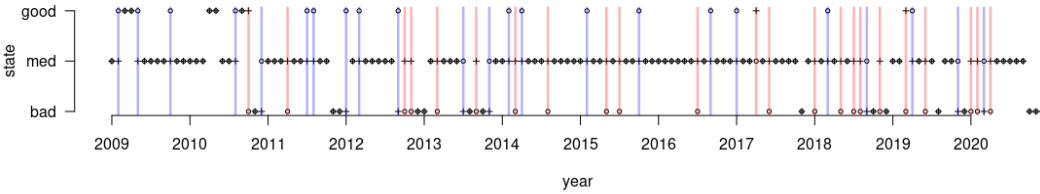
The models ranged from 58.3% correct state prediction for YFT to 71.5% correct in the case of albacore. These numbers indicate that there may be a tighter coupling between ocean and catch states in some species.

yellowfin ETBF bullseye chart: 58.3% correct



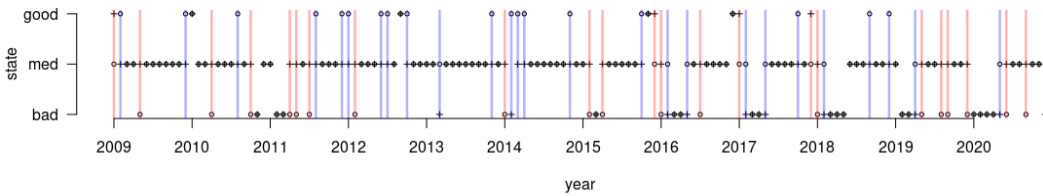
(A)

bigeye ETBF bullseye chart: 68.1% correct



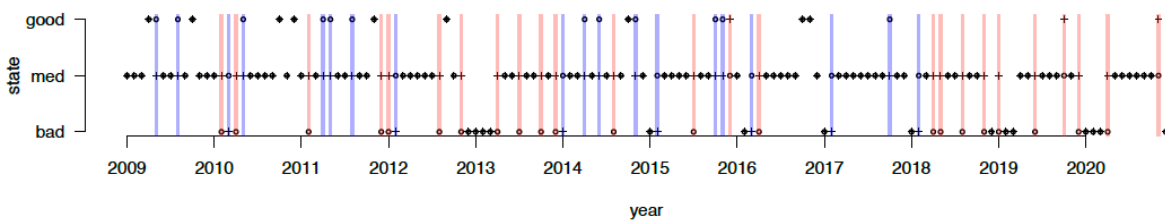
(B)

swordfish ETBF bullseye chart: 66% correct



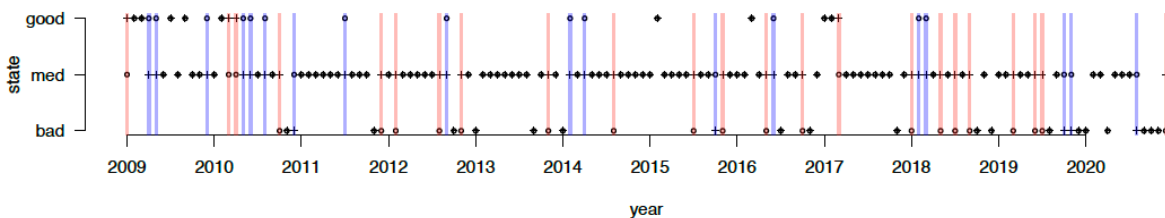
(C)

Striped Marlin ETBF bullseye chart: 69.4% correct



(D)

albacore ETBF bullseye chart: 71.5% correct



(E)

Figure 80 - State predictions for each species through time. See text for explanation of the plots.

### 8.4 Discussion

To recap, the results of the modelling were only moderately successful. The deviance explained by the models was low and while the models typically did better than a random prediction of state, their success at predicting the next state based on current state and oceanography was variable. The results shown here use the ETBF as a focal region for prediction and show that (best to worst)

ALB, STM, BBL, BET and YFT states were predicted with accuracy between 71 and 58% accuracy. This indicates that useful predictions may be generated for some species. There was, however, a lower degree of predictability for BET and YFT. We discuss aspects of the modelling that may be investigated in further work, which may improve the success rates.

The aim of this chapter was to trial a new approach to prediction of catch rates based on ocean data. For this we selected a period of relatively stable nominal CPUE from which we produced a categorized set of discrete states which we labelled Good, Medium and Bad. We then considered whether these states could be predicted through time for each month based on knowledge of the previous months state in both the region of interest and adjacent regions and descriptors of oceanography in the current state.

The results we obtained suggest that the models were generally able to predict better than a random guess. However, the models we fit here are probably insufficient to be used as a highly accurate predictive tool. Further development is required to determine if the accuracy of the models can be improved. For this there are several lines of inquiry which could be explored in future work.

#### **8.4.1 Selection of thresholds for categorisation of states**

One aspect where improvements may be gained is in the categorisation of the state itself. For uniformity across the species, our categorisation of state using the 25th and 85th percentiles as thresholds. This may not be optimal for the following reasons:

- These thresholds may not capture what the industry considers to be a good / poor catch rate. If there is interest in developing an approach similar to that considered here, we hope that this initial exploration of the method will allow for focused discussion in industry/management forums such as TTRAG. This may elucidate the thresholds considered by industry to be exceptionally good or bad years.
- The ability of the model to correctly estimate the state is likely to be a function of how many times it “sees” transitions to and from states. The number of these will be a function of the thresholds we selected. In other words, if you used an inappropriate threshold, you could have no observations of a given state etc.
- The use of the same percentiles may not be appropriate across all species.

The latter two aspects of these may be improved by shifting from the approach we took, where the state is considered to be directly observable (once thresholds have been selected), to a more sophisticated model where the states are considered to be latent variables. In the latter formulation, the model ‘decides’ the probability that a given observation is drawn from a set of underlying state-distributions. This is known as a Hidden Markov Model (MacDonald and Zucchini, 2016).

While this approach would be more objective from a statistical standpoint, as it allows the data to decide whether a given observation is to be considered “Good”, “Medium” or “Bad”, the approach is more complex – especially when the transitions between states is a function of covariates. Such models are widely used in a range of problems (e.g. finance, medical applications, speech recognition). Typically, these require a large amount of data but in principle these approaches could address the dependence on selected cut-offs.

## 8.4.2 Spatial configuration

In all species, the adjacent models which depended on state categorisations from neighbouring regions were preferred. On the face of it, this may indicate that there is spatiotemporal dependence in catch rates. This may be the case, but there are some caveats that should be raised on this point.

First, the adjacent models may be preferred simply because there is more covariate data to inform the model. We consider this possible but not necessarily likely. Our conclusion of a general tendency for better performance in the adjacent models was based on AIC. This criterion should penalize the addition of spurious covariates and reduce overfitting.

Further, and in the same vein as the discussion above regarding the dependence on choice of thresholds in the catch rate time series, the spatial units considered here may not be appropriate for all species. The results of section 4 on oceanographic regimes/regions of course gives us a physical basis for the spatial configuration used. However, the target species considered here may not respond to oceanography in the same way or at the same spatial/time scales. Nevertheless, the fact that some variables were more consistently selected may point to common influences across species.

# Discussion and Conclusion

The results from this exploration into a suite of habitat models for investigating drivers in the ETBF and surrounding regions has suggested that sub-surface variables are important in explaining the variance. Although much variance is explained by effort (and we have been constrained to using fishery-dependant data for the most part), there is still a significant part of the variance in CPUE that is linked to the environment for some species and regions.

Our results also suggest the importance of developing regionally trained models. A model that is conditioned in an area dominated by a specific set of drivers is not always applicable to the other areas where a different environment dominates (eg EAC vs CS), and this needs to be taken into account.

The method we investigated in the categorical approach showed promise for some species (ALB/SWO and STM). For BET and YFT our results were not encouraging. However, as we considered in the discussion in that section, there are aspects which may improve the ability of models to predict catch states.

In principle, the models could be fitted to historical 'nowcast data' and, in conjunction with predictive ocean models, provide a near-term future forecast of catch rates. As with any aspect of the fishery, care would need to be taken to consider predictions in light of the dynamics of the target species stock. Obviously for a highly depleted stock, we would expect relatively poor catch rates, irrespective of the ocean dynamics. Therefore, any usage of these models in a truly predictive mode (i.e. predictive of the future catch state) would need to consider this information. Future work could consider how to include stock assessment model projections in predictions of catch rate.

# Implications

The outcomes of this work will have utility for fisheries stock assessments and management in the face of climate change. It is expected that as the ocean continues to warm, and fish distributions change, there will be a need to use environmental nowcasts and forecasts to aid support sustainable harvest and management and inform the debate about spatial management tools such as static and dynamic protected areas.

Ongoing provision of environmental status reports and forecasts (situational reports) will be useful for managers managing these resources in a changing environment.

## Recommendations

Based on continual project engagement with end users over four years, there is a clear interest from industry and need for continued and improved delivery of oceanographic information and insight to Australian fisheries management and industry. During the evolution of this project, the team has worked closely with Bureau of Meteorology staff and CSIRO oceanographers to incorporate the various reanalysis and forecast products into our work. The outputs of the modelling work show that primary (e.g., temperature at 500m) and derived (e.g., depth of the 20°C isotherm, heat content in the upper 300m, and mixed layer depth) sub-surface oceanographic variables are important, and yet these are limited in their availability to be forecast. Many of these variables are yet to be fully assessed for forecast skill (a measure of accuracy), and when this has been done, efforts to make these available should be pursued. The analysis-ready datasets produced by this project should be considered in the regular workflow of the TTRAG for use in standardising CPUE and providing updates of current ocean state. Ongoing development of operational systems and engagement with the Bureau of Meteorology (and continued provision and assessment of additional ocean variables) that include the sub-surface variables of interest should be pursued.

## Further development

A substantial limitation in assessing the environmental influence on tuna and billfish availability in the ETBF and surrounding regions is the limited or absent fishery independent data such as that obtained from electronic tags. There is a need for targeted studies of species of interest in the Australian region to explore the influences in more detail. Catch data are clearly influenced by decisions made by fishers and managers, primarily to do with economics (e.g., distance from port, market price or demand), or harvest controls, which confound the ocean influences on fish distribution.

# Extension and Adoption

A variety of aspects of this work has been presented at scientific meetings and are outlined in Appendix 5 – project updates.

In addition, we wrote an article for the SPC Newsletter (<https://coastfish.spc.int/en/publications/bulletins/fisheries-newsletter>), that is attached at Appendix 6.

We will continue the development and population of the project website for delivery of timeseries of key indices (from section 4).

Investigate partnering with Climate Resilient Enterprise (API delivery of climate products to end-users).

# Project materials developed

We have one paper that is in review at Fisheries Oceanography:

**"Forecast-ready models to support fisheries adaptation to global variability and change"**

Kylie L. Scales<sup>1</sup>, Thomas S. Moore II<sup>2</sup>, Bernadette Sloyan<sup>2</sup>, Claire Spillman<sup>3</sup>, J. Paige Eveson<sup>2</sup>, Toby A. Patterson<sup>2</sup>, Ashley Williams<sup>2</sup>, Alistair J. Hobday<sup>2</sup>, Jason R. Hartog<sup>2</sup>

<sup>1</sup>School of Science, Technology and Engineering, University of the Sunshine Coast, Queensland, Australia.

<sup>2</sup>CSIRO Oceans & Atmosphere, Castray Esplanade, Hobart, Tasmania, Australia.

<sup>3</sup>Bureau of Meteorology, Melbourne, Victoria, Australia.

During the project, we delivered 6 written project updates to TTRAG and SPC (these can be found in Appendix 5. In addition, formal presentations were made to TTRAG and the Steering Committee through the life of the project.

# Appendices

**Appendix 1 – Initial Habitat Modelling exploration (attached)**

**Appendix 2 – Boosted Regression Tree results for all species and regions (attached)**

**Appendix 3 – Categorical Timeseries (attached)**

**Appendix 4 – Project Staff**

Jason Hartog (CSIRO) – Project leader (co-Project leader at inception)  
Alistair Hobday (CSIRO) – co-Project leader (Project leader at inception)  
Paige Eveson (CSIRO)  
Thomas Moore (CSIRO)  
Bernadette Sloyan (CSIRO)  
Kylie Scales (USC)  
Toby Patterson (CSIRO)  
Shane Baylis (CSIRO)  
Robert Campbell (CSIRO)  
Ashley Williams (CSIRO)  
Claire Spillman (BOM)  
Don Bromhead (AFMA)

**Appendix 5 – Project Updates (attached)**

**Appendix 6 – SPC Newsletter article (attached)**

## References

- Alexander, M. A., I. Bladé, M. Newman, J. R. Lanzante, N.-C. Lau, and J. D. Scott, 2002: The atmospheric bridge: The influence of ENSO teleconnections on air–sea interaction over the global oceans. *J. Climate*, 15, 2205–2231.
- Bi, Dave; Marsland, Simon; Uotila, Petteri; O'Farrell, Siobhan; Fiedler, Russell; Sullivan, Arnold; Griffies, Stephen; Zhou, Xiaobing; Hirst, Tony. ACCESS-OM: the Ocean and Sea ice Core of the ACCESS Coupled Model. *Australian Meteorological and Oceanographic Journal*. 2013; 63(1):213-232. <http://hdl.handle.net/102.100.100/97081?index=1>
- Bjerknes, J., 1969: Atmospheric teleconnections from the equatorial Pacific. *Mon. Wea. Rev.*, 97, 163–172.
- Chamberlain, M. A., Oke, P. R., Fiedler, R. A. S., Beggs, H. M., Brassington, G. B., and Divakaran, P.: Next generation of Bluelink ocean reanalysis with multiscale data assimilation: BRAN2020, *Earth Syst. Sci. Data*, 13, 5663–5688, <https://doi.org/10.5194/essd-13-5663-2021>, 2021.
- Dell, J. T., C. Wilcox, R. J. Matear, M. A. Chamberlain and A. J. Hobday (2015). Potential impacts of climate change on the distribution of longline catches of yellowfin tuna (*Thunnus albacares*) in the Tasman Sea. *Deep Sea Research II* 113: 235-245.
- Delworth, T. L., Broccoli, A. J., Rosati, A., Stouffer, R. J., Balaji, V., Beesley, J. A., Cooke, W. F., Dixon, K. W., Dunne, J., Dunne, K. A., Durachta, J. W., Findell, K. L., Ginoux, P., Gnanadesikan, A., Gordon, C. T., Griffies, S. M., Gudgel, R., Harrison, M. J., Held, I. M., Hemler, R. S., Horowitz, L. W., Klein, S. A., Knutson, T. R., Kushner, P. J., Langenhorst, A. R., Lee, H., Lin, S., Lu, J., Malyshev, S. L., Milly, P. C. D., Ramaswamy, V., Russell, J., Schwarzkopf, M. D., Shevliakova, E., Sirutis, J. J., Spelman, M. J., Stern, W. F., Winton, M., Wittenberg, A. T., Wyman, B., Zeng, F., & Zhang, R. (2006). GFDL's CM2 Global Coupled Climate Models. Part I: Formulation and Simulation Characteristics, *Journal of Climate*, 19(5), 643-674 <https://journals.ametsoc.org/view/journals/clim/19/5/jcli3629.1.xml>
- Elith, J., Leathwick, J. R., & Hastie, T. (2008). A working guide to boosted regression trees. *Journal of Animal Ecology*, 77(4), 802-813.
- Eveson, J. P., A. J. Hobday, J. R. Hartog, C. M. Spillman and K. M. Rough (2015). Seasonal forecasting of tuna habitat in the Great Australian Bight. *Fisheries Research* 170: 39–49.
- Feng, M., Y. Li, and G. Meyers (2004), Multidecadal variations of Fremantle sea level: Footprint of climate variability in the tropical Pacific, *Geophys. Res. Lett.*, 31, L16302, doi:10.1029/2004GL019947.
- Folland, C. K., J. A. Renwick, M. J. Salinger, and A. B. Mullan (2002), Relative influences of the Interdecadal Pacific Oscillation and ENSO on the South Pacific Convergence Zone, *Geophys. Res. Lett.*, 29(13), 1643, doi:10.1029/2001GL014201.
- Frankcombe LM, McGregor S, England MH (2015) Robustness of the modes of Indo-Pacific sea level variability. *Clim Dyn* 45:1281–1298. doi:10.1007/s00382-014-2377-0
- Greenwell, B., Boehmke, B., Cunningham, J. and GBM Developers (2020).gbm: Generalized Boosted Regression Models. R package version 2.1.8. <https://CRAN.R-project.org/package=gbm>
- Hartog, J., A. J. Hobday, R. Matear and M. Feng (2011). Habitat overlap of southern bluefin tuna and yellowfin tuna in the east coast longline fishery - implications for present and future spatial management. *Deep Sea Research Part II* 58: 746-752.
- Hill, K.L., Rintoul, S.R., Coleman, R., Ridgway, K.R., 2008. Wind forced low frequency variability of the East Australia Current. *Geophysical Research Letters* 35, L08602. doi:10.1029/2007GL032912.
- Hobday, A. J. (2010). Ensemble analysis of the future distribution of large pelagic fishes in Australia. *Progress in Oceanography* 86(1-2): 291-301 doi:10.1016/j.pocean.2010.1004.1023.

- Hobday, A. J. and G. T. Pecl (2014). Identification of global marine hotspots: sentinels for change and vanguards for adaptation action. *Reviews in Fish Biology and Fisheries* 24: 415-425. DOI 410.1007/s11160-11013-19326-11166.
- Hobday, A. J., C. M. Spillman, J. P. Eveson and J. R. Hartog (2016). Seasonal forecasting for decision support in marine fisheries and aquaculture. *Fisheries Oceanography* 25(S1): 45-56.
- Hobday, A. J., Hartog, J. R., Spillman, C. M., & Alves, O. (2011). Seasonal forecasting of tuna habitat for dynamic spatial management. *Canadian Journal of Fisheries and Aquatic Sciences*, 68(5), 898-911. doi:10.1139/f2011-031
- Hobday, A. J., Spillman, C. M., Eveson, J. P., Hartog, J. R., Zhang, X., & Brodie, S. (2018). A Framework for Combining Seasonal Forecasts and Climate Projections to Aid Risk Management for Fisheries and Aquaculture. *Frontiers in Marine Science*, 5(137). doi:10.3389/fmars.2018.00137
- Holbrook, N. J., I. D. Goodwin, S. McGregor, E. Molina, and S. B. Power, 2011, ENSO to multi-decadal time scale changes in East Australian Current transports and Fort Denison sea level: Oceanic Rossby waves as the connecting mechanism, *Deep-Sea Research II*, 58, 547–558.
- Hudson, D., Alves, O., Hendon, H.H., Lim, E., Liu, G., Luo J.-J., MacLachlan, C., Marshall, A.G., Shi, L., Wang, G., Wedd, R., Young, G., Zhao, M., Zhou X. 2017: ACCESS-S1: The new Bureau of Meteorology multi-week to seasonal prediction system. *Journal of Southern Hemisphere Earth Systems Science*, 67:3 132-159 doi: 10.22499/3.6703.001.
- Kelly, P., Clementson, L. and Lyne, V.: Decadal and seasonal changes in temperature, salinity, nitrate, and chlorophyll in inshore and offshore waters along southeast Australia, *J Geophys Res-Oceans*, 120(6), 4226–4244, doi:10.1002/2014JC010646, 2015.
- Last, P. R., W. T. White, D. C. Gledhill, A. J. Hobday, R. Brown, G. J. Edgar and G. T. Pecl (2011). Long-term shifts in abundance and distribution of a temperate fish fauna: a response to climate change and fishing practices. *Global Ecology and Biogeography* 20: 58-72 DOI: 10.1111/j.1466-8238.2010.00575.x.
- Lehodey, P., I. Senina, S. Nicol and J. Hampton (2015). Modelling the impact of climate change on South Pacific albacore tuna. *Deep Sea Research II* 113: 246-259.
- Lehodey, Patrick, 'Climate and Fisheries: An Insight from the Central Pacific Ocean', in Nils Chr. Stenseth and others (eds), *Marine Ecosystems and Climate Variation: The North Atlantic: A Comparative Perspective* (Oxford, 2005)
- MacDonald, I. L., & Zucchini, W. (2016). Hidden Markov models for discrete-valued time series. *Handbook of discrete-valued time series*, 267-286.
- MacLachlan, C., Arribas, A., Peterson, K.A., Maidens, A., Fereday, D., Scaife, A.A., Gordon, M., Vellinga, M., Williams, A., Comer, R.E., Camp, J., Xavier, P. and Madec, G. (2015), Global Seasonal forecast system version 5 (GloSea5): a high-resolution seasonal forecast system. *Q.J.R. Meteorol. Soc.*, 141: 1072-1084. <https://doi.org/10.1002/qj.2396>
- Mantua, N. J., and S. R. Hare (2002), The Pacific Decadal Oscillation, *J. Oceanogr.*, 58, 35–44, doi:10.1023/A:1015820616384.
- Madec, G. (2012). NEMO ocean engine (Note du P<sup>o</sup>le modelisation, Vol. 27, 357 pp.). Institute Pierre Simon Laplace.
- Muhling, B. A., R. Brill, J. T. Lamkin, M. A. Roffer, S.-K. Lee, Y. Liu and F. Muller-Karger (2017). Projections of future habitat use by Atlantic bluefin tuna: mechanistic vs. correlative distribution models. *ICES Journal of Marine Science* 74(3): 698–716.
- Newman, M., and Coauthors, 2016: The Pacific decadal oscillation, revisited. *J. Climate*, 29, 4399–4427, <https://doi.org/10.1175/JCLI-D-15-0508.1>.
- O’Kane, T. J., Sandery, P. A., Kitsios, V., Sakov, P., Chamberlain, M. A., Collier, M. A., Fiedler, R., Moore, T. S., Chapman, C. C., Sloyan, B. M., & Matear, R. J. (2021). CAFE60v1: A 60-Year Large Ensemble Climate Reanalysis. Part I: System Design, Model Configuration, and Data Assimilation, *Journal of Climate*, 34(13), 5153-5169.
- O’Kane, T. J., Sandery, P. A., Kitsios, V., Sakov, P., Chamberlain, M. A., Squire, D. T., Collier, M. A., Chapman, C. C., Fiedler, R., Harries, D., Moore, T. S., Richardson, D., Risbey, J. S., Schroeter, B. J. E., Schroeter, S., Sloyan, B. M., Tozer, C., Watterson, I. G., Black, A., Quinn,

C., & Matear, R. J. (2021). CAFE60v1: A 60-Year Large Ensemble Climate Reanalysis. Part II: Evaluation, *Journal of Climate*, 34(13), 5171-5194.

- R Core Team (2022). R: A language and environment for statistical computing. R Foundation for Statistical Computing, Vienna, Austria. <https://www.R-project.org/>.
- Ridgway, K. R.; Dunn, J. R.; Cahill, M. L.; Griffin, D. A. SynTS: a 3-D ocean observational analysis for the Australian region [poster]. In: Second Argo science workshop, March 12-18; 2006; Venice, Italy. 2006.
- Robinson, L., A. J. Hobday, H. P. Possingham and A. J. Richardson (2015). Trailing edges projected to move faster than leading edges for large pelagic fish under climate change. *Deep Sea Research II* 113: 225-234.
- Robinson, L., J. Elith, A. J. Hobday, R. G. Pearson, B. E. Kendall, H. P. Possingham and A. J. Richardson (2011). Pushing the limits in marine-based species distribution modelling: lessons from the land present challenges and opportunities. *Global Ecology and Biogeography* 20(6): 789–802 DOI: 10.1111/j.1466-8238.2010.00636.x.
- Saha, S., Moorthi, S., Pan, H.-L., Wu, X., Wang, J., Nadiga, S., . . . Goldberg, M. (2010). The NCEP Climate Forecast System Reanalysis. *Bulletin of the American Meteorological Society*, 91(8), 1015-1058. doi:10.1175/2010bams3001.1
- Scales K. L., E. L. Hazen, S. M. Maxwell, H. Dewar, S. Kohin, M. G. Jacox, C. A. Edwards, D. K. Briscoe, L. B. Crowder, R. L. Lewison, S. J. Bograd (2017) Fit to predict? Ecoinformatics for modeling the catchability of a pelagic fish in near real-time. *Ecological Applications*, 27(8): 2313-2329 DOI: 10.1002/eap.1610
- Smith G and Spillman CM (2019) New high-resolution sea surface temperature forecasts for coral reef management on the Great Barrier Reef. *Coral Reefs* 38:1039-1056. <https://doi.org/10.1007/s00338-019-01829-1>
- Sunday, J. M., G. T. Pecl, S. D. Frusher, A. J. Hobday, N. Hill, N. J. Holbrook, G. J. Edgar, R. Stuart-Smith, N. S. Barrett, T. Wernberg, R. Watson, D. A. Smale, E. A. Fulton, D. Slawinski, M. Feng, B. T. Radford, P. A. Thompson and A. E. Bates (2015). Species traits and climate velocity explain geographic range shifts in an ocean-warming hotspot. *Ecology Letters*: doi: 10.1111/ele.12474.
- Thompson, D. W. J., and J. M. Wallace, 2000: Annular modes in the extratropical circulation. Part I: Month-to-month variability. *J. Climate*, 13, 1000–1016.
- Timmerman, A. and co-authors, 2018, El Niño–Southern Oscillation complexity, *Nature*, 559, 535-545, doi: 10.1038/s41586-018-0252-6.
- Tommasi, D., C. Stock, A. J. Hobday, R. Methot, I. Kaplan, P. Eveson, K. Holsman, T. Miller, S. Gaichas, M. Gehlen, A. Pershing, G. Vecchi, R. Msadek, T. Delworth, M. Eakin, M. Haltuch, R. Sefarian, C. Spillman, J. Hartog, S. Siedlecki, J. Samhuri, B. Muhling, R. Asch, M. Pinsky, V. Saba, S. Kapnick, C. Gaitan, R. Rykaczewski, M. Alexander, Y. Xue, K. Pegion, P. Lynch, M. Payne, T. Kristiansen, P. Lehodey and C. Werner (2017). Managing living marine resources in a dynamic environment: the role of seasonal to decadal climate forecasts. *Progress in Oceanography* 152: 15-49.
- Wedd R., Alves O., de Burgh-Day C., Down C., Gray-Weale A., Griffiths M., Hendon H.H., Hudson D., Li S., Lim E., Marshall A.G., Shi L., Smith P., Smith G., Spillman C.M., Wang G., Wheeler M.C., Yan H., Yin Y., Young G., Zhao M., Yi X. and Zhou X. In Review. ACCESS-S2: The upgraded Bureau of Meteorology multi-week to seasonal prediction system. *Journal of Southern Hemisphere Earth System Science*, 2022
- Williams, K. D., Harris, C.M., et al. 2015. The Met Office Global Coupled model 2.0 (GC2) configuration, *Geoscientific Model Development*, 8, 1509-1524, doi:10.5194/gmd-8-1509-2015.
- Wong, A. P. S., Wijffels, S. E., Riser, S. C., Pouliquen, S., Hosoda, S., Roemmich, D., . . . Park, H.-M. (2020). Argo Data 1999–2019: Two Million Temperature-Salinity Profiles and Subsurface Velocity Observations From a Global Array of Profiling Floats. *Frontiers in Marine Science*, 7. doi:10.3389/fmars.2020.00700

- Wood, S. N., Pya, N., & Säfken, B. (2016). Smoothing parameter and model selection for general smooth models. *Journal of the American Statistical Association*, 111(516), 1548-1563.
- Wood, Simon N. *Generalized additive models: an introduction with R*. Chapman and Hall/CRC, 2006.
- Zhang, X., and J. A. Church (2012), Sea level trends, interannual and decadal variability in the Pacific Ocean, *Geophys. Res. Lett.*, 39, L21701, doi:10.1029/2012GL053240.